BUCKLING OF CYLINDRICAL SHELLS UNDER NON-UNIFORM LATERAL PRESSURES

by

KUNDURPI S. PRABHU, B.E.,M.E.

A Doctoral Thesis

Submitted in Partial Fulfilment of the Requirements

For the Award of

Doctor of Philosophy of the

Loughborough University of Technology

September 1975

Supervisors:

Professor D. J. Johns,
Ph.D.,C.Eng.,F.R.Ae.S.,A.F.A.I.A.A.

and

Dr. S. Gopalacharyulu,
B.E.,M.Sc.,Ph.D.

SUMMARY

This thesis presents static equilibrium and stability analyses of cylindrical shells subjected to non-uniform external pressures. This problem is of practical importance in the design of launch vehicles, oil storage tanks, cooling towers subjected to wind loads and other engineering structures submerged in flowing water. The non-uniform pressure distributions considered are due to - a) Wind at high Reynold's numbers

b) Flow of water on submerged cylinders.

In the static equilibrium analysis for the pre-buckled state both Donnell and Flugge shell theories are employed. The results of pre-buckle deformations and stress resultants, when compared with results obtained using beam or semi-membrane theories show that the beam theory is inadequate and unsafe, whereas the semi-membrane theory is conservative and safe for wind loaded structures.

Stability analyses are carried out using both continuum and finite element approaches. The stagnation critical pressures are obtained for various shell geometries and end conditions. The criterion used for determining the buckling pressures is the vanishing of the second variation of total potential energy. The second variation of energy is expressed in terms of the pre-buckling (equilibrium) membrane strains and the assumed buckling virtual displacement components. Non-linear strain displacement relations are employed in the buckling analysis. The finite element method is generalised to take into account the effect of axial variation in shell thickness and the influence of additional ring stiffeners.

An experimental study of the problem is also reported. A series of experiments are conducted on model cylindrical shells in both a low speed wind tunnel facility and a low speed water tunnel. Based on the theoretical and experimental results obtained, the existing codes for the design of oil storage tanks subjected to wind loads are examined and are found to be conservative. Recommendations are made regarding the codes and the use of empirical relations for the stagnation buckling pressures in terms of shell parameters.

ACKNOWLEDGEMENTS

I would like to express my sincere thanks to Professor D.J. Johns and Dr. S. Gopalacharyulu for the inspiring guidance and advice throughout this work.

The help and assistance provided by all the technician staff in fabricating and testing the models is gratefully acknowledged.

The financial assistance provided by the Department of Trade and Industry is gratefully acknowledged.

Table of Contents

List of Figures

List of Tables

List of Appendices

Notation

A_1 to A_8	- arbitrary constants of integration.
A_R	- area of cross-section of ring.
a	- radius of the shell.
a_{i1}, a_{i2}, a_{i3}	- constants given in Appendix IV.
$[A]$	- row matrix of arbitrary constants.
B_1 to B_8	- arbitrary constants of integration.
b_{mn} , b_n	- Fourier coefficients in the loading.
$[B], [BI], [\bar{B}], [\bar{BI}]$	- the matrices given in Appendix VII.
C_1 to C_8	- arbitrary constants of integration.
C_{11} to C_{18} C_{21} to C_{28}	- constants given in Appendix III.
$\{C\}$	- column matrix in equation (4.11).
A_{mn}, B_{mn}, C_{mn}	- arbitrary constants in virtual displacements.
D	- $\frac{Eh}{1-\nu^2}$ membrane stiffness of shell.
b, d	- breadth and width of stiffening ring.
$[D], [D_n]$	- matrices given in Appendix VIII.
E	- Young's modulus of the material of shell.
e	- eccentricity of ring ($= d/2$)
e_{ij}	- error in pressure measured
$[F(x)], [\bar{F}(x)]$	- matrices of polynomial terms.
f_{ij}	- functions in stability determinant.
G, G_n	- particular solutions.
g_k	- constants in equation (3.16).
h	- thickness of the shell.

H_P	- max. permitted height of the shell.
H_f	- max. free height of the shell.
H_R	- reduced height of the shell.
H_n	- height of n^{th} course of shell.
h_n	- thickness of n^{th} course of shell.
h_a	- Average thickness of shell.
I_x, I_z	- moments of inertia of ring.
i	- counter for the elements of harmonics.
j	- counter for elements of harmonics.
J_η	- torsional stiffness of ring.
K	- $\frac{E h^3}{12(1-\gamma^2)}$ - bending stiffness of shell.
$\bar{K}$	- $K/D = \frac{h^2}{12}$
K_1, K_2	- spring constants at the base.
$[K_n], [K_n], [K_E]$ and $[K_G]$	- stiffness matrices for element and for the shell.
$[\bar{K}_1]$	- constant in equation (6.6).
$K_x, K_\theta, K_{x\theta}$	- curvatures of the shell.
L	- length of shell.
l	- length of shell element.
m	- suffix used as a counter.
$M_x, M_\theta, M_{x\theta}$	- the moment resultants in shell.
M_1, M_1', M_2, M_2'	- constants given in Appendix III.
n	- suffix used as a counter or for denoting harmonic.
N_1, N_1', N_2, N_2'	- constants given in Appendix III.
$N_x, N_\theta, N_{x\theta}$	- the stress resultants.

P	-	represents lateral load.
P_x, P_θ, P_z	-	components of external load on shell
P_o	-	stagnation pressure under wind load.
P_{ij}	-	pressure measured at point (i, j).
Q_z, Q_θ	-	transverse shear in the shell
$\{Q_n\}$	-	generalised displacements of shell.
$\{q\}_j, \{q_n\}$	-	jth nodal displacements and nth harmonic displacements of an element.
$\{\eta\}$	-	element load vector.
$\{R\}_n$	-	load vector for the shell for nth harmonic.
U	-	strain energy of the shell.
U_m	-	membrane strain energy.
U_b	-	bending strain energy.
V	-	potential energy of shell.
W	-	work done by external loads.
u, v, w	-	displacements in co-ordinate directions.
u_n, v_n, w_n	-	nth harmonics of displacements.
u_p, v_p, w_p	-	particular integrals for displacement.
x	-	axial co-ordinate.
x_1 to x_4 x_{1n} to x_{4n} x'_{1n} to x_{4n}	-	functions defined in Appendix IV.
z	-	the radial co-ordinate.
$\{\}$	-	denotes a column matrix.
$\lfloor \rfloor$	-	denotes a row matrix.
$[\ ]$	-	denotes a rectangular matrix.

Note the parameters u, v,w and x, z have been non-dimensionalised w.r.t. the radius of the shell, a.

Thus u = u*/a etc where u* is actual displacement.

$\alpha_1, \beta_1, \alpha_2, \beta_2$	-	roots of the characteristic equations.
α, β	-	indices in equation (6.1)
γ	-	the factor of safety.
Δ	-	denotes increment.
δ	-	denotes first variation on the quantity.
δ^2	-	denotes second variation.
$\epsilon_x, \epsilon_\theta, \epsilon_{x\theta}$	-	the membrane strains in the shell.
ξ, η, ζ	-	virtual displacements in x, θ and z direction.
ϕ_{ij}	-	functions in second variation.
$\Phi_1, \Phi_1', \Phi_2, \Phi_2'$	-	functions given in Appendix III.
Φ, Φ_n	-	function defined in Appendix II.
$\Psi_1, \Psi_1', \Psi_2, \Psi_2'$	-	defined in Appendix III.
$\Psi_K(L)$	-	Lagrangian multiplier in equation (3.16)
λ, λ_{cnit}	-	load parameters.
$\bar{\lambda}$	-	the factor in equation (6.1)
Ω, μ	-	defined in Appendix III.
ν	-	Poisson's ratio.
θ	-	circumferential co-ordinate.
$\sigma_x, \sigma_\theta, \sigma_{x\theta}$	-	the stresses in the shell in the co-ordinate direction.
ρ	-	(a/L), the length ratio.

CHAPTER 1

INTRODUCTION

1.1. General Remarks

The problem of static and stability analysis of shells subjected to non-uniform lateral pressure loads finds extensive application in many branches of Engineering. The collapse of cooling towers at Ferrybridge in 1965 and the collapse of oil storage tanks which were under construction at Haydock in 1967 have generated considerable interest in analysing this problem. The oil storage tanks at Haydock after collapse are shown in Figure 1.1. (The collapse mode of a model cylinder is shown in Fig.1.1a.)

Cooling towers, oil storage tanks, silos used for grain storage are all subjected to the action of wind loads and are a few examples of cylindrical shells under non-uniform lateral pressure. Off shore structures and marine structures under hydrodynamic loading and launch vehicles under ground winds are some further examples which come under this class of problems. All of these structures can be idealised as cylindrical shells with specified boundary conditions at the ends. The external pressure on the shell in general varies both in the axial and circumferential directions. The loads imposed on the external surface of the shell either due to wind or fluid flow are typical examples of the

non-uniform external pressure.

1.2. Review of Literature

Many aspects of static buckling of shells are discussed in the literature[1,2,3], although these references are essentially for the uniform pressure loads. The buckling pressures obtained by using the infinitesimal deformation theory are called the Euler critical loads. The theoretical buckling pressures show a reasonably good agreement with experiments for long shells. However, for the case of short cylinders the agreement is not satisfactory due to the snap-through action. It is observed that the shell can be in a weak equilibrium state at loads which are lower than the Euler critical loads and due to finite disturbances it will jump into a neighbouring equilibrium state, causing a considerable change in the geometry of the shell during the process. The load at which the shell tends to jump to another equilibrium configuration is called the snap-through critical load. The Euler critical load and the snap-through load can be represented on the pressure-deflection diagram as in Fig. 1.2.

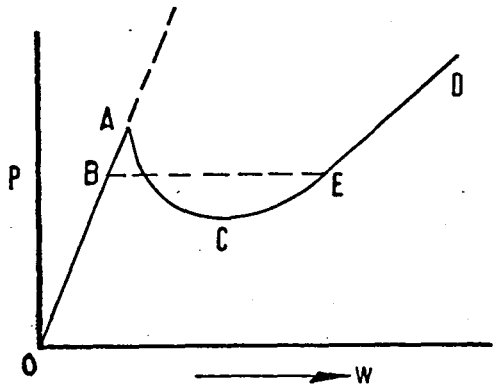

Fig- 1.2 Pressure-deflection Diagram

OA is the primary equilibrium path and the load at point A is the Euler critical load. AC is the unstable secondary equilibrium path. CD is the stable secondary equilibrium path. At the point B the shell may jump from state B to state E and the load at B is the snap-through load. The determination of complete pressure-deflection diagram is very involved and in the literature only Euler critical loads are generally reported. In the literature very few works are reported on the stability analysis of cylindrical shells under non-uniform loads. The work due to Almroth[4] seems to be the first one in which a general theory and its application for stability analysis for a simple non-uniform pressure is presented. All other published literature related to this aspect is concerned mainly with the stability analysis of shells under wind loads. However the wind loading is only an example of the general non-uniform loading on the shell varying both axially and circumferentially. Hence the stability analysis developed for this particular problem can be very easily adapted to the general non-uniform load by suitably altering the load parameters. Different approaches have been employed for this particular problem. Rish[5] has conducted experiments in the wind tunnel on shells made out of paper to obtain the buckling pressures and has compared these results with theoretical results obtained by a simple strain energy consideration.

Langhaar and Miller[6] have given a theoretical solution for estimation of buckling pressures based on the differential geometry of surfaces in which considerable simplifications are made to obtain the numerical results.

Realising the difficulties of the theoretical investigation, Holownia[7] has conducted a series of experiments on the closed ended shells. Based on these experiments empirical results have been developed for quick calculation of the buckling pressures which are convenient for design purposes.

Experimental investigation on the hyperbolic cooling tower models is reported by Der and Fidler[8] in which the effects of imperfections are studied.

After observing that the deformations in the shell are large even prior to buckling, Brave-Boy[9] attempted to analyse the problem by a large deflection analysis ab initio, starting with the non-linear differential equations and employing a Galerkin type of approximation to solve them.

Alnajafi[10] has also attempted a similar analysis by the finite element technique using a load increment and iteration procedure. These methods in Ref. (9) and (10) have not apparently yielded useful results.

Ewing[11] has used a simple Rayleigh type of method for determining the buckling loads.

Billington and Wang[12] have re-investigated the problem by utilising the theory given by Langhaar and Miller[6]

and have pointed out certain discrepancies noted in the Ref. (6)

Chian and Firmin[13] have used the finite element method to carry out a large deflection analysis of cooling towers under wind load. The buckling loads are obtained in this method by noting the deflection in each harmonic; and if at any load level, the deflection in one particular harmonic tends to be large that is considered to be critical load.

1.3. Scope of Present Work

In the present investigation the cylindrical shells are considered to be homogenous and isotropic. As the stability of such shells under lateral pressure loading is not considered to be imperfection sensitive, the material and geometric imperfections in the shell are ignored. The thickness variation in the axial direction as well as the variation of the pressure load both in circumferential and axial directionsare considered in the analysis.

The aims of the present work are:

a) To estimate the stresses in the circular cylindrical shells based on continuum and finite element methods. In the continuum analysis linear thin shell theories Viz. semi-membrane, Donnell and Flugge theories are employed. Relative merits of these theories are studied. A higher order cylindrical shell element is developed to estimate the stresses by the Finite Element method.

b) To develop a satisfactory theoretical method based on energy considerations by both the continuum and Finite Element methods to determine the critical buckling pressures under the action of non-uniform loads, such as due to wind, for various edge boundary conditions of the shell. The second variation of the total potential energy forms the basis for the criterion for the estimation of critical loads. The Finite Element method is employed to analyse variable thickness shells, and ring stiffened shells.

c) To determine the buckling pressures experimentally by testing model cylindrical shells in the wind tunnel and to compare theoretical and experimental results.

d) To examine the current codes of practice for the design of wind loaded structures and indicate their validity in the light of the present investigation.

e) It should be emphasised that the principal assumption made in (a) and (b) relates to the linearity of the pre-buckle deflection behaviour followed by a bifurcation buckling analysis.

CHAPTER 2.

STATIC ANALYSIS - CONTINUUM THEORY

2.1 Introduction

Stress analyses of cylindrical shells have been carried out by many research workers using different shell theories in Ref. (14) to (32).

Martin et al have presented a series of papers[14 to 16] on stress analyses of cooling towers. Membrane theory is used in Refs. (14) and (15) where as in Ref. (16) a more general theory is employed. Because of the simplicity of the membrane theory this has been applied for cylindrical shells under wind loads in Ref. (21). Due to the limitations of the membrane theory other approximate versions of the general shell theory have also been developed in the literature; these approximate theories have the advantage of simple explicit forms of solution that are convenient in the preliminary design stage. In fact even the elementary beam theory is sometimes used for this purpose.

Vlasov's[17] semi-membrane theory is well known in the above class of approximate theories. Krajicinovic[18] and Rish[19] have used Vlasov's theory for analysis of cantilever cylindrical shells under wind load.

Wang and Billington[20] have presented a slightly different version of the semi-membrane theory.

Among the general theories of shells, Donnell's[22] theory has been extensively used.

In Refs. (23)&(25) the different shell theories including that of Donnell have been compared with one another on the basis of the roots of the characteristic equation.

The accuracy of the Donnell's theory has been studied by Hoff[26] Kempner[27] and Moe[23].

Hoff[26] has calculated the error in the characteristic roots of Donnell's equations as compared with the roots given by Flugge's equations.

Kempner[27] has reduced Flugge's shell equations to a form analogous to Donnell's equations and has shown the error to be small except for thick cylindrical shells under loads represented by lower harmonics.

The analysis given by Hoff[28] using the Donnell's equations seems to be very convenient for the problem of wind loaded shells, and therefore the accuracy of the Donnell's equations as applied to this problem will be studied in detail.

The Flugge's shell theory[29] is considered to be accurate and this theory will be used for comparison purpose in the present analysis. In recent years there have been further improvements in the first order linear thin shell theories such as due to Morley[30], Koiter[31] and Sanders[32]. However these will not be considered in the present investigation.

In this Chapter the equilibrium stress analysis of the shells under the action of external pressure loads by the semi-membrane, Donnell and Flugge theories is presented.

The validity of the semi-membrane theory is studied as applied to these problems. The shell is considered to be thin, isotropic and homogenous. The loading considered on the shells is only an external pressure acting on the curved surface, typical of that due to wind.

2.2. Representation of Lateral Pressure Loads

The representation of pressure distribution around a two dimensional circular cylindrical shell due to an external potential flow is quite simple analytically. However, the pressure distribution is modified by vortex shedding and by the presence of real fluid (viscous) effects. It is also very much dependent on height to diam. ratio of the shell (i.e. three dimensional effects), approach velocity profile as a function of the height, natural turbulence in the free stream, Reynold's number, etc. As it is not possible to consider all these effects analytically, the pressure distribution has to be determined only by experiments. Such experimental data are reported by Roshko[33], Gould[34] Cowdrey and O'Neil[35] and Purdy[36] and coworkers. The data given by Roshko and Gould is for long cylinders at high Reynolds numbers whereas the data given by Purdy is for short closed ended shells. Cowdrey and O'Neil have given the data for cooling towers of hyperbolic shape.

In general the pressure distribution will vary both in the axial and circumferential directions. The experimentally

measured pressure distribution can be represented by an equation of the form

$$P = P_o \sum_{m=0}^{m_1} \sum_{n=0}^{n_1} b_{mn} x^m \cos n\theta \qquad (2.1)$$

where the variation in the axial direction is represented by polynomials and the variation in the circumferential direction is represented by the Fourier series.

The data from Ref.(37) for the closed ended cylindrical shells tested in water tunnels has been reduced to the double series form as given by Eqn.(2.1) in the present analysis. The least square method is used to evaluate the arbitrary constants, b_{mn}, in the double series. The pressure represented in this form differs from the experimentally measured pressure distribution by a maximum of 5%. The least square method of evaluating the constants is given in Appendix 1.

In many cases the variation in the axial direction is very insignificant. As a consequence, the static and stability analyses can be slightly simplified if the axial variation of pressure is completely neglected. Making such a simplification, the data given in Ref. (33-35) has been represented by Rish[19] as

$$P = P_o \sum_{n=0}^{6} b_n \cos n\theta \qquad (2.2)$$

The values of the constants b_n obtained by Rish are

$b_0 = -0.387$ $b_1 = 0.338$ $b_2 = 0.533$ $b_3 = 0.471$

$b_4 = 0.166 \quad b_5 = 0.066 \quad b_6 = 0.055$

The values of the coefficients for harmonics above six are very small and hence they are neglected.

When the cylinder is open ended it is also noted that the internal surface of the cylinder is under the action of a uniform suction load of magnitude 0.607 Po. When this effect is taken into account the value of the first coefficient b_o changes to 0.22.

The pressure data either in the form of Eqn.(2.1) or Eqn.(2.2) are used in the appropriate analyses presented in the subsequent sections of this chapter.

2.3. Basic Equations

The geometry of the shell and the coordinate axes with the corresponding displacements of the shell are shown in Fig. 2.1. The shell is considered to be thin, isotropic and homogenous. For static stress analysis purpose the deflections are considered to be small in comparison with thickness, and only first order linear thin shell theories will be used.

Assuming that the material of the shell obeys Hooke's law, the stress-strain relations can be written as:

$$\sigma_x = \frac{E}{1-\nu^2}(\epsilon_x + \nu\epsilon_\theta)$$

$$\sigma_\theta = \frac{E}{1-\nu^2}(\epsilon_\theta + \nu\epsilon_x) \qquad (2.3)$$

$$\sigma_{x\theta} = \frac{E}{2(1+\nu)}\epsilon_{x\theta}$$

The stress resultants and the moment resultants acting on a differential shell element are shown in Fig. 2.2. Considering the equilibrium of the forces and moments acting on the element in the three coordinate directions, one arrives at the equations of equilibrium: (Ref. 29).

$$\frac{\partial N_x}{\partial x} + \frac{\partial N_{x\theta}}{\partial \theta} + a\, p_x = 0$$

$$\frac{\partial N_{\theta x}}{\partial x} + \frac{\partial N_\theta}{\partial \theta} - Q_\theta + a\, p_\theta = 0$$

$$\frac{\partial Q_x}{\partial x} + \frac{\partial Q_\theta}{\partial \theta} + N_\theta + a\, p_z = 0 \qquad (2.4)$$

$$\frac{\partial M_x}{\partial x} + \frac{\partial M_{x\theta}}{\partial \theta} - a\, Q_x = 0$$

$$\frac{\partial M_\theta}{\partial \theta} + \frac{\partial M_{\theta x}}{\partial x} - a\, Q_\theta = 0$$

$$a\, N_{x\theta} - a\, N_{\theta x} + M_{\theta x} = 0$$

These equations are to be solved in conjunction with the strain-displacement relations and stress-strain relations, to determine the state of stress in the shell. However, by making certain assumptions regarding the state of stress or strain the solution of these equations can be simplified.

2.4. Semi-membrane Theory

The additional assumptions made in semi-membrane analysis are:

1. The bending moments M_x and $M_{x\theta}$ are small compared with M_θ except for a small region near the fixed edges of the shell. Hence these moments are neglected.
2. The circumferential strain and the shear strain are neglected in comparison with axial strain.
   Hence $\epsilon_\theta = \epsilon_{x\theta} = 0$

By the first assumption, and by assuming that $N_{x\theta} = N_{\theta x}$ and $M_{x\theta} = M_{\theta x}$, the equations of equilibrium can be reduced to:

$$\frac{\partial N_x}{\partial x} + \frac{\partial N_{x\theta}}{\partial \theta} + a P_x = 0$$

$$\frac{\partial N_\theta}{\partial \theta} + \frac{\partial N_{\theta x}}{\partial x} - \frac{1}{a}\frac{\partial M_\theta}{\partial \theta} + a P_\theta = 0 \qquad (2.5)$$

$$\frac{1}{a}\frac{\partial^2 M_\theta}{\partial \theta^2} + N_\theta + a P_z = 0$$

Eliminating N_θ and $N_{x\theta}$ from the above set, one gets:

$$\frac{\partial^2 N_x}{\partial x^2} + \frac{1}{a}\frac{\partial^4 M_\theta}{\partial \theta^4} + \frac{1}{a}\frac{\partial^2 M_\theta}{\partial \theta^2} + \bar{P} = 0 \qquad (2.6)$$

where $$\bar{P} = a\left[\frac{\partial P_x}{\partial x} - \frac{\partial P_\theta}{\partial \theta} + \frac{\partial^2 P_z}{\partial \theta^2}\right]$$

The strain-displacement relations considered are:

$$\epsilon_x = \frac{\partial u}{\partial x} \qquad \epsilon_\theta = \frac{\partial v}{\partial \theta} - w \qquad (2.7)$$

$$\epsilon_{x\theta} = \frac{\partial u}{\partial \theta} + \frac{\partial v}{\partial x} \qquad K_\theta = \frac{1}{a}\frac{\partial}{\partial \theta}\left(v + \frac{\partial w}{\partial \theta}\right)$$

Because of the second assumption, one obtains

$$\epsilon_\theta = \frac{\partial v}{\partial \theta} - w = 0 \qquad i.e \quad w = \frac{\partial v}{\partial \theta} \tag{2.8}$$

To satisfy the condition $\epsilon_{x\theta} = 0$, the displacements u and v are selected as

$$u = -\frac{\partial \phi}{\partial x} \quad and \quad v = \frac{\partial \phi}{\partial \theta} \tag{2.9}$$

where ϕ is an arbitrary function.

The remaining stress resultants can be expressed in terms of the function ϕ as

$$N_x = -\frac{Eh}{1-\nu^2}\frac{\partial^2 \phi}{\partial x^2}$$

$$M_\theta = -\frac{Eh^3}{12(1-\nu^2)} K_\theta = \frac{-Eh^3}{12(1-\nu^2)}\frac{1}{a}\frac{\partial^2}{\partial \theta^2}\left(\phi + \frac{\partial^2 \phi}{\partial \theta^2}\right) \tag{2.10}$$

substituting the expressions in Eqn.(2.10) into Eqn.(2.6) the governing differential equation reduces to:

$$\frac{\partial^4 \phi}{\partial x^4} + \frac{h^2}{12a^2}\frac{\partial^4}{\partial \theta^4}\left(1 + \frac{\partial^2}{\partial \theta^2}\right)^2 \phi = -\frac{(1-\nu^2)}{Eh}\bar{p} \tag{2.11}$$

The solution of this equation for the case of a shell under non-uniform load is given in Appendix II.

2.5. Donnell's Shell Theory

Donnell's shell theory given in Ref. (22) has been extensively applied for analysis of cylindrical shells. In this theory the shell is considered to be shallow and as a result the strain pattern in the shell is considered to be analagous to that of thin plate. It is also assumed that $M_{x\theta} = M_{\theta x}$ and $N_{x\theta} = N_{\theta x}$.

The mid-surface (Neutral) strains and curvatures are related to the displacements of the mid-surface as:

$$\epsilon_x = \frac{\partial u}{\partial x} \qquad K_x = \frac{1}{a}\frac{\partial^2 w}{\partial x^2}$$

$$\epsilon_\theta = \frac{\partial v}{\partial \theta} - w \qquad K_\theta = \frac{1}{a}\frac{\partial^2 w}{\partial \theta^2} \tag{2.12}$$

$$\epsilon_{x\theta} = \frac{\partial u}{\partial \theta} + \frac{\partial v}{\partial x} \qquad K_{x\theta} = \frac{1}{a}\frac{\partial^2 w}{\partial x\, \partial \theta}$$

The stress resultants and moment resultants at any point in the shell are given as:

$$N_x = \frac{Eh}{1-\nu^2}(\epsilon_x + \nu\epsilon_\theta) \qquad M_x = \frac{Eh^3}{12(1-\nu^2)}(K_x + \nu K_\theta)$$

$$N_\theta = \frac{Eh}{1-\nu^2}(\epsilon_\theta + \nu\epsilon_x) \qquad M_\theta = \frac{Eh^3}{12(1-\nu^2)}(K_\theta + \nu K_x)$$

$$N_{x\theta} = \frac{Eh}{2(1+\nu)}\epsilon_{x\theta} \quad \text{and} \quad M_{x\theta} = \frac{Eh^3}{12(1-\nu^2)}K_{x\theta} \tag{2.13}$$

In the equations of equilibrium (2.4b), neglecting Q_θ term and the last equation of equilibrium, the remaining equations can be reduced to:

$$\frac{\partial N_x}{\partial x} + \frac{\partial N_{x\theta}}{\partial \theta} + a\, p_x = 0$$

$$\frac{\partial N_{\theta x}}{\partial x} + \frac{\partial N_\theta}{\partial \theta} + a\, p_\theta = 0$$

$$\frac{\partial^2 M_x}{\partial x^2} + \frac{\partial^2 M_\theta}{\partial \theta^2} + 2\frac{\partial^2 M_{x\theta}}{\partial x\, \partial \theta} + a N_\theta + a^2 p_z = 0 \qquad \text{— (2.14)}$$

Substituting for the stress resultants from Eqns. (2.13) and (2.12), one has the equations of equilibrium in terms of the displacements as:

$$\frac{\partial^2 u}{\partial x^2} + \frac{(1-\nu)}{2}\frac{\partial^2 u}{\partial \theta^2} + \frac{(1+\nu)}{2}\frac{\partial^2 v}{\partial x\, \partial \theta} - \nu w + \frac{a\, p_x}{D} = 0$$

$$\left(\frac{1+\nu}{2}\right)\frac{\partial^2 u}{\partial x\, \partial \theta} + \frac{\partial^2 v}{\partial \theta^2} + \left(\frac{1-\nu}{2}\right)\frac{\partial^2 v}{\partial x^2} - \frac{\partial w}{\partial \theta} + \frac{a\, p_\theta}{D} = 0 \qquad \text{—(2.15)}$$

$$\nu \frac{\partial u}{\partial x} + \frac{\partial v}{\partial \theta} - w - \frac{h^2}{12a^2}\nabla^4 w + \frac{a\, p_z}{D} = 0$$

where $D = \dfrac{Eh}{1-\nu^2}$ and $\nabla^4 = \left(\dfrac{\partial^2}{\partial x^2} + \dfrac{\partial^2}{\partial \theta^2}\right)^2$

The general solution of these equations for any set of boundary conditions and external loading is given in Appendix III, and applied in Refs. (38) and (39)

2.6. Flugge's Shell Theory

The Flugge shell theory for the analysis of circular cylindrical shells, given in Ref. (29), is considered to be accurate. No simplifications of the equations of equilibrium of Eqn.(2.4) are made. Starting from the basic assumptions, as in the engineers theory of bending the stress and moment resultants are obtained in terms of the displacements as:

$$N_x = D\left[\frac{\partial u}{\partial x} + \nu\left(\frac{\partial v}{\partial \theta} - w\right)\right] + \frac{k}{a}\frac{\partial^2 w}{\partial x^2}$$

$$N_\theta = D\left[\frac{\partial v}{\partial \theta} - w + \nu\frac{\partial u}{\partial x}\right] - \frac{k}{a}\left(w + \frac{\partial^2 w}{\partial \theta^2}\right)$$

$$N_{\theta x} = \frac{D(1-\nu)}{2}\left(\frac{\partial u}{\partial \theta} + \frac{\partial v}{\partial x}\right) + \frac{k(1-\nu)}{2a}\left(\frac{\partial u}{\partial \theta} - \frac{\partial^2 w}{\partial x \partial \theta}\right)$$

$$N_{x\theta} = \frac{D(1-\nu)}{2}\left(\frac{\partial u}{\partial \theta} + \frac{\partial v}{\partial x}\right) + \frac{k(1-\nu)}{2a}\left(\frac{\partial v}{\partial x} - \frac{\partial^2 w}{\partial x \partial \theta}\right)$$

$$M_x = \frac{k}{a}\left(\frac{\partial^2 w}{\partial x^2} + \nu\frac{\partial^2 w}{\partial \theta^2} - \frac{\partial u}{\partial x} - \nu\frac{\partial v}{\partial \theta}\right)$$

$$M_\theta = \frac{k}{a}\left(w + \frac{\partial^2 w}{\partial \theta^2} + \nu\frac{\partial^2 w}{\partial x^2}\right) \qquad \text{— (2.16)}$$

$$M_{x\theta} = \frac{k}{a}(1-\nu)\left(\frac{\partial^2 w}{\partial x \partial \theta} - \frac{\partial v}{\partial x}\right)$$

$$M_{\theta x} = \frac{k}{a}(1-\nu)\left[\frac{\partial^2 w}{\partial x \partial \theta} + \frac{1}{2}\left(\frac{\partial u}{\partial \theta} - \frac{\partial v}{\partial x}\right)\right]$$

where $k = \dfrac{E h^3}{12(1-\nu^2)}$

Substituting these in the equations of equilibrium (2.4) one obtains the governing equations of the shell as:

$$\frac{\partial^2 u}{\partial x^2} + \frac{1-\nu}{2}\frac{\partial^2 u}{\partial \theta^2} + \frac{1+\nu}{2}\frac{\partial^2 v}{\partial x \partial \theta} - \nu\frac{\partial w}{\partial x} + \frac{h^2}{12a^2}\left[\frac{1-\nu}{2}\frac{\partial^2 u}{\partial \theta^2} + \frac{\partial^3 w}{\partial x^3} + \frac{1-\nu}{2}\frac{\partial^3 w}{\partial x \partial \theta^2}\right] + \frac{p_x a}{D} = 0$$

$$\frac{(1+\nu)}{2}\frac{\partial^2 u}{\partial x \partial \theta} + \frac{\partial^2 v}{\partial \theta^2} + \frac{1-\nu}{2}\frac{\partial^2 v}{\partial x^2} - \frac{\partial w}{\partial \theta} + \frac{h^2}{12a^2}\left[\frac{3(1-\nu)}{2}\frac{\partial^2 v}{\partial x^2} + \frac{3-\nu}{2}\frac{\partial^3 w}{\partial x \partial \theta^2}\right] + \frac{p_\theta a}{D} = 0$$

$$\nu\frac{\partial u}{\partial x} + \frac{\partial v}{\partial \theta} - w + \frac{h^2}{12a^2}\left[\frac{1-\nu}{2}\frac{\partial^3 u}{\partial x \partial \theta^2} - \frac{\partial^3 u}{\partial x^3} + \frac{3-\nu}{2}\frac{\partial^3 v}{\partial x^2 \partial \theta} + \nabla^4 w + 2\frac{\partial^2 w}{\partial \theta^2} + w\right] + \frac{p_z a}{D} = 0 \qquad \text{— (2.17)}$$

The solution of these equations for the case of cylindrical shells under non-uniform load is developed in Appendix IV.

2.7. Results and Discussions

The different shell theories discussed here have been applied to the following problems.

a) To analyse the cantilever cylindrical shell under wind load assumed by Krajicinovic[18].

b) To calculate the characteristic roots of Flugge's shell theory for different shell geometries.

c) To compare the shell theories due to Flugge and Donnell for different shell geometries and end conditions.

d) To calculate the displacements and stresses due to each of the harmonics for two typical shell geometries.

e) To represent the complete displacement, stress and moment distribution for a typical shell.

Krajicinovic has applied the semi-membrane theory for wind load of the form:

$$p_z = p_{z1} + p_{z2}$$

where $p_{z1} = P \cos 2\theta \qquad -\frac{\pi}{4} \leq \theta \leq \pi/4$

$= 0 \qquad$ elsewhere

$$p_{z2} = \frac{p}{2} \cos 2\theta \qquad 0 \leq \theta \leq 2\pi$$

The results given by Krajicinovic are incorrect as indicated in Appendix II. The correct solution for the problem are also presented in this appendix. This problem is analysed by both Donnell's and Flugge's theories also. The maximum stresses at the root of the windward and leeward generators are calculated and are plotted in Fig. 2.3 and 2.4 for various shell geometries. The circumferential variation of the axial stress at the root for two typical shell geometries is plotted in Fig. 2.5. in which the solution by the beam theory is also given. These results show that the beam theory is inadequate in preliminary estimation of stresses and also it misrepresents the state of stress at the leeward generator. From the results presented in Fig. 2.3 and 2.4, it can also be concluded that the semi-membrane

theory over estimates the axial stresses for all shell geometries. The error in the semi-membrane theory is large for short thin shells but the error is small for long thick shells. The design based on the semi-membrane theory is considered to be conservative. The accuracy of the Donnell shell theory for determining stresses in shells is examined next. The characteristic roots of the Donnell equations for various shell thicknesses and harmonics are given by Hoff[28]. The corresponding roots by Flugge's theory are given in Fig. 2.6. and Fig. 2.7. From these and Ref. 28, it may be seen, for $n \geq 2$ the characteristic roots of Donnell's theory differ from those of Flugge's theory by a maximum of 5% for shells of thickness ratio considered here ($100 \leq a/h \leq 500$). Next the stresses are calculated by both the theories under the action of idealised harmonic loading as well as wind loading, of Section 2.1, for various shell geometries and end conditions. The geometries of shells considered are $1 \leq L/a \leq 5$ and $100 \leq \frac{a}{h} \leq 500$. Various combinations of end conditions such as clamped-free, clamped-s.s., etc. have been considered. A few typical results obtained for different harmonic loadings such as maximum deflections, maximum stresses and maximum moments are given in Tables 2.1 to 2.3. As the Donnell theory is suspected to give results with large error for the lower harmonics, only the results obtained for harmonics 1 and 2 are presented in these tables. The stresses given by Donnell's theory differ

by a maximum of 1% as compared with Flugge's theory. For higher harmonics the difference is still smaller. The distribution of deflections, stresses and moments for a typical cantilever shell ($L/a = 1$, $a/h = 100$) along three generators and along five meridian circles are plotted in Fig. 2.8. - 2.13. under the action of the wind loads given by Eqn.(2.2.). From these figures it can be seen that the root of the windward generator is under maximum stress and the stress at the leeward generator is quite small.

The analysis for any other type of loading on the shell can be easily performed by suitably summing the stresses and deflections for each harmonic provided the solution for each harmonic is already known. As an example for two typical shell geometries, the maximum radial displacement and the maximum stresses are calculated. The variation of these quantities in the axial direction for each of the harmonics is given in Figs. 2.14. - 2.19. Clearly since these have been obtained from a linear elastic analysis, they may be quite simply added in proportion to the Fourier harmonic in loading, provided that the stresses caused by combined loading are still in the linear elastic range.

CHAPTER 3

STABILITY ANALYSIS - CONTINUUM THEORY

3.1. Introduction

The stability analysis of circular cylindrical shells subjected to uniform external pressure has been extensively studied in the literature[2,29,40,41,42,43]. Most of the problems considered are for the case of simply supported shells, the types of loading considered being hydrostatic pressure or a band load. The problem of stability of shells subjected to non-uniform load is much more involved than that of the uniform pressure because of the coupling between harmonics in the assumed mode caused by the non-linear terms. The first paper presenting an appropriate energy theory for shells under circumferentially varying pressure is apparently due to Almroth[4], who has considered a pressure loading of the form $P = P_0 (b_0 + b_1 \cos \theta)$ on simply supported shells.

Maderspach[44] and co-workers have followed Almroth's approach for their investigation on simply supported shells subjected to wind loading given in Ref(36). Bushnell[45] has developed a computer code called BOSOR4 that can be applied for buckling analysis of axisymmetric structures. Recently his work has been extended to non-uniform lateral pressures by Sheinmann and Tene[46]. Ewing[11] has used a simplified energy theory for the estimation of buckling loads of the cooling towers.

Langhaar and Miller[6] have used a semi-membrane theory for the problem of cylindrical shells under wind loads. Their analysis is extended further by Wang and Billington[12] as the original analysis has given inconsistent results. Brave-Boy and Johns[9] have attempted to integrate the non-linear large deflection equations of equilibrium by the Galarkin method. In Ref(47) the analysis of cantilever cylindrical shells under wind load is presented.

In the present chapter the stability analysis of cylindrical shells under the action of non-uniform loads, such as due to wind, by the energy theory is presented. The infinitesimal energy theory of buckling, that gives the 'Euler buckling loads' as defined by Langhaar[3] is employed. Complete non-linear analysis and snap through actions are not considered. Dynamic effects and shell imperfections are ignored. The shell is considered to be uniform, isotropic and homogeneous. The prebuckling deformations are considered to be small and as a result the change in the shape of shell due to these deformations is neglected. As the shell under the action of lateral pressure is not imperfection sensitive, the classical buckling theory is considered to be adequate. Only static instability due to a known non-uniform pressure is investigated in the present analysis. The convergence of the buckling pressures with the number of terms in virtual displacements is studied. Numerical results for buckling pressures of cantilever cylindrical shells under wind load for

various shell geometries are presented. The influence of constraint and relaxation of edge conditions and the influence of form of pressure distribution on the buckling loads is examined.

3.2. Second Variation Principle

The buckling analysis is based on the energy theory given in Ref (3). The advantages of this theory as compared with other theories of buckling are discussed by Langhaar and Boresi[2]. The theory is based on the principle that for a conservative mechanical system to be in stable equilibrium, the total potential energy should be a minimum. For any elastic system one can write the potential energy as:

$$V = U - W \qquad (3.1.)$$

where

U - strain energy stored in the system

W - work done by the external loads

To study the nature of potential energy in any equilibrium state, variational calculus is employed. Change in potential energy during a small load increment or due to a virtual displacement state around the equilibrium position is:

$$\Delta V = \Delta U - \Delta W \qquad (3.2.)$$

The increments in strain energy and work done can be written as: (Ref 3)

$$\Delta U = \delta U + \frac{1}{2!}\delta^2 U + \frac{1}{3!}\delta^3 U + \cdots$$

$$\Delta W = \delta W + \frac{1}{2!}\delta^2 W + \frac{1}{3!}\delta^3 W + \cdots \qquad - (3.3)$$

where $\delta^n U$ and $\delta^n W$ are nth variation of U and W respectively. Hence the change in potential energy can be written as:

$$\Delta V = (\delta U - \delta W) + \frac{1}{2!}(\delta^2 U - \delta^2 W) + \frac{1}{3!}(\delta^3 U - \delta^3 W) + \cdots$$

$$= \delta V + \frac{1}{2!}\delta^2 V + \frac{1}{3!}\delta^3 V + \cdots \qquad (3.4.)$$

From the principle of virtual work, for an elastic system to be in equilibrium, the first variation of potential energy should be equal to zero.

i.e.

$$\delta V = \delta U - \delta W = 0 \qquad (3.5.)$$

Thus the nature of ΔV in an equilibrium position is determined by $\delta^2 V \; (= \delta^2 U - \delta^2 W)$. If ΔV is to be a relative minimum one gets that

$$\delta^2 V > 0 \qquad (3.6.)$$

When the condition (3.6.) is satisfied one can conclude that the equilibrium state is stable. The equilibrium will not be stable if $\delta^2 V$ becomes negative for any of the possible virtual displacement states.

Hence the criterion used for determining the buckling loads is that the sign of the second variation of the total potential energy changes from positive definite character to an indefinite character at the critical loads.

3.3. Potential Energy - Second Variation

The potential energy of the cylindrical shell can be written as: (Ref 4)

$$V = U_m + U_b - W \qquad (3.7a.)$$

where

U_m = membrane strain energy of the shell

$$= \frac{E a^2 h}{2(1-\nu^2)} \int_0^{4/a} \int_0^{2\pi} \left[\epsilon_x^2 + \epsilon_\theta^2 + 2\nu \epsilon_x \epsilon_\theta + \frac{1-\nu}{2} \epsilon_{x\theta}^2 \right] dx\, d\theta$$

U_b = bending strain energy of shell

$$= \frac{E h^3}{24(1-\nu^2)} \int_0^{4/a} \int_0^{2\pi} \left[K_{xx}^2 + K_{\theta\theta}^2 + 2\nu K_{xx} K_{\theta\theta} + 2(1-\nu) K_{x\theta}^2 \right] dx\, d\theta \quad \text{— (3.7b.)}$$

and

W = the work done by the external loads

$$= \frac{a^3}{2} \int_0^{4/a} \int_0^{2\pi} P \left[w - \frac{1}{2} \left\{ w^2 + 2v \frac{\partial w}{\partial \theta} + v^2 - w \frac{\partial u}{\partial x} + u \frac{\partial w}{\partial x} \right\} \right] dx\, d\theta$$

In the buckling analysis recognising the importance of the non-linear terms in the strain displacement relations, which represent the rotation component of the strain, these are selected as: (Ref 4)

$$\bar{\epsilon}_x = \bar{u}_{,x} + \frac{1}{2} \bar{w}_{,x}^2$$

$$\bar{\epsilon}_\theta = (\bar{v}_{,\theta} - \bar{w}) + \frac{1}{2} (\bar{v} + \bar{w}_{,\theta})^2$$

$$\bar{\epsilon}_{x\theta} = (\bar{u}_{,\theta} + \bar{v}_{,x}) + \bar{w}_{,x} (\bar{v} + \bar{w}_{,\theta}) \quad \text{(3.8a.)}$$

where the bars are used over the quantities to indicate that these are the total quantities consisting of both the equilibrium state and the virtual displacement state. The suffixes for the displacements indicate differentiation. The expressions for curvatures are identical to those used in linear analysis.

i.e. $\bar{K}_{xx} = \bar{w}_{,xx}$

$$\bar{K}_{\theta\theta} = \bar{\omega} + \bar{\omega}_{,\theta\theta}$$

$$\bar{K}_{x\theta} = \bar{\omega}_{,x\theta} \qquad (3.8b.)$$

The components of the displacements in the equilibrium state be denoted by u, v and ω. The corresponding components of displacements in the virtual displacements be ξ, η and ζ. The total displacements can be written as:

$$\begin{aligned} \bar{u} &= u + \xi \\ \bar{v} &= v + \eta \\ \bar{w} &= w + \zeta \end{aligned} \qquad (3.9.)$$

Substituting these displacement components in equation (3.8) one gets:

$$\begin{aligned} \bar{\epsilon}_x &= u_{,x} + \xi_{,x} + \tfrac{1}{2}\zeta_{,x}^2 \\ \bar{\epsilon}_\theta &= (v_{,\theta} - w) + (\eta_{,\theta} - \zeta) + \tfrac{1}{2}(\eta + \zeta_{,\theta})^2 \\ \bar{\epsilon}_{x\theta} &= (u_{,\theta} + v_{,x}) + (\xi_{,\theta} + \eta_{,x}) + \zeta_{,x}(\eta + \zeta_{,\theta}) \\ \bar{K}_{xx} &= w_{,xx} + \zeta_{,xx} \\ \bar{K}_{\theta\theta} &= w + w_{,\theta\theta} + \zeta + \zeta_{,\theta\theta} \\ \bar{K}_{x\theta} &= w_{,x\theta} + \zeta_{,x\theta} \end{aligned} \qquad (3.10.)$$

In these expressions the prebuckling rotations have been neglected as they are small except possibly at the free edges. Substituting (3.10.) in (3.7.) and calculating the second variation, one obtains:

$$\delta^2 V = \frac{E a^2 h}{2(1-\nu^2)} \int_0^{L/a} \int_0^{2\pi} \Big\{ \xi_{,x}^2 + (\eta_{,\theta} - \zeta)^2 + 2\nu \xi_{,x}(\eta_{,\theta} - \zeta) + \frac{1-\nu}{2}(\xi_{,\theta} + \eta_{,x})^2 + \frac{1}{12}\frac{h^2}{a^2}\Big[\zeta_{,xx}^2 + (\zeta + \zeta_{,\theta\theta})^2 + 2\nu(\zeta + \zeta_{,\theta\theta})\zeta_{,xx} + 2(1-\nu)\zeta_{,x\theta}^2 \Big] + \underline{u_{,x}}\Big[\zeta_{,x}^2 + \nu(\eta + \zeta_{,\theta})^2 \Big] + \underline{(v_{,\theta} - w\theta)}\Big[(\eta + \zeta_{,\theta})^2 + \nu \zeta_{,x}^2 \Big] + \underline{(u_{,\theta} + v_{,x})}(1-\nu)\zeta_{,x}(\eta + \zeta_{,\theta}) \Big\} dx\, d\theta + \frac{a^3}{2} \int_0^{L/a} \int_0^{2\pi} P\Big[\zeta^2 + 2\eta\zeta_{,\theta} + \eta^2 - \xi_{,x}\zeta + \zeta_{,x}\xi \Big] dx\, d\theta \qquad -(3.11.)$$

The underlined quantities in the above expression are the prebuckling membrane strains. It can also be seen that the second variation is quadratic in virtual displacements with the load appearing as a parameter.

The critical buckling pressures are calculated from this quadratic expression by forming the Hessian determinant. $\delta^2 V$ is positive definite if the Hessian determinant is positive.

It can be noted that in Eqn.(3.11.) the first part of the integral, which does not contain the prebuckling membrane strains, is identical to the linear strain

energy of the shell and it is always positive. Hence only the second part of the integral containing both the prebuckling strains and the virtual displacements is reponsible for changing the nature of $\delta^2 V$. Thus it is clear that the prebuckling membrane strains are very important in the buckling analysis and therefore are to be determined accurately. (see Section 3.7)

3.4. Virtual Displacements

The virtual displacements chosen should satisfy the geometric constraint on the shell and they should be continuous with continuous first derivatives in the region of the shell. Depending on the boundary conditions at the ends one can choose beam functions or Fourier series. Beam functions can satisfy automatically certain end conditions, but they are mathematically difficult to handle. The selection of polynomials in the axial direction has certain advantages as these can be manipulated to satisfy any geometric constraint at the circular ends. Selection of Fourier harmonics to represent the virtual displacements in the circumferential direction is very well suited. Thus the virtual displacements for the case of cantilever cylindrical shells are represented as:

$$\begin{aligned} \xi &= \sum_{m=1}^{m_1} \sum_{n=n_1}^{n_2} A_{mn}\, x^m \cos n\theta \\ \eta &= \sum_{m=1}^{m_1} \sum_{n=n_1}^{n_2} B_{mn}\, x^m \sin n\theta \\ \zeta &= x \sum_{m=1}^{m_1} \sum_{n=n_1}^{n_2} C_{mn}\, x^m \cos n\theta \end{aligned} \qquad (3.12)$$

These satisfy the requirements that $\xi = \eta = \zeta = \zeta_{,x} = 0$ at $x=0$, representing the fixed edge. At $x=L/a$ the free edge, they are not constrained.

The advantages of polynomials will be evident, if one wants to consider the case of clamped-simply supported shells. Instead of starting from a completely new set of functions, the virtual displacements can be written as:

$$\xi = \sum_{m=1}^{m_1} \sum_{n=n_1}^{n_2} A_{mn}\, x^m \cos n\theta$$

$$\eta = (1-\rho x) \sum_{m=1}^{m_1} \sum_{n=n_1}^{n_2} B_{mn}\, x^m \sin n\theta \qquad \text{—(3.13)}$$

$$\zeta = x(1-\rho x) \sum_{m=1}^{m_1} \sum_{n=n_1}^{n_2} C_{mn}\, x^m \cos n\theta$$

where $\rho = a/L$

These satisfy the end conditions:

$\xi = \eta = \zeta = \zeta_{,x} = 0$ at $x=0$, the fixed edge

and $\eta = \zeta = 0$ at $x = L/a$ the simply supported edge

It can also be seen that by setting $\rho = 0$ in equation (3.13.) the virtual displacements for a cantilever shell are recovered. This serves as a check in the numerical work in the problem. Any other set of boundary conditions on the shell can be taken care of either by suitably defining a new set of virtual displacements or by retaining the virtual displacements in equation (3.12.) and suitably modifying them to satisfy the edge condition.

3.5. Stability Determinant

Substituting the assumed functions for ξ, η and ζ of equation (3.12) in the expression for the second variation equation (3.11.) and carrying out the integration, the resulting expression is found to be a quadratic in the arbitrary coefficients A_{mn}, B_{mn} and C_{mn}. To study the positive definite character of this algebraic quadratic function, it is differentiated with respect to each of the coefficients A_{mn}, B_{mn} and C_{mn} in succession and the resulting equation in each case is set to zero. This results in a system of linear homogenous equations of the form:

$$\sum_m \sum_n \left[(f_{K1} + \lambda \phi_{K1}) A_{mn} + (f_{K2} + \lambda \phi_{K2}) B_{mn} + (f_{K3} + \lambda \phi_{K3}) C_{mn} \right] = 0$$

where $K = 1, 2$ and 3: $\lambda = \frac{P_0}{E}\left(\frac{a}{h}\right)^3$ —(3.14)

The functions f_{cj} and ϕ_{cj} are given in Appendix V. The coefficient matrix of these equations is the stability determinant (Hessian determinant).

The lowest value of λ which makes the stability determinant singular is denoted as λ_{crit} and this corresponds to the lowest buckling pressure of the shell. The value of λ_{crit} is determined in the present analysis by determinant search method. In this method the value of stability determinant is evaluated for successively increasing values of λ until a change in the sign of the stability determinant is noted. Then by the process of iteration, within the last two values of

λ , the value of λ_{crit} is obtained to a desired degree of accuracy.

If the expressions in Eqn.(3.13) are used for the clamped-simply supported shell, the stability determinant will have a few additional terms. These additional terms are given in Appendix VI.

3.6. Effect of Boundary Condition on Buckling Pressures

The boundary conditions at the circular ends of the shell influence to a considerable degree the buckling pressures, especially when the shell is short.

In Ref. 47. the discrepancy between the theoretical and experimental results for buckling of shells subjected to wind loads is attributed to the lack of proper fixed edge conditions. The influence of boundary conditions on the stability of simply supported cylinders under uniform pressure has been discussed by Sobel[48], Gallatly and Bart[49], Singer and Rosen[50] and Heyman[51]. The effects of boundary conditions on the buckling pressures is studied in this section by imposing additional constraints or by relaxing the existing constraints.

The application of the Lagrangian multipliers technique to impose additional constraints is well known. Budiansky and Pai[52] have applied this method to obtain the bounds to the critical stresses of plates. Using this method the critical buckling pressures of cantilever shells fixed at the base (i.e. at $x = 0$) with different tip boundary conditions (i.e. at $x = L/a$) are obtained by

imposing the required additional constraints on the virtual displacements.

As an example let the edge $x = L/a$ be fixed.

The additional constraints to be imposed are:

$$\xi(\bar{L}) = \eta(\bar{L}) = \varphi(\bar{L}) = \varphi_{,x}(\bar{L}) = 0 \qquad (3.15)$$

where $\bar{L} = L/a$

These conditions are to be satisfied by each harmonic in the virtual displacements and hence one has:

$$\xi_n(\bar{L}) = \sum_m A_{mn}\, \bar{L}^m = 0$$

$$\eta_n(\bar{L}) = \sum_m B_{mn}\, \bar{L}^m = 0$$

$$\varphi_n(\bar{L}) = \sum_m C_{mn}\, \bar{L}^{m+1} = 0 \qquad (3.15b.)$$

$$\varphi_{n,x}(\bar{L}) = \sum_m (m+1)\, C_{mn}\, \bar{L}^m = 0$$

This set of $(4 \times n)$ additional equations are incorporated into the buckling determinant by introducing a set of Lagrangian multipliers g_k as follows:

$$\delta^2 \bar{V} = \delta^2 V + g_k \Psi_k(\bar{L}) \qquad (3.16.)$$

where $\delta^2 \bar{V}$ - the second variation with constraints.

g_k - Lagrangian multipliers.

$\Psi_k(\bar{L})$ - the constraint conditions in Eqn.(3.15b.)

To obtain the stability determinant $\delta^2 \bar{V}$ is differentiated not only with respect to the arbitrary coefficient A_{mn} etc. but also with respect to the unknown multipliers g_k.

This in turn increases the size of the stability determinant by ($k = 4 \times n$).

For any other additional constraint at the 'free top' only the appropriate geometric constraints are imposed. For example if the end is simply supported the constraint conditions are $\eta(\bar{L}) = \tau_\theta(\bar{L}) = 0$ and this adds only ($2 \times n$) additional equations. The other additional conditions considered at the top in the analysis are:

Pinned condition – $\xi(\bar{L}) = \eta(\bar{L}) = \tau_\theta(\bar{L}) = 0$

and clamped-sliding condition i.e. $\eta(\bar{L}) = \tau_\theta(\bar{L}) = \tau_{\theta,x}(\bar{L}) = 0$

In all these cases, when using the Lagrangian multipliers in buckling analysis, the prebuckling membrane strains are to be determined with the appropriate boundary conditions taken into account.

3.6.1. Effect of Base Stiffness

As shown in Ref.(47), the buckling pressure will be drastically reduced if the fixed edge conditions are not properly realised during experiments. The influence of axial stiffness and the rotational stiffness at the base of a cantilever cylindrical shell on the buckling pressure are studied theoretically. The shell is considered to be resting on two springs one giving only axial stiffness and the other imparting only rotational stiffness. The boundary conditions corresponding to this representation is chosen, as explained in Appendix III, as:

$$N_x(0) + k_1\, u(0) = 0$$

$$M_x(0) + k_2\, w_{,x}(0) = 0 \qquad (3.17.)$$

By suitably altering the values of the spring constants k_1 and k_2 one can obtain either a clamped edge condition or a simply support edge condition as shown in Appendix III.

When the axial displacement and rotation at the base are not fully prevented, the corresponding virtual displacements ζ_φ, ξ in eqn. (3.12) are modified as

$$\zeta_\varphi = \sum_{m=1}^{m_1} \sum_{n=n_1}^{n_2} C_{mn}\, x^m \cos n\theta$$

$$\xi_\varphi = \sum_{m=0}^{m_1-1} \sum_{n=n_1}^{n_2} A_{mn}\, x^m \cos n\theta \qquad (3.18.)$$

As the spring constants k_1 and k_2 are finite, their contribution to the second variation of potential energy in the form of strain energy of the support springs is to be added. The addition to the second variation is:

$$\frac{a}{2} \int_0^{2\pi} \left[k_1\, \xi^2(0) + k_2\, \zeta_{,x}^2(0) \right] d\theta$$

3.7. Results and Discussions

The buckling analysis presented in this chapter has been applied to the following problems:

a) cantilever cylindrical shell under wind loading.

b) submerged cylindrical shell under flow of water.

Numerical results for cantilever cylindrical shells are presented for the following shell geometries:

$$1 \leq L/a \leq 5 \quad , \quad 100 \leq a/h \leq 500$$

To ascertain the adequacy of the polynomials for the virtual displacements, the analysis is first employed to obtain the critical buckling pressures of cantilever cylindrical shells under uniform radial compression. The results for this problem are given by Billington and Wang[12] using a semi-inextensional theory, and by Cole[53] by a finite element analysis. The number of polynomial terms representing the axial mode in the present analysis is selected as five. For this problem as there is no coupling between the harmonics, only one harmonic is needed in virtual displacements. As a result the buckling determinant is of order (15 x 15). The buckling pressure for each successive harmonic selected is computed and the minimum of these is chosen as the critical buckling pressure. The results obtained are compared with those in Ref.(12) and (53) in Table 3.1. These show that the critical buckling pressures obtained by the present analysis are more accurate as they are lower.

For analysis of shell under non-uniform pressure due to wind, the harmonics selected should correspond to those representing the buckled pattern of the shell. Considering the number of polynomial terms as five, to find the significant harmonics, the buckling pressures are calculated by selecting successive

harmonics, only one at a time in the virtual displacements for various shell geometries. The results obtained, given in Table 3.2., show that the buckling pressures are one order lower for a certain range of harmonics as compared with others. The range containing the significant harmonics, for the shell geometries considered in most cases is about 5. When the number of polynomial terms and the harmonics is five each, the buckling determinant is of the order 75x75. The buckling pressures are computed for different shell geometries with various lower limit of the harmonics. These results are given in Table 3.3. and for a few shell geometries are plotted in Fig. 3.1. and 3.2. The minimum buckling pressures from these tables are considered to be the critical buckling pressures.

To confirm the present method of selection of harmonics, the following three other methods of selecting harmonics have been studied.

a) only five odd harmonics

b) only five even harmonics

c) one set of random combination

The buckling pressures obtained by these methods of combinations are compared with the previous results in Table 3.4.; these indicate that selecting five successive harmonics yields lower buckling pressures. Next a convergence study of the buckling pressures with the number of terms selected is carried out. First to study the convergence with the number of

terms in axial direction, the number of harmonics is considered to be fixed at five in the significant harmonic range. The number of polynomial terms is varied from 2 to 5 in the virtual displacements and the buckling pressures are obtained for a few typical shell geometries. These results are given in Table 3.5.

Next to study the convergence with number of terms in the circumferential direction, the number of polynomial terms is considered to be fixed at five: starting from the lower limit of the significant harmonic range, the number of harmonics selected in the virtual displacements is successively increased up to 5. The buckling pressures are calculated for each case. The results obtained for a few typical shell geometries are given in Table 3.6. and Fig. 3.3. These results confirm that five terms in axial direction and five terms in circumferential direction (i.e. a total of 25 terms for each virtual displacement component) are sufficient to get satisfactory results for buckling pressures. The final critical buckling pressures obtained for the case of cantilever cylindrical shells under wind load are plotted in Fig. 3.4. for various shell geometries.

Using the Lagrangian multiplier method given in Section 3.6., the buckling pressures obtained for a few shell geomet ries with different tip constraints are presented in Tables 3.7. and 3.8. The variation

of buckling pressure versus thickness ratio is plotted for free, s.s. and clamped tip conditions in Fig. 3.5. Comparing the clamped and pinned conditions in Table 3.8., it can be seen that the rotation of the tip has negligible influence on the critical buckling pressures.

The results obtained by relaxing the fixed edge condition at the base, as described in Section 3.6.1. are given in Table 3.9. and Fig. 3.6. The results in Table 3.9. are obtained when only the moment constraint is relaxed. The results in Fig. 3.6. indicate the variation of buckling pressure with the axial stiffness at the base. These results confirm that the rotation at the ends does not significantly influence the buckling pressures whereas the relaxation of the axial stiffness at the base can reduce the buckling pressure considerably. Similar qualitative conclusions have been drawn by Ewing[11].

Next the influence of the pressure distribution on buckling pressure is studied. First the influence of the negative suction peak on the buckling pressure has been considered. The magnitude of the suction peak has been altered arbitrarily and the corresponding buckling pressures obtained. The results obtained are shown in Fig. 3.8. and it can be seen that the buckling pressures are not very sensitive to the magnitude of the suction peak. The pressure distribution measured by Gould[34] is considered next to study this aspect.

These pressure distributions and the corresponding buckling pressures obtained are shown in Fig.3.7. The Fourier pressure coefficients for the three pressure forms are given in Table 3.10. These results indicate that the axisymmetric component of the pressure distribution (i.e. b_o) has more influence on the buckling pressures than the magnitude of the suction peak. To study the influence of the axisymmetric component of the pressure distribution, the magnitude of b_o is varied in steps and the buckling pressure is calculated. These results are presented in Fig. 3.9. The present analysis is also used to obtain the critical buckling pressure for the shell submerged under a flow of water. As these results are used to compare with experimental results, these are given in Chapter 5. During this analysis it is noted that the variation of pressure in the axial direction has very little influence on the buckling pressure. Thus the simplifying assumption that the pressure does not vary in the x direction used in the other examples seems to be justified. Through numerical examples it has also been found that the set of virtual displacements in Eqn.(3.13) even though more appropriate for the clamped-simply supported shell, the buckling pressures obtained by using the set in Eqn.(3.12) with Lagrangian multipliers for this problem, are as accurate as those obtained by using Eqn.(3.13.). Thus we can conclude that the Lagrangian multiplier method can be applied to any type of boundary conditions in the problem.

The influence of prebuckling deformations on the buckling pressure has been discussed in Ref. (54) and (55). In the present analysis, this aspect has been examined numerically. The buckling pressures obtained by neglecting any of the prebuckling membrane strains were unduly large. When semi-membrane theory is used to obtain the prebuckling strains, the buckling pressures obtained are at least 10 times higher than the values obtained by the present analysis.

A satisfactory method of estimating the buckling pressures of cylindrical shells under non-uniform pressure loads is developed. It should also be noted that the major factor influencing the stability of shell is the magnitude and the extent of the positive pressure near the windward generator of the shell. Refs. (56) and (57) present some of the results of the present analyses on convergence, edge boundary effects, etc.

CHAPTER 4.

STATIC AND STABILITY ANALYSES - FINITE ELEMENT THEORY

4.1 Introduction:

The application of finite element method for the analysis of shells is reported extensively in the literature. The work reported by Grafton and Strome[58], Klien[59], Percy, Pian and Navaratna[60] are some of the earlier papers on this topic. These papers have shown that the finite element method can be used successfully for static analysis of shells of revolution. The stability analysis by the finite elements is treated by some authors as a large deflection problem.

The derivation of stiffness matrices for large deflection and stability analysis is given by Martin[61], Mallett and Marcel[62]. These matrices are also called the incremental stiffness matrices.

The application of finite element analysis for stability analysis of shells is presented by Gallaghar[63] and Gallaghar and Mau[64].

Treating the additional terms arising due to the large deflection strain-displacement relations as extra loadings on the shell, Striklin[65] and co-workers have analysed the problem of stability of shells by load increment and iteration using finite elements. The numerical solution procedures for these problems are discussed in Ref.(66). This method has been adopted by Alnajafi[10] for the problem of cylindrical shells under lateral pressure loading and apparently no useful numerical results could be obtained.

Ch'an and Firmin[13] have also attempted a large deflection stability analysis on the basis of the geometric stiffness approach given by Argyris[67] and obtained approximate buckling pressures for cylindrical shells. In the present analysis the second variation principle of total potential energy is used for studying the stability of cylindrical shells under non-uniform loads in the finite element formulation. The theoretical basis of this method is given in sections 3.2 and 3.3. The prebuckling equilibrium strains are determined by using a cylindrical shell element that retains continuity of strains at the inter element boundaries. In the buckling analysis a simpler form of element representation is used which retains only the continuity of displacements. The buckling analysis is used to study the influence of variable wall thickness ((68)) and the influence of stiffening ring on buckling pressures. The problem of optimum location of axial supports for a simply supported shell under wind load is examined.

4.2 Equilibrium state of stresses:

The equilibrium state of stresses in the shell at any given load level is determined by a linear theory. The cylindrical shell is idealised into a series of cylindrical finite elements as shown in Fig. 4.1. By this representation the problem of assembly of the elements into the shell is reduced to a one dimensional problem. This results in considerable saving in computer storage and time. The stiffness matrices for the elements are derived based on energy considerations.

As shown in Chapter 3. the prebuckling strains can influence the critical buckling pressures to a considerable extent. Hence to determine these strains accurately without any discontinuity across the inter-element boundaries the nodal displacements selected include the displacements and their derivatives that appear in the prebuckling strains. Thus the nodal displacements considered are

$$\lfloor q_j \rfloor = \lfloor u \; u' \; v \; v' \; w \; w' \; w'' \rfloor \tag{4.1}$$

where primes denote differentiation w.r.t.x.

In the present analysis as we are mainly concerned with loads that are represented by Fourier harmonics in the circumferential direction (as given in eqn. 2.2), the resulting displacements by a linear analysis can also be written as

$$\begin{aligned} u &= \sum_n u_n \cos n\theta \\ v &= \sum_n v_n \sin n\theta \\ w &= \sum_n w_n \cos n\theta \end{aligned} \tag{4.2}$$

where u_n, v_n and w_n are functions of x only.

n varies over the same range as the applied loads. For any jth element these functions are written in terms of the element nodal coordinates as

$$\begin{Bmatrix} u_n \\ v_n \\ w_n \end{Bmatrix} = [B] \begin{Bmatrix} q_i \\ q_{i+1} \end{Bmatrix}_n \tag{4.3}$$

The matrix $[B]$ is the matrix of interpolation functions and its derivation is given in Appendix VII.

In the linear analysis the strain displacement relations considered are

$$\epsilon_x = \frac{\partial u}{\partial x} \qquad K_{xx} = \frac{\partial^2 w}{\partial x^2}$$

$$\epsilon_\theta = \frac{\partial v}{\partial \theta} - w \qquad K_{\theta\theta} = w + \frac{\partial^2 w}{\partial \theta^2} \qquad (4.4)$$

$$\epsilon_{x\theta} = \frac{\partial u}{\partial \theta} + \frac{\partial v}{\partial x} \qquad K_{x\theta} = \frac{\partial^2 w}{\partial x \, \partial \theta}$$

The expression for the strain energy of the shell element is

$$U = \frac{E a^2 h}{2(1-\nu^2)} \int_0^{l/a} \int_0^{2\pi} \Big\{ \epsilon_x^2 + \epsilon_\theta^2 + 2\nu \epsilon_x \epsilon_\theta + \frac{1-\nu}{2} \epsilon_{x\theta}^2 + \frac{h^2}{12 a^2} \Big[K_{xx}^2 + K_{\theta\theta}^2 + 2(1-\nu) K_{x\theta}^2 + 2\nu K_{xx} K_{\theta\theta} \Big] \Big\} dx \, d\theta \qquad (4.5)$$

Substituting for strains in terms of the nodal displacements from eqns. (4.2) to (4.4), the strain energy for any harmonic can be written as

$$U_n = \frac{1}{2} \{q\}_n [k]_n \{q\}_n \qquad (4.6)$$

where $\{q\}_n$ - is the column vector of the nodal displacements of the shell element

and $[k]_n$ - stiffness matrix for the nth harmonic.

The matrix k_n is of the form

$$k_n = \frac{E a^2 h}{1-\nu^2} \pi [B1]^T \Big[\int_0^{l/a} [D] \, dx \Big] [B1] \qquad (4.7)$$

The matrices $[B1]$ and $[D]$ are given in Appendix VII and VIII respectively.

4.2.1 Generalised loads:

The generalised load vector corresponding to the nodal parameters selected is obtained by the consideration of the work done.

i.e. $$W = \sum_n W_n = \frac{a^3}{2} \int_0^{l/a} \int_0^{2\pi} p\, w \, dx \, d\theta$$

and (4.8)

$$W_n = \frac{a^3}{2} P_0 \pi b_n \int_0^{l/a} w_n \, dx = \frac{\pi a^3 P_0 b_n}{2} [A] \int_0^{l/a} \{c\} dx$$

substituting for $[A]$ from Appendix VII

$$W_n = \frac{a^3 \pi P_0 b_n}{2} [q]_n [B1]^T \int_0^{l/a} \{c\} dx \quad (4.9)$$

This can be written as

$$W_n = \frac{1}{2} [q]_n \{\eta_n\} \quad (4.10)$$

where $\{\eta_n\}$ - column matrix of generalised loads for the element and

$$= a^3 \pi P_0 b_n [B1]^T \int_0^{l/a} \{c\} dx \quad (4.11)$$

The elements of the matrix $[c]$ are

$$[c] = [0\ 0\ 0\ 0\ 0 \,!\, 0\ 0\ 0\ 0 \,!\, 1\ x\ x^2\ x^3\ x^4\ x^5]$$

knowing the element stiffness and load matrices these two matrices are assembled to form the equilibrium equations for a particular harmonic as

$$[K]_n \{Q\}_n = \{R\}_n \quad (4.12)$$

where $[K]_n$ assembled stiffness matrix of the complete shell.

$\{R\}_n$ assembled load vector of the shell.

$\{Q\}_n$ the unknown generalised nodal displacements of the shell.

Solving the set of equations in (4.12) for the nodal displacements and substituting in equations (4.1) to (4.4) the prebuckling strains throughout the shell are determined. By repeating the analysis for each harmonic in the loading, the complete stress state of the shell is determined.

The analysis for the case of axisymmetric compression (i.e. n = 0) needs special mention while using the above equations. For this type of loading, as it is known before hand that $v \equiv 0$, the corresponding terms in all the equations (4.1) to (4.12) are deleted. This ensures that stiffness matrix does not become singular and also it reduces the number of equations to be solved in the final set of equations (4.12).

4.3 Stability Analysis:

The second variation principle explained in section 3.2 is used in this section to derive the stiffness matrices for stability analysis. The theoretical basis of the investigation of stability by examining the positive definite nature of the second variation of total potential energy is explained in section 3.2. The shell is again considered to be subdivided into a series of short cylindrical shell elements referred to as "ring" elements as shown in Fig. 4.1. But their number need not necessarily be equal to the number considered in prebuckling analysis. The second variation of the total potential energy of the shell is now obtained as a summation over all the elements. In the stability investigations as the main interest is only the energy,

a simple element description is believed to be adequate. The selection of a simpler element reduces to a considerable extent the size of the stability determinant. With these considerations the nodal parameters selected are

$$\left[\bar{q}_{..}\right]_j = \left[\xi_{..} \;\; \eta_{..} \;\; \zeta_{..} \;\; \zeta'_{..}\right]_j \qquad (4.13)$$

where $\{\bar{q}\}_j$ - column vector of j th nodal displacements

The notation used in the Chapter 3. for the virtual displacements is still continued here.

These virtual displacements are again considered to be represented as a summation of Fourier harmonics in the circumferential direction as

$$\begin{aligned} \xi &= \sum_{n=n_1}^{n_2} \xi_n \cos n\theta \\ \eta &= \sum_{n=n_1}^{n_2} \eta_n \sin n\theta \\ \zeta &= \sum_{n=n_1}^{n_2} \zeta_n \cos n\theta \end{aligned} \qquad (4.14)$$

The shape functions ξ_n, η_n and ζ_n are related to the nodal displacements as

$$\begin{Bmatrix} \xi_n \\ \eta_n \\ \zeta_n \end{Bmatrix} = \left[\bar{B}\right] \begin{Bmatrix} \bar{q}_i \\ \bar{q}_{i+1} \end{Bmatrix}_n \qquad (4.15)$$

where the matrix $\left[\bar{B}\right] = \left[\bar{F}(\omega)\right]\left[\bar{B}1\right]$

The matrices $\left[\bar{F}(\omega)\right]$ and $\left[\bar{B}1\right]$ are given in Appendix VII.

The matrix $\left[\bar{B}\right]$ is the matrix of interpolation functions connecting the shape functions and the nodal displacements.

Having selected the shape function these are to be substituted in the expression for the second variation of total potential energy and its value evaluated. For the sake of convenience this process is carried out in two steps. As already explained in Section 3.4 the second variation of total potential energy consists of two distinct parts: one that is dependent entirely on the virtual displacements and another that is dependent both on the equilibrium strains and the virtual displacements. The two parts are evaluated separately as

$$\delta^2 V = \delta^2 V_a + \delta^2 V_b$$

Considering the first part only we have

$$\delta^2 V_a = \frac{E a^2 h}{2(1-\nu^2)} \int_0^{l/a} \int_0^{2\pi} \left\{ \xi_{,x}^2 + (\eta_{,\theta} - \zeta)^2 + 2\nu\, \xi_{,x}(\eta_{,\theta} - \zeta) + \left(\frac{1-\nu}{2}\right)(\xi_{,\theta} + \eta_{,x})^2 + \frac{h^2}{12a^2}\left[\zeta_{,xx}^2 + (\zeta + \zeta_{,\theta\theta})^2 + 2\nu\, \zeta_{,xx}(\zeta + \zeta_{,\theta\theta}) + 2(1-\nu)\, \zeta_{,x\theta}^2 \right] \right\} dx\, d\theta \tag{4.16}$$

substituting for the virtual displacements from (4.14) it will be noticed that this quantity can be evaluated separately for each harmonic. Substituting for the shape functions and carrying out the integration this quantity can be written for each element as

$$\delta^2 V_a = \sum_{n=n_1}^{n_2} \delta^2 V_{an} \tag{4.17}$$

and

$$\delta^2 V_{an} = \frac{E a^3 h}{2(1-\nu^2)} \pi \lfloor \bar{A}_n \rfloor [\bar{D}_n] \{\bar{A}_n\} \tag{4.18}$$

substituting for $\lfloor \bar{A}_n \rfloor$ from Eqn. (AVII.9) we get

$$\delta^2 V_{an} = \frac{E a^2 h}{2(1-\nu^2)} \pi [\bar{q}_n][\bar{B}1]^T[\bar{D}_n][\bar{B}1]\{\bar{q}_n\} \quad (4.19)$$

where $\bar{q}_n$ are the nodal displacements of the jth element for the harmonic n.

The matrix $[\bar{B}1]$ is given in Appendix VII.

The detailed elements of the matrix $[\bar{D}_n]$ are given in Appendix VIII.b. Comparing the equation (4.19) with equation (4.7) and noting its close resemblance we can write this equation as

$$\delta^2 V_{an} = \frac{E a^2 h}{2(1-\nu^2)} \pi [\bar{q}_n][K_{En}]\{\bar{q}_n\} \quad (4.20)$$

where $K_{En} = [\bar{B}1]^T[\bar{D}_n][\bar{B}1]$

= stiffness matrix for the j th element and for harmonic n.

Now we can evaluate the second part that is dependent on both the virtual displacements and load and the equilibrium strains for a particular element.

$$\delta^2 V_b = \frac{E a^2 h}{2(1-\nu^2)} \int_0^{l/a}\int_0^{2\pi} \Big\{ \big[u_{,x} + \nu(v_{,\theta} - w) \big] \zeta_{,x}^2 + \big[(v_{,\theta} - w) + \nu u_{,x}\big](\eta + \zeta_{,\theta})^2 + (1-\nu)(u_{,\theta} + v_{,x})\zeta_{,x}(\eta + \zeta_{,\theta}) \Big\} dx\, d\theta + \frac{a^3 P_0}{2} \int_0^{l/a}\int_0^{2\pi} b_n \cos n\theta \big[\zeta^2 + 2\eta\zeta_{,\theta} + \eta^2 - \zeta\xi_{,x} + \xi\zeta_{,x}\big] dx\, d\theta \quad (4.21)$$

substituting for the membrane strains and the virtual displacements and carrying out the integration the resulting expression is a quadratic algebraic expression.

This can be represented for the j th element as

$$\delta^2 V_b = \frac{E a^2 h}{2(1-\nu^2)} \lambda \lfloor \bar{q}_{..} \rfloor [K_G] \{\bar{q}_{..}\} \qquad (4.22)$$

where $[K_G]$ is the geometric stiffness matrix

λ = load parameter = $\frac{P_0}{E}\left(\frac{a}{h}\right)$

It has to be noted that the elements of the matrix $[K_G]$ are dependent on all the harmonics of the equilibrium strains and also on all the nodal displacements for different harmonics. It should also be noted that this is <u>not</u> so for the matrix K_{En} (eqn. 4.20).

The detailed derivation of the matrix $[K_G]$ is given in Appendix IX.

The second variation of total potential energy can now be written for each element as

$$(\delta^2 V)_j = \frac{E a^2 h}{2(1-\nu^2)} \left[\sum_{n=n_1}^{n_2} \lfloor \bar{q}_n \rfloor [K_{En}] \{\bar{q}_n\} + \lambda \lfloor \bar{q} \rfloor [K_G] \{\bar{q}\} \right] \qquad (4.23)$$

Assembling for all the elements this quantity can be written for the complete shell as

$$\delta^2 V = \frac{E a^2 h}{2(1-\nu^2)} \lfloor \bar{Q} \rfloor [K_E + \lambda K_G] \{\bar{Q}\} \qquad (4.24)$$

where $\{\bar{Q}\}$ is the column vectors of all the nodal displacements of the shell for each of the harmonics considered in virtual displacements

ie $\lfloor \bar{Q} \rfloor = \lfloor \bar{Q}_{n_1} \quad \bar{Q}_{n_1+1} \quad \cdots \quad \bar{Q}_{n_2} \rfloor$

$\{\bar{Q}_n\}$ - column vector of the nodal displacements for the nth harmonics

$[K_E]$ The diagonal stiffness matrix of the shell for all the harmonics considered with the stiffness of the shell for each harmonic as a diagonal element.

i.e. $[K_E] = \begin{bmatrix} k_{En_1} & & & \\ & k_{En_1+1} & & \\ & & \ddots & \\ & & & k_{En_2} \end{bmatrix}$

K_G – The geometric stiffness matrix for the shell. This will be a fully populated matrix indicating the influence of each harmonic.

Thus it can be seen that the final size of the stability matrix is dependent on (a) the number of elements chosen (b) the number of degrees of freedom at each node and (c) the number of harmonics selected in the virtual displacements. In the linear analysis the harmonics are uncoupled.

4.4 Stability determinant:

Having obtained the expression for the second variation of the total potential energy as in eqn. (4.24), the positive definite character of this quantity is to be examined as explained in section 3.6. However, the process is very much simplified because of the representation in matrix language and the stability determinant is simply

$$|K_E + \lambda K_G| = 0 \qquad (4.25)$$

The lowest value of λ which satisfies this condition is the critical buckling pressure (λ crit).

To find the value of λ crit from (4.25) the determinant

search method is employed. In this method the value of the stability determinant is evaluated for successively increasing values of λ until a change in the sign of the stability determinant is noted. Then the value of λ_{crit} is obtained by iteration to a desired degree of accuracy.

4.5 Ring stiffened shells:

The advantage of the finite element analysis is its adaptability to complex situations for which continuum solutions are not practicable. One such problem is to find the buckling pressures for ring stiffened shells. For analysing the problem one needs to take into account the stiffening effects of rings both in the prebuckling stress calculations and in the buckling analysis. The rings are considered to be attached to the shell at a nodal circle, so that compatibility of displacements between ring and shell can be easily maintained.

In the prebuckling analysis, the stiffness elements of the ring are added to the corresponding stiffness elements of the shell in eqn. (4.12) and the resulting equations are solved for equilibrium stresses. To evaluate the influence of a ring in buckling analysis one needs to calculate the contribution of the ring to the buckling determinant apart from the stiffness matrix. The details of these matrices which are taken from Ref. (69) are given in Appendix X. After adding these contributions to the corresponding nodal displacements in the buckling determinant, the critical buckling pressures can be calculated as explained in section 4.4.

4.6 Results and Discussions:

The finite element analysis developed in this Chapter is first applied to a few cases, for which the results are known, to assess its accuracy. The convergence of the results is also examined. Next the method is used for analysing (a) ring stiffened shells, (b) variable thickness shells and (c) to find optimum axial location of supports in a simply-supported uniform shell.

The accuracy of the stresses obtained by the present method is first examined. In the prebuckling analysis, the maximum radial displacement (w) and the maximum stresses obtained by the Finite element analysis are compared with those obtained by using Donnell's theory by considering only one harmonic at a time in the loading. The results obtained are presented in Tables 4.1 to 4.3 for a few typical shell geometries considered. The number of 'ring' elements considered for this analysis is ten. From these results it can be seen that the displacements, the axial stress and the circumferential stress are estimated accurately, the maximum error being only 5%; whereas the error in the shearing stress is of the order of 10%. Hence it is assumed that the stresses obtained by considering ten elements in the prebuckling analysis are satisfactory.

To study the convergence of buckling pressures with the number of elements selected, the problem of a simply supported shell under hydrostatic loading is considered; the results for which are given by Flugge[29]. For a few shell geometries the results obtained are plotted in

Fig. 4.2. It is seen from these graphs that the improvement in buckling pressure beyond five elements is negligible compared to the extra computer time required. Hence five elements to represent the shell in buckling analysis are considered to be adequate. The buckling pressures obtained by considering only five elements for this problem are given in Table 4.4. The maximum error in buckling pressures is seen to be about 10%.

To study the convergence of the results with number of effective harmonics, the problem of the cantilever cylindrical shell under wind loading is considered, the results for which are given in Chapter 3 by continuum analysis. The buckling pressures obtained for successively increasing number of harmonics for a few shell geometries are plotted in Fig. 4.3. These results again confirm that the selection of five effective harmonics gives sufficiently converged results for buckling pressures under non-uniform loads.

When the number of elements selected is five and the number of harmonics selected is also five, the resulting buckling determinant is of the order (100 x 100). With this stability determinant the buckling pressures are obtained for the following two problems: (a) simply supported shell under non-uniform pressure assumed by Almroth[4]. The results obtained are compared with those given by Almroth in Table 4.5 for a few shells, (b) cantilever cylindrical shells under wind load. The results obtained are compared with those obtained by continuum theory in Fig. 4.4. These results indicate that the

buckling pressures obtained by the Finite Element Method differ from those obtained in Chapter 3 by a maximum of 10%

Having studied the accuracy of the method, the analysis is used for determining the critical buckling pressures for the case of cantilever cylindrical shell with a ring stiffener at the free top. The results obtained for few shells are given in Fig. 4.5. Comparison of these results with those in Fig. 3.5 indicates that when the ring dimensions are large compared to thickness the tip boundary conditions are close to a clamped end. When the ring dimensions are reduced the critical buckling pressures are also reduced. For a few cases when the ring is thin, the results obtained correspond to the case of clamped-simply supported shell. It is also observed that in the limiting case when the ring dimensions are zero, the critical buckling pressures corresponding to the cantilever shell are obtained.

The present method has also been used to obtain the critical buckling pressures for variable thickness cantilever shells, such as the ones used for oil storage in the petroleum industry, under wind load. The results obtained for certain shell geometries typical of such shells are given in Table 4.6.

The third problem for which the present analysis is applied is to find the optimum axial location of supports for a simply supported uniform shell under wind load. This problem is often encountered in the design of Radomes. For analysis purpose, the supports are

considered to be placed symmetrically. (See Fig. 4.6). The stress and stability analysis of the shell are carried out for different support locations. The variation of the maximum radial displacement, the maximum axial and shearing stresses, for each of the harmonics in the loading, are calculated for different support locations. These results for the case of shell with L/a = 2, a/h = 500 are presented in Fig. 4.6 to 4.8. The corresponding results for a shell with L/a = 6, a/h = 400 are plotted in Fig. 4.9 - 4.11. The variation of critical buckling pressures for these two shells for different support locations are presented in Fig. 4.12. These results indicate that the deflections and stresses are minimum and the buckling pressure is a maximum when the supports are located at 0.22L from the ends of the shell. The finite element analysis presented is seen to be a very convenient tool for analysing problems for which continuum solutions are impracticable.

CHAPTER 5

EXPERIMENTAL INVESTIGATION

5.1 Introduction

In the field of stability of shells, in general, there are significant differences between theoretical and experimental results. Even for simple problems such as that of shell under uniform axial compression or uniform lateral pressure, all the available theories do not agree qualitatively and considerable scatter is observed in experimental results. It is difficult to simulate exact boundary conditions assumed in the theory and imperfections in the shell can also influence the buckling pressures. Since the theoretical buckling results are invariably non-conservative, an assessment of their usefulness in design can only be made by comparing those values with experimental results. Therefore an experimental study of buckling of shells under non-uniform pressure is undertaken here.

The theoretical analysis assumes that the loading is gradually applied and that the dynamic effects are absent. However the lateral loadings considered in the experimental work viz:

a) pressure loading due to a steady wind simulated in the wind tunnel and

b) pressure due to flow of water in the water tunnel

are such that the shells are not completely free of the dynamic effects. The main reason for choosing these

loadings despite this deficiency is that they represent realistic problems of practical interest.

5.2 Wind Tunnel Testing

Testing of cylindrical shells in the wind tunnel enables to determine the critical buckling pressures under the action of wind pressures on the lateral surface of the shell. It is possible to vary the type of flow in the wind tunnel and simulate various wind conditions. The pressure distribution on the shell is dependent on the type of flow. The influence of various parameters on the pressure distribution such as the surface roughness, Reynolds numbers and gust effects have been studied by Scheubel[70] and Niemann[71]. Neimann has shown that the form of the pressure distribution can be determined accurately by knowing the magnitude of the suction peak for circular cylindrical shells. Extensive experiments are carried out to measure pressure distribution on rigid cylindrical shells and to check the uniformity of flow in the wind tunnel by Brave-Boy[9] and the pressure distribution is shown to be in good agreement with that given by Rish[19]. Experiments on buckling of cantilever cylindrical shells have been reported in Refs (5) to (8) and in (51). Rish[5] used model cylindrical shells made of paper as these shells buckle at very low wind speed. Langhaar and Miller[6] also used similar models in the qualitative study of the nature of buckling. Der and Fidler[8] conducted experiments on hyperbolic cooling towers to study the effect of base uplift and other possible structural damages on the buckling pressures. Heyman[51] has

presented some more experimental data and a theoretical study of these effects. Croll[72] has shown that the flexibility at the base has influence on buckling pressures only when the external pressure is distributed on the surface of shell based on an experimental investigation. Holownia[7] has reported the experimental buckling pressures for both open ended and closed ended shells under wind loading.

5.2.1 Wind Tunnel

The wind tunnel used for conducting the tests is an open jet return circuit type. The test section dimensions are $3\frac{1}{2}'$ x $2\frac{1}{2}'$ rectangle. The maximum velocity of flow attainable at the test section is 90 ft/sec. The velocity distribution across the test section is fairly constant. The jet velocity is controlled by means of two biased switches. By operating these switches, the velocity can be varied in steps. A schematic diagram of the wind tunnel is shown in Fig. 5.1.

5.2.2 Selection of Geometry of Models

The selection of sizes of the shells for testing in the wind tunnel has been based on the following considerations:

a) The maximum dynamic pressure attainable in the wind tunnel and

b) the blockage effects due to the presence of model in the test section.

The shells are to be such that they collapse within the maximum dynamic pressure attainable in the wind tunnel. This can be ensured either by choosing very thin shells

or by using materials of low elastic moduli for the shell. By these considerations Flovic/Darvic plastic sheets are used for fabricating the shells. The thickness of the sheets used are; 0.25 m.m. (0.01") 0.5 m.m. (0.02") and 0.75 m.m. (0.03").

The flovic material has certain other advantages as compared with metal sheets for forming the shells. It is easier to form and joining the edges of the shell presents no difficulty. Unlike the metal shells that undergo permanent plastic deformations after buckling, the Flovic shells return to their original position and recover almost entirely the circular shape with only a small amount of permanent set (creasing) at the fixed edge of the windward generator. The flovic shells can therefore be tested in a different orientation. By removing the small region that may have a permanent set, it is also possible to obtain a shorter shell on which further tests can be conducted.

The blockage effects in the test section determine to a considerable extent the length and the diameter of the shells. The height at the test section is about 30 inches. If the height of the model is well within this height, the shell will be in a completely submerged flow and the internal suction in the shell will be ensured. Therefore the height of the shell is restricted to a maximum of about 24 inches. The maximum diameter of the shell is to be chosen such that the frontal area of the shell does not exceed the maximum permitted blockage area of

the tunnel, which is 20% of the area of the test section. If the diameter exceeds this limit blockage correction needs to be applied to the results obtained. However it has not been possible to strictly adhere to this rule in all the cases tested. The maximum frontal area of the shells in a few cases has been 22% of the test section area. As a result of this some spillage of flow has been noticed in these cases. The corrections required for these cases are nevertheless quite small as the wind tunnel is open jet type.

5.2.3 Construction of the Shell

The shells are made out of Flovic/Darvic plastic sheets. The shells are formed by rolling sheets and joining the ends by a buttweld (or a joint). This results in a seam along one generator. To avoid excessive stiffness along this generator the thickness of overlapping parts of the ends are reduced by sand papering. In the initial experiments on clamped free shells the models have been mounted on a base ring which holds the shell in the interior and an outer ring has been used to clamp the shell at the base. This method of fixing is shown in Fig. 5.2a. This arrangement has been later discarded as it has been suspected that fixed edge conditions may not have been completely realised because of the possible movement of the shell in the axial direction. In the later experiments the base of the shell is set in an epoxy resin after placing the shell in the grooves made in the base plate. After setting the resin provides a good fixity for the shell as shown in Fig. 5.2.b.

To simulate the stiffening effect of the rings, the shell is stiffened at the free end by a perspex ring which fits snugly inside the shell. The ring and the shell are bonded by an araldite glue. The arrangement is shown in Fig. 5.2.b.

To construct shells of variable thickness, sheets of different thickness are first bonded in an appropriate manner. The composite sheet is rolled to obtain shells with varying thickness in the axial direction. A schematic diagram of the variable thickness shells is shown in Fig. 5.3.

5.2.4 Determination of Material Properties

The Young's modulus for the Flovic/Darvic plastic is given by the manufacturers as 0.45×10^5 lbs/in.^{2}. However the properties of plastic change quite considerably with time and temperature. Also as the material used for some of the models was stored for considerable time, it has been regarded as appropriate to check the Young's modulus, as this is very important in assessing the experimental results. The following two methods have been used to determine the Young's modulus.

In the first method a rectangular specimen is prepared out of the sheet and a bending test is carried out. The specimen is supported at two points and two equal loads applied symmetrically. The central deflection in the beam is measured by a capacitance transducer. Knowing the central deflection and the cross sectional dimensions the Young's modulus is determined.

In the second method a standard tension specimen is prepared and it is tested in a strain rate controlled universal testing machine which is specially designed to test plastics. The stress-strain curve is automatically plotted during the test. The slope of the stress-strain curve directly gives the required Young's modulus. The values of the Young's modulus obtained by both the methods differ very little from the value given by the manufacturers. Hence the value of Young's modulus for all the further tests has been assumed as 0.45×10^5 lbs/in^2.

5.2.5 Test Technique

After a shell is mounted in the test section, the velocity of flow in the wind tunnel is gradually increased by means of the biased switches till the shell collapses. During this process the behaviour of the shell is carefully observed. The dynamic pressure of the free stream just before the front surface of the shell collapses is noted on the manometer. This is taken as the critical buckling pressure of the shell.

5.2.6 Experimental Observations

While conducting the buckling tests on cylindrical shells in the wind tunnel it has been noted that:

1. The long shells ($L/a \geq 4$) tend to vibrate very violently. The vibrations are initiated in the wake region of the shell at a dynamic pressure which is much lower than the critical pressure. These oscillations gradually build up as the

velocity of flow is increased and they are transmitted to the front surface of the shell. The amplitude of vibration is sometimes as large as 30 times the thickness of the shell. The number of waves in the circumferential direction is between 3 and 7, depending on the thickness of the shell. The amplitude of vibrations is maximum just before the collapse.

2. For certain shell geometries it has been noted that the windward generator of the shell tends to move in the direction of the upstream just before final collapse. Similar observation has been reported by Heyman[51] and this is called the formation of cusp.

These observations are considered to be due to the unsteady nature of the pressure distribution due to vortex shedding. Attempts to study this nature of pressure distribution is reported in Ref. (34). It is also reported in the above reference that the long shells ($L/a \geq 8$) do not collapse in the wind as do the short shells. The dynamic effect seems to be influencing the buckling pressures for shell of intermediate length ratio.

5.3 Testing in the Water Tunnel

Experiments have been conducted on cylindrical shells submerged in water at N.P.L. by Maybrey and Bryer[37]. A schematic diagram of the arrangement used for testing the shell is shown in Fig. 5.4. The base of the shell is fixed to the tunnel wall and the top of the shell is

closed by a diaphragm. The diaphragm is connected by a rod to the outside pressure compensating chamber which balances the pressure acting on the diaphragm. This arrangement is used to eliminate any axial load on the shell due to presence of different pressures on either side of the end diaphragm. This also enables to maintain any desired internal pressure inside the shell without developing any axial load.

The model shell is made out of a solid plastic bar by removing the core material and making it hollow till a uniform thin shell is obtained. The following two different shell geometries are tested:

1. $L/a = 1.827$ $\quad a/h = 214$
2. $L/a = 4.728$ $\quad a/h = 149$

Only the following two velocities of flow are considered for analysis, i.e. 52 in/sec and 73 in/sec. In the water tunnel the following three different flow conditions are simulated.

a) smooth flow without grids.

b) only turbulent flow.

c) turbulent shear flow.

The distribution of pressure is different from one another in all these cases.

5.3.1 Test Technique

The tests on the model shells are conducted in two stages. In the first part of the test, the pressure measurements on a rigid cylindrical shell are obtained. The pressure is measured at seven points along one generator on a

manometer. This generator is aligned at different angles with respect to the flow by rotating the cylinder and at each setting, the pressures are noted at all the points on this generator to obtain the complete pressure distribution on the shell. This process is repeated for the three different flow conditions and for the two velocities on the two shell geometries.

In the second part the buckling tests are carried out on the flexible shells. The shell is mounted in the test section and one of the possible velocities of flow is maintained steadily. The internal pressure is gradually reduced till the shell starts to collapse. As the internal pressure is reduced still further the number of lobes in the circumferential direction into which the shell buckles ~~increases~~ changes. The value of the internal suction pressure p^*_{cr} at each stage of the collapse is noted. The pressure measurements and the buckling pressures are given in Ref. 37 and this data is used here for theoretical analysis and comparison. (see Tables 5.3 and 5.4)

The two shells are tested under internal pressure only without any external pressure due to flow. The critical buckling pressures are also given in Ref.(37). (See Table 5.2)

5.4 Results and Discussions

In the first stage of the experimental work on cantilever cylindrical shells, the arrangement shown in Fig. 5.2a is used. The experimental results obtained by such a fixity are compared with theoretical results obtained by the continuum theory in Fig. 5.5. The error in the experimental results is, in a few cases about, 50%. The

discrepancy has been attributed to improper edge conditions at the base. The buckling pressures obtained by using the arrangement in Fig. 5.2b are compared with the theoretical results in Fig. 5.6. The theoretical results obtained by the continuum theory is chosen for all comparisons with experiments. The maximum difference in experimental and theoretical results is now only about 15% for the case of short shells ($L/a \simeq 1$); and it is about 30% for the long shells ($L/a \simeq 5$).

During the experiments it has been observed that the short shells are almost steady during the test and the buckling occurs more or less suddenly in a snap through action: in the case of long shells quite violent oscillations of the shell are first noticed before the final collapse takes place. Whether or not these or any dynamic/static interaction influencing the collapse requires further study.

In the subsequent test conducted to evaluate the repeatability of the experimental data, the base of the shell has been always embedded in the epoxy resin. At least four shells have been tested for each shell geometry. The experimental results obtained for the clamped free shells are shown in Fig. 5.7 to 5.9 along with theoretical results for three thickness ratios.

Experiments have also been conducted on clamped-free shells with a stiffening ring at the free top. For comparison purpose the ring is considered to act as a simply supported end. The test results are compared with theory

in Fig. 5.10 to 5.12 for three thickness ratios. In a few cases the difference between the two results is only about 10%. Hence it is considered that the ring acts more like a clamped end than as a simply supported end.

A few tests have also been conducted on cantilever cylindrical shells with variable thickness. The theoretical results for these cases have been obtained by the Finite Element analysis. These results are given in Table 5.1. The maximum error between the two results is about 30%. Noting that F.E. method gives buckling pressures which are about 10% higher than the continuum results for similar geometries, the results are considered to be satisfactory.

The experimental results obtained by tests in the water tunnel are analysed by using the theory given in earlier chapters. The following methods have been employed to obtain the theoretical results:

a) Considering the shell to be clamped - s.s., and using the virtual displacements in Eqn.(3.13) by employing the continuum method.

b) By using the virtual displacements in Eqn. (3.12) in conjunction with the Lagrangian multipliers to get s.s. condition at the end .

c) By employing the Finite Element method for the problem.

While using the first two methods, the external loading is represented as in Eqn.(2.1.) to consider the variation of pressure in the axial direction. For a few shell

geometries the simplified pressure distribution in the form of Eqn.(2.2.) is also used for obtaining the buckling pressure. It is found that the axial variation of pressure has very little influence on the buckling pressures. Hence the simplified pressure form is used in method (c). The results obtained by the three methods have been reasonably close. The results obtained by using the finite element method are generally higher than those obtained by the other two methods. The theoretical and experimental results for the case of axisymmetric compression (i.e. for the zero velocity of flow) are given in Table 5.2. The results for other flow conditions for the two shell geometries are given in Tables 5.3 and 5.4. In these tables the results in Column (a) are the theoretical buckling pressure obtained by the above methods.

From the results in Table 5.2, ignoring the scatter in experimental data, the theoretical results are seen to be much higher. To make certain that the present theoretical results are of right order, the circular cylindrical shell of similar geoemtry subjected to suction loading but simply supported at both ends is considered. The results for this problem is given by Flugge[29] for the two shells as 0.373 and 0.33. By clamping one end of the shell the buckling pressures will be higher, and hence it is considered that present results are in the correct trend. The discrepancy between the theoretical results in column (a) and the experimental results is considered to be due to:

(i) Imperfections in the shell and the boundary conditions.

(ii) The end cap may be exerting some axial force on the shell.

To investigate the second possibility the internal suction load acting on the end cap is assumed to be transmitted to the shell as an axial compression. The buckling pressures obtained by this assumption are given in Column (b). This gives a closer agreement between theory and experiment for the zero velocity case.

It should be noted from the experimental data presented in Table 5.3 that the number of lobes increases initially and then decreases as the internal suction pressure P^*_{cr} is increased. We believe that the highest value of P^*_{cr} is the best approximation to the critical pressure determined theoretically.

CHAPTER 6

DESIGN ASPECTS

6.1 Introduction:

The static and the stability analyses of cylindrical shells presented in the previous chapters have important application in the design of oil storage tanks, radomes and other engineering structures. However, because of the complexity of the analyses, it is not practicable to use these exact theoretical methods for all stress and stability problems. As an alternative empirical equations are often used for rapid estimation of buckling pressures. Even though the empirical equations are approximate and have limited range of applicability, they are considered to be convenient for design purposes. Wiengarton[73] has presented a series of empirical equations for cylindrical shells under different types of loading. In Ref. (7 to 9) similar equations have been developed for the case of cylindrical shells under wind loads based on the experimental results obtained for the above problem. In Ref. (47) similar attempts have been made based on the theoretical results. In Ref. (74) these empirical equations are discussed and a theoretical basis for the derivation of these is discussed. In all the above works, the empirical equations are developed based either only on experimental results or only on the theoretical results. Hence, it is considered, they may have only a limited applicability.

In this chapter certain design considerations for oil storage tanks are discussed. Existing codes and empirical

equations used in the design are examined and their deficiencies are pointed out. New empirical equations based on the results obtained in the earlier chapters will be presented.

6.2 Critical pressures:

For a given shell geometry, material properties and boundary conditions, the value of P_o at which the shell buckles will be termed of the stagnation critical pressure (P_{cr}). This is to be distinguished from the gas critical pressures obtained for the case of uniform external pressure.

Numerical results have shown that the stagnation critical pressures are always greater than the gas pressures. As an example the results for a clamped-free shell are plotted in Fig. 6.1 in which the experimental results are also shown. As compared with experimental results, the gas critical pressures are lower i.e., conservative. On the other hand the stagnation critical pressures are higher. It is therefore necessary to reduce the present theoretical results by an appropriate factor (γ) to approximate the experimental results. This fact has not been considered by Maderspach[44].

6.3 Empirical criterion:

By plotting the numerical results on log-log graph sheets and following the general theoretical basis given in Ref. (74), it has been found that all the results for cylindrical shells under wind loads regardless of boundary conditions can be fitted satisfactorily

by an equation of the form

$$\left(\frac{P_{cr}}{E}\right) = \bar{\lambda}\,(L/a)^{\alpha}\,(a/h)^{\beta} \qquad (6.1)$$

As an example the log-log plots of the theoretical buckling pressures for clamped-free shells are shown in Fig. 6.2 and 6.3. The values of the indices α and β, as measured by the slopes of these graphs, differ very slightly from (-1) and (-2.5) respectively. For all practical purposes they can be considered as -1 and -2.5. Hence the equation can be written as

$$\left(\frac{P_{cr}}{E}\right) = \bar{\lambda}\,(a/L)\,(h/a)^{2.5}$$

The value of $\bar{\lambda}$ depends on the boundary conditions at the ends. For certain combinations of clamped, simply supported and free conditions, the values of $\bar{\lambda}$ are given in Table 6.1. The values of $\bar{\lambda}$ are obtained by assuming that the value of γ found for clamped-free case is valid for other cases as well.

It is convenient to re-write the equation (6.1) in another form. For a given design wind speed, shell geometry and boundary conditions, the maximum permissible height, H_p, can be obtained as

$$H_p = \bar{\lambda}\,\frac{E}{P_{cr}}\,a\left(\frac{h}{a}\right)^{2.5} \qquad (6.2)$$

As an example if we consider a simply-supported steel shell under a wind which produces a dynamic pressure of

0.25 P.S.i we have

$$P_{cr} = 0.25\,Psi\,, \quad E = 30\times10^{6}\ P.S.i$$

$$\bar{\lambda} = 1.1$$

Hence $$\left(\frac{H_P}{a}\right) = 13.2\times10^{7}\left(\frac{h}{a}\right)^{2.5} \qquad (6.3)$$

6.4 Current standards:

As applied to oil storage tanks certain empirical equations have been recommended by the American Petrolium Institute Ref. (76) and the British Standards Institution Ref. (75). For open top tanks, a primary stiffening ring is to be used at or near the top end. No mention has been made regarding the boundary conditions at either ends, but simple supported conditions are implied. It is considered that a more realistic base condition is that of a clamped edge. However, the value of $\bar{\lambda}$ for this case is only marginally higher than the simply supported base, with the top being supported, as shown in Table 6.1. Therefore, the lower value is preferred. For the maximum permissible height of "unstiffened" shells, the formula recommended by API is

$$H_p = 600h\sqrt{\left(\frac{100h}{2a}\right)^{3}} \qquad (6.4)$$

where H_p and a are in feet and h in inches. Here the design wind speed implied is 100 mph, which

gives a dynamic pressure of 0.1776 psi . This wind velocity is increased by 20% for gust allowance, etc., making the total dynamic pressure as 0.25 psi . Equation (6.4) in a non-dimensional form becomes

$$\left(\frac{H_P}{a}\right) = 9.0 \times 10^{7} \left(\frac{h}{a}\right)^{2.5} \qquad (6.5)$$

The British Standard Institution recommends the following formula for the corresponding height as

$$H_P = \bar{K}_1 \sqrt{h^5/(2a)^3} \qquad (6.6)$$

where H_P and a are in metres and h in millimetres and $\bar{K}_1$, is a constant obtained as

$$\bar{K}_1 = \frac{95\,000}{3.563\, V_m^2 + 580\, V_a}$$

V_m - design wind speed in m/sec.

V_a - vacuum for design of girders in m bars.

For a design wind speed of 100 mph. (=45 m/sec.) and taking the value of V_a = 5 m bars, Equation (6.6) in a non-dimensional form becomes

$$\frac{H_P}{a} = 9.0 \times 10^{7} \left(\frac{h}{a}\right)^{2.5} \qquad (6.7)$$

This agrees with the API specifications. The BSI formula clearly applies for design at various wind speeds.

Comparing Equations (6.7 and (6.5) with (6.3), it can be considered that the current standards are conservative.

In the foregoing discussion, the shells are considered to be of constant thickness. However, the shells may also be made up of a number of courses of different thickness. In this situation it is recommended to consider the height of an equivalent shell of average thickness by API. Let H_n be the height of n^{th} course of thickness h_n, and let h_a be the average thickness, the reduced height H_R is defined as

$$H_R = \sum_n H_n \left(\frac{h_a}{h_n}\right)^{2.5} \qquad (6.8)$$

where $$h_a = \frac{\sum h_n H_n}{\sum H_n}$$

This reduced height H_R is to be compared against the maximum permissible height H_p in which h_a is now the average uniform thickness of shell. In the B.S.I. recommendations the reduced heights are calculated based on the minimum thickness instead of the average thickness.

In Fig. 6.4 is plotted in non-dimensional form, the maximum permissible height for a given thickness ratio of the shell with simply supported ends. These are obtained using (1) the theoretical stagnation pressures

(2) the empirical equation proposed here i.e. Equation (6.3); (3) the theoetical gas pressures and (4) the equations recommended by standards; i.e. Equations (6.4) and (6.6). Apparently the standards are based on the gas pressures with a factor of safety of about 1.25. Assuming the same factor of safety on the present theoretical critical stagnation pressures we arrive coincidentally at the values given by the proposed empirical Equations (6.1) and (6.3). As stated earlier, the experimental values of buckling pressures are never less than the values given by Equation (6.1). Hence, this equation can be considered to be more appropriate for design purposes than the formulae given in standards.

6.5 Secondary wind girders:

Whenever the actual height of the shell (or the reduced height in the case of shells of variable thickness) exceeds the maximum permissible height H_p, a secondary wind girder will be required to stiffen the shell. For typical Appendix A-type tanks of API (Ref. 76), which are of constant thickness the maximum permissible heights are computed using Equations (6.3), (6.5) and (6.7). The results are shown in Table 6.2 in columns (5) and (4) respectively. It can be seen that none of these tanks require any secondary girder.

For some typical Appendix K-type tanks of Ref. (76), the corresponding results are shown in Table 6.3. It can be seen that many of these tanks require a secondary wind girder if the design is based on the current

standards; where as most of the shells do not need secondary girders if the present formula in Equations (6.3) and (6.8) is used.

6.5.1 Free height of shells:

While the shells are under construction, the top of the shell is not supported and hence it has to be treated as free edge in the analysis. Assuming the base to be clamped, the maximum height up to which the shell may be constructed without the risk of the shell buckling due to wind, at the maximum speed expected, can be calculated from Equation (6.1) as

$$\left(\frac{H_f}{a}\right) = \frac{0.66\,E}{P_{cr}}\left(\frac{h}{a}\right)^{2.5} \qquad (6.9)$$

where H_f is the maximum permitted free height.

Assuming $P_{cr} = 0.25$ p.s.i. we have

$$H_f = 2.64\,E\,a\left(\frac{h}{a}\right)^{2.5}$$

(E in p.s.i.)

If the boundary condition at the base is not a perfect clamped end, appropriate value of $\bar{\lambda}$ has to be selected. For some typical Appendix A-type tanks, Ref. (76), the value of H_f are shown in column (6) of Table 6.2, assuming clamped-free end conditions. Should the base condition be clamped-sliding due to deficiency in design or construction, the low value of $\bar{\lambda}$ (=0.22) for this case would reduce the values of H_f to one third of

those given in column (6), Table 6.2. In these cases the shell becomes very susceptible to collapse at the maximum expected winds and remedial action will be required.

Similar results for the Appendix D and Appendix G-type tanks are given in Table 6.4 and 6.5. For a few cases in Table 6.5, the ratio of reduced height to the maximum permitted spacing is some times more than two. In these cases two intermediate girders will be required if the current standards are employed; Whereas the present formulae in these cases still suggests only one intermediate girder.

6.6 Discussion:

An empirical criterion based on the results obtained in the previous chapters is presented for the stability design of cylindrical shells under wind loads. The existing codes are valid only for the case of simply supported ends , whereas the present equation can be used for any boundary condition. As compared with the current standard, the difference between the maximum free height and the maximum permitted ring spacing is clearly brought out in the current analysis. The current standards are considered to be conservative. As has been discussed in Refs. (77) and (78).

CHAPTER 7

CONCLUSIONS & RECOMMENDATIONS

7.1 Conclusions:

The problem of cylindrical shells under non-uniform lateral pressure has been analysed using both continuum and finite elements methods. From the theoretical results it can be concluded that:

1. The beam theory is inadequate for estimation of stresses in shells and the stress may even be misrepresented as only the first harmonic component of loading is considered in this theory.
2. The semi-membrane theory over-estimates stresses and in the preliminary design it is convenient but conservative.
3. The stress analysis of the shells can be carried out with sufficient accuracy using the Donnell's shell theory which is simpler than the Flugge's theory.
4. The second variation principle applied here provides a convenient tool for stability analysis of shells subjected to lateral non-uniform pressures.
5. The buckling mode of a shell under non-uniform pressure will consist of a range of significant harmonics. The range of significant harmonics increases for thinner shells and decreases for longer shells. The buckling pressure is a minimum only when the assumed displacement mode includes all the significant harmonics. The number of effective harmonics required is generally five or more.

6. The buckling mode of the shell in the axial direction can be satisfactorily represented by polynomial terms. Five polynomials terms are considered to be adequate.

7. The variation of pressure distribution in the axial direction due to boundary layer, end effects due to three dimensional flow effects, etc., do not influence the buckling pressure to any significant extent.

8. The buckling of cylindrical shells under wind loading is influenced mainly by the positive pressure area on the windward generator. The suction peak has a negligible influence on the buckling loads.

9. The relaxation or constraint of the edge rotation of the shell does not significantly alter the buckling pressures, whereas the relaxation or constraint of the axial displacement can alter the buckling pressures enormously.

10. By stiffening the free top edge of a cantilever shell, the buckling pressures can be increased considerably.

11. The current engineering practice for estimation of buckling pressures of shells is conservative. The second variation principle yields critical pressures that are higher than the experimental values. The empirical equations developed here yield results which are closer to the experimental buckling pressures.

7.2 Suggestions for further work:

1. An improvement in the continuum analysis may be

possible by looking for means to reduce the size of the stability determinant for a selected range of harmonics. One such avenue seems to be to relate the arbitrary constants in the virtual displacements before using them in the expression for the second variation of total potential energy by noting that these virtual displacements are required to satisfy the equilibrium equations. For the case of cantilever cylindrical shells no useful simplification was achieved by this process.

2. On the other hand by selecting a wider range of harmonics lower buckling pressures could be obtained: however, this will further increase the size of the stability determinant which necessitates a larger computer storage and time.

3. The method can be easily extended to the case of orthotropic shells which finds direct application in analysing stiffened shells with closely spaced reinforcements.

4. The method can be extended by including the dynamic effects to analyse the dynamic instability of long shells ($L/a \geq 4$) under oscillatory loads such as due to wind considering the flow separation effects. An outline procedure for this is given in Ref. (79).

REFERENCES

1. Hoff, N. J. — "Buckling and stability" Forty-first Wilber-Wright memorial lecture, J. of Royal Aero. Soc., Jan., 1954.

2. Langhaar, H. L. and Boresi, A. P. — "Snap through and post buckling behaviour of cylindrical shells under the action of external pressure". University of Illinois, Engg. experimental station, Bulletin 443, 1957.

3. Langhaar, H. L. — "General theory of buckling". Applied Mechanics reviews, Vol. 11, Nov.1958, pp 585 - 588.

4. Almroth, B.O. — "Buckling of cylindrical shells subjected to non-uniform external pressure". J.of Appl. Mech. pp 675 - 682, Dec., 1962.

5. Rish, R. F. — "Collapse of cylindrical elastic shells under wind load". The Engineer, Oct., 1963, pp 669 - 672.

6. Langhaar, H. L. and Miller, R. E. — "Buckling of an elastic isotropic cylindrical shell subjected to wind pressure". Proc. of symp. on "Theory of Shells" to honour L. H. Donnell, University of Houston, Texas, 1967, pp 405 - 430.

7. Holownia, B. P. — "Buckling of cylindrical shells under wind loading". Proc. of Symp. on "Wind Effects on Buildings and Structures" Loughborough University of Technology, 1968.

8. Der, T. J. and Fidler, R. — "A model study of the buckling behaviour of hyperbolic shells". Proc. of Inst. of Civil Engnrs. Vol.41, Sept. 1968, pp 705 - 108.

9. Brave-Boy, G. K. and Johns, D. J. — "Static Stability of thin cylindrical shells under lateral pressure loading". Report TT 70 R 07, Loughborough University of Technology, Aug., 1970.

10. Alnajafi, A.M.J. — "Non-linear behaviour of cylindrical shells under lateral pressure loading". Report TT 7003, Oct., 1970. Loughborough University of Technology.

11. Ewing, D. J. F. — "The buckling and vibrations of cooling tower shells", Parts I and II. Central Electricity Research Laboratories, Leatherhead, C.E.G.B. RD/L/R 1763.

12. Wang, Y. and Billington, D.P. "Buckling of cylindrical shells by wind pressure". Proc. of A.S.C.E., J. of Engs. Mech.Division, EM5, Vol.100, Oct., 1974, pp 1005 - 1023.

13. Chian, A.S.L. and Firmin, A. "The analysis of cooling towers by the matrix finite element method". Part II, -Large displacements. The Aeronautical Journal of the Royal Aero. Soc., Vol.74, Dec., 1970, pp 971 - 983.

14. Martin, D. W. and Scriven, W.E. "Calculation of membrane strains in hyperbolic cooling towers". Proc. of Inst. Civil Engnrs., Vol. 19, Aug., 1961, pp 503 - 514

15. Martin, D. W. Maddock, J. S. and Scriven, W. E. "Membrane displacements in hyperbolic cooling towers due to wind and dead loading". Proc.Inst.Civil Engnrs., Vol.28, July, 1964, pp 327 - 337.

16. Albasiny, E. L. and Martin, D. W. "Bending and membrane equilibrium in cooling towers". J. of Engng. Mech. Division, Proc. of A.S.C.E., EM3, Vol. 93, June 1967, pp 1 - 17.

17. Vlasov, V. Z. "General theory of shells and its application in Engineering". NASA N. 64 - 19883, Washington, D.C., 1964.

18. Krajicinovic, D. "Semi-membrane analysis of cylindrical shells subjected to wind loading". J. of Appl. Mech., Trans. of A.S.M.E., Vol.37, Dec. 1970, pp 995 - 1001.

19. Rish, R. F. "Forces in cylindrical shells due to wind". Proc. of Inst. of Civil Engnrs., Vol. 36, April, 1967, pp 791 - 803.

20. Billington, D. P. and Yung-Shih Wang "A simplified theory of thin cylindrical shells". Proc. of A.S.C.E., J. of Engs., Mech. Division, EM-4, Vol.100, Aug., 1974, pp 719 - 735.

21. Tanniru, V. N. "Discussion on 'Cantilever cylindrical shells under assumed wind load' ". Proc. of A.S.C.E., J. of Engs., Mech. Division, EM-6, Vol.100, Dec., 1974. pp 1256 - 1261.

22. Donnell, L. H. "Stability of thin walled tubes under torsion". N.A.C.A. Report No. 479, Washington, D.C., 1933.

23. Moe, J. "On the theory of cylindrical shells - explicit solution of the characteristics equation and discussion of the accuracy of various shell theories". Int. Assoc. for Bridge and Struct. Engs. Vol.13, 1953, p 283.

24. Houghton, D. S. and Johns, D. J. "A comparison of the characteristic equations in the theory of circular cylindrical shells". The Aero. Quarterly, Vol. XII, Sept. 1961, pp 228 - 236.

25. Morris, A. J. "A comparison of solution in the first approximation shell theories". Quart. J.Mech.Appl.Math., Vol.XXVI, No. 1, 1973, pp 43 - 51.

26. Hoff, N. J. "The accuracy of Donnell's equations". J.of Appl. Mech., Vol. 22, No. 3, Sept. 1955, pp 329 - 334.

27. Kempner, J. "Remarks on Donnell's equations". J. of Appl. Mech. Vol. 22, No. 1, March, 1955, pp 117 - 118.

28. Hoff, N. J. "Boundary value problems of the thin walled circular cylinder". J.of Appl. Mech., Vol. 21, No. 4, Dec. 1954, pp 343 - 350.

29. Flugge, W. "Stresses in Shells". 4th printing, Springer - Verlag 1967.

30. Morley, L. S. D. "An improvement in Donnell's approximation for thin walled circular cylinders". Quart. J. Mech. Appl. Math., Vol. 12, 1959, pp 89 - 99.

31. Koiter, W. T. "A consistent first approximation in the general theory of thin elastic shells". Proc. of IUTAM Symp. on the theory of thin elastic shells. North Holland publishing Co., Amsterdam, 1960, pp 12 - 33.

32. Sanders, J. L. "An improved first approximation theory for thin shells". N.A.S.A. Report R.24, 1959.

33. Roshko, A. "Experiments on the flow past a circular cylinder at high Reynolds numbers". J. of Fluid Mechanics, Vol. 10, No. 3, 1961, pp 345 - 356.

34. Gould W. R. E. Reymer, W. E. and Pensford, P. J. "Wind tunnel tests on chimneys of circular section at high Reynolds numbers". Symp. on Wind Effects on Buildings and Structures. Loughborough University of Technology, 1968.

35. Cowdrey, C. F. and O'Neil, P. G. "Reports of tests on a model cooling tower". N.P.L. Report, Aero. No. 316a, Dec., 1956.

36. Purdy, M. D. Moher, J. F. and Frederick, D. "Model studies of wind load on flat top cylinders". Proc. of A.S.C.E., J.of Struct. Division, Vol.93, No. 2, April, 1962, pp 379 - 395.

37. Maybrey, J. F. M. and Bryen D.W. Private Communication -

38. Gopalacharyulu,S. and Johns, D. J. "Cantilever cylindrical shells under assumed wind pressure". J.of Engs. Mech. Division, Proc. of A.S.C.E., EM-5, Oct., 1973, pp 943 - 956.

39. Prabhu, K. S. Gopalacharyulu,S. and Johns, D. J. "Cantilever cylindrical shells under wind load". Trans. of A.S.M.E., J.of Appl.Mech., Vol. 42, No. 1, March, 1975, pp 233 - 234.

40. Timoshenko, S. and Gere, J. H. "Theory of elastic stability". McGraw-Hill Book Co., Inc., 1961.

41. Nash, W. A. "Buckling of thin cylindrical shells subjected to Hydrostatic pressure". J.of Aero.Sci., Vol. 21, 1954, pp 354 - 355.

42. "Collected papers on Instability of shell structures", 1962. N.A.S.A. TN D1510, Langley Research Center, Hampton, Virginia.

43. Almroth, B. O. and Brush, D. O. "Buckling of a finite length cylindrical shell under a circumferential Band of pressure". J.of Aero.Space Sci. Vol. 28, July, 1961, pp 573 - 579.

44. Maderspach, V. Gaunt, J. T. and Sword, J. H. "Buckling of cylindrical shells due to wind loading". College of Engineering, Virginia Polytechnic Institute and State University, Report VPI - E - 71 - 25, Oct., 1971.

45. Bushnell, D. "Stress, stability and vibration of complex branched shells of revolution". Analysis and users manual for BOSOR4 NASA CR-2116, Oct. 1972.

46. Shienmann, I. and Tene, Y. "Buckling of segmented shells of revolution subjected to symmetric and antisymmetric loads". A.I.A.A. Journal, Vol. 12, No. 1, Jan., 1974, pp 15 - 20

47. Gopalacharyulu, S. and Johns, D. J. "Buckling of thin clamped-free circular cylindrical shells subjected to wind load". Report TT 7113, Loughborough University of Technology, Dec., 1971.

48. Sobel, L. H. "Effect of boundary conditions on the stability of cylinders subjected to lateral and axial pressure". A.I.A.A. Journal, Vol. 2, No. 8, Aug. 1964, pp 1437 - 1440.

49. Gallatly, G. D. and Bart, R. "Effects of boundary conditions and initial out of roundness on the strength of thin walled cylinders subjected to external hydrostatic pressure". J. of Appl. Mech., Vol 23, No. 3, Sept. 1956, pp 351 - 358.

50. Singer, J. and Rosen, A. "The influence of boundary conditions on the buckling of stiffened cylindrical shells". AFOSR TR T.A.E. Report No. 213, Technion, Israel Institute of Technology, Haifa.

51. Heyman, B. "The stability of degenerate structures" Ph.D. thesis, University College, London, September, 1970.

52. Budiansky, B. and Pai, C. Hu "The Lagrangian multiplier method for finding upper and lower limits to critical stresses of clamped plates". NACA TN 1103, July, 1946.

53. Cole, P.P. "Buckling of hyperbolic cooling tower shells". Report No. 73 - SM - 2, Dept. of Civil and Geological Engs. Princeton University, Princeton, N.J., 1973.

54. Hiroyuki, A. "On the influence of prebuckling deformations on the buckling of thin elastic shells". Int. J. Of Non-linear mechanics, Vol. 8, No. 3, 1973, pp 409 - 430.

55. Yamaki, N. "Influence of prebuckling deformations on the buckling of circular cylindrical shells under external pressure". A.I.A.A. Journal, Vol. 7, 1969, pp 735 - 739.

56. Prabhu, K. S. Gopalacharyulu,S. and Johns, D. J. "Collapse of cylindrical shells under non-uniform external pressure". Aero. Soc. of India, Silver Jubilee Tech. Conference, Bangalore, 1974.

57. Prabhu, K. S. Gopalacharyulu, S. and Johns, D. J. "Stability of cantilever shells under wind loads". To appear in Proc. of A.S.C.E., J.of Engs. Mech. Division, Oct., 1975.

58. Grafton, P. E. and Strome, D. R. "Analysis of axisymmetric shells by direct stiffness method". A.I.A.A. Journal, Vol. 1, No. 10, Oct., 1963, pp 2342 - 2347.

59. Klien, S. "A study of matrix displacement method as applied to shells of revolution". AFFDL - TR - 80, Proc. of Conference on 'Matrix methods of structural analysis'. Airforce Flight Dynamic Laboratory, OHIO., 1965.

60. Percy, J. H. Pian, T. H. H. and Navaratna, D. R. "Application of matrix displacement method to linear elastic analysis of shells of revolution". A.I.A.A. Journal, Vol. 3, No. 11, Nov. 1965, pp 2138 - 2145.

61. Martin, H. C. "On the derivation of stiffness matrices for the analysis of large deflection and stability". AFFDL - TR - 66 - 80, Proc. of Conference on 'Matrix methods in structural analysis'. Wright-Patterson Airforce Base, Dayton, Ohio, Dec., 1965.

62. Mallett, R. H. and Marcel, P. V. "Finite element analysis of non-linear structures". Proc. of A.S.C.E., J. of Structural Division, Vol. 94, ST9, Sept. 1968, pp 2081 - 2105.

63. Gallagher, R. H. "The finite element method in shell stability analysis". Int. J. of computers and structures, Vol. 3, 1973, pp 543 - 557.

64. Gallagher, R. H. and Mau, S. T. "A Finite element procedure for non-linear prebuckling and initial post buckling analysis". N.A.S.A. CR-1936, Jan., 1972.

65. Striklin, J. A. Haisler, W. E. McDougall, H. R. and Stebbins, F. J. "Non-linear analysis of shells of revolution by the matrix displacement method". A.I.A.A. Journal Vol. 6, No. 12, Dec., 1968, pp 2306 - 2312.

66. Haisler, W. E. Striklin, J. A. and Stebbins, F. J. "Development and evolution of solution procedures for geometrically non-linear structural analysis by the direct stiffness method". A.I.A.A./A.S.M.E., 12th Structures, Structural Dynamics and Material Conference, Anahiem, California, April, 1971.

67. Argyris, J. H. "Recent advances in matrix method of structural analysis" - progress in Aeronautical Sciences, Vol. 4, Pergamon Press, 1964.

68. Pap, A.A. and Maderspach, V. "Critical buckling gas pressure of cylindrical shells with changing wall thickness". Report VPI - E - 70 - 12, Sept., 1970, College of Engineering, Virginia Polytechnic Institute and State University, Blacksburg, Virginia.

69. Alnajafi, A. M. J. and Warburton, G. B. "Free vibration of Ring Stiffened cylindrical shell". J. of Sound and Vibration, Vol. 13, No. 1, 1970, pp 9 - 25.

70. Scheubel, F. N. "Comments on wind effects on water cooling towers". Technische Hochschule Darmstadt, VGB, Kraftswerksten, Vol. 54, No. 6, June, 1974, pp 396 - 398.

71. Neimann, H. J. "Stationary wind loads on hyperbolic cooling towers". Proceedings of the 3rd International Conference on "Wind Effects on buildings and Structures", Tokyo, 1971.

72. Croll, J. G. A. "The Buckling of hyperbolic cooling towers under lateral loading". I.A.S.S. Conference, Session VII, Madrid, Sept. - Oct., 1969.

73. Weingarton, V. I. "Buckling of thin walled circular cylinders". NASA SP 8007, Aug., 1968.

74. Johns, D. J. "Static Stability of thin circular cylindrical shells under wind loading and uniform pressure loading". Report TT 71 R 08, Loughborough University of Technology.

75. "Vertical Steel Welded Storage tanks with butt welded shells for the petroleum Industry". BS 2654, 1973, British Standards Institution, London.

76. "Welded Steel Tanks for oil storage". API Standard 650, July, 1973, American Petroleum Institute, Washington, D.C.

77. Prabhu, K. S. Gopalacharyulu, S. and Johns, D. J. "Design criteria for stability of cylindrical shells subjected to wind load". Presented at the 4th International Conference on 'Wind Effects on Buildings and Structures", Sept., 1975, London.

78. Prabhu, K. S. Gopalachayulu, S. and Johns, D. J. "Stress and stability aspects of cylindrical structures subjected to wind loads". Presented at 2nd U.S. National Conference on Wind Engineering Research, Colorado, June, 1975.

79. Nataraja, R. "Response of thin walled cylinders to Aerodynamic excitation". Ph.D. Thesis, Loughborough University of Technology, 1974.

APPENDICES

APPENDIX-I

Least square method for representation of experimental data.

The application of least square method for analytical representation of experimental data is given in this appendix. The pressure data from Ref. (37) is represented by a double series consisting of polynomials in the axial direction and harmonics in the circumferential direction by this method. The coefficients in the double series are evaluated by the condition that the square of the total error in analytical representation of data over the complete surface of shell is minimum. The results obtained by this method for one particular set of data are also presented.

Let us consider that the pressure measurements are made at regular intervals both in the axial and circumferential directions, such that the points at which the measurements are made forms a regular grid on the surface of the shell. Let $\overline{P}_{ij}$ be the measured pressure at a discrete point (i, j) : where i being the counter for the point in the axial direction, and j being the counter for the point in circumferential direction. i.e. the pressure is measured at a total of $(i \times j)$ points. To represent the pressure in analytical form, we choose the double series as:

$$P = \sum_m \sum_n b_{mn} x^m \cos n\theta \qquad -(AI.1)$$

where P = pressure at any point on the surface of shell

b_{mn} - arbitrary constants to be evaluated.

The error in the representation of pressure by equn. (AI.1) at the discrete point (i, j) is

$$e_{ij} = \left[\overline{P}_{ij} - P(i,j) \right] \qquad -(AI.2)$$

$$= \left[\bar{P}_{ij} - \sum_m \sum_n b_{mn} x^m \cos n\theta \right]$$

The square of the total error in the pressure representation over the complete shell is obtained as

$$\sum_i \sum_j e_{ij}^2 = \sum_i \sum_j \left[\bar{P}_{ij} - \sum_m \sum_n b_{mn} x^m \cos n\theta \right]^2 \quad -(AI.3)$$

The coefficients b_{mn} are evaluated by the condition that square of the total error $\sum\sum e_{ij}^2$ given in equn.(AI.3) is minimum. This condition is achieved by minimising the above expression w.r.t. each coefficient as:

$$\frac{\partial}{\partial b_{mn}} \left(\sum_i \sum_j e_{ij}^2 \right) = 0 \quad -(AI.4)$$

This results in a set of linear algebraic equations of the form

$$\sum_i \sum_j \sum_m \sum_n \sum_r \sum_s b_{mn} x^{m+r} \cos n\theta_j \cos s\theta_j = \sum_i \sum_j \sum_m \sum_n \bar{P}_{ij} x_i^m \cos n\theta_j \quad -(AI.5)$$

The indices r and s vary over the same range as m and n respectively.

The indices m and n should be such that $m \leq i$, $n \leq j$.

As an example the pressure distribution measured on a shell with $L/a = 4.728$, $a/h = 149.0$ in turbulent shear flow at a velocity of V = 52.5 in/sec. is considered. These data are given in Table - AI-1; The measurements are made at 7 points in the axial direction and 24 points in the circumferential direction. The indices m and n are considered to vary between 0 to 3. and the indices n and j are considered to vary between 0 to 6. In Table AI-2 pressure coefficients obtained by the above procedures are presented.

This method can be very easily simplified for obtaining the pressure coefficients from experimental data. in which the axial variation is neglected. In this particular case all the terms containing x and the corresponding summations in equations (AI.1) to (AI.5) are neglected.

TABLE AI-1

PRESSURE DATA

Hole No.At → x / ↓ θ	1 0.022	2 0.1815	3 0.341	4 0.50	5 0.660	6 0.82	7 0.978
0	0.045	0.055	0.072	0.080	0.089	0.094	0.054
10	0.037	0.050	0.063	0.070	0.081	0.087	0.047
20	0.021	0.030	0.038	0.045	0.052	0.059	0.023
30	0.000	0.001	0.003	0.011	0.011	0.015	-0.008
40	-0.023	-0.033	-0.036	-0.033	-0.034	-0.036	-0.047
50	-0.049	-0.062	-0.068	-0.070	-0.074	-0.080	-0.088
60	-0.072	-0.085	-0.092	-0.099	-0.105	-0.114	-0.120
70	-0.087	-0.099	-0.102	-0.110	-0.118	-0.127	-0.133
75	-0.089	-0.100	-0.102	-0.107	-0.118	-0.124	-0.133
80	-0.089	-0.099	-0.100	-0.102	-0.112	-0.114	-0.131
85	-0.088	-0.097	-0.098	-0.098	-0.107	-0.109	-0.127
90	-0.087	-0.094	-0.096	-0.094	-0.103	-0.105	-0.120
95	-0.086	-0.091	-0.090	-0.091	-0.099	-0.100	-0.113
100	-0.080	-0.087	-0.087	-0.088	-0.096	-0.099	-0.105
105	-0.078	-0.084	-0.085	-0.087	-0.094	-0.096	-0.100
110	-0.077	-0.081	-0.083	-0.085	-0.091	-0.094	-0.097
115	-0.076	-0.080	-0.080	-0.084	-0.090	-0.092	-0.094
120	-0.074	-0.078	-0.078	-0.083	-0.089	-0.091	-0.092
130	-0.072	-0.076	-0.077	-0.080	-0.088	-0.089	-0.091
140	-0.070	-0.074	-0.076	-0.079	-0.087	-0.089	-0.089
150	-0.069	-0.073	-0.074	-0.077	-0.085	-0.089	-0.089
160	-0.069	-0.072	-0.074	-0.077	-0.085	-0.091	-0.091
170	-0.069	-0.072	-0.074	-0.076	-0.085	-0.091	-0.092
180	-0.069	-0.072	-0.074	-0.074	-0.085	-0.091	-0.095

TABLE AI-2

b_{mn} for m \ n	0	1	2	3	4	5	6
0	-0.0477	0.0445	0.0476	0.0278	0.0087	-0.0018	-0.0017
1	-0.0101	-0.0033	0.0066	0.0064	0.0026	0.0006	-0.0040
2	-0.0016	0.0071	0.000	-0.008	0.0009	0.0002	+0.0016
3	-0.0002	-0.0014	-0.0003	-0.0004	-0.0004	-0.0001	-0.0002

The coefficients b_{mn} for the above data

APPENDIX - II

Application of Semi-membrane theory for Cantilever cylindrical shells:

The analysis of cantilever cylindrical shells under non-uniform loads such as due to wind using the semi-membrane theory is presented here. The analysis is presented by Krajicinovic[18] : But as his analysis contains an error, the results given are not correct. The corrected analysis is presented here.

The external loading considered on the shell is

$$p_x = p_\theta = 0 \quad \text{and} \quad p_z = p_{z1} + p_{z2} \qquad -(A\text{II}\cdot 1)$$

where $p_{z1} = P \cos 2\theta \qquad -\frac{\pi}{4} \leq \theta \leq \pi/4$

$= 0 \qquad$ elsewhere

$p_{z2} = P/2 \cos 2\theta \qquad 0 \leq \theta \leq 2\pi$

This loading can be represented in the form

$$p_z = P \sum_n b_n \cos n\theta \qquad -(A\text{II}\cdot 2)$$

The values of the coefficients b_n are

$$b_0 = \frac{1}{2\pi} \quad b_1 = \frac{2\sqrt{2}}{3\pi} \quad b_2 = 3/4 \quad b_3 = \frac{2\sqrt{2}}{5\pi}$$

$$b_4 = \frac{1}{3\pi} \quad b_5 = \frac{2\sqrt{2}}{24\pi} \quad b_6 = 0 \quad b_7 = \frac{-2\sqrt{2}}{45\pi} \qquad -(A\text{II}\cdot 3)$$

$$b_8 = \frac{-1}{15\pi} \quad b_9 = \frac{-2\sqrt{2}}{77\pi} \quad b_{10} = 0 \quad b_{11} = \frac{-2\sqrt{2}}{117\pi}$$

Only the first eight harmonics are considered in the analysis as the coefficients for the higher harmonics are comparatively small.

The governing equation (2.11) given in section 2.4 is to be solved subjected to the boundary conditions

$$u = v = w = \frac{\partial w}{\partial x} = 0 \qquad \text{at } x = 0 \text{ the fixed edge} \qquad -(A\text{II}\cdot 4)$$

$$N_x = N_{x\theta} = 0 \qquad \text{at } x = L/a \text{ the free edge}$$

When the loading is represented by Fourier harmonics as in equn. AII.2 the solution for ϕ is also assumed as

$$\phi = \sum \phi_n \cos n\theta \qquad -(A\text{II}.5)$$

With this representation the governing equation and the boundary conditions reduce to

$$\frac{d^4\phi_n}{dx^4} + \frac{h^2}{12a^2} n^4 (1-n^2)^2 \phi_n + \frac{1-\nu^2}{Eh} n^2 b_n = 0 \qquad -(A\text{II}.6)$$

and $\phi_n = \frac{d\phi_n}{dn} = 0$ at $x=0$, $\frac{d^2\phi_n}{dx^2} = \frac{d^3\phi_n}{dx^3} = 0$ at $x = L/a$

The solution for the case $n=0$ is trivial and there are no stresses due to axisymmetric loading.

The solution for the case $n=1$ can be easily written as

$$\phi_1 = \frac{1-\nu^2}{Eh} a b_1 \left[x^4 - 4\bar{L}x^3 + 6x^2\bar{L}^2 \right] \qquad -(A\text{II}.7)$$

This can be easily identified to be the solution given by beam theory. For example the max. stress at the root is obtained as $N_{x\,max} = -\frac{b_1 L^2}{2}$ at $x=0$ which is the same as that given by beam theory.

The solution for all other harmonics ($n \geq 2$) can be developed in the form

$$\phi_n = A_1 \cosh \mu x \cos \mu x + A_2 \cosh \mu x \sin \mu x + A_3 \sinh \mu x \cos \mu x + A_4 \sinh \mu x \sin \mu x + G_n$$

where $\mu = \sqrt[4]{\frac{h^2 n^4 (1-n^2)^2}{48a^2}}$, $G_n = -\frac{(1-\nu^2) n^2 a b_n}{4Eh\mu^4}$ $\qquad -(A\text{II}.8)$

and A_1, A_2, A_3 and A_4 are arbitrary constants of integration. For the case of a cantilever shell, with the B.C. as in equn. (AII.6), these can be evaluated to be

$$A_1 = -G_n \qquad A_2 = -A_3$$

$$A_3 = \left[\frac{\cosh \mu\bar{L} \sinh \mu\bar{L} + \sin \mu\bar{L} \cos \mu\bar{L}}{\cos^2 \mu\bar{L} + \cosh^2 \mu\bar{L}} \right] \qquad -(A\text{II}.9)$$

$$A_4 = \left[\frac{\cosh^2 \mu\bar{L} - \cos^2 \mu\bar{L}}{\cosh^2 \mu\bar{L} + \cos^2 \mu\bar{L}} \right]$$

In the analysis presented by Krajicinovic[18], the expression for A_4 contains an error. Hence the results presented are invalid.

Knowing the function ϕ_n for each harmonic, the stresses can be calculated by using equn.(2.10) after summing over all the harmonics.

APPENDIX - III

Solution of Donnell's equations for non-uniform loads:

The solution of the Donnell shell equations for a cantilever cylindrical shell under non-uniform load is presented in this appendix. Following the general solution procedure given by Hoff [28], the problem has been analysed in Ref.(38). The external loading on the shell considered is

$$p_x = p_\theta = 0 \quad \text{and} \quad p_z = P_0 \sum_n b_n \cos n\theta \qquad -(A\text{III}\cdot 1)$$

When the external loading on the shell is represented by Fourier harmonics, the displacements can also be selected in a similar form as

$$\begin{aligned} u &= \sum_n u_n \cos n\theta \\ v &= \sum_n v_n \sin n\theta \\ w &= \sum_n w_n \cos n\theta \end{aligned} \qquad -(A\text{III}\cdot 2)$$

By this representation, the displacements u_n and v_n can be connected to w_n by the equn. 2.15.

The boundary conditions for the cantilever cylindrical shell are; at $x=0$, the fixed edge conditions $u=v=w=$ $-(A\text{III}\cdot 3)$ $\frac{dw}{dx}=0$ and at $x=L/a$, the free edge conditions $\sigma_x = \sigma_{x\theta} = M_x = Q_{x_{eff}} = 0$

The solution for axisymmetric component of loading is developed first as it is quite simple:

The differential equation reducesto (for $n=0$)

$$\frac{du_0}{dx} - \nu w_0 = 0$$

$$-(1-\nu^2) w_0 - \left(\frac{k}{D}\right) \frac{d^4 w_0}{dx^4} = \frac{P_0 b_0}{D} \qquad -(A\text{III}\cdot 4)$$

The boundary conditions become

$$w_0 = \frac{dw_0}{dx} = 0 \quad \text{at } x=0$$

$$\frac{d^2 w_0}{dx^2} = \frac{d^3 w_0}{dx^3} = 0 \quad \text{at } x = L/a$$

The solution can be easily written down as

$$w_0 = \frac{P_0 b_0}{D(1-\nu^2)} \left[\begin{array}{l} 1 - \cosh \mu x \cos \mu x + \\ A_1 (\sinh \mu x \cos \mu x - \cosh \mu x \sin \mu x) \\ + A_2 \sinh \mu x \sin \mu x \end{array} \right] \quad - (A\text{III}\cdot 5)$$

where $$\mu = \sqrt[4]{\frac{3(1-\nu^2)}{h^2}}$$

$$A_1 = \frac{\sinh \mu \bar{L} \cosh \mu \bar{L} + \sin \mu \bar{L} \cos \mu \bar{L}}{\cosh^2 \mu \bar{L} + \cos^2 \mu \bar{L}}$$

$$A_2 = \frac{\sinh^2 \mu \bar{L} + \sin^2 \mu \bar{L}}{\cosh^2 \mu \bar{L} + \cos^2 \mu \bar{L}}$$

The solution for other harmonics ($n \geq 1$): The particular solution can be developed for the displacements as:

$$u_p = 0 \qquad v_p = \sum v_{pn} \sin n\theta$$

$$w_p = \sum w_{pn} \cos n\theta \quad - (A\text{III}\cdot 6)$$

where $$v_{pn} = \lambda \frac{12(1-\nu^2) b_n}{n^5}$$

$$w_{pn} = \lambda \frac{12(1-\nu^2) b_n}{n^4}$$

and $$\lambda = \frac{P_0 a^3}{E h^3}$$

The homogeneous part of the solution is developed as in Hoff's[28] analysis. The characteristic roots are

$$\alpha_1 = \frac{1}{2}\left[\Omega + \mu + \frac{n^2}{\Omega}\right] \qquad \beta_1 = \frac{1}{2}\left[\Omega - \mu - \frac{n^2}{\Omega}\right]$$

$$\alpha_2 = \frac{1}{2}\left[\Omega - \mu + \frac{n^2}{\Omega}\right] \qquad \beta_2 = \frac{1}{2}\left[\Omega + \mu - \frac{n^2}{\Omega}\right]$$

where $$\Omega = \left\{ -\mu^2/2 + \sqrt{\frac{\mu^4}{4} + n^4} \right\}^{1/2} \quad - (A\text{III}\cdot 7)$$

The solution for each displacements can be written as

$$
\begin{aligned}
u = \sum_n \frac{1}{2\mu^2} \Big[& -A_1 (N_1' \cos\beta_1 x + N_1 \sin\beta_1 x) e^{-\alpha_1 x} \\
& + A_2 (N_1 \cos\beta_1 x - N_1' \sin\beta_1 x) e^{-\alpha_1 x} \\
& + A_3 (N_2' \cos\beta_2 x + N_2 \sin\beta_2 x) e^{-\alpha_2 x} \\
& + A_4 (N_2 \cos\beta_2 x - N_2' \sin\beta_2 x) e^{-\alpha_2 x} \\
& + A_5 (N_1' \cos\beta_1 x - N_1 \sin\beta_1 x) e^{\alpha_1 x} \\
& - A_6 (N_1 \cos\beta_1 x + N_1' \sin\beta_1 x) e^{\alpha_1 x} \\
& + A_7 (N_2' \cos\beta_2 x - N_2 \sin\beta_2 x) e^{\alpha_2 x} \\
& - A_8 (N_2 \cos\beta_2 x + N_2' \sin\beta_2 x) e^{\alpha_2 x} \Big] \cos n\theta
\end{aligned}
\qquad - (A\text{III}\cdot 8a)
$$

$$
\begin{aligned}
v = \sum_n \Big\{ \frac{n}{2\mu^2} \Big[& A_1 (M_1' \cos\beta_1 x + M_1 \sin\beta_1 x) e^{-\alpha_1 x} \\
& - A_2 (M_1 \cos\beta_1 x - M_1' \sin\beta_1 x) e^{-\alpha_1 x} \\
& + A_3 (M_2' \cos\beta_2 x + M_2 \sin\beta_2 x) e^{-\alpha_2 x} \\
& - A_4 (M_2 \cos\beta_2 x - M_2' \sin\beta_2 x) e^{-\alpha_2 x} \\
& + A_5 (M_1' \cos\beta_1 x - M_1 \sin\beta_1 x) e^{\alpha_1 x} \\
& - A_6 (M_1 \cos\beta_1 x + M_1' \sin\beta_1 x) e^{\alpha_1 x} \\
& + A_7 (M_2' \cos\beta_2 x - M_2 \sin\beta_2 x) e^{\alpha_2 x} \\
& - A_8 (M_2 \cos\beta_2 x + M_2' \sin\beta_2 x) e^{\alpha_2 x} \Big] \\
& + v_{pn} \Big\} \sin n\theta
\end{aligned}
\qquad - (A\text{III}\cdot 8b)
$$

$$
\begin{aligned}
w = \sum_n \Big[& (A_1 \cos\beta_1 x + A_2 \sin\beta_1 x) e^{-\alpha_1 x} \\
& + (A_3 \cos\beta_2 x + A_4 \sin\beta_2 x) e^{-\alpha_2 x} \\
& + (A_5 \cos\beta_1 x - A_6 \sin\beta_1 x) e^{\alpha_1 x} \\
& + (A_7 \cos\beta_2 x - A_8 \sin\beta_2 x) e^{\alpha_2 x} \\
& + w_{pn} \Big] \cos n\theta
\end{aligned}
\qquad - (A\text{III}\cdot 8c)
$$

where

$$
N_1 = \left[\frac{n^2}{\alpha_1^2 + \beta_1^2} + \nu \right] \alpha_1 \quad , \qquad N_1' = \left[\frac{n^2}{\alpha_1^2 + \beta_1^2} - \nu \right] \beta_1
$$

$$N_2 = \left[\frac{n^2}{\alpha_2^2+\beta_2^2} + \nu\right]\alpha_2 , \qquad N_2' = \left[\frac{n^2}{\alpha_2^2+\beta_2^2} - \nu\right]\beta_2$$

$$M_1 = \frac{n^2(\alpha_1^2-\beta_1^2)}{(\alpha_1^2+\beta_1^2)^2} - (2+\nu), \qquad M_1' = \frac{2n^2\alpha_1\beta_1}{(\alpha_1^2+\beta_1^2)^2}$$

$$M_2 = \frac{n^2(\alpha_2^2-\beta_2^2)}{(\alpha_2^2+\beta_2^2)^2} - (2+\nu), \qquad M_2' = \frac{2n^2\alpha_2\beta_2}{(\alpha_2^2+\beta_2^2)^2}$$

Using the equn.(2.12), (2.3) and (2.13), and making use of certain properties of roots given by Hoff, the required stresses and moments can be written as

$$\begin{aligned}\sigma_x = \sum_n \frac{En^2}{2\mu^2}\Big[&(A_1 \sin\beta_1 x - A_2\cos\beta_1 x)\, e^{-\alpha_1 x} \\ &+ (A_3 \sin\beta_2 x - A_4\cos\beta_2 x)\, e^{-\alpha_2 x} \\ &- (A_5 \sin\beta_1 x + A_6\cos\beta_1 x)\, e^{\alpha_1 x} \\ &- (A_7 \sin\beta_2 x + A_8\cos\beta_2 x)\, e^{\alpha_2 x}\Big]\cos n\theta\end{aligned} \qquad - (A\,III\cdot 9a)$$

$$\begin{aligned}\sigma_{x\theta} = \sum_n \frac{En^2}{2\mu^2}\Big[&-A_1(\beta_1\cos\beta_1 x - \alpha_1\sin\beta_1 x)\, e^{-\alpha_1 x} \\ &- A_2(\alpha_1\cos\beta_1 x + \beta_1\sin\beta_1 x)\, e^{-\alpha_1 x} \\ &- A_3(\beta_2\cos\beta_2 x - \alpha_2\sin\beta_2 x)\, e^{-\alpha_2 x} \\ &- A_4(\alpha_2\cos\beta_2 x + \beta_2\sin\beta_2 x)\, e^{-\alpha_2 x} \\ &+ A_5(\beta_1\cos\beta_1 x + \alpha_1\sin\beta_1 x)\, e^{\alpha_1 x} \\ &+ A_6(\alpha_1\cos\beta_1 x - \beta_1\sin\beta_1 x)\, e^{\alpha_1 x} \\ &+ A_7(\beta_2\cos\beta_2 x + \alpha_2\sin\beta_2 x)\, e^{\alpha_2 x} \\ &+ A_8(\alpha_2\cos\beta_2 x - \beta_2\sin\beta_2 x)\, e^{\alpha_2 x}\Big]\sin n\theta\end{aligned} \qquad - (A\,III\cdot 9b)$$

$$\begin{aligned}M_x = \frac{D}{a}\sum_n \Big[&A_1(\psi_1\cos\beta_1 x - \psi_1'\sin\beta_1 x)\, e^{-\alpha_1 x} \\ &+ A_2(\psi_1'\cos\beta_1 x + \psi_1\sin\beta_1 x)\, e^{-\alpha_1 x}\end{aligned}$$

$$+ A_3(\psi_2 \cos\beta_2 x - \psi_2' \sin\beta_2 x)\, e^{-\alpha_2 x}$$
$$+ A_4(\psi_2' \cos\beta_2 x + \psi_2 \sin\beta_2 x)\, e^{-\alpha_2 x}$$
$$+ A_5(\psi_1 \cos\beta_1 x + \psi_1' \sin\beta_1 x)\, e^{\alpha_1 x}$$
$$+ A_6(\psi_1' \cos\beta_1 x - \psi_1 \sin\beta_1 x)\, e^{\alpha_1 x}$$
$$+ A_7(\psi_2 \cos\beta_2 x + \psi_2' \sin\beta_2 x)\, e^{\alpha_2 x}$$
$$+ A_8(\psi_2' \cos\beta_2 x - \psi_2 \sin\beta_2 x)\, e^{\alpha_2 x}$$
$$+ \nu n^2 \omega_{pn}\Big] \cos n\theta \qquad -(A\text{III}\cdot 9c)$$

$$Q_{x\,eff} = \left(-\frac{D}{a^2}\right) \sum \Big[A_1(-\theta_1 \cos\beta_1 x + \theta_1' \sin\beta_1 x)\, e^{-\alpha_1 x}$$
$$+ A_2(-\theta_1' \cos\beta_1 x - \theta_1 \sin\beta_1 x)\, e^{-\alpha_1 x}$$
$$+ A_3(-\theta_2 \cos\beta_2 x + \theta_2' \sin\beta_2 x)\, e^{-\alpha_2 x}$$
$$+ A_4(-\theta_2' \cos\beta_2 x - \theta_2 \sin\beta_2 x)\, e^{-\alpha_2 x}$$
$$+ A_5(\theta_1 \cos\beta_1 x + \theta_1' \sin\beta_1 x)\, e^{\alpha_1 x}$$
$$+ A_6(\theta_1' \cos\beta_1 x - \theta_1 \sin\beta_1 x)\, e^{\alpha_1 x}$$
$$+ A_7(\theta_2 \cos\beta_2 x + \theta_2' \sin\beta_2 x)\, e^{\alpha_2 x}$$
$$+ A_8(\theta_2' \cos\beta_2 x - \theta_2 \sin\beta_2 x)\, e^{\alpha_2 x}\Big] \cos n\theta$$
$$-(A\text{III}\cdot 9d)$$

where

$$\psi_1 = \nu n^2 - \alpha_1^2 + \beta_1^2 \qquad \psi_1' = 2\alpha_1\beta_1$$
$$\psi_2 = \nu n^2 - \alpha_2^2 + \beta_2^2 \qquad \psi_2' = 2\alpha_2\beta_2$$
$$\theta_1 = \alpha_1^3 - 3\alpha_1\beta_1^2 - \alpha_1 n^2(2-\nu)$$
$$\theta_1' = \beta_1^3 - 3\alpha_1^2\beta_1 + (2-\nu) n^2 \beta_1$$
$$\theta_2 = \alpha_2^3 - 3\alpha_2\beta_2^2 - (2-\nu) n^2 \alpha_2$$
$$\theta_2' = \beta_2^3 - 3\alpha_2^2\beta_2 + (2-\nu) n^2 \beta_2$$

Using these equations the required eight equations for determining the eight constants A_1 to A_8 are obtained. These constants are evaluated for each harmonics; Adding these solutions to that of the uniform component the total solution is obtained from which the complete stress pattern can be determined.

To consider other possible boundary conditions and the case of supports which behave like springs, the following procedure is adopted in numerical work. The boundary conditions at the two ends of the shell are written as

$$\left.\begin{aligned} &C_{11}\, u(0) + C_{12}\, N_x(0) = 0 \\ &C_{21}\, v(0) + C_{22}\, N_{x\theta}(0) = 0 \\ &C_{31}\, w(0) + C_{32}\, Q_x(0) = 0 \\ &C_{41}\, \frac{\partial w(0)}{\partial x} + C_{42}\, M_x(0) = 0 \end{aligned}\right\} \quad \text{at } x = 0 \qquad -(A\text{III}\cdot 10)$$

$$\left.\begin{aligned} &C_{51}\, M_x(\bar{L}) + C_{52}\, \frac{\partial w(\bar{L})}{\partial x} = 0 \\ &C_{61}\, Q_x(\bar{L}) + C_{62}\, w(\bar{L}) = 0 \\ &C_{71}\, N_x(\bar{L}) + C_{72}\, u(\bar{L}) = 0 \\ &C_{81}\, N_{x\theta}(\bar{L}) + C_{82}\, v(\bar{L}) = 0 \end{aligned}\right\} \quad \text{at } x = L/a = \bar{L}$$

By this representation, to obtain the case of cantilever shell, the constants C_{ij} are selected as

$$C_{i1} = 1 \quad \text{and} \quad C_{i2} = 0 \quad \text{for } i = 1, 8 \qquad -(A\text{III}\cdot 11)$$

For the case of a simply supported shell, the coefficients are

$$C_{21} = C_{31} = C_{51} = C_{71} = C_{12} = C_{42} = C_{62} = C_{82} = 1.0$$

and

$$C_{11} = C_{41} = C_{61} = C_{81} = C_{22} = C_{32} = C_{52} = C_{72} = 0.0 \qquad -(A\text{III}\cdot 12)$$

Similarly by suitably choosing the values of coefficients all other possible boundary conditions can be represented.

When the shell is considered to be supported on the springs at the ends the values of the coefficients C_{ij} will be between 0 and 1.

When the cantilever cylindrical shell is considered to be supported at the base, which imparts both axial and rotational stiffnesses, these conditions are written as

$$\left(\frac{C_{11}}{C_{12}}\right) u(0) + N_x(0) = 0 \qquad -(A\,III\cdot 13)$$

$$\left(\frac{C_{41}}{C_{42}}\right) \frac{\partial w(0)}{\partial x} + M_x(0) = 0$$

where the coefficients (C_{11}/C_{12}) and (C_{41}/C_{42}) can be regarded as the spring constants. By this representation, if (C_{11}/C_{12}) and $(C_{41}/C_{42}) \to 0$, one has the case of simply supported end: and if (C_{11}/C_{12}) and $(C_{41}/C_{42}) \to \infty$ one has the case of fixed edge. This representation of end conditions is made use of not only in determining the stresses but also in buckling analysis.

APPENDIX - IV

Solution of Flugge's shell equations for a cantilever shell under non-uniform load:-

The solution of the Flugge's shell equations for a cantilever cylindrincal shell given in equation (2.17) will be developed for the case of non-uniform load. The external loading on the shell is again considered as

$$p_x = p_\theta = 0 \qquad \text{and}$$
$$p_z = P_0 \sum b_n \cos n\theta \qquad \text{(A IV.1)}$$

As a result the displacements can be selected as

$$u = \sum u_n \cos n\theta$$
$$v = \sum v_n \sin n\theta \qquad \text{(A IV.2)}$$
$$w = \sum w_n \cos n\theta$$

When the displacements are represented by Fourier harmonics, the governing differential equations (2.17) reduce to a set of ordinary differential equations for each harmonic as

$$\frac{d^2u_n}{dx^2} - \frac{(1-\nu)}{2} n^2 (1+\bar{k})\, u_n + \frac{1+\nu}{2} n \frac{dv_n}{dx} + \nu \frac{dw_n}{dx} - \bar{k}\left[\frac{d^3w_n}{dx^3} + \left(\frac{1-\nu}{2}\right) n^2 \frac{dw_n}{dx}\right] = 0 \qquad \text{(A IV.3)}$$

$$-\frac{(1+\nu)}{2} n \frac{du_n}{dx} - n^2 v_n + \left(\frac{1-\nu}{2}\right)(1+3\bar{k}) \frac{d^2v_n}{dx^2} - n w_n + \bar{k}\left(\frac{3-\nu}{2}\right) n \frac{d^2w_n}{dx^2} = 0$$

$$\nu \frac{du_n}{dx} + n v_n + w_n + \bar{k}\left[-\frac{(1-\nu)}{2} n^2 \frac{du_n}{dx} - \frac{d^3 u_n}{dx^3} - \left(\frac{3-\nu}{2}\right) n \frac{d^2 v_n}{dx^2} + \right.$$

$$\left. \frac{d^4 w_n}{dx^4} - 2n^2 \frac{d^2 w_n}{dx^2} + n^4 w_n - 2n^2 w_n + w_n \right] = \frac{P_0 b_n}{D}$$

where

$$\bar{k} = k/D$$

For the case of cantilever cylindrical shell, these equations are to be solved subjected to the boundary conditions

$$u(0) = 0$$

$$v(0) = 0$$

$$w(0) = 0 \qquad \text{at } x = 0$$

$$\frac{\partial w(0)}{\partial x} = 0 \qquad \text{(A IV.4)}$$

and

$$N_x(\bar{L}) = 0 \qquad \text{at } x = \bar{L} = L/a$$

$$M_x(\bar{L}) = 0$$

$$Q_{xef} = Q_x(\bar{L}) + \frac{\partial M_{x\theta}(\bar{L})}{\partial \theta} = 0$$

$$T(\bar{L}) = N_{x\theta}(\bar{L}) - \frac{M_{x\theta}(\bar{L})}{a} = 0$$

As the solution of these equations for the case of axisymmetric component of load (b_0) and for the case $n = 1$ are of different form, as compared with other harmonics, they will be developed first.

Solution for the axisymmetric loading ($n=0$):

For this case $v \equiv 0$ and the equations (A IV.3) reduce to

$$\frac{d^2 u(0)}{dx^2} + \nu \frac{dw_0}{dx} - \bar{k} \frac{d^3 w_0}{dx^3} = 0 \qquad \text{(A IV.5)}$$

$$\nu \frac{du_0}{dx} + w_0 + \bar{k}\left[-\frac{d^3 u_0}{dx^3} + \frac{d^4 w_0}{dx^4} + w_0\right] = \frac{P_0 b_0}{D}$$

Eliminating u_0, this becomes

$$\frac{d^4 w_0}{d x^4} + 2 c_1^2 \frac{d^2 w_0}{d x^2} + c_2^4 w_0 = \frac{P_0 b_0}{k(1-\bar{k})} \quad \text{—(A IV.6)}$$

where $c_1^2 = \frac{\nu}{1-\bar{k}}$ and $c_2^4 = \frac{1-\nu+\bar{k}}{\bar{k}(1-\bar{k})}$

The solution for w_0 can be written as

$$w_0 = A_1 \cosh \alpha_1 x \cos \beta_1 x + A_2 \cosh \alpha_1 x \sin \beta_1 x + A_3 \sinh \alpha_1 x \cos \beta_1 x + A_4 \sinh \alpha_1 x \sin \beta_1 x + G \quad \text{— (A IV.7)}$$

where $\alpha_1 = \sqrt{\frac{c_2^2 - c_1^2}{2}}$, $\beta_1 = \sqrt{\frac{c_2^2 + c_1^2}{2}}$

and $G = \frac{P_0}{k} \frac{n^2 b_0}{(1-\nu^2+\bar{k})}$

The constants of integration A_1 to A_4 are evaluated by the conditions $w_0(0) = \frac{d w(0)}{d x} = 0$ at $x = 0$

and $M_x(\bar{L}) = Q_{xef}(\bar{L}) = 0$ at $x = \bar{L} = L/a$

Solutions for the harmonic $n = 1$:

The governing differential equation for this case can be written, after eliminating u_1 and v_1, as

$$\frac{d^4}{d x^4}\left[\frac{d^4 w_1}{d x^4} - 2(2-\nu)\frac{d^2 w_1}{d x^2} + \frac{1-\nu^2}{\bar{k}} w_1\right] = \frac{P_0 b_1}{k} \quad \text{(A IV.8)}$$

The displacement u_1 and v_1 can be related to w_1 as

$$\nabla^4 u_1 = -\nu \frac{d^3 w_1}{d x^3} - \frac{d w_1}{d x} \quad \text{(A IV.9)}$$

$$\nabla^4 v_1 = (2+\nu)\frac{d^2 w_1}{dx^2} - w_1$$

The particular solution for these equations can be written as

$$\begin{aligned} w_{1p} &= \lambda \frac{\bar{k} b_1}{2} x^4 \\ u_{1p} &= -\lambda \bar{k} b_1 \left[12(2+\nu)x + 2x^3\right] \\ v_{1p} &= -\lambda \bar{k} b_1 \left[12(1+2\nu) + 6\nu x^2 - \frac{x^4}{2}\right] \end{aligned} \qquad \text{(A IV.10)}$$

The homogeneous part of the solution is written as

$$\begin{aligned} u_1 = {} & A_1 X_1 + A_2 X_2 + A_3 X_3 + A_4 X_4 + A_5 + \\ & A_6 x + A_7 x^2 + A_8 x^3 \\ v_1 = {} & B_1 X_1 + B_2 X_2 + B_3 X_3 + B_4 X_4 + B_5 + \\ & B_6 x + B_7 x^2 + B_8 x^3 \\ w_1 = {} & C_1 X_1 + C_2 X_2 + C_3 X_3 + C_4 X_4 + C_5 + \\ & C_6 x + C_7 x^2 + C_8 x^3 \end{aligned} \qquad \text{(A IV.11)}$$

where

$$\begin{aligned} X_1 &= \cosh \alpha_1 x \cos \beta_1 x \\ X_2 &= \cosh \alpha_1 x \sin \beta_1 x \\ X_3 &= \sinh \alpha_1 x \cos \beta_1 x \\ X_4 &= \sinh \alpha_1 x \sin \beta_1 x \end{aligned}$$

$$\alpha_1 = \sqrt{\frac{\sqrt{\frac{1-\nu^2}{\bar{k}}} + 2 - \nu}{2}} \qquad \beta_1 = \sqrt{\frac{\sqrt{\frac{1-\nu^2}{\bar{k}}} - (2-\nu)}{2}}$$

The constants A_1 to A_8 and B_1 to B_8 are related to the constants C_1 to C_8 by the equations of equilibrium (A IV.9). The constants C_1 to C_8 are evaluated by using the boundary conditions in equation (A IV.4).

Solution for other harmonics ($n \geq 2$):

The solution of Flugge's set of differential equations is developed in a general form as sum of complementary function and particular Integral.

The particular Integrals for the loading considered are

$$u_{pn} = 0$$

$$v_{pn} = -12(1-\nu^2)\,\lambda\,\frac{b_n}{n(n^2-1)} \qquad \text{(A IV.12)}$$

$$w_{pn} = -12(1-\nu^2)\,\lambda\,\frac{b_n}{(n^2-1)}$$

The complimentary functions for the homogeneous part of the equations (A IV.3) can be written after calculating the characteristic roots and adding this to the particular solution, we have the total solution as

$$u_n = A_{1n}X_{1n} + A_{2n}X_{2n} + A_{3n}X_{3n} + A_{4n}X_{4n} + A_{5n}X'_{1n} + A_{6n}X'_{2n} + A_{7n}X'_{3n} + A_{8n}X'_{4n} + u_{pn}$$

$$v_n = B_{1n}X_{1n} + B_{2n}X_{2n} + B_{3n}X_{3n} + B_{4n}X_{4n} + B_{5n}X'_{1n} + B_{6n}X'_{2n} + B_{7n}X'_{3n} + B_{8n}X'_{4n} + v_{pn}$$

$$w_n = C_{1n}X_{1n} + C_{2n}X_{2n} + C_{3n}X_{3n} + C_{4n}X_{4n} + C_{5n}X'_{1n} + C_{6n}X'_{2n} + C_{7n}X'_{3n} + C_{8n}X'_{8n} + w_{pn}$$

where

$$X_{1n} = \cosh\alpha_{1n}x\,\cos\beta_{1n}x \qquad \text{(A IV.13)}$$

$$X_{2n} = \cosh\alpha_{1n}x\,\sin\beta_{1n}x$$

$$X_{3n} = \sinh\alpha_{1n}x\,\cos\beta_{1n}x$$

$$X_{4n} = \sinh\alpha_{1n}x\,\sin\beta_{1n}x$$

$$X'_{1n} = \cosh\alpha_{2n}x\,\cos\beta_{2n}x$$

$$X'_{2n} = \cosh\alpha_{2n}x\,\sin\beta_{2n}x$$

$$X'_{3n} = \sinh \alpha_{2n} x \cos \beta_{2n} x$$

$$X'_{4n} = \sinh \alpha_{2n} x \sin \beta_{2n} x$$

α_{1n}, β_{1n}, α_{2n} and β_{2n} are the real and imaginary parts of the two sets of complex conjugate roots of the characteristic equation.

The coefficients A_{1n} to A_{8n}, B_{1n} to B_{8n} and C_{1n} to C_{8n} are related to each other by the equations of equilibrium (A IV.3) and this yields sixteen equations. Eight further equations are written down by the boundary conditions (A IV.4). Solving these twenty four equations, the arbitrary constants A_{in}, B_{in} and C_{in} ($i = 1,8$) are evaluated, and thus the displacements are determined. Knowing the displacements, the stress resultants are calculated from equation (2.16) for the particular harmonic considered. The total stresses in the shell are obtained by summing over all the harmonics.

General form of the particular solution:

When the external loading on the shell is represented as in equation (2.1), it will be very convenient to write the particular solution for each term.

For the case of axisymmetric loading ($n = 0$) the loading can be written as

$$P = P_0 \sum_{m=0}^{3} b_{m0} x^m$$

The particular solution from equation (A IV.6) is

$$\omega_{P_0} = \frac{P_0}{k} \frac{\bar{k}}{(1-\nu^2+\bar{k})} \left[\sum_{m=0}^{3} b_{m0} x^m - \frac{2\nu\bar{k}}{1-\nu^2+\bar{k}} (2 b_{00} + 6 b_{10} x) \right] \quad \text{— (A IV.14)}$$

For all other harmonics the particular solution is written as

$$u_p = \lambda\, 12(1-\nu^2) \sum_m \sum_n b_{mn} X_1 \cos n\theta$$
$$v_p = \lambda\, 12(1-\nu^2) \sum_m \sum_n b_{mn} X_2 \sin n\theta \qquad \text{(A IV.15)}$$
$$w_p = \lambda\, 12(1-\nu^2) \sum_m \sum_n b_{mn} X_3 \cos n\theta$$

The functions X_1, X_2 and X_3 are of different form for the harmonic one, and hence they are given in a seperate table below.

m ↓	X_1	X_2	X_3
0	$12x(2+\nu) + 2x^3$	$12(2+\nu) + 6\nu x^2 - \frac{x^4}{2}$	$\frac{x^4}{2}$
1	$12(3+2\nu) + 6x^2(2+\nu) + \frac{x^4}{2}$	$12x(1+2\nu) - 2\nu x^3 - \frac{x^5}{10}$	$\frac{x^5}{10}$
2	$24x(3+2\nu) + 4x^3(2+\nu) + x^5/5$	$48(1+\nu) + 12x^2(1+2\nu) + \nu x^4 - \frac{x^6}{30}$	$\frac{x^6}{30}$
3	$72(4+3\nu) + 36x^2(3+2\nu) + 3x^4(2+\nu) + \frac{x^6}{10}$	$48x(1+\nu) + 12x^3(1+2\nu) + \frac{3}{5}\nu x^5 - \frac{x^7}{70}$	$\frac{x^7}{70}$

particular Integrals for harmonic $n = 1$

The functions in the particular solution for all other harmonics ($n \geq 2$) is written as

$$X_1 = \sum_{i=0}^{3} a_{i1} x^i$$
$$X_2 = \sum_{i=0}^{3} a_{i2} x^i \qquad \text{(A IV.16)}$$
$$X_3 = \sum_{i=0}^{3} a_{i3} x^i$$

The constants a_{ij} are evaluated in terms of b_{mn} and these are given in the table below.

$i \downarrow$	a_{i1}	a_{i2}	a_{i3}
3	0	$\frac{-b_{3n}}{n(n^2-1)^2}$	$\frac{b_{3n}}{(n^2-1)^2}$
2	$\frac{-3(1+\bar{K}n^2)\,b_{3n}}{(1+\bar{K})n^2(n^2-1)^2}$	$\frac{-b_{2n}}{n(n^2-1)^2}$	$\frac{b_{2n}}{(n^2-1)^2}$
1	$\frac{-2(1+\bar{K}n^2)\,b_{2n}}{(1+\bar{K})n^2(n^2-1)^2}$	$-\frac{a_{13}+6\Omega_2 a_{33}}{n}$	$\frac{b_{1n}}{(n^2-1)^2} - \frac{6\Omega_1 b_{3n}}{\bar{K}(n^2-1)^4}$
0	$-\frac{(1+\bar{K}n^2)\,a_{23}}{n^2(1+\bar{K})} + \frac{12\,a_{33}}{(1-\nu^2)n^2(1+\bar{K})}\left[\frac{1+\nu}{2}\Omega_2 - \bar{K} - \frac{1+\bar{K}n^2}{n^2(1+\bar{K})}\right]$	$\frac{2\Omega_2 a_{23} - a_{03}}{n}$	$\frac{b_{0n}}{(n^2-1)^2} - \frac{2\Omega_1 a_{23}}{\bar{K}(n^2-1)^2}$

where

$$\Omega_1 = \left[\frac{1-\nu}{2}\,\frac{(1+\bar{K}n^2)^2}{n^2(1+\bar{K})} - \frac{1-\nu}{2n^2}(1+3\bar{K}) - 2n^2\bar{K}\right]$$

$$\Omega_2 = \left[\frac{1+\nu}{2}\,\frac{1+\bar{K}n^2}{n^2(1+\bar{K})} - \frac{1-\nu}{2n^2}(1+3\bar{K}) - \frac{\bar{K}(3-\nu)}{2}\right]$$

APPENDIX V

FUNCTIONS IN STABILITY DETERMINANT

The functions appearing in the stability determinant are given here in detail for the case of a clamped-free shell using the virtual displacement in Equation (3.12).

$$f_{11} = 2\pi\delta_{nj}\left(\frac{L}{a}\right)^{m+i+1}\left[\frac{mi}{(m+i-1)} + \left(\frac{1-\nu}{2}\right)\frac{nj}{(m+i+1)}\right]$$

$$f_{12} = \pi\delta_{nj}\left(\frac{L}{a}\right)^{m+i}\left[\frac{2\nu\, in}{(m+i)} - \frac{(1-\nu)\, jm}{(m+i)}\right]$$

$$\phi_{11} = \phi_{12} = 0$$

$$f_{13} = -\frac{2\pi\delta_{nj}\, i\,\nu}{(m+i+1)}\left(\frac{L}{a}\right)^{m+i+1}$$

$$\phi_{13} = (1-\nu)\frac{(m+1-i)}{(m+i+1)}\left(\frac{h}{a}\right)^{2}\left(\frac{L}{a}\right)^{m+i+1} RC(n,j)$$

$$f_{22} = \pi\delta_{nj}\left(\frac{L}{a}\right)^{m+i-1}\left[\frac{2nj}{m+i+1}L^{2} + \frac{(1-\nu)\, mi}{m+i-1}\right]$$

$$\phi_{22} = 2(1-\nu^{2})\left(\frac{h}{a}\right)^{2}\left(\frac{L}{a}\right)^{m+i+1}\frac{RS(n,j)}{m+i+1} +$$

$$2\nu\, SS(m+i+1,n,j) + 2\, TS(m+i+1,n,j) + G4(m+i+1)$$

$$f_{23} = -\frac{2\pi\delta_{nj}\, j}{m+i+2}\left(\frac{L}{a}\right)^{m+i+2}$$

$$\phi_{23} = -2(1-\nu^{2})\left(\frac{h}{a}\right)^{2}\left(\frac{L}{a}\right)^{m+i+2}\frac{n\, RS(n,j)}{m+i+2} -$$

$$2\nu n\, SS(m+i+1,n,j) - 2n\, TS(m+i+2,n,j) +$$

$$(1-\nu)(m+1)\, US(m+i+1,n,j) +$$

$$2\pi\delta_{nj}\, n(1-\nu^{2})\, G4(m+i+2).$$

$$f_{33} = \delta_{nj}\frac{\pi}{6}\left(\frac{h}{a}\right)^2\left\{\frac{mi\,(m+1)\,(i+1)}{(m+i-1)}\left(\frac{L}{a}\right)^{m+i-1} + \frac{(1-n^2)\,(1-j^2)}{(m+i+3)}\left(\frac{L}{a}\right)^{m+i+3} + \nu\frac{m(m+1)\,(1-j^2)}{(m+i+1)}\left(\frac{L}{a}\right)^{m+i+1} + \frac{2(1-\nu)(m+1)\,(i+1)\,nj}{(m+i+1)}\left(\frac{L}{a}\right)^{m+i+1} + \nu\frac{i\,(i+1\,(1-n^2)}{m+i+1}\left(\frac{L}{a}\right)^{m+i+1}\right\} + \frac{2\pi\delta_{nj}}{m+i+3}\left(\frac{L}{a}\right)^{m+i+3}$$

$$\Phi_{33} = 2(1-\nu^2)\left(\frac{h}{a}\right)^2(L/a)^{m+i+3}\frac{RC(n,j)}{m+i+3} +$$

$$2\nu nj\;SS(m+i+3,n,j) + 2(m+1)(i+1)\;SC(m+i+1,n,j)$$

$$+2nj\;TS(m+i+3,n,j) + 2\nu(m+1)(i+1)\;WS(m+i+1,n,j)$$

$$-(1-\nu)(m+i)\,j\;US(m+i+2,n,j)$$

$$-(1-\nu)(1+i)\,n\;US(m+i+2,j,n)$$

$$-2(1-\nu^2)\,\pi\,\delta_{nj}\;G4\,(m+i+3)$$

where

$$RS(n,j) = \sum_{n=0}^{6} b_n \int_0^{2\pi} \cos n\theta\;\sin j\theta\;\sin n\theta\;d\theta$$

$$RC(n,j) = \sum_{n=0}^{6} b_n \int_0^{2\pi} \cos n\theta\;\cos j\theta\;\cos n\theta\;d\theta$$

$$SS(m,n,j) = \sum_{n=1}^{6} \int_0^{L/a} F_{1n}(x)\,x^{m-1}\,dx \int_0^{2\pi} \cos n\theta\;\sin n\theta\;\sin j\theta\;d\theta$$

$$SC(m,n,j) = \sum_{n=1}^{6} \int_0^{4/a} F_{1n}(x)\, x^{m-1} dx \int_0^{2\pi} \cos n\theta \cos j\theta \cos n\theta \, d\theta$$

$$TS(m,n,j) = \sum_{n=1}^{6} \int_0^{4a} F_{2n}(x)\, x^{m-1} dx \int_0^{2\pi} \cos n\theta \sin n\theta \sin j\theta \, d\theta$$

$$WS(m,n,j) = \sum_{n=1}^{6} \int_0^{4/a} F_{2n}(x)\, x^{m-1} dx \int_0^{2\pi} \cos n\theta \cos n\theta \cdot \cos j\theta \, d\theta$$

$$US(m,n,j) = \sum_{n=1}^{6} \int_0^{4/a} F_{3n}(x)\, x^{m-1} dx \int_0^{2\pi} \sin n\theta \cos n\theta \sin j\theta \, d\theta$$

$$US(m,j,n) = \sum_{n=1}^{6} \int_0^{4/a} F_{3n}(x)\, x^{m-1} dx \int_0^{2\pi} \sin n\theta \cos j\theta \sin n\theta \, d\theta$$

where

F_{1n}, F_{2n}, F_{3n} are the expressions in the pre-buckling membrane strains ($\epsilon_x, \epsilon_\theta, \epsilon_{x\theta}$ respectively) due to the non-uniform loading components i.e.

$$P = P_0 \sum_{n=1}^{6} b_n \cos n\theta$$

$$\epsilon_x = u_{,x} = \sum_{n=1}^{6} F_{1n} \cos n\theta$$

$$\epsilon_\theta = v_{,\theta} - w = \sum_{n=1}^{6} F_{2n} \cos n\theta$$

$$\epsilon_{x\theta} = u_{,\theta} + v_{,x} = \sum_{n=1}^{6} F_{3n} \cos n\theta$$

and

$$G4(m) = \left(\frac{h}{a}\right)^3 \int_0^{4/a} \omega^0 \, x^{m-1} \, dx$$

where ω^0 is displacement due to b_0 the axisymmetric component

Here

i and j vary over the same range as m and n.

The function δ_{nj} is defined as

$$\delta_{nj} = 1 \quad \text{for} \quad n = j$$

$$= 0 \quad \text{for} \quad n \neq j$$

The other elements of the stability determinant can be written down by symmetry of matrix as these are obtained from a quadratic expression.

APPENDIX VI

The additional terms in the stability determinant due to the modification of the virtual displacements as in Equation (3.13) are given below for each term.

f_{11}, ϕ_{11}, ϕ_{12}, ϕ_{21} - No additional terms

$$f_{12} - -\rho\delta_{nj}\left[2\nu\, i n - (1-\nu)\, j\,(m+1)\right]\frac{(L/a)^{m+i+1}}{(m+i+1)}$$

$$f_{13} - \rho\, 2\nu\,\delta_{nj}\, i\pi\,\frac{(L/a)^{m+i+2}}{m+i+2}$$

$$f_{22} - 2\pi\delta_{nj}\, n\left[2\rho\,\frac{(L/a)^{m+i+3}}{(m+i+3)} - \rho^2\,\frac{(L/a)^{m+i+4}}{(m+i+4)}\right]$$

$$f_{23} - 2\pi\delta_{nj}\, j\,(L/a)^{m+i+3}\left[\frac{2\rho}{(m+i+3)} - \frac{\rho^2 L}{(m+i+4)}\right]$$

$$f_{33} - -4\rho\pi\delta_{nj}\left[\frac{1}{12}\left(\frac{h}{a}\right)^2\left\{(m+1)(i+1)\,\frac{(mi+m+i)}{m+i}(L/a)^{m+i}\right.\right.$$

$$+ (1-n^2)(1-j^2)\,\frac{(L/a)^{m+i+4}}{(m+i+4)} + \nu\,\frac{(1-n^2)(1+i)^2(L/a)^{m+i+2}}{m+i+2}$$

$$+\nu\,(1+m)^2\,\frac{(1-j^2)(L/a)^{m+i+2}}{m+i+2} + (1-\nu)\,nj\,\frac{(2mi+3m+3i+4)(L/a)^{m+i+2}}{m+i+2}\Bigg\}$$

$$\left. + \frac{(L/a)^{m+i+4}}{m+i+4}\right]$$

$$+\rho^2 2\pi\delta_{nj}\left[\frac{1}{12}\left(\frac{h}{a}\right)^2\left\{(m+1)\,\frac{(m+2)(i+1)(i+2)}{m+i+1}(L/a)^{m+i+1}\right.\right.$$

$$\left.\left. + (1-n^2)(1-j^2)\,\frac{(L/a)^{m+i+5}}{m+i+5} + \right.\right.$$

$$+\nu(1-n^2)(i+1)(i+2)\frac{(L/a)^{m+i+3}}{m+i+3}+$$

$$\nu(m+1)(m+2)(1-j^2)\frac{(L/a)^{m+i+3}}{m+i+3}+$$

$$2(1-\nu)nj(m+2)(i+2)\frac{(L/a)^{m+i+3}}{m+i+3}\Big\}$$

$$+\frac{(L/a)^{m+i+5}}{m+i+5}\Big]$$

$$\Phi_{13} = -\rho(1-\nu^2)\left(\frac{h}{a}\right)^2 RC(n,j)\frac{(m+2-i)(L/a)^{m+i+2}}{m+i+2}$$

$$\Phi_{22} = -2\rho\Big[2\nu\,SS(m+i+2,n,j)+2TS(m+i+2,n,j)$$

$$+2(1-\nu^2)\left(\frac{h}{a}\right)^2\frac{RS(n,j)(L/a)^{m+i+2}}{m+i+2}$$

$$-(1-\nu^2)2\pi\delta_{nj}\,G4(m+i+2)\Big]$$

$$+\rho^2\Big[2\nu\,SS(m+i+3,n,j)+2TS(m+i+3,n,j)$$

$$+2(1-\nu^2)\left(\frac{h}{a}\right)^2\frac{RS(n,j)(L/a)^{m+i+3}}{m+i+3}$$

$$-(1-\nu^2)2\pi\delta_{nj}\,G4(m+i+3)\Big]$$

$$\Phi_{23} = -2\rho\Big[-2\nu n\,SS(m+i+3,n,j)-2n\,TS(m+i+3,n,j)$$

$$+2(1-\nu^2)n\pi\delta_{nj}\,G4(m+i+3)$$

$$-2(1-\nu^2)n\left(\frac{h}{a}\right)^2 RS(n,j)\frac{(L/a)^{m+i+3}}{m+i+3}$$

$$+\frac{(1-\nu)}{2}(2m+3)\,US(m+i+2,n,j)\Big]$$

$$+\rho^2\Big[-2\nu n\,SS(m+i+4,n,j)-2n\,TS(m+i+4,n,j)$$
$$+2(1-\nu^2)\,\Pi\,\delta_{nj}\,n\,G4(m+i+4)$$
$$-2(1-\nu^2)\left(\frac{h}{a}\right)^2 n\,RS(n,j)\,\frac{(L/a)^{m+i+4}}{m+i+4}$$
$$+(1-\nu)(m+2)\;US(m+i+3,n,j)\Big]$$

$$\Phi_{33} - -2\rho\Big[2\nu nj\,SS(m+i+4,n,j)+2nj\,TS(m+i+4,n,j)$$
$$+(2mi+3m+3i+4)\,SC(m+i+2,n,j)$$
$$+\nu(2mi+3m+3i+4)\,WS(m+i+2,n,j)$$
$$+2(1-\nu^2)\left(\frac{h}{a}\right)^2 RC(n,j)\,\frac{(L/a)^{m+i+4}}{m+i+4}$$
$$+\frac{(1-\nu)}{2}\,j(2m+3)\;US(m+i+3,n,j)$$
$$+\left(\frac{1-\nu}{2}\right)n(2i+3)\;US(m+i+3,j,n)$$
$$-2(1-\nu^2)\,\Pi\,\delta_{nj}\,nj\;G4(m+i+4)\Big]$$
$$+\rho^2\Big[2\nu nj\,SS(m+i+5,n,j)+2nj\,TS(m+i+5,n,j)$$
$$+2(m+2)(i+2)\;SC(m+i+3,n,j)$$
$$+2\nu(m+2)(i+2)\;WS(m+i+3,n,j)$$
$$+2(1-\nu^2)\left(\frac{h}{a}\right)^2 RC(n,j)\,\frac{(L/a)^{m+i+5}}{m+i+5}$$
$$+\left(\frac{1-\nu}{2}\right)j(m+2)\cdot 2\;US(m+i+4,n,j)$$
$$+(1-\nu)\,n\,(i+2)\;US(m+i+4,j,n)$$

$$- 2(1-\nu^2)\, nj\, \pi\, \delta nj\, G4(m+i+5)\Big]$$

The other additional terms can be again written down by noting the symmetry of the stability determinant.

The functions RC, RS, US, WS etc. are as defined in Appendix V.

The terms in ϕ_{ki} which are dependent only on the internal suction load (i.e. b_o) are given here seperately for convenience of analysing the problem in Section 5.3. The virtual displacements in Equation (3.13) are employed to obtain these expressions.

$$\phi_{11} = \phi_{12} = \phi_{21} = 0$$

$$\phi_{13} = (1-\nu^2)\left(\frac{h}{a}\right)^2 \pi\, \delta nj \left[(m+1-i)\, \frac{(L/a)^{m+i+1}}{m+i+1} - \rho\,(m+2-i)\, \frac{(L/a)^{m+i+2}}{m+i+2} \right]$$

$$\phi_{22} = -2(1-\nu^2)\, \pi\, \delta nj \left[CN(m+i+1) - 2\rho\, CN(m+i+2) + \rho^2\, CN(m+i+3) \right.$$

$$\left. -\left(\frac{h}{a}\right)^2 \left\{ \frac{(L/a)^{m+i+1}}{(m+i+1)} - 2\rho\, \frac{(L/a)^{m+i+2}}{(m+i+2)} + \rho^2\, \frac{(L/a)^{m+i+3}}{(m+i+3)} \right\} \right]$$

$$\Phi_{23} = 2(1-\nu^2)\,\Pi\, n\, \delta_{nj} \left[CN(m+i+2) - 2\rho\, CN(m+i+3) + \rho^2 CN(m+i+4) \right.$$

$$\left. - \left(\frac{h}{a}\right)^2 \left\{ \frac{(L/a)^{m+i+2}}{m+i+2} - 2\rho \frac{(L/a)^{m+i+3}}{m+i+3} + \rho^2 \frac{(L/a)^{m+i+4}}{m+i+4} \right\} \right]$$

$$\Phi_{33} = -2(1-\nu^2)\,\Pi\, \delta_{nj} \left[nj \left\{ CN(m+i+3) - 2\rho\, CN(m+i+4) + \rho^2 CN(m+i+5) \right\} \right.$$

$$\left. - \left(\frac{h}{a}\right)^2 \left\{ \frac{(L/a)^{m+i+3}}{m+i+3} - 2\rho \frac{(L/a)^{m+i+4}}{m+i+4} + \rho^2 \frac{(L/a)^{m+i+5}}{m+i+5} \right\} \right]$$

Where $$CN(m) = \left(\frac{h}{a}\right)^2 \int_0^{L/a} \bar{\omega}^{\circ}\, x^{m-1}\, dx$$

and $\bar{\omega}^{\circ}(x)$ - is the displacement at any point due to unit internal suction pressure.

The other terms can again be written by symmetry.

APPENDIX VII - Interpolation functions

AVII.a The Interpolation functions for higher order element

In the equilibrium stress analysis the nodal displacements at j^{th} node selected are given in equation (4.1)

$$\lfloor q_j \rfloor_n = \lfloor u_j \; u'_j \; v_j \; v'_j \; w_j \; w'_j \; w''_j \rfloor_n \qquad \text{(A.VII.1)}$$

The interpolation function selected can have

4 arbitrary constants in u

4 " in v

6 " in w

corresponding to the number of degrees of freedom of the element. The conditions which the functions selected should satisfy are discussed in Ref. (59)

Subjected to these conditions the polynomials are selected for the shape functions as

$$u_n = a_1 + a_2 x + a_3 x^2 + a_4 x^3 \qquad \text{(A VII.2)}$$

$$v_n = a_5 + a_6 x + a_7 x^2 + a_8 x^3$$

$$w_n = a_9 + a_{10} x + a_{11} x^2 + a_{12} x^3 + a_{13} x^4 + a_{14} x^5$$

These can be written in the matrix form as

$$\begin{Bmatrix} u_n \\ v_n \\ w_n \end{Bmatrix} = \left[\begin{array}{cccc|cccc|ccccc} 1 & x & x^2 & x^3 & & & & & & & & & \\ & & & & 1 & x^2 & x^3 & x^3 & & & & & \\ & & & & & & & & 1 & x & x^2 & x^3 & x^4 & x^5 \end{array}\right] \begin{bmatrix} a_1 \\ a_2 \\ a_3 \\ \vdots \\ \vdots \\ a_{14} \end{bmatrix}$$

$$= [F(x)]\{A\} \qquad \text{(A VII.3)}$$

where $[F(x)]$ is the matrix of polynomial terms

$\{A\}$ column matrix of the arbitrary constants.

The arbitrary constants a_1 to a_{14} in equation (AVII·2) can be related to the nodal displacements of the elements in (A VII.1). These relations can be written in the form:

$$\{A\} = [B1] \begin{Bmatrix} q_j \\ q_{j+1} \end{Bmatrix}_n \qquad \text{(A VII.4)}$$

The matrix $[B1]$ is given in Figure A VII.1. Substituting for $\{A\}$ in equation (A VII.3) we have

$$\begin{Bmatrix} u_n \\ v_n \\ w_n \end{Bmatrix} = [F(x)][B1] \begin{Bmatrix} q_j \\ q_{j+1} \end{Bmatrix}_n$$

$$= [B] \begin{Bmatrix} q_j \\ q_{j+1} \end{Bmatrix}_n \qquad \text{(A VII.5)}$$

where $[B] = [F(x)][B1]$

is the matrix of interpolation function referred to in equation (4.3).

$$
\begin{bmatrix} a_1 \\ a_2 \\ a_3 \\ a_4 \\ a_5 \\ a_6 \\ a_7 \\ a_8 \\ a_9 \\ a_{10} \\ a_{11} \\ a_{12} \\ a_{13} \\ a_{14} \end{bmatrix}
=
\begin{bmatrix}
1 & 0 & & & & & & & & & & & & \\
0 & 1 & & & & & & & & & & & & \\
-3/\bar{\ell}^2 & -2/\bar{\ell} & & & & & 3/\bar{\ell}^2 & -1/\bar{\ell} & & & & & & \\
2/\bar{\ell}^3 & 1/\bar{\ell}^2 & & & & & -2/\bar{\ell}^3 & 1/\bar{\ell}^2 & & & & & & \\
 & & 1 & 0 & & & & & & & & & & \\
 & & 0 & 1 & & & & & & & & & & \\
 & & -3/\bar{\ell}^2 & -2/\bar{\ell} & & & 3/\bar{\ell}^2 & -1/\bar{\ell} & & & & & & \\
 & & 2/\bar{\ell}^3 & 1/\bar{\ell}^2 & & & -2/\bar{\ell}^3 & 1/\bar{\ell}^2 & & & & & & \\
 & & & & 1 & 0 & 0 & & & & & & & \\
 & & & & 0 & 1 & 0 & & & & & & & \\
 & & & & 0 & 0 & 1/2 & & & & & & & \\
 & & & & -10/\bar{\ell}^3 & -6/\bar{\ell}^2 & -3/2\bar{\ell} & & & & 10/\bar{\ell}^3 & -4/\bar{\ell}^2 & 1/2\bar{\ell} & \\
 & & & & 15/\bar{\ell}^4 & 8/\bar{\ell}^3 & 3/2\bar{\ell}^2 & & & & -15/\bar{\ell}^3 & 7/\bar{\ell}^3 & -1/\bar{\ell}^2 & \\
 & & & & -6/\bar{\ell}^5 & -3/\bar{\ell}^4 & -1/2\bar{\ell}^3 & & & & 6/\bar{\ell}^5 & -3/\bar{\ell}^4 & 1/2\bar{\ell}^3 &
\end{bmatrix}
\begin{bmatrix} u_j \\ u'_j \\ \theta_j \\ \theta'_j \\ w_j \\ w'_j \\ w''_j \\ u_{j+1} \\ u'_{j+1} \\ \theta_{j+1} \\ \theta'_{j+1} \\ w_{j+1} \\ w'_{j+1} \\ w''_{j+1} \end{bmatrix}
$$

A VII.b Interpolation functions for simpler element representation

To represent the virtual displacement state the nodal variables selected at j /th node are

$$\left[\bar{q}_n\right]_j = \left[\bar{\xi}_n \;\; \eta_n \;\; \zeta_n \;\; \zeta_n'\right]_j \qquad \text{(A VII. 6.)}$$

The shape functions selected consistent with the number of degrees of freedom of the element are

$$\begin{aligned} \bar{\xi}_n &= \bar{a}_{1n} + \bar{a}_{2n}\, x \\ \eta_n &= \bar{a}_{3n} + \bar{a}_{4n}\, x \\ \zeta_n &= \bar{a}_{5n} + \bar{a}_{6n} x + \bar{a}_{7n} x^2 + \bar{a}_{8n}\, x^3 \end{aligned} \qquad \text{(A VII.7)}$$

These are written in the matrix notation as

$$\begin{Bmatrix} \bar{\xi}_n \\ \eta_n \\ \zeta_n \end{Bmatrix} = \left[\begin{array}{cc|cc|cccc} 1 & x & & & & & & \\ & & 1 & x & & & & \\ & & & & 1 & x & x^2 & x^3 \end{array}\right] \begin{bmatrix} a_{1n} \\ a_{2n} \\ a_{3n} \\ a_{4n} \\ a_{5n} \\ a_{6n} \\ a_{7n} \\ a_{8n} \end{bmatrix}$$

$$= \left[\bar{F}(x)\right] \left\{\bar{A}_n\right\} \qquad \text{(A VII.8)}$$

where $[\bar{F}(x)]$ is the matrix of polynomial terms

$\{\bar{A}_n\}$ is column matrix of arbitrary constants.

Considering each displacement, the arbitrary constants can be related to the nodal displacements of the element as

$$\{\bar{A}_n\} = [\bar{B}1] \begin{Bmatrix} \bar{q}_j \\ \bar{q}_{j+1} \end{Bmatrix}_n \qquad \text{(A VII.9)}$$

The matrix $[\bar{B}1]$ is given in Figure AVII.2.

Substituting for $\bar{A}_n$ we have

$$\begin{Bmatrix} \xi_n \\ \eta_n \\ \zeta_n \end{Bmatrix} = [\bar{F}(x)][\bar{B}1] \begin{Bmatrix} \bar{q}_j \\ \bar{q}_{j+1} \end{Bmatrix}_n = [\bar{B}] \begin{Bmatrix} \bar{q}_j \\ \bar{q}_{j+1} \end{Bmatrix}_n$$

This is the equation referred to in equn (4.15)

$$\begin{bmatrix}
1 & 0 & 0 & 0 \\
-1/\bar{\ell} & 0 & 1/\bar{\ell} & 0 \\
0 & 1 & 0 & 0 \\
0 & -1/\bar{\ell} & 0 & 1/\bar{\ell} \\
1 & 0 & & \\
0 & 1 & & \\
-3/\bar{\ell}^2 & -2/\bar{\ell} & 3/\bar{\ell}^2 & -1/\bar{\ell} \\
2/\bar{\ell}^3 & 1/\bar{\ell}^2 & -2/\bar{\ell}^3 & 1/\bar{\ell}^2
\end{bmatrix}$$

$\bar{\ell} = \ell/a$

FIG A VII.2

APPENDIX VIII

STIFFNESS MATRICES

The elements of the stiffness matrices obtained from considering the strain energy are given in this Appendix.

A VIII.a Equilibrium stress analysis:

Starting from the strain energy expression in Equation (4.5) and substituting for the strains and curvatures from Equations (4.4) and (4.2) while making use of the interpolation functions of Equation (A VII.2), we obtain the strain energy for any harmonic as

$$U_n = \frac{E a^2 h}{2(1-\nu^2)} \pi \lfloor A \rfloor \int_0^{1/a} [D]\, dx \, \{A\}$$

The matrix $[D]$ is obtained from $[F(\alpha)]$. The matrix $[D]$ is written as

$$[D] = [D_1] + \alpha \begin{bmatrix} 0 & 0 \\ 0 & D_2 \end{bmatrix}$$

(α being $= \frac{h^2}{12a^2}$)

where D_1 - is that part of the matrix corresponding to the membrane strains, and is of order (14 x 14)

D_2 - is obtained from the bending constribution of the shell, and is of order (6 x 6).

The matrices D_1, and D_2 are given in Tables (A VIII.1) and (A VIII.2).

TABLE A VIII.1

$\frac{1-\nu}{2}n^2$	$\frac{1-\nu}{2}n^2x$	$\frac{1-\nu}{2}n^2x^2$	$\frac{1-\nu}{2}n^2x^3$		$-n\frac{(1-\nu)}{2}$	$-nx(1-\nu)$	$-\frac{(1-\nu)}{2}3nx^2$						
	$\frac{1-\nu}{2}n^2x^2$	$2x+\frac{1-\nu}{2}n^2x^3$	$3x^2+\frac{1-\nu}{2}n^2x^4$	$n\nu$	$\nu nx-\frac{(1-\nu)}{2}nx$	$\nu nx^2-(1-\nu)nx^2$	$\nu nx^3-\frac{1-\nu}{2}3nx^3$	$-\nu$	$-\nu x$	$-\nu x^2$	$-\nu x^3$	$-\nu x^4$	$-\nu x^5$
		$4x^2+\frac{1-\nu}{2}n^2x^4$	$6x^3+\frac{1-\nu}{2}n^2x^5$	$2n\nu x$	$2\nu nx^2-\frac{1-\nu}{2}nx^2$	$2\nu nx^3-(1-\nu)nx^3$	$2\nu nx^4-\frac{1-\nu}{2}3nx^4$	$-2\nu x$	$-2\nu x^2$	$-2\nu x^3$	$-2\nu x^4$	$-2\nu x^5$	$-2\nu x^6$
			$9x^4+\frac{1-\nu}{2}n^2x^6$	$3nx^2\nu$	$3\nu nx^3-\frac{1-\nu}{2}nx^3$	$3\nu nx^4-(1-\nu)nx^4$	$3\nu nx^5-\frac{1-\nu}{2}3nx^5$	$-3\nu x^2$	$-3\nu x^3$	$-3\nu x^4$	$-3\nu x^5$	$-3\nu x^6$	$-3\nu x^7$
				n^2	n^2x	n^2x^2	n^2x^3	$-n$	$-nx$	$-nx^2$	$-nx^3$	$-nx^4$	$-nx^5$
					$n^2x^2+\frac{1-\nu}{2}n^2$	$n^2x^3+\frac{1-\nu}{2}n^2 2x$	$n^2x^4+\frac{1-\nu}{2}3n^2x^2$	$-nx$	$-nx^2$	$-nx^3$	$-nx^4$	$-nx^5$	$-nx^6$
						$n^2x^4+\frac{1-\nu}{2}n^2 4x^2$	$n^2x^5+\frac{1-\nu}{2}n^2 6x^3$	$-nx^2$	$-nx^3$	$-nx^4$	$-nx^5$	$-nx^6$	$-nx^7$
							$n^2x^6+\frac{1-\nu}{2}9n^2x^4$	$-nx^3$	$-nx^4$	$-nx^5$	$-nx^6$	$-nx^7$	$-nx^8$
								1	x	x^2	x^3	x^4	x^5
									x^2	x^3	x^4	x^5	x^6
										x^4	x^5	x^6	x^7
											x^6	x^7	x^8
												x^8	x^9
													x^{10}

Sym.

TABLE - A VIII.2

$(1-n^2)^2$	$(1-n^2)^2 x$	$(1-n^2)^2 x^2 + 2\nu(1-n^2)$	$(1-n^2)^2 x^3 + 6\nu x(1-n^2)$	$(1-n^2)^2 x^4 + 12\nu x^2(1-n^2)$	$(1-n^2)^2 x^5 + 20\nu x^3(1-n^2)$
	$(1-n^2)^2 x^2 + 2(1-\nu)n^2$	$(1-n^2)^2 x^3 + 2\nu(1-n^2)x + 4n^2 x(1-\nu)$	$(1-n^2)^2 x^4 + 6\nu(1-n^2)x^2 + 6n^2 x^2(1-\nu)$	$(1-n^2)^2 x^5 + 12\nu(1-n^2)x^3 + 8(1-\nu)n^2 x^3$	$(1-n^2)^2 x^6 + 20\nu(1-n^2)x^4 + 10(1-\nu)n^2 x^4$
		$4 + (1-n^2)^2 x^4 + 4\nu x^2(1-n^2) + 8n^2 x^2(1-\nu)$	$12x + (1-n^2)^2 x^5 + 8\nu(1-n^2)x^3 + 12n^2 x^3(1-\nu)$	$24x^2 + (1-n^2)^2 x^6 + 14\nu(1-n^2)x^4 + 16(1-\nu)n^2 x^4$	$40x^3 + (1-n^2)^2 x^7 + 22\nu(1-n^2)x^5 + 20(1-\nu)n^2 x^5$
			$36x^2 + (1-n^2)^2 x^6 + 12\nu(1-n^2)x^4 + 18n^2(1-\nu)$	$72x^3 + (1-n^2)^2 x^7 + 18\nu(1-n^2)x^5 + 24(1-\nu)n^2 x^5$	$120x^4 + (1-n^2)^2 x^8 + 26\nu(1-n^2)x^6 + 30(1-\nu)n^2 x^6$
				$144x^4 + (1-n^2)^2 x^8 + 24\nu(1-n^2)x^6 + 32(1-\nu)n^2 x^6$	$240x^5 + (1-n^2)^2 x^9 + 32\nu(1-n^2)x^7 + 40(1-\nu)n^2 x^7$
					$400x^6 + (1-n^2)^2 x^{10} + 40\nu(1-n^2)x^8 + 50(1-\nu)n^2 x^8$

Sym.

$\frac{1-\nu}{2} n^2 \bar{l}$	$\frac{1-\nu}{2} n^2 \frac{\bar{l}^2}{2}$		$-\frac{1-\nu}{2} n \bar{l}$				
	$\bar{l} + \frac{1-\nu}{2} n^2 \frac{\bar{l}^3}{3}$	$\nu n \bar{l}$	$\frac{n(3\nu-1)\bar{l}^2}{4}$	$-\nu \bar{l}$	$-\nu \frac{\bar{l}^2}{2}$	$-\nu \frac{\bar{l}^3}{3}$	$-\nu \frac{\bar{l}^4}{4}$
		$n^2 \bar{l}$	$\frac{n^2 \bar{l}^2}{2}$	$-n \bar{l}$	$-\frac{n \bar{l}^2}{2}$	$-\frac{n \bar{l}^3}{3}$	$-\frac{n \bar{l}^4}{4}$
			$\frac{1-\nu}{2} \bar{l} + n^2 \bar{l}^3/3$	$-\frac{n \bar{l}^2}{2}$	$-\frac{n \bar{l}^3}{3}$	$-\frac{n \bar{l}^4}{4}$	$-\frac{n \bar{l}^5}{5}$
				$\alpha\beta \bar{l}$	$\alpha\beta \frac{\bar{l}^2}{2}$	$\alpha[\beta \bar{l}^3/3 + 2\nu(1-n^2)\bar{l}]$	$\alpha[\beta \bar{l}^4/4 + 3\nu(1-n^2)\bar{l}^2]$
					$\alpha[\beta \bar{l}^3/3 + 2(1-\nu) n^2 \bar{l}]$	$\alpha[\beta \bar{l}^4/4 + 2(1-\nu) n^2 \bar{l}^2 + \nu(1-n^2)\bar{l}^2]$	$\alpha[\beta \bar{l}^5/5 + 2\nu(1-n^2)\bar{l}^3 + 2(1-\nu) n^2 \bar{l}^3]$
						$\alpha[\beta \bar{l}^5/5 + 4\nu(1-n^2)\bar{l}^3/3 + 2(1-\nu) n^2 4 \bar{l}^3/3 + 4\bar{l}]$	$\alpha[\beta \bar{l}^6/6 + 8\nu(1-n^2)\bar{l}^4/4 + 3(1-\nu) n^2 \bar{l}^4 + 6\bar{l}^2]$
							$\alpha[\beta \bar{l}^7/7 + 12\nu(1-n^2)\bar{l}^5/5 + 18(1-\nu) n^2 \bar{l}^5/5 + 12\bar{l}^3]$

Sym.

$\alpha = \frac{h^2}{12a^2}$

$\beta = (1-n^2)^2 + 1/\alpha$

APPENDIX IX

DERIVATION OF GEOMETRIC STIFFNESS MATRIX

To obtain this matrix starting from the expression in Equation (4.21), we need the prebuckling membrane strains. These are determined for each harmonic separately as described in Section 4.2 and these are represented here as

$$\begin{aligned}
\epsilon_x &= u_{,x} + \nu(v_{,\theta} - w) \\
&= \sum_{n=0}^{6} AS_n \cos n\theta \\
\epsilon_\theta &= (v_{,\theta} - w) + \nu\, u_{,x} \\
&= \sum_{n=0}^{6} CS_n \cos n\theta \qquad \text{(A IX.1)} \\
\epsilon_{x\theta} &= u_{,\theta} + v_{,x} \\
&= \sum_{n=0}^{6} SS_n \sin n\theta
\end{aligned}$$

where

$$\begin{aligned}
AS_n &= u_{n,x} + \nu(n v_n - w_n) \\
CS_n &= (n v_n - w_n) + \nu\, u_{n,x} \\
SS_n &= -n u_n + v_{n,x}
\end{aligned}$$

Substituting these quantities into the Equation (4.21) we get for an element

$$\delta^2 V_b = \frac{E a^2 h}{2(1-\nu^2)} \sum_{n=0}^{6} \int_0^{\ell/a} \int_0^{2\pi} \Big\{ \Big[AS_n \zeta_{1x}^2 + CS_n (\eta + \zeta_{1\theta})^2 \Big] \cos n\theta + SS_n (1-\nu) \zeta_{1x} (\eta + \zeta_{1\theta}) \sin n\theta + P_0 b_n \cos n\theta \Big[\zeta^2 + 2\eta \zeta_{1\theta} + \eta^2 - \xi_{1x} \zeta + \xi \zeta_{1x} \Big] \Big\} \, d\alpha \, d\theta$$

(A IX.2)

Substituting for the virtual displacements from Equations (4.14) and (4.15) one encounters the following type of integrals in evaluating the above quantity.

$$CCC(n,i,j) = \int_0^{2\pi} \cos n\theta \cos i\theta \cos j\theta \, d\theta$$

$$CSS(n,i,j) = \int_0^{2\pi} \cos n\theta \sin i\theta \sin j\theta \, d\theta$$

$$SCS(n,i,j) = \int_0^{2\pi} \sin n\theta \cos i\theta \sin j\theta \, d\theta$$

$$F1(n,m) = \int_0^{\ell/a} AS_n \, x^{m-1} \, d\alpha$$

$$F2(n,m) = \int_0^{\ell/a} CS_n \, x^{m-1} \, d\alpha$$

$$F3(n,m) = \int_0^{\ell/a} SS_n \, x^{m-1} \, d\alpha$$

(A IX.3)

where η - varies between 0-6 (the No. of harmonics in the load)

i and j vary over the same range as the No. of harmonics in virtual displacements.

With this notation carrying out the integration in Equation A IX .2 one gets the typical value of the matrix SK_G for the element, for the harmonic, n, selected. This matrix is given in Figure A IX.1. By Summation of all such matrices for the element over the complete range of the harmonics in the load, the matrix $[K_G]$ in Equation (4.2 2) is obtained.

					$b_n \cdot ccc \cdot \bar{l}$	$b_n \cdot ccc \cdot \bar{l}^2$	$b_n \cdot ccc \cdot \bar{l}^3$
				$-b_n \cdot ccc \cdot \bar{l}$		$b_n \cdot ccc \cdot \bar{l}^3/3$	$b_n \cdot ccc \cdot \bar{l}^4/2$
		$b_n \cdot css \cdot \bar{l} + css \cdot F2(n,1)$	$b_n \cdot css \cdot \bar{l}^2/2 + css \cdot F2(n,2)$	$-b_n j \bar{l} \cdot css \cdot - j\, css \cdot F1(n,1)$	$-b_n css \cdot j\, \bar{l}^2/2 - j \cdot css \cdot F2(n,2)$	$-b_n j \cdot css \cdot \bar{l}^3/3 - j \cdot css \cdot F2(n,3)$	$-b_n \cdot j \frac{\bar{l}^4}{4} \cdot css \cdot - j \cdot css \cdot F2(n,4)$
		$b_n \cdot css \cdot \bar{l}^2/2 + css \cdot F2(n,2)$	$b_n \cdot css \cdot \bar{l}^3/3 + css \cdot F2(n,3)$	$-b_n \cdot j \frac{\bar{l}^2}{2} \cdot css - j \cdot css \cdot F2(n,2)$	$-b_n j \cdot css \cdot \bar{l}^3/3 - j \cdot css \cdot F2(n,3)$	$-b_n j \cdot css \cdot \bar{l}^4/4 - j \cdot css \cdot F2(n,4)$	$-b_n j \cdot css \cdot \bar{l}^5/5 - j \cdot css \cdot F2(n,5)$
		$-b_n \cdot css \cdot i \bar{l} - i \cdot css \cdot F2(n,1)$	$-b_n \cdot css \cdot i \frac{\bar{l}^2}{2} - i \cdot css \cdot F2(n,2)$	$b_n \cdot ccc \cdot \bar{l} + ij \cdot css \cdot F2(n,1)$	$b_n \cdot ccc \cdot \frac{\bar{l}^2}{2} + ij \cdot css \cdot F2(n,2)$	$b_n \cdot ccc \cdot \frac{\bar{l}^3}{3} + ij \cdot css \cdot F2(n,3)$	$b_n \cdot ccc \cdot \frac{\bar{l}^4}{4} + ij \cdot css \cdot F2(n,4)$
		$-b_n \cdot css \cdot i \frac{\bar{l}^2}{2} - i \cdot css \cdot F2(n,2) + (1-\nu) scs \cdot F3(n,1)$	$-b_n \cdot css \cdot i \bar{l}^3/3 - i\, css \cdot F2(n,3) + (1-\nu) \cdot scs \cdot F3(n,2)$	$b_n ccc \cdot \bar{l}^2/2 + ij \cdot css \cdot F2(n,2) - j(1-\nu)\, scs \cdot F3(n,1)$	$b_n \cdot ccc \cdot \bar{l}^3/3 + ccc \cdot F1(n,1) + ij \cdot css \cdot F2(n,3) - j(1-\nu) \cdot scs \cdot F3(n,2)$	$b_n \cdot ccc \cdot \bar{l}^4/4 + 2 \cdot ccc \cdot F1(n,2) + ij \cdot css \cdot F2(n,4) - j(1-\nu) \cdot scs \cdot F3(n,3)$	$b_n \cdot ccc \cdot \bar{l}^5/5 + 3ccc \cdot F1(n,3) + ij\, css\, F2(n,5) - j(1-\nu)\, scs \cdot F3(n,4)$
		$-b_n \cdot css \cdot i \bar{l}^3/3 - i\, css \cdot F2(n,3) + 2(1-\nu) \cdot scs \cdot F3(n,2)$	$-b_n \cdot css \cdot i \bar{l}^4/4 - i\, css \cdot F2(n,4) + 2(1-\nu) \cdot scs \cdot F3(n,3)$	$b_n ccc \cdot \bar{l}^3/3 + ij \cdot css \cdot F2(n,3) + (1-\nu) \cdot 2 \cdot scs \cdot F3(n,2) \cdot (-j)$	$b_n \cdot ccc \cdot \bar{l}^4/4 + 2 ccc \cdot F1(n,2) + ij\, css \cdot F2(n,4) - 2j(1-\nu) \cdot scs \cdot F3(n,3)$	$b_n \cdot ccc \cdot \bar{l}^5/5 + 4\, ccc \cdot F1(n,3) + ij \cdot css \cdot F2(n,5) - 2j(1-\nu) \cdot scs \cdot F3(n,4)$	$b_n \cdot ccc \cdot \bar{l}^6/6 + 6 \cdot ccc \cdot F1(n,4) + ij \cdot css \cdot F2(n,6) - 2j \cdot (1-\nu) scs \cdot F3(n,5)$
		$-b_n \cdot css \cdot \frac{\bar{l}^4}{4} \cdot i - i\, css \cdot F2(n,4) + 3(1-\nu) \cdot scs \cdot F3(n,3)$	$-b_n css \cdot \bar{l}^5/5 - i \cdot css \cdot F2(n,5) + 3(1-\nu) \cdot scs \cdot F2(n,4)$	$b_n \cdot ccc \cdot \bar{l}^4/4 + ij \cdot css \cdot F2(n,4) - 3j(1-\nu) \cdot scs \cdot F3(n,3)$	$b_n \cdot ccc \cdot \bar{l}^5/5 + 3ccc \cdot F1(n,3) + ij \cdot css \cdot F2(n,5) - 3j(1-\nu) \cdot scs \cdot F3(n,4)$	$b_n \cdot ccc \cdot \bar{l}^6/6 + 6 \cdot ccc\, F1(n,4) + ij \cdot css \cdot F2(n,6) - 3j(1-\nu) \cdot scs \cdot F3(n,5)$	$b_n ccc\, \bar{l}^7/7 + 9 \cdot ccc \cdot F1(n,5) + ij\, css \cdot F2(n,7) - 3i(1-\nu) \cdot scs\, F3(n,6)$

FIG A IX · 1

APPENDIX X

Stiffness Matrices of the Ring

The basic geometry of the ring and its attachment to the shell is shown in Figure A X.1. The ring is considered to be attached to the shell at one of the nodes. Then the displacements of the ring are connected to the displacements of the shell at the node as

$$\begin{aligned} u_r &= u - e\beta \\ v_r &= \frac{a_r}{a} v - \frac{e}{a}\frac{\partial w}{\partial \theta} \\ w_r &= w \\ \beta_r &= \beta = \frac{\partial w}{\partial x} \end{aligned} \qquad \text{(A X. 1)}$$

The suffix r refers to the ring.

With these four parameters as the degrees of freedom for the ring, the stiffness matrix for linear analysis is obtained by Alnajafi [69]. This matrix is given in Figure A X.2 and it is made use of in obtaining the equilibrium stresses for a ring stiffened shell for each harmonic.

Consideration of ring in the buckling analysis:

Here we adopt the same notation as in chapters 3 and 4 and differentiate the corresponding quantitites for the ring by the subscript r. Hence the strain displacement relations for the ring during buckling are

$$\bar{\epsilon}_{\theta n} = (\bar{v}_{n,\theta} - \bar{w}_n) + \tfrac{1}{2}(\bar{v}_n + \bar{w}_{n,\theta})^2$$

$$\bar{K}_{n\,\theta\theta} = \bar{w}_{n,\theta\theta} + \bar{w}_n$$

$$\bar{K}_{n\,xx} = \bar{w}_{n,x} + \frac{\bar{u}_{n,\theta\theta}}{1+e} \qquad \text{(A.X.2)}$$

$$\bar{K}_{n\,x\theta} = -\bar{w}_{n,x\theta} + \frac{\bar{u}_{n,\theta}}{1+e}$$

The total displacements are written as the sum of equilibrium displacements (u_n, v_n and w_n) and the virtual displacements ξ_n, η_n and $\zeta_{\varphi n}$ so that

$$\bar{u}_n = u_n + \xi_n$$

$$\bar{v}_n = v_n + \eta_n \qquad \text{(A.X.3)}$$

$$\bar{w}_n = w_n + \zeta_{\varphi n}$$

The virtual displacements of the ring are connected to the virtual displacements of the shell by similar relations as in (A.X.1).

The strain energy of the ring is given by

$$U_n = \frac{E_n a^3}{2(1+e)} \int_0^{2\pi} \Big[I_{zz} K_{n\,xx}^2 + A_n \epsilon_{\theta n}^2 + \frac{I_{xx} K_{n\theta\theta}^2}{(1+e)^2} + \Big(\frac{G_n J}{E_n}\Big) K_{n\,x\theta}^2 \Big] d\theta \qquad \text{(A.X.4)}$$

where I_{xx}, I_{zz}, J , E_n , G_n are the cross-sectional parameters and the material constants of the ring.

Assuming the virtual displacements of the ring to be represented

by a summation of Fourier harmonics, substituting (A X.2) and (A X.3) into equation (A X.4) and then calculating the second variation, one gets

$$\delta^2 U_n = \frac{E_n a^3}{2(1+e)} \pi \sum_n \left[I_{zz} \left(\zeta_{nn,x} - n^2 \frac{\xi_{nn}}{1+e} \right)^2 + \frac{I_{xx}}{(1+e)^2} \left(\zeta_{nn} - n^2 \zeta_{nn} \right)^2 + A_n \left(n\eta_{nn} - \zeta_{nn} \right)^2 + \frac{G_n J}{E_n} \left(n\zeta_{nn,x} - \frac{n\xi_{nn}}{1+e} \right)^2 \right]$$

$$+ \frac{E_n a^3}{2(1+e)} A_n \epsilon_{\theta nn} \cdot \left(\eta_{nn} - n\zeta_{nn} \right)^2 \cdot CSS(n,i,j) \qquad \text{—(A X.5)}$$

where $$CSS(n,i,j) = \int_0^{2\pi} \cos n\theta \sin i\theta \sin j\theta \, d\theta$$

and

$-\epsilon_{\theta nn}$ is the equilibrium state of strain in the ring for the harmonic n.

The expression for the second variation of the ring can again be identified to consist of the two distinct parts. The first part that is dependent only on the virtual displacements can be evaluated to be

$$\delta^2 U_{na} = \frac{E a^3 \pi}{2(1+e)} \sum_n \left[\bar{q}_n \right]_n \left[\bar{K}_{nn} \right] \left\{ \bar{q}_{nn} \right\} \qquad \text{—(A X.6)}$$

The elements of the matrix $\bar{K}_{nn}$ are identical to those given in Figure A X.2.

These additional stiffness terms are to be added to the matrix $[K_E]$ at the appropriate nodes in the buckling analysis.

The second part of the equation (A X.5) that is dependent both on prebuckling strains and the virtual displacement is

$$\delta^2 U_{nb} = \frac{E_n a^3}{2(1+e)} A_n \epsilon_{\theta nn} \, CSS(n,i,j) (\eta_{nn} - n\zeta_{nn})^2$$

$$= \frac{E_n a^3}{2(1+e)} A_n \, CSS(n,i,j) \, [q_n]_i \, [SK_{Gn}] \, \{q_n\}_j \cdot (1+e)^2$$

(A X.7)

where $[SK_{Gn}] =$

$$\begin{bmatrix} 0 & 0 & 0 & 0 \\ 0 & 1 & -j/2 & 0 \\ 0 & -j/2 & jj & 0 \\ 0 & 0 & 0 & 0 \end{bmatrix}$$

and $[q_n]_n$ – nodal displacements of the nth harmonic at junction.

$$= [\xi \; \eta \; \psi \; \zeta_{1x}]_n$$

Again it has to be noted that the summation of $[SK_{Gn}]$ over all the harmonics in the load gives the geometric stiffness matrix $[K_{Gn}]$ of the ring.

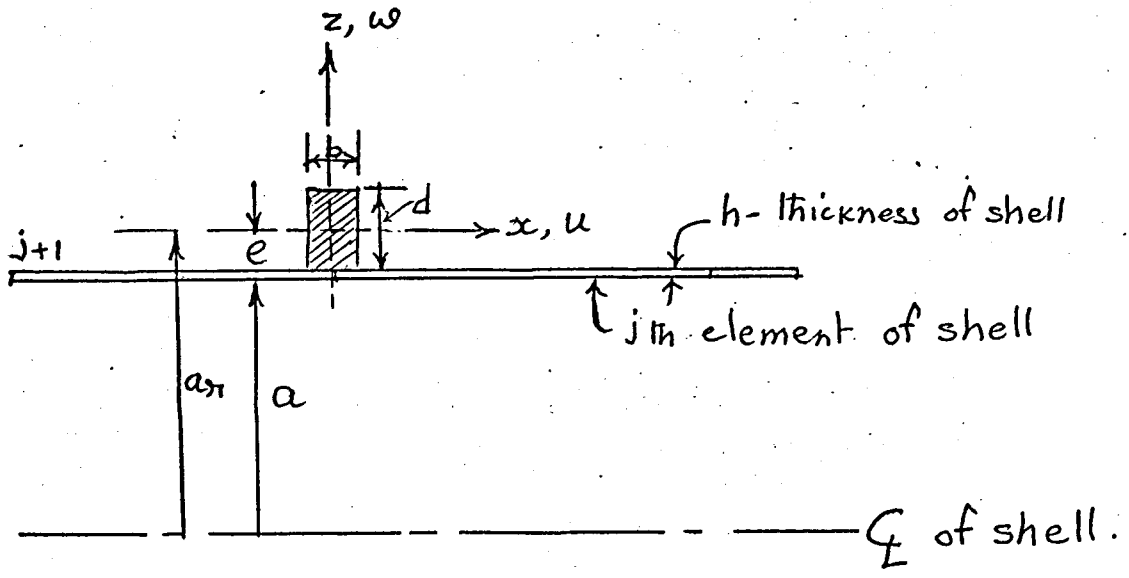

FIGURE A X.1

I_{xx}, I_{zz} - moment of inertia on xx and zz axes.

A_n - Area of cross-section of ring.

J - Torsional stiffness of ring.

E_n, G_n - Young's modulus and rigidity modulus of the ring material.

$\frac{E_n a^3 \pi}{(1+e)}$

$\frac{n^4}{(1+e)^2} I_z + \frac{G_n J}{E_n} \frac{n^2}{(1+e)^2}$			$\frac{-n^2}{1+e}\left\{1-\frac{en^2}{(1+e)}\right\} I_z - \frac{G_n J}{E_n} \frac{n^2}{1+e}\left(1-\frac{e}{1+e}\right)$
	$A_n n^2 (1+e)^2$	$-n(1+e)(1+en^2)\cdot A_n$	
Symm.		$\frac{I_x}{(1+e)^2}(1-n^2)^2 + A_n (1+en^2)^2$	
			$I_z \left(1-\frac{en^2}{1+e}\right)^2 + \frac{G_n J}{E_n} \frac{n^2}{(1+e)^2}$

FIGURE A X.2

FIGURES

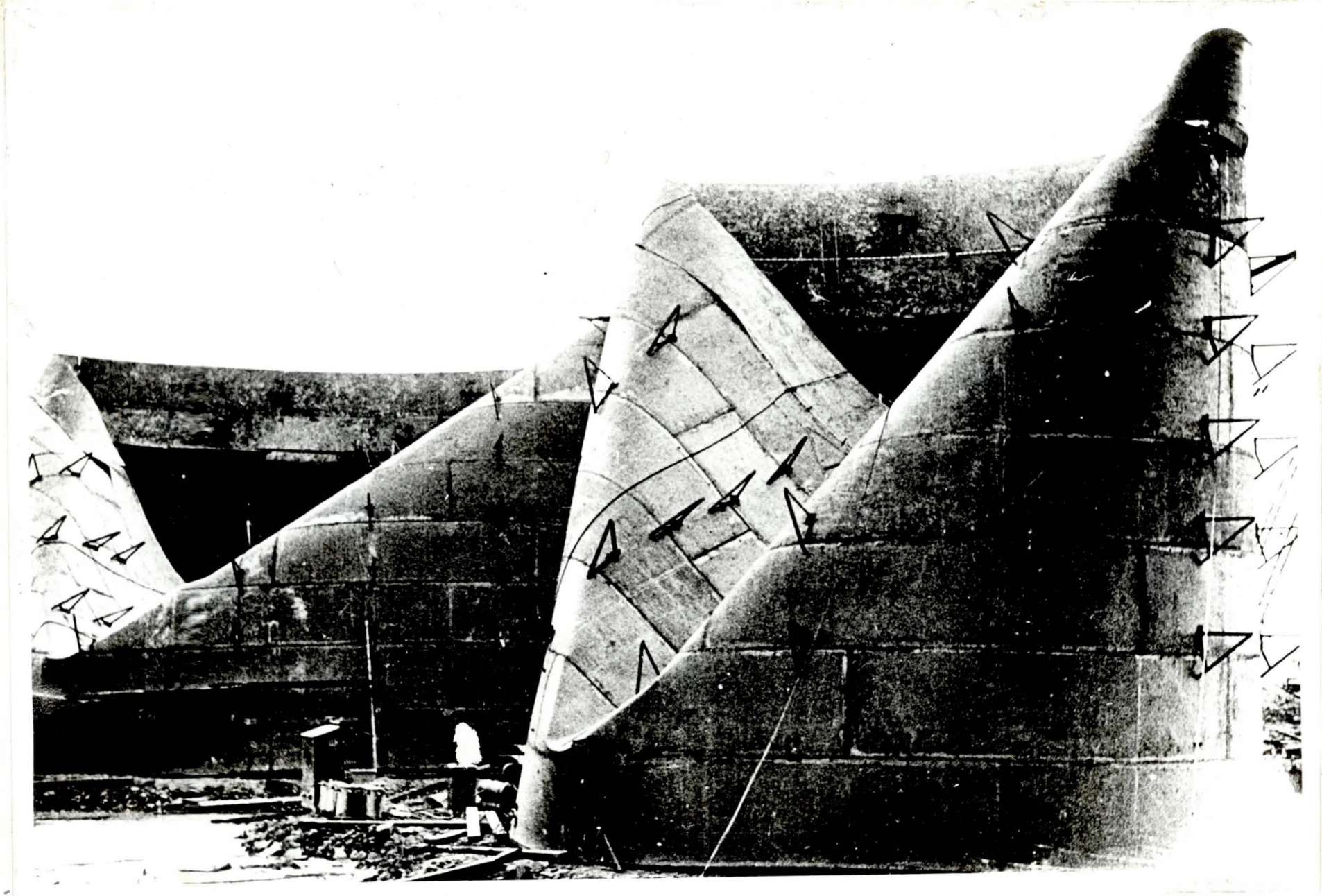

Fig. 1.1 Collapse mode of full size structure

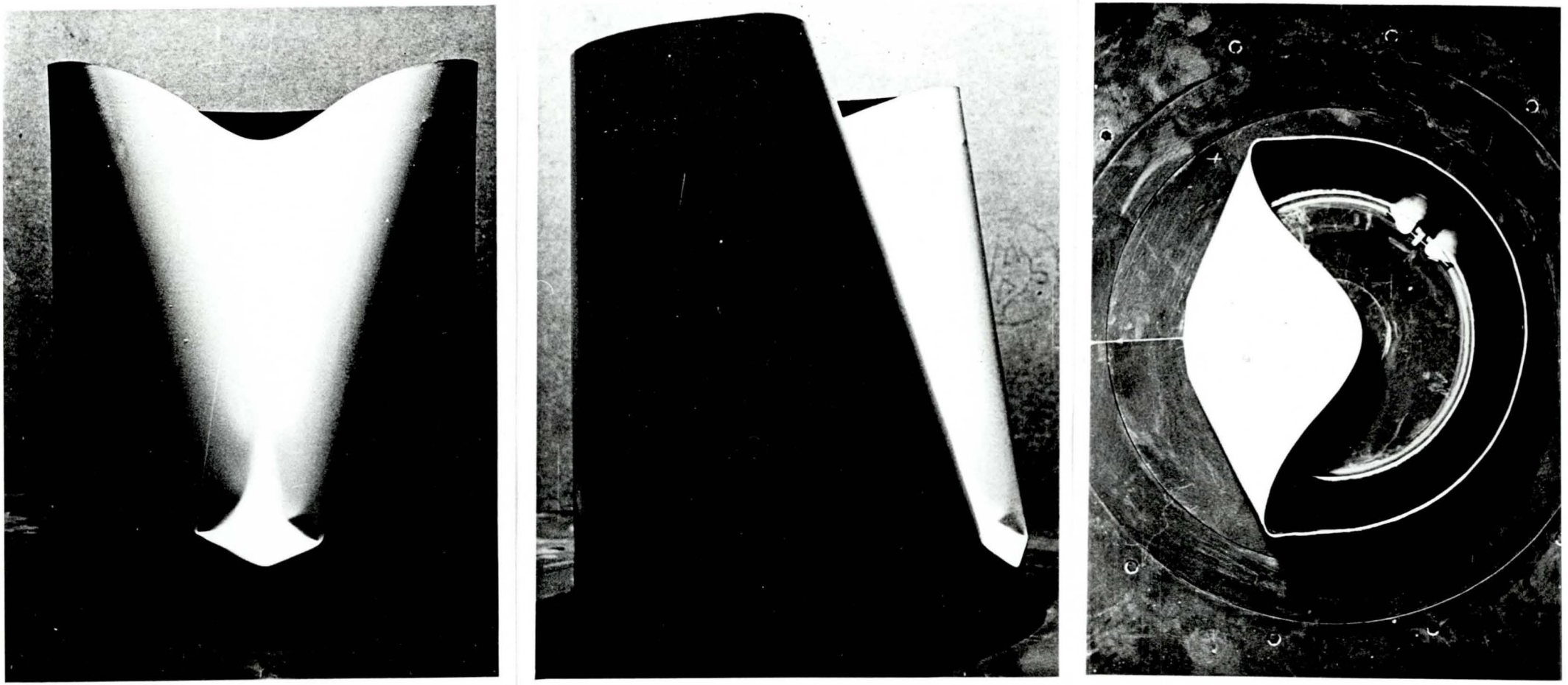

FIG 1·1a COLLAPSE MODE OF MODEL CYLINDERS

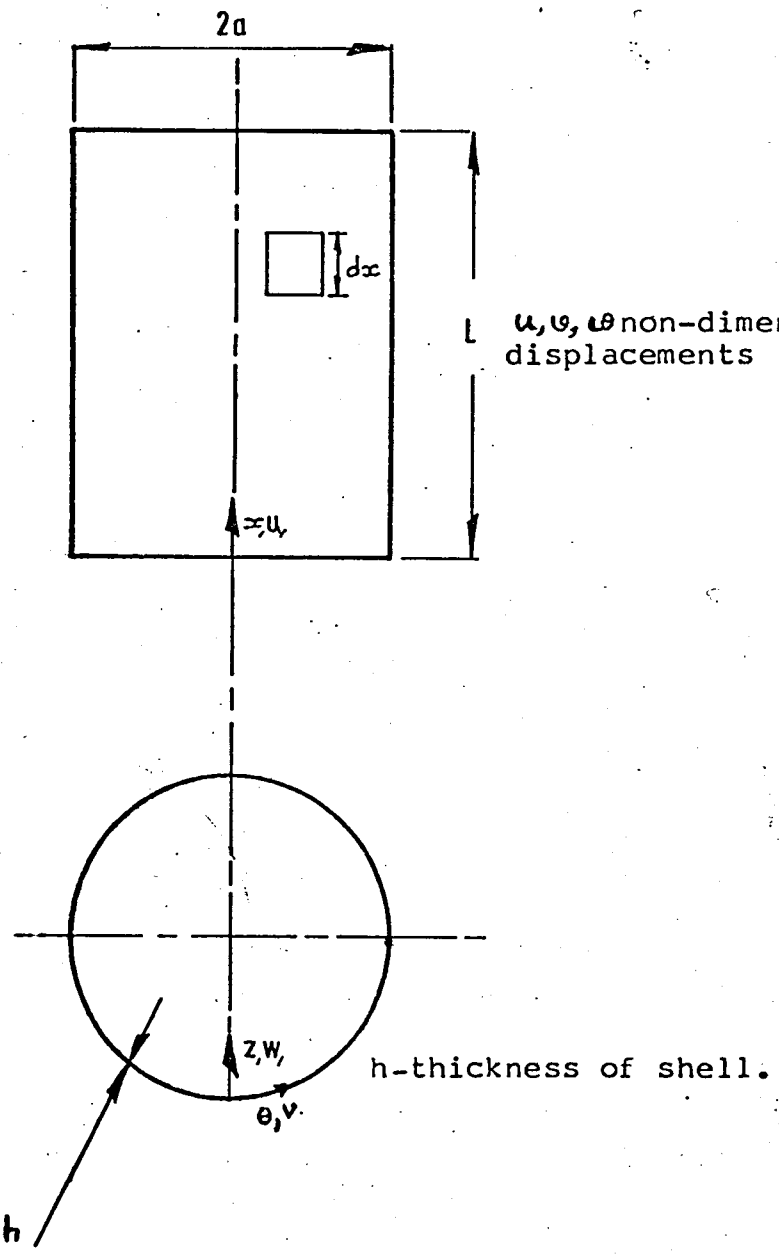

Fig. 2.1 Shell geometry and co-ordinates

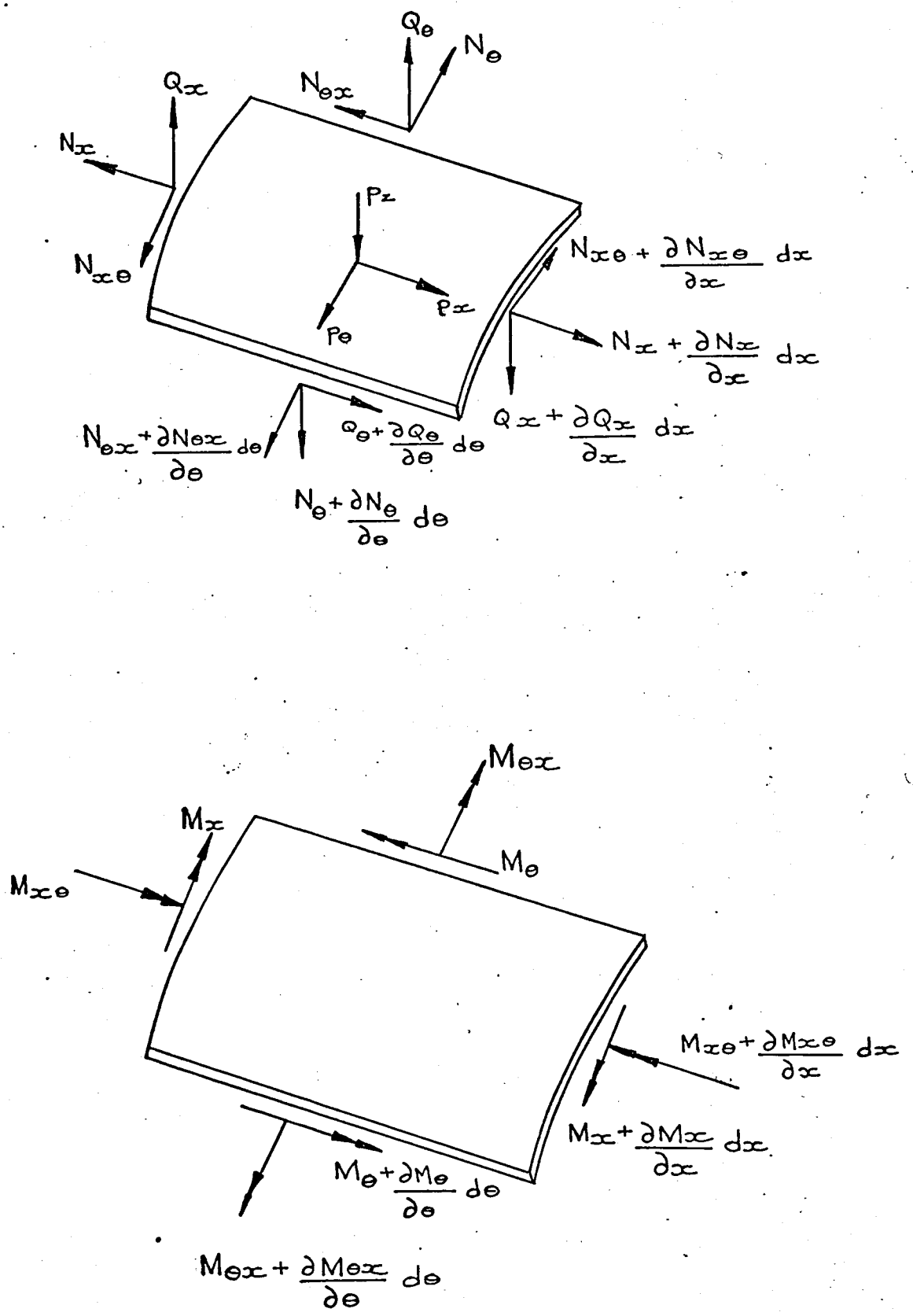

Fig. 2.2 Stress and moment Resultants.

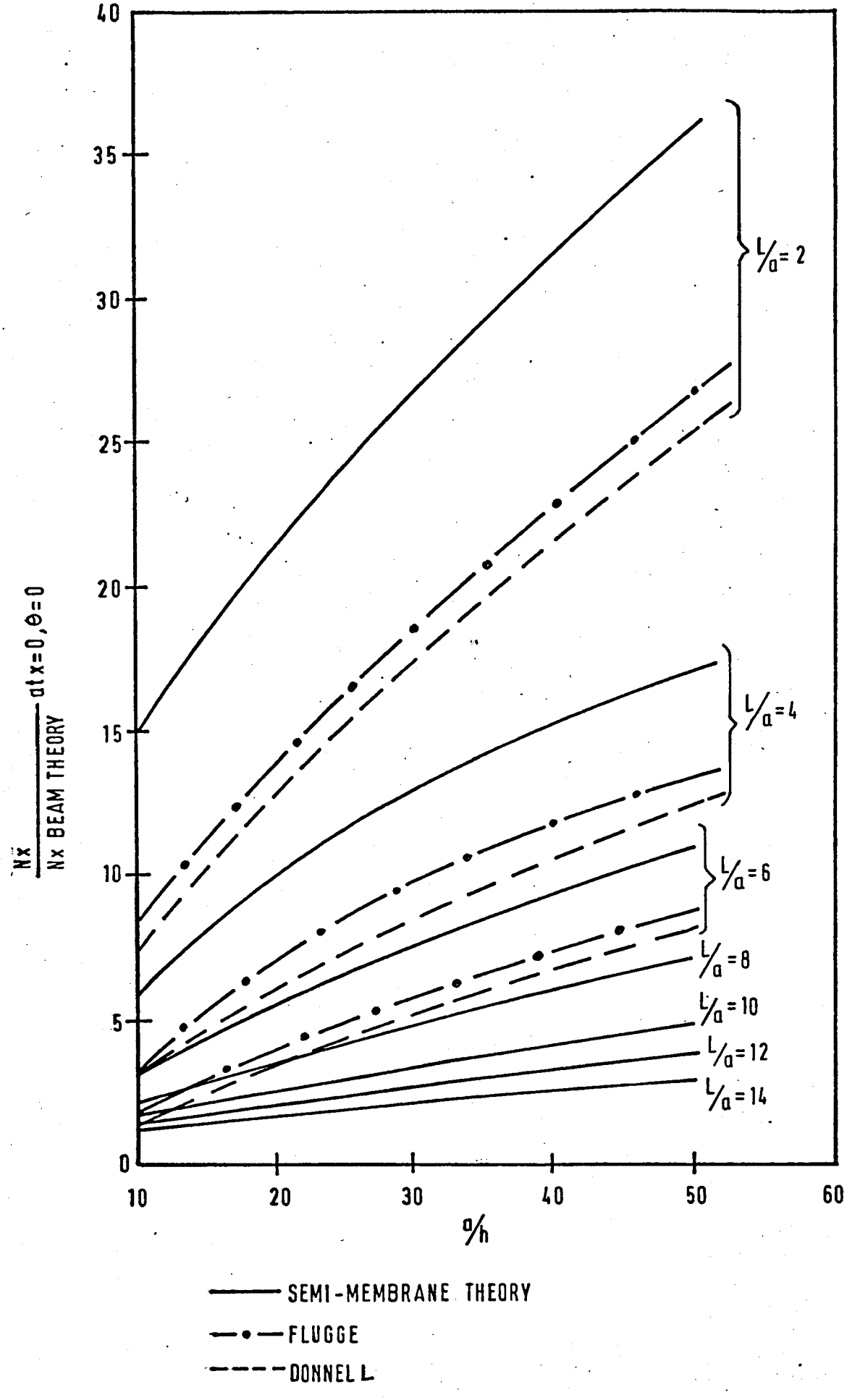

Figure 2.3

Comparison of axial stress at the root of windward generator

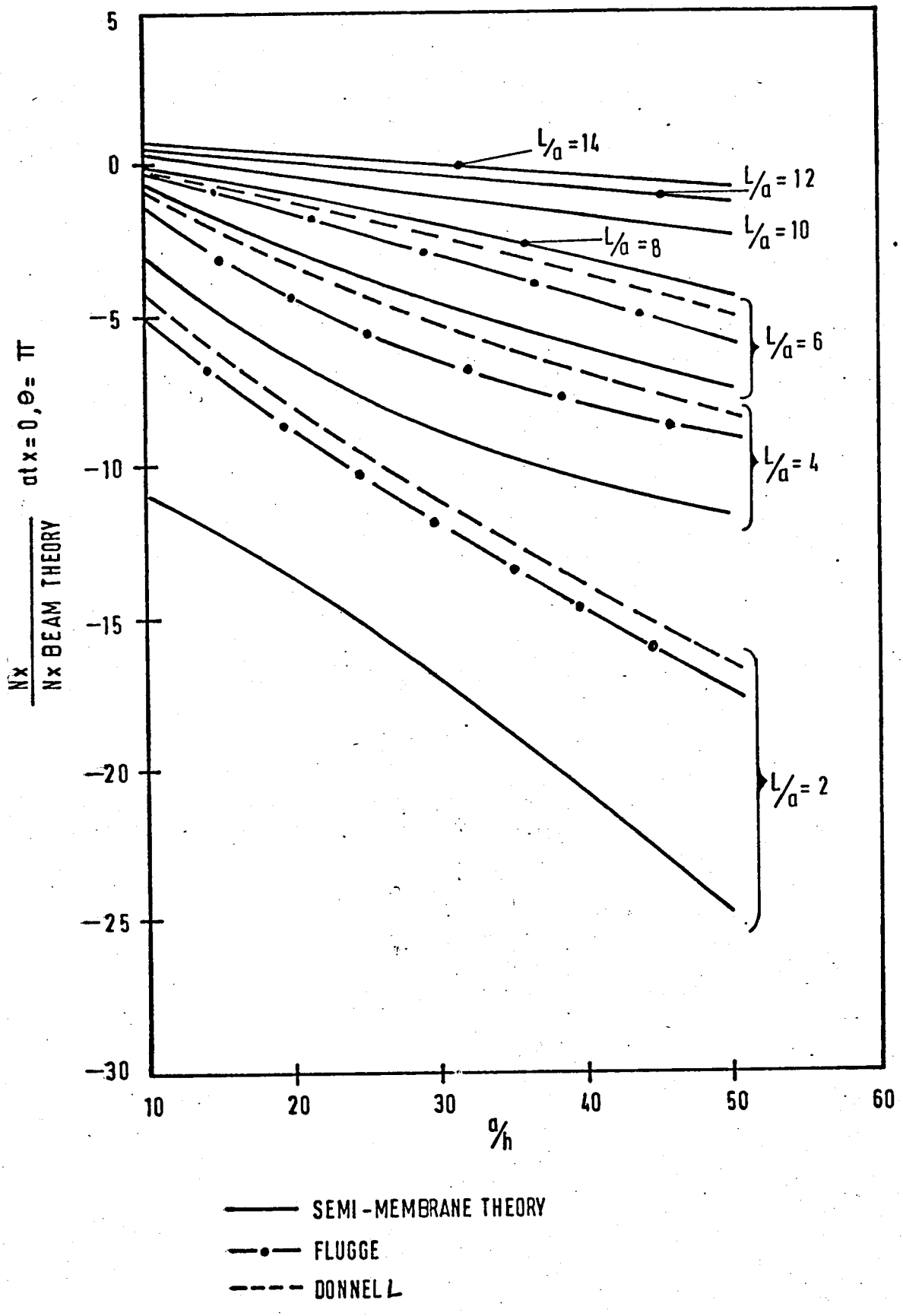

Figure 2.4

Comparison of axial stress at the root of leeward generator.

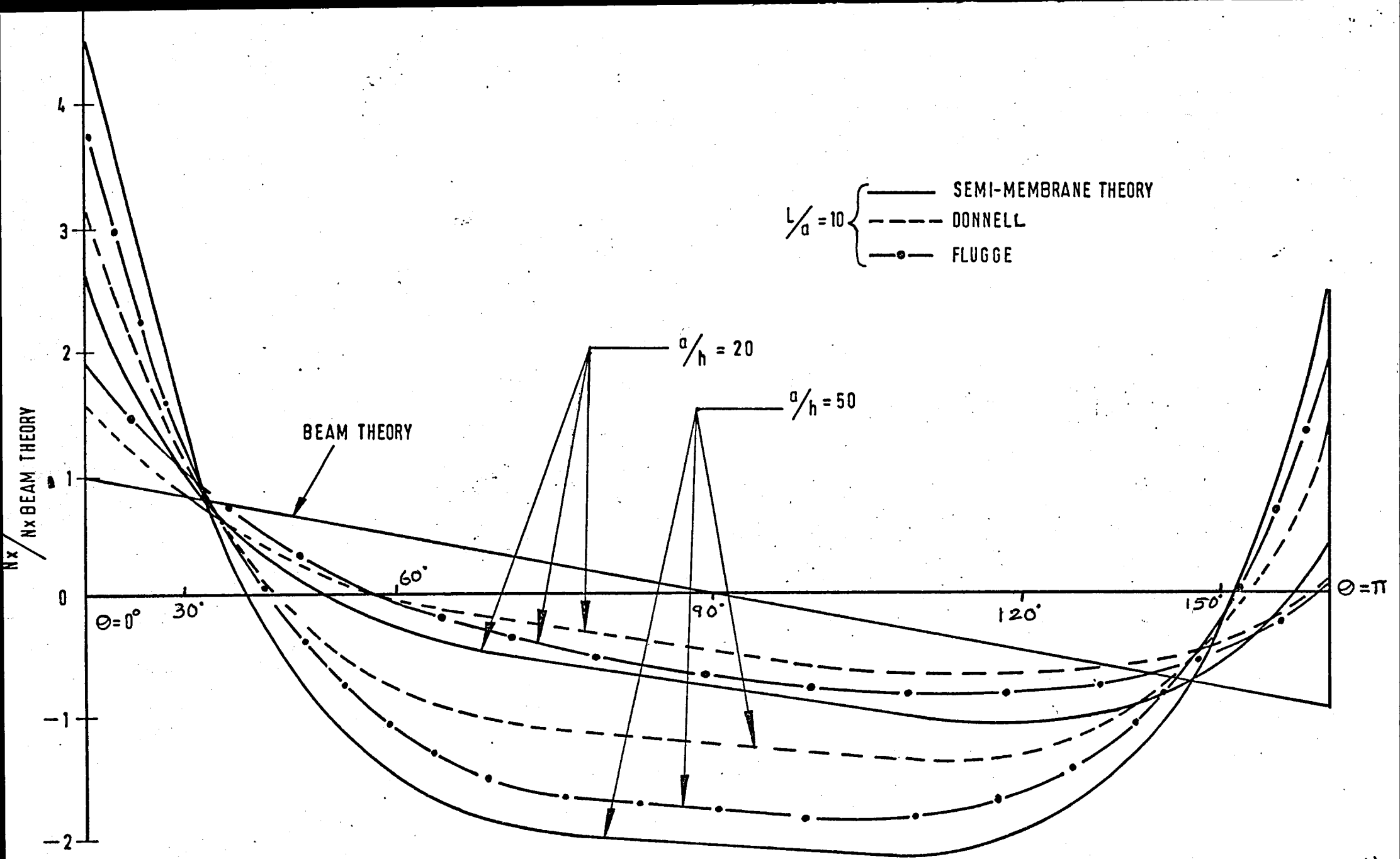

Figure 2.5 Circumferential Distribution of N_x at x = 0

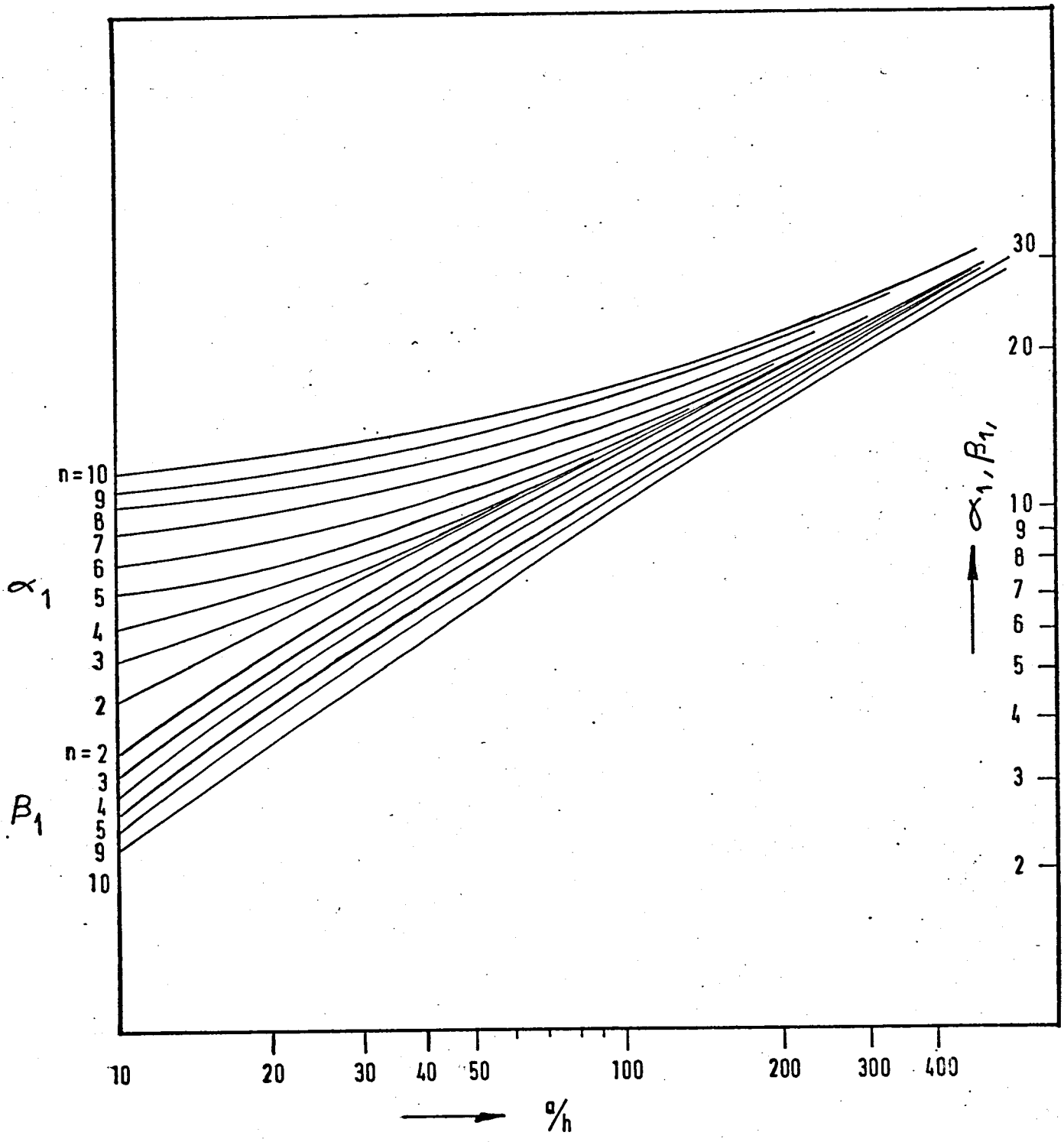

Fig. 2.6 Real and Imaginery parts : first root.

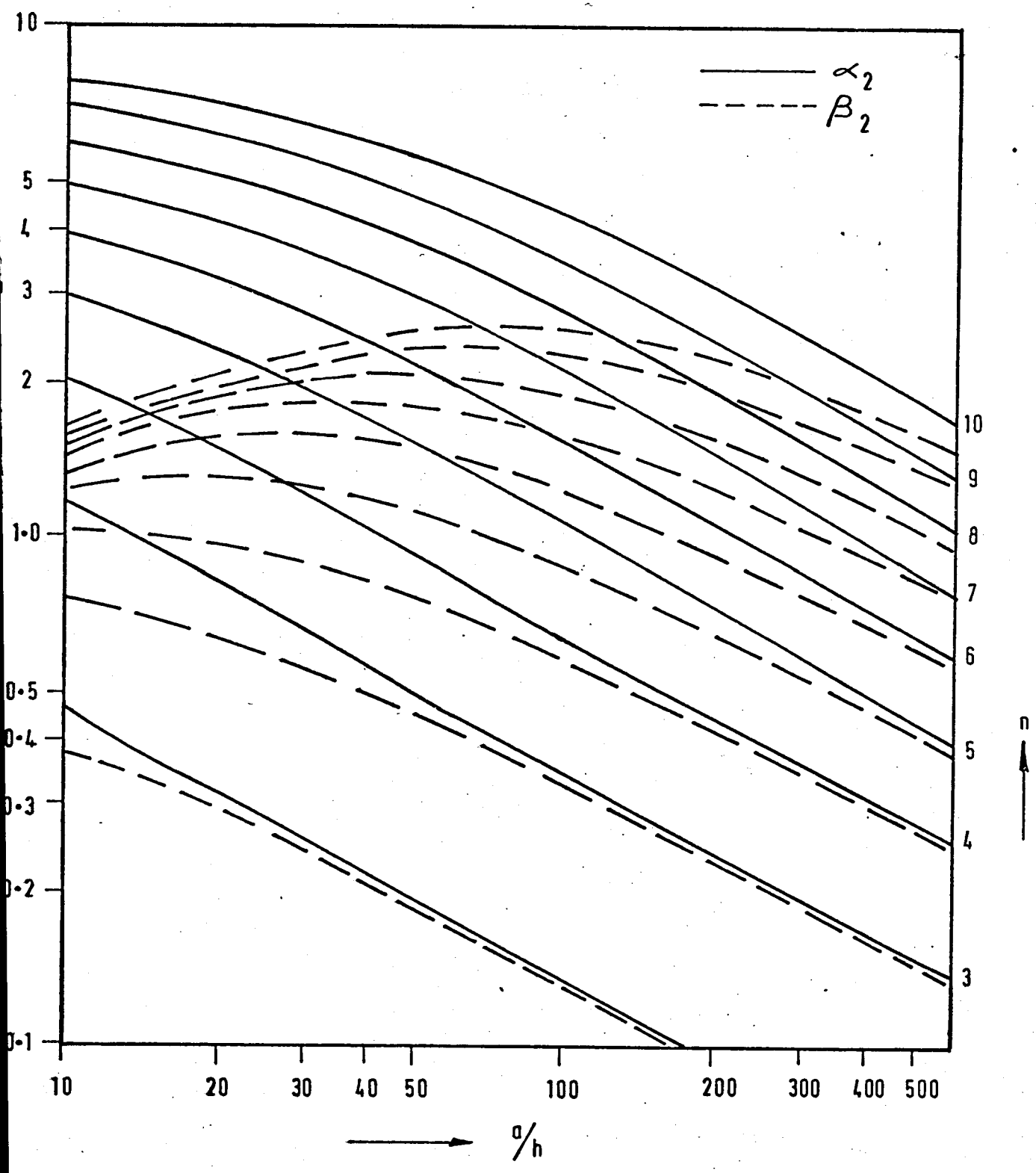

Fig. 2.7 Real and Imaginary parts: Second root.

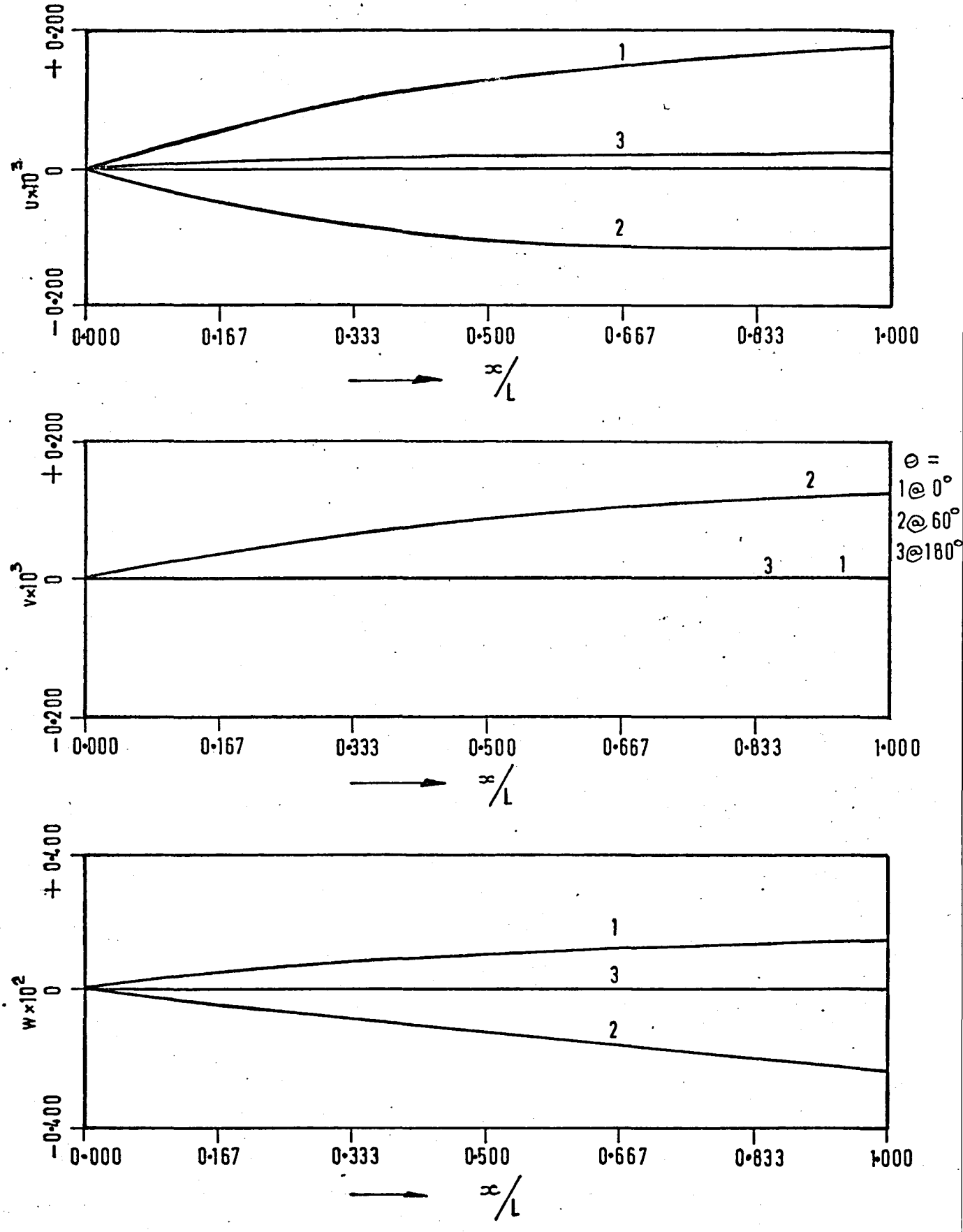

Fig. 2.8 The displacement distribution in axial direction.

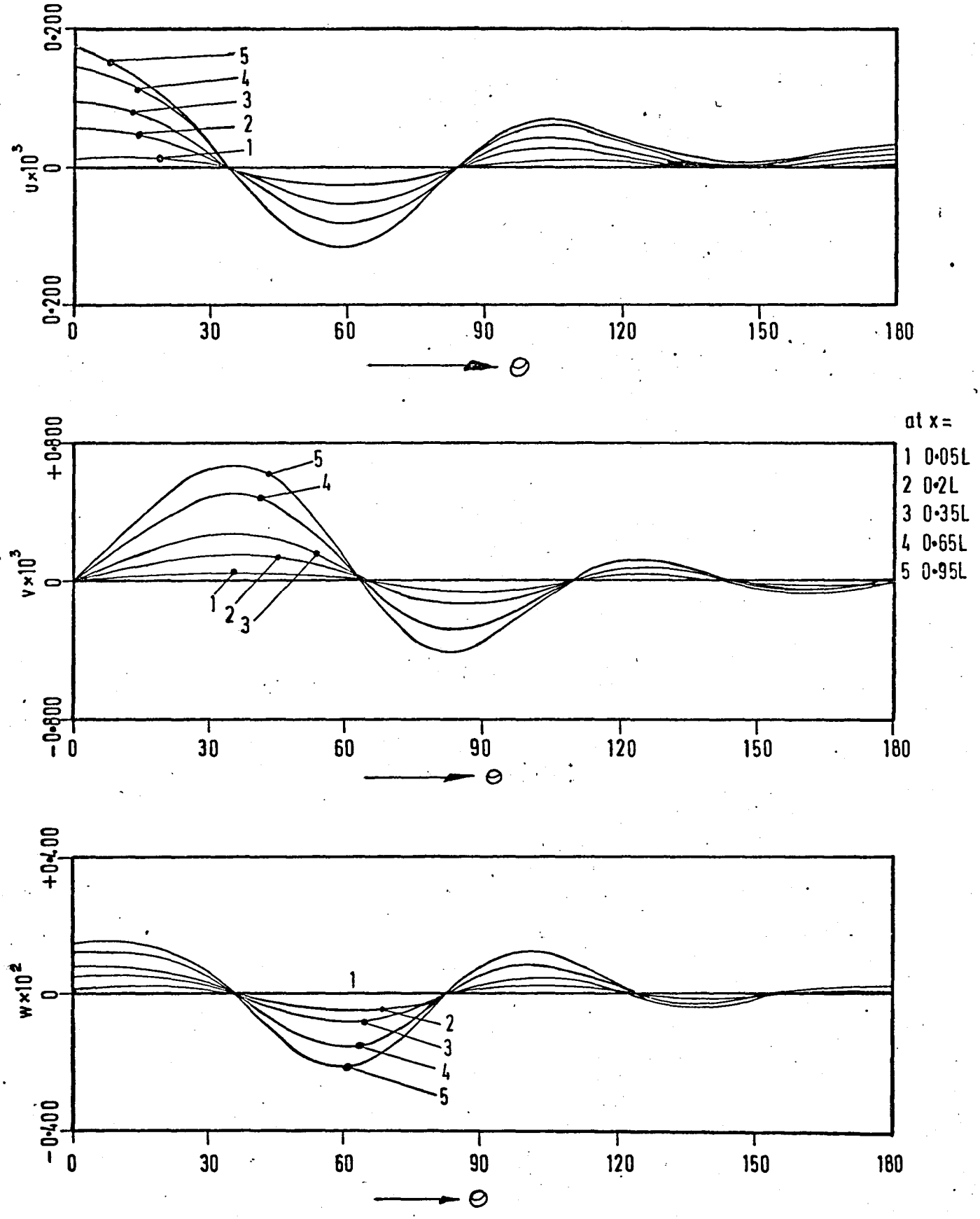

Fig. 2.9 The displacement distribution in circumferential direction.

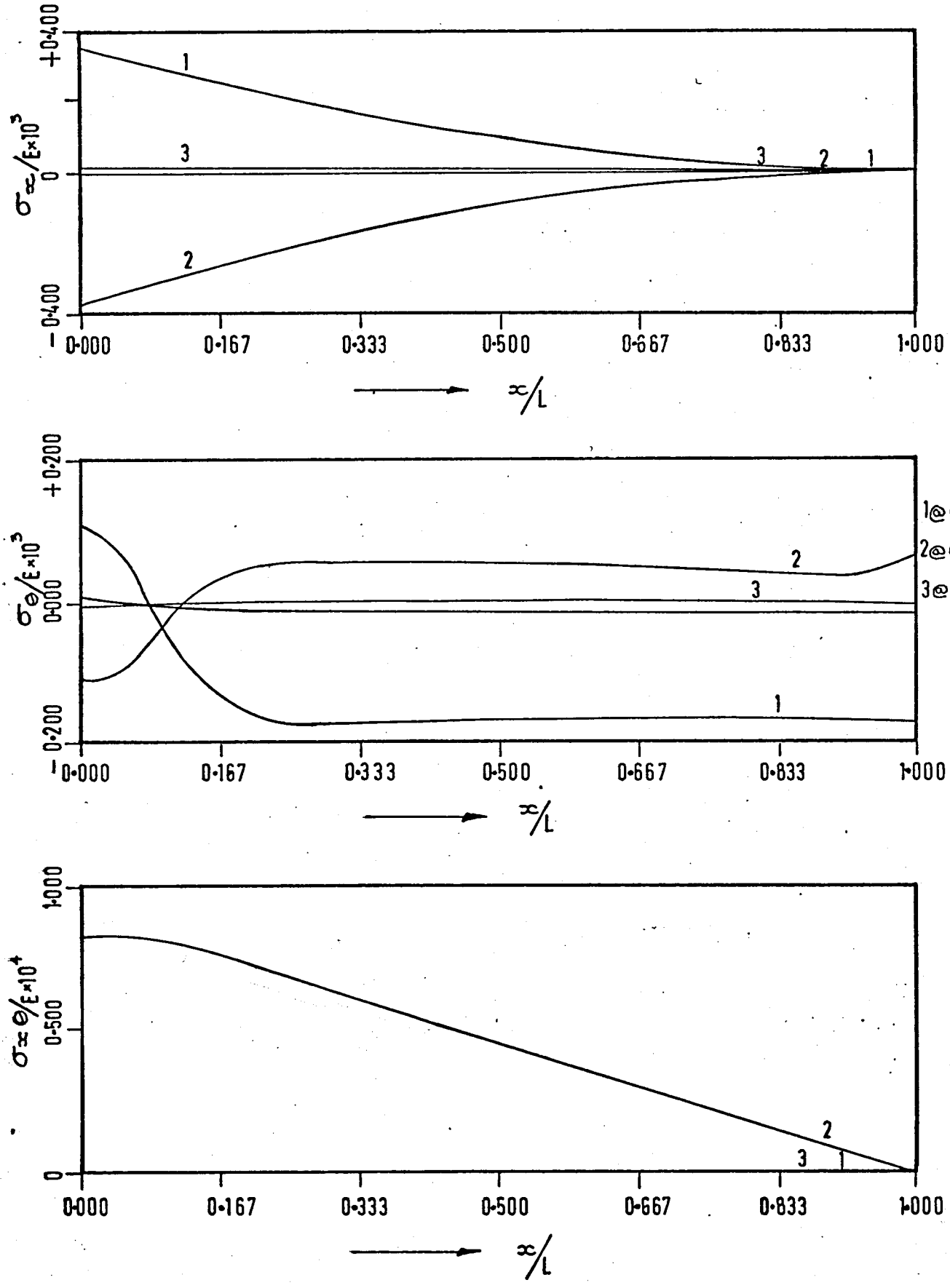

Fig. 2.10 The stress distribution in axial direction.

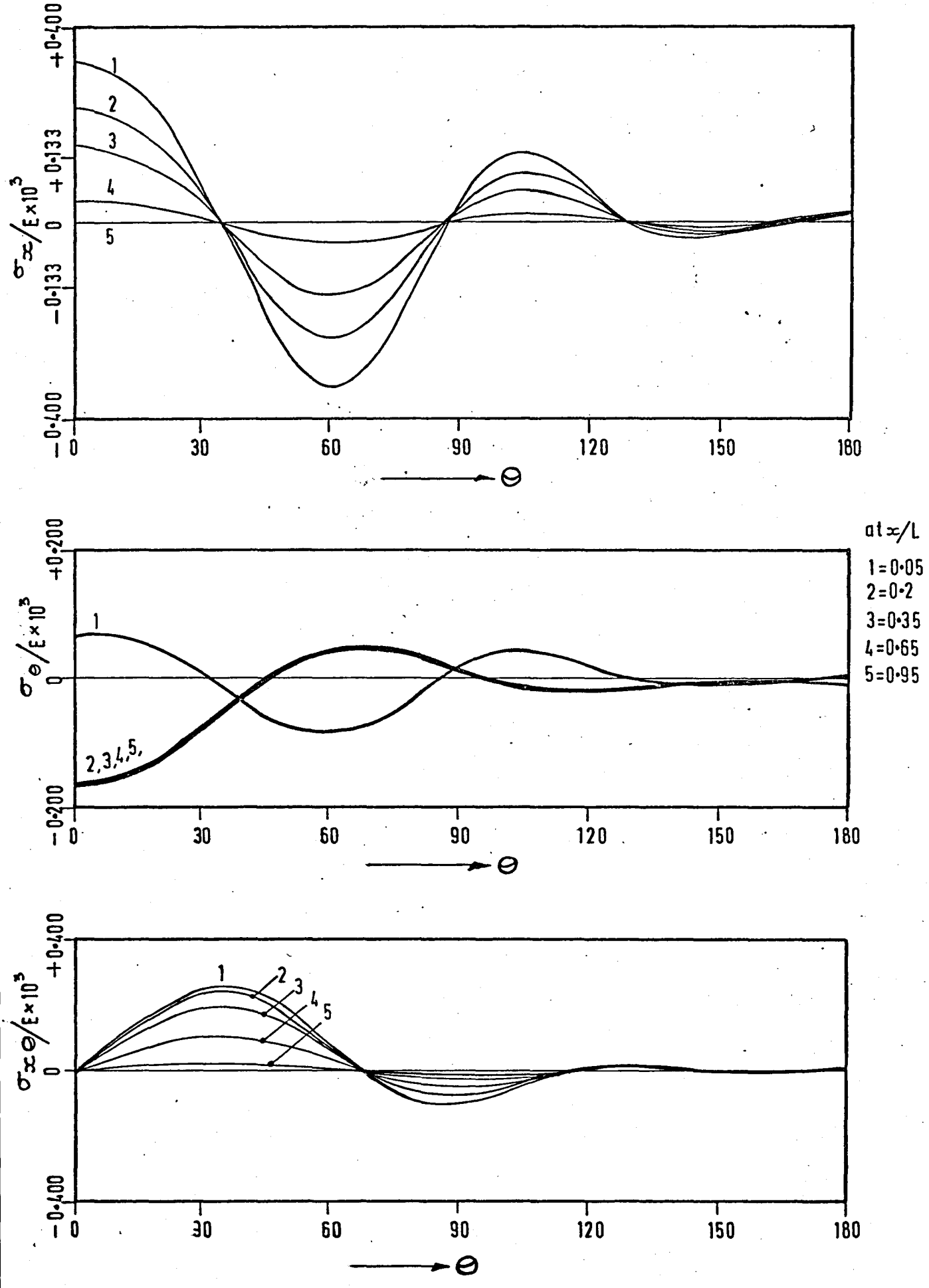

Fig.2.11 The stress distribution in circumferential direction.

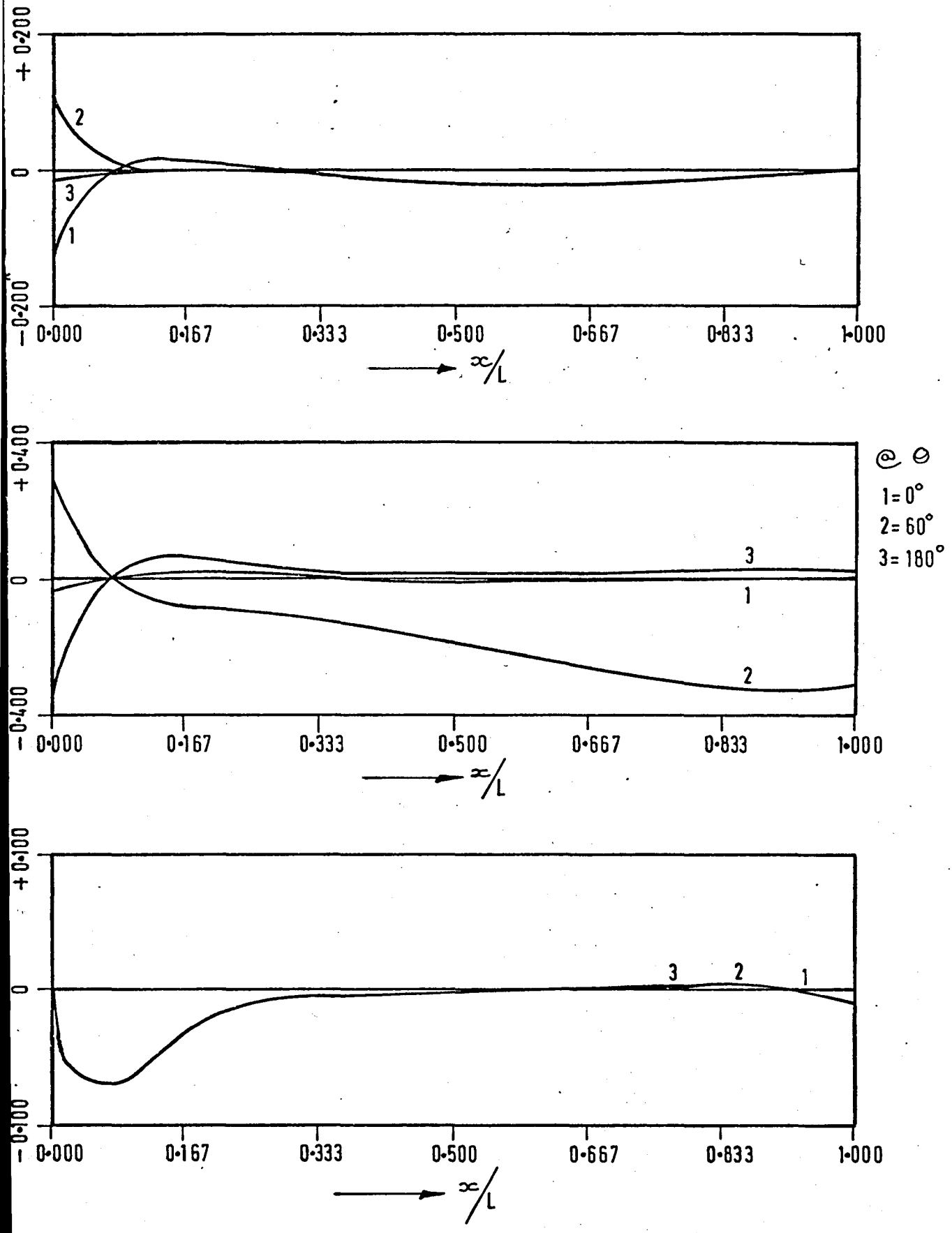

Fig. 2.12 The distribution of moment resultants in axial direction.

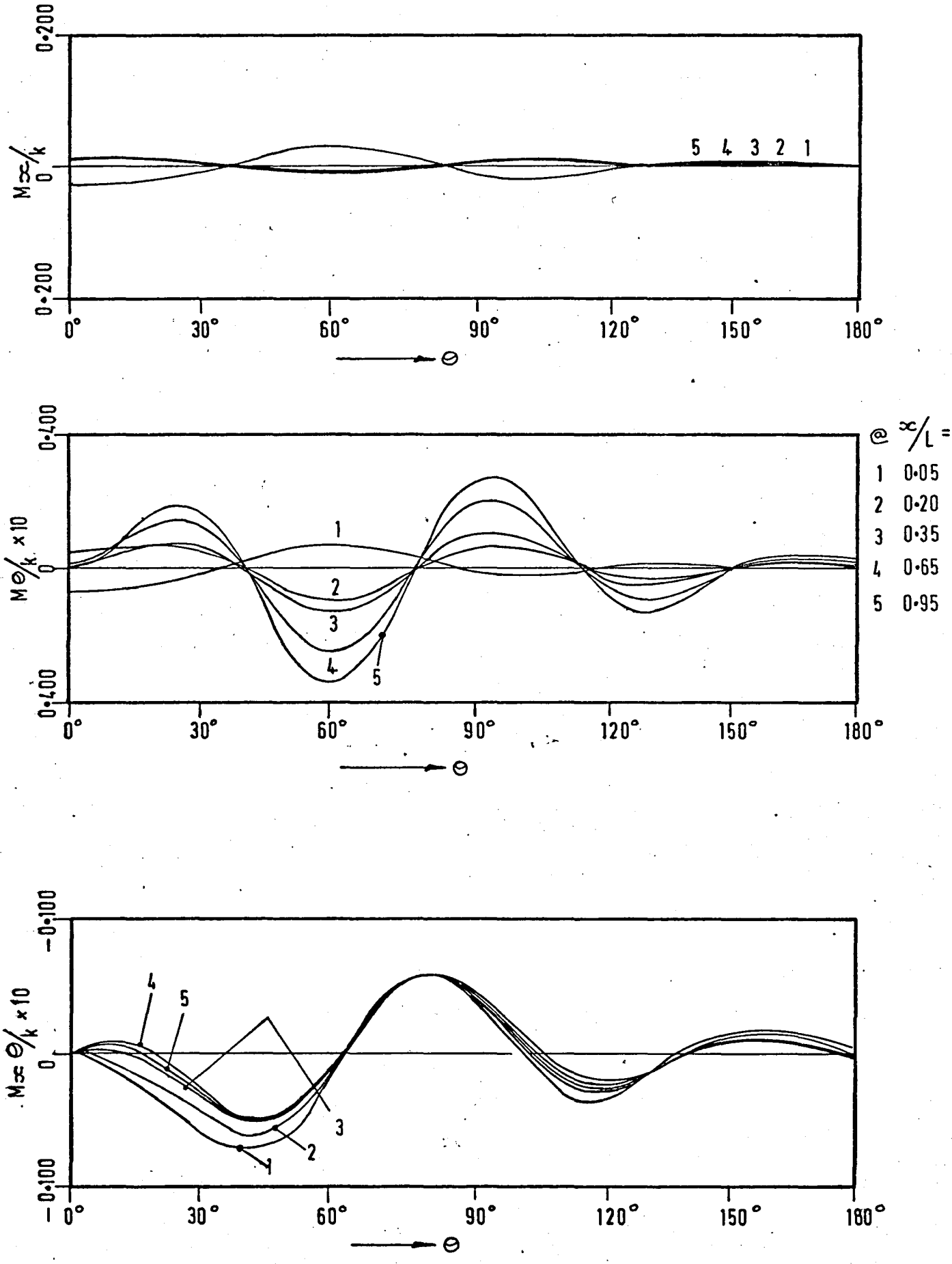

Fig. 2.13 The distribution of moment resultants in circumferential direction.

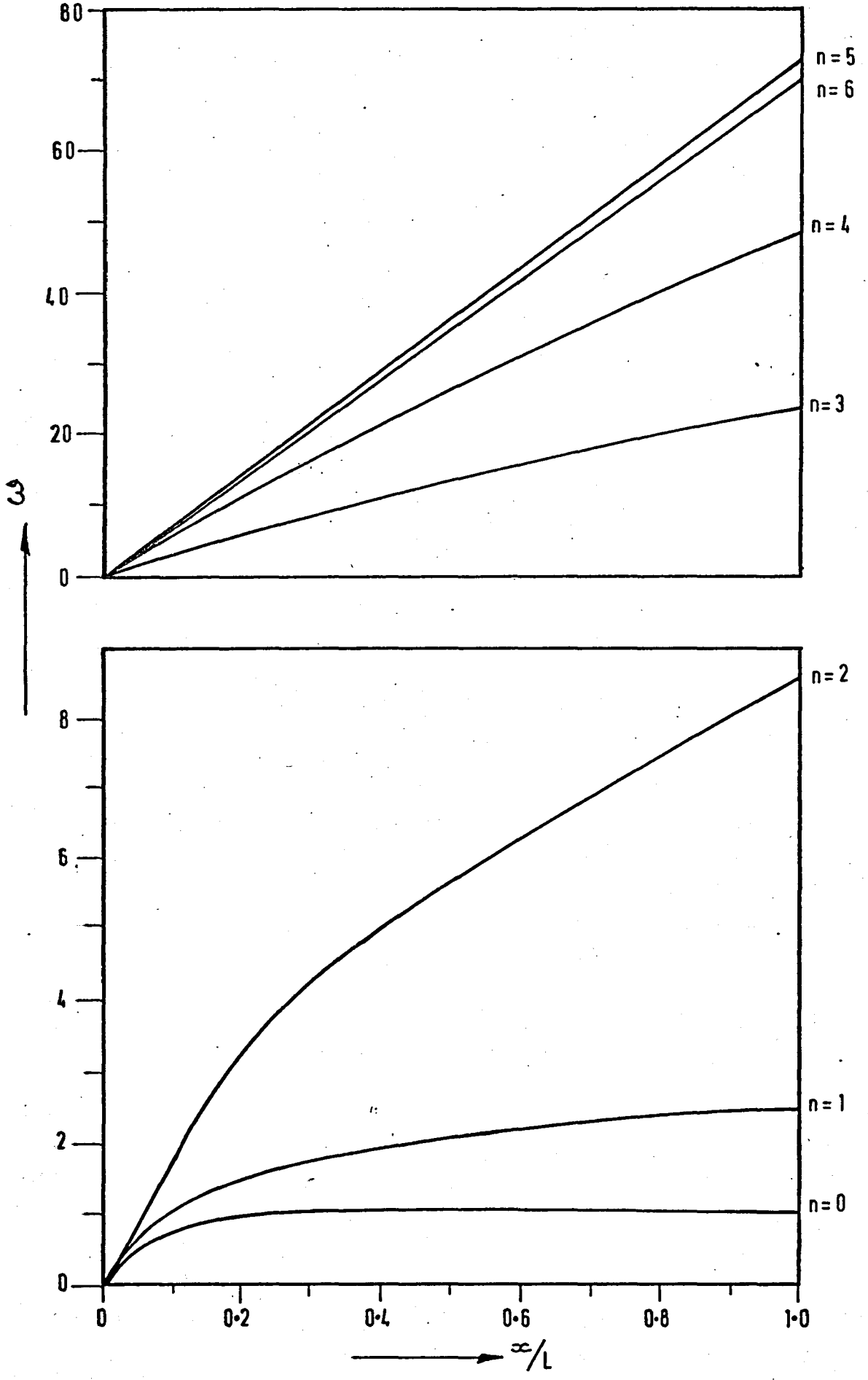

Fig. 2.14 The displacements distribution in axial direction for various harmonics.
Shell geometry: L/a = 1 (a/h) = 100 .

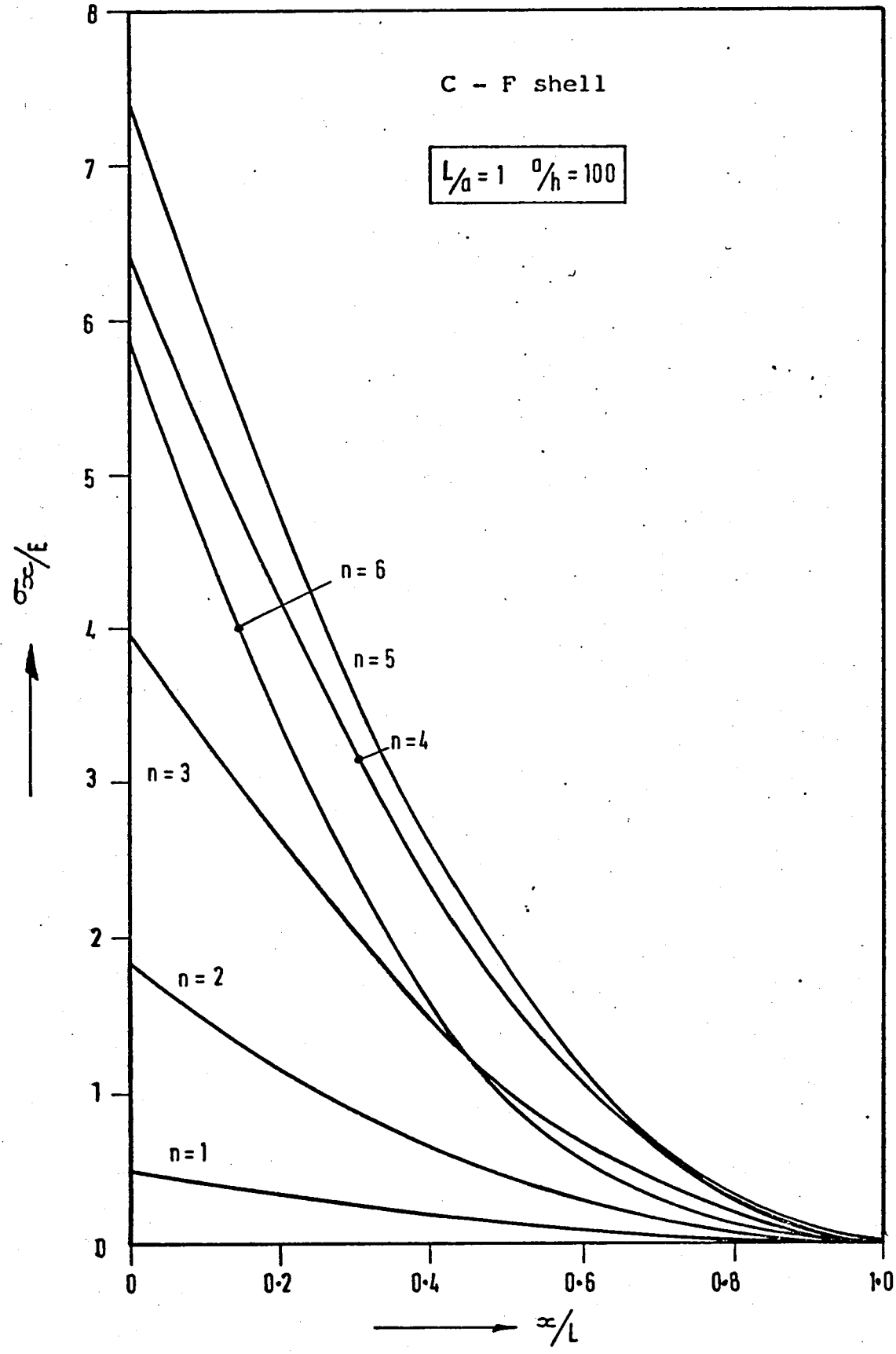

Fig. 2.15 The distribution of normal stress in the axial direction for different harmonics.

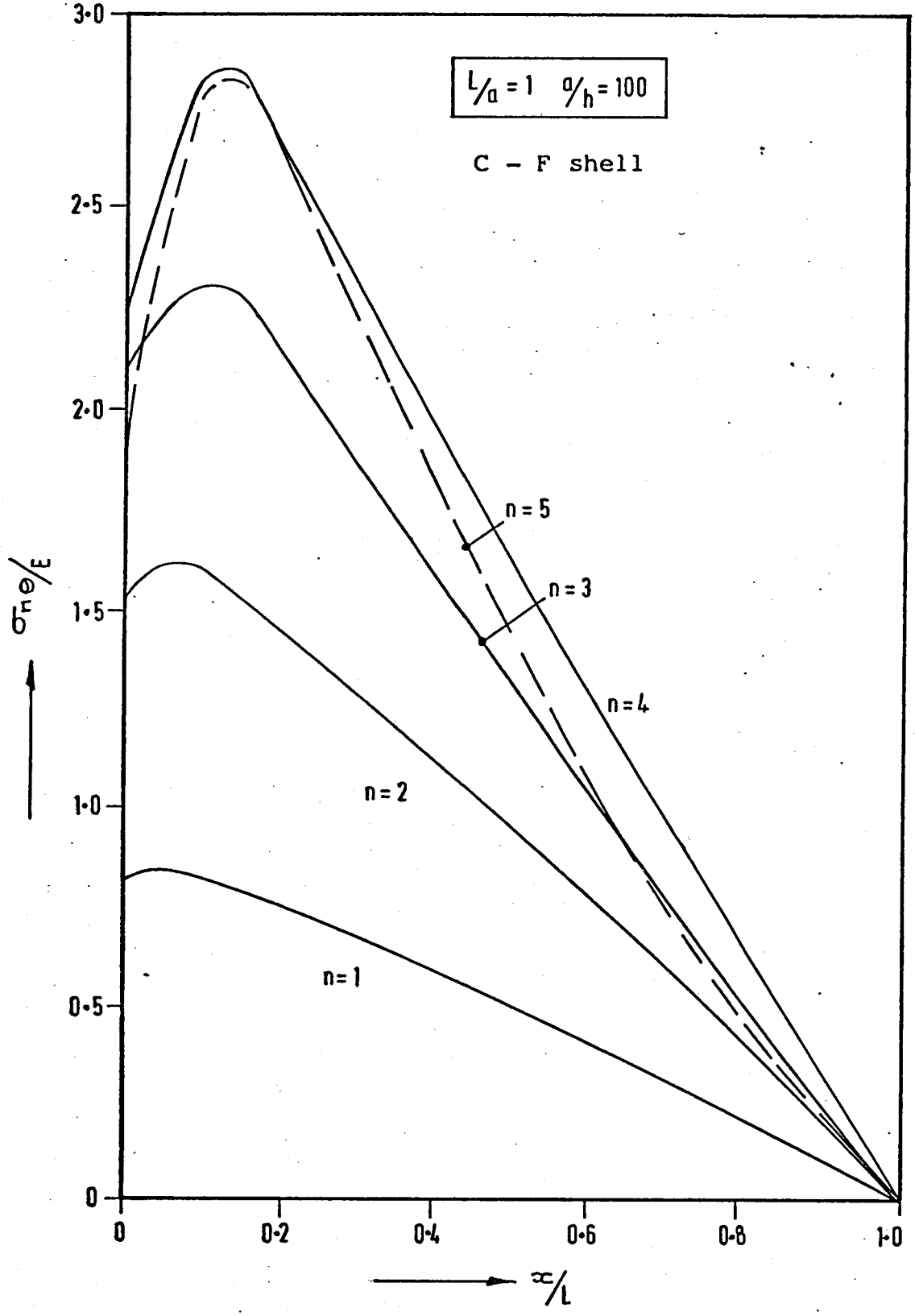

Fig. 2.16 The distribution of shear stress for each harmonic in axial direction.

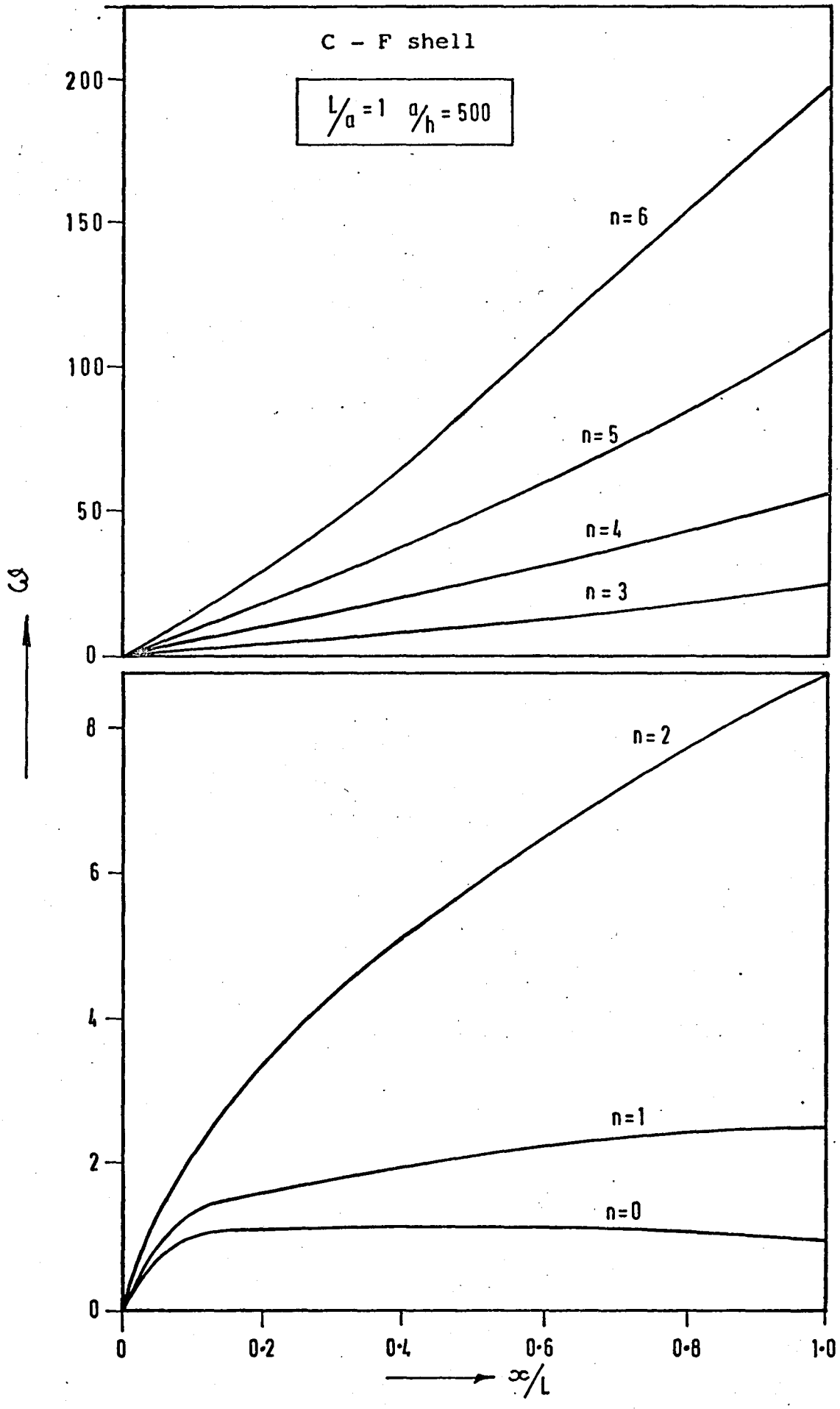

Fig. 2.17 Distribution of radial displacement in axial direction for different harmonics.

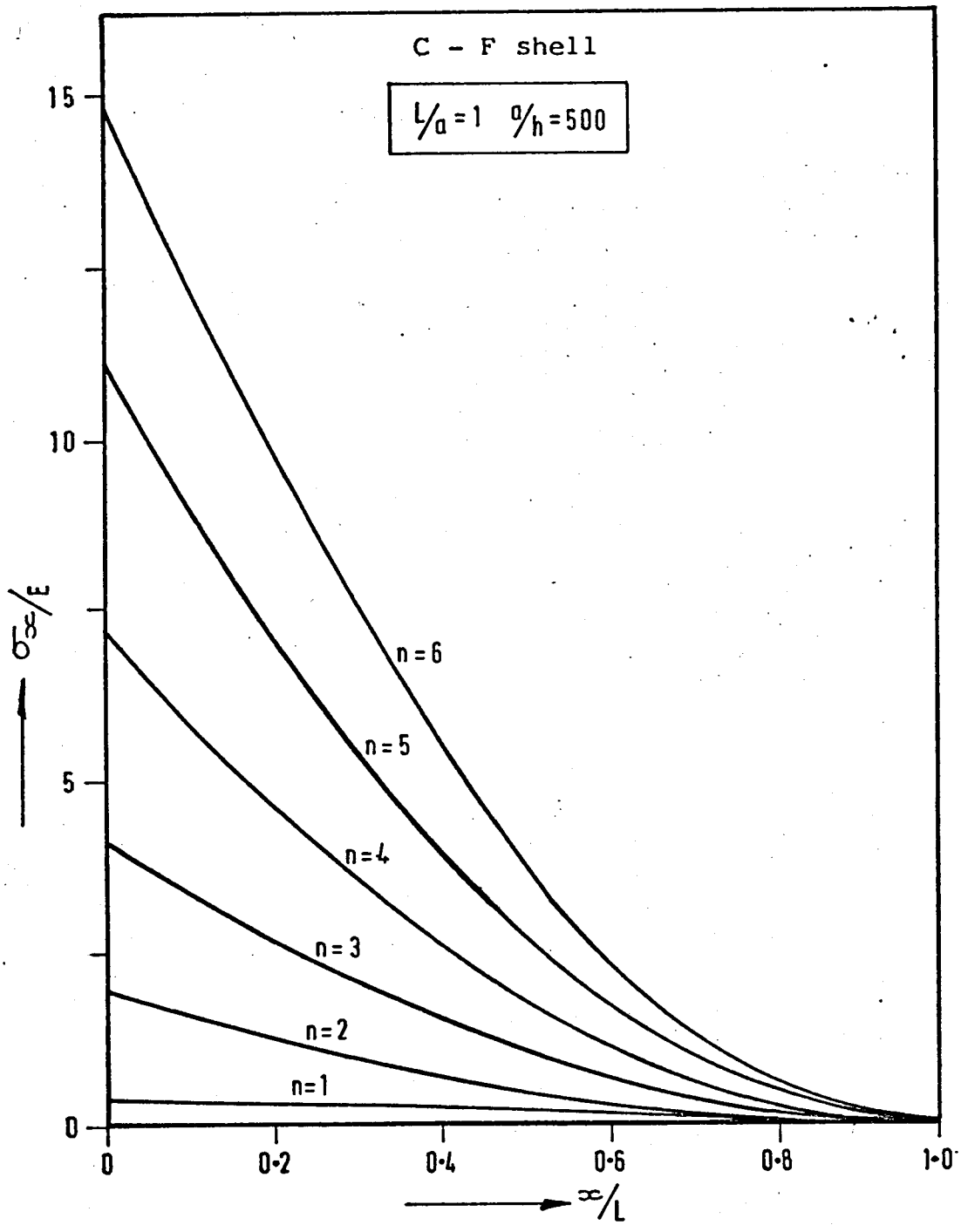

Fig. 2.18 The distribution of normal stress in the axial direction for different harmonics.

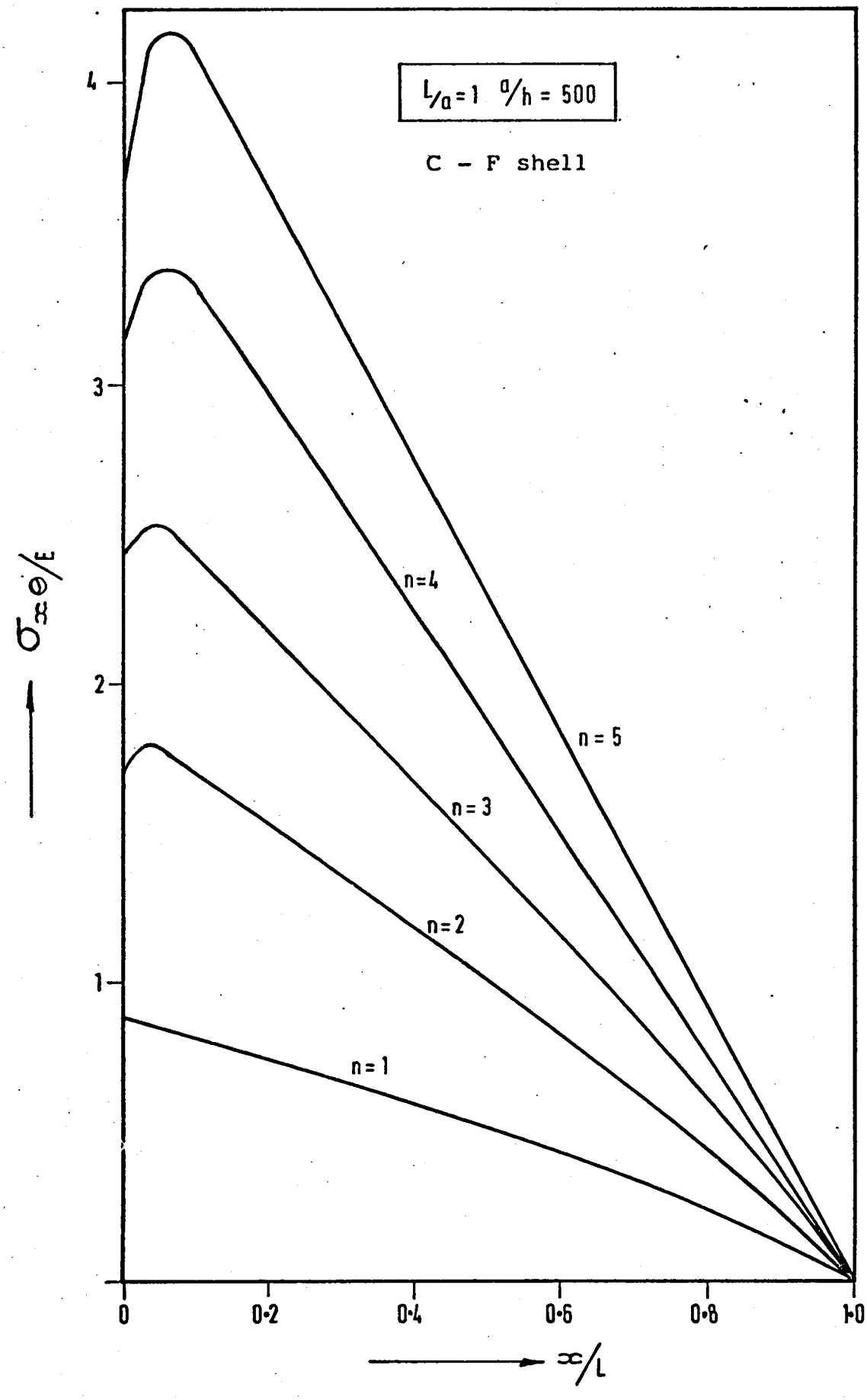

Fig. 2.19 Distribution of shear stress in the axial direction for different harmonics.

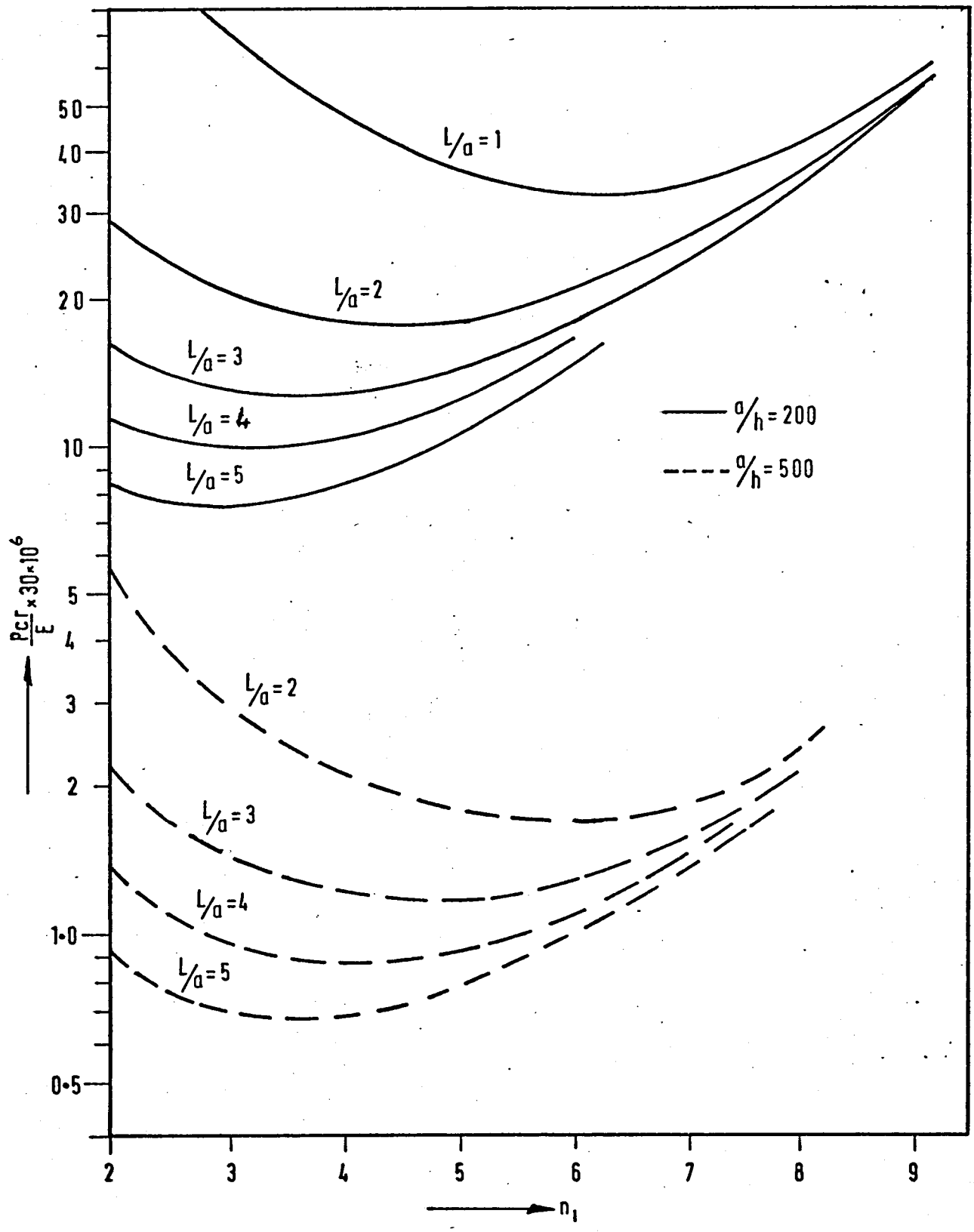

Fig. 3.1 Variation of P_{cr} with lower limit of harmonics.

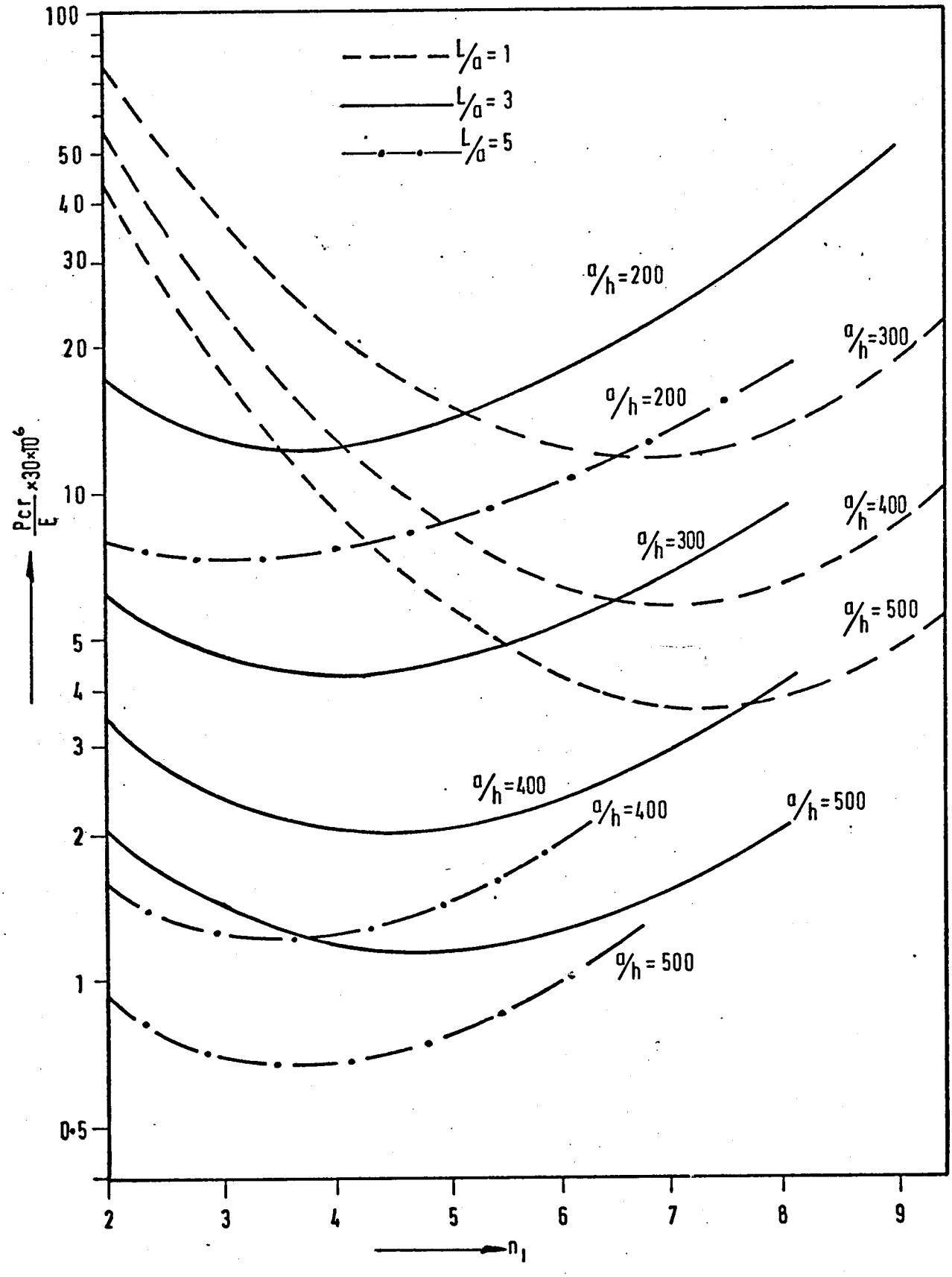

Fig. 3.2 Variation of P_{cr} with lower limit of harmonics.

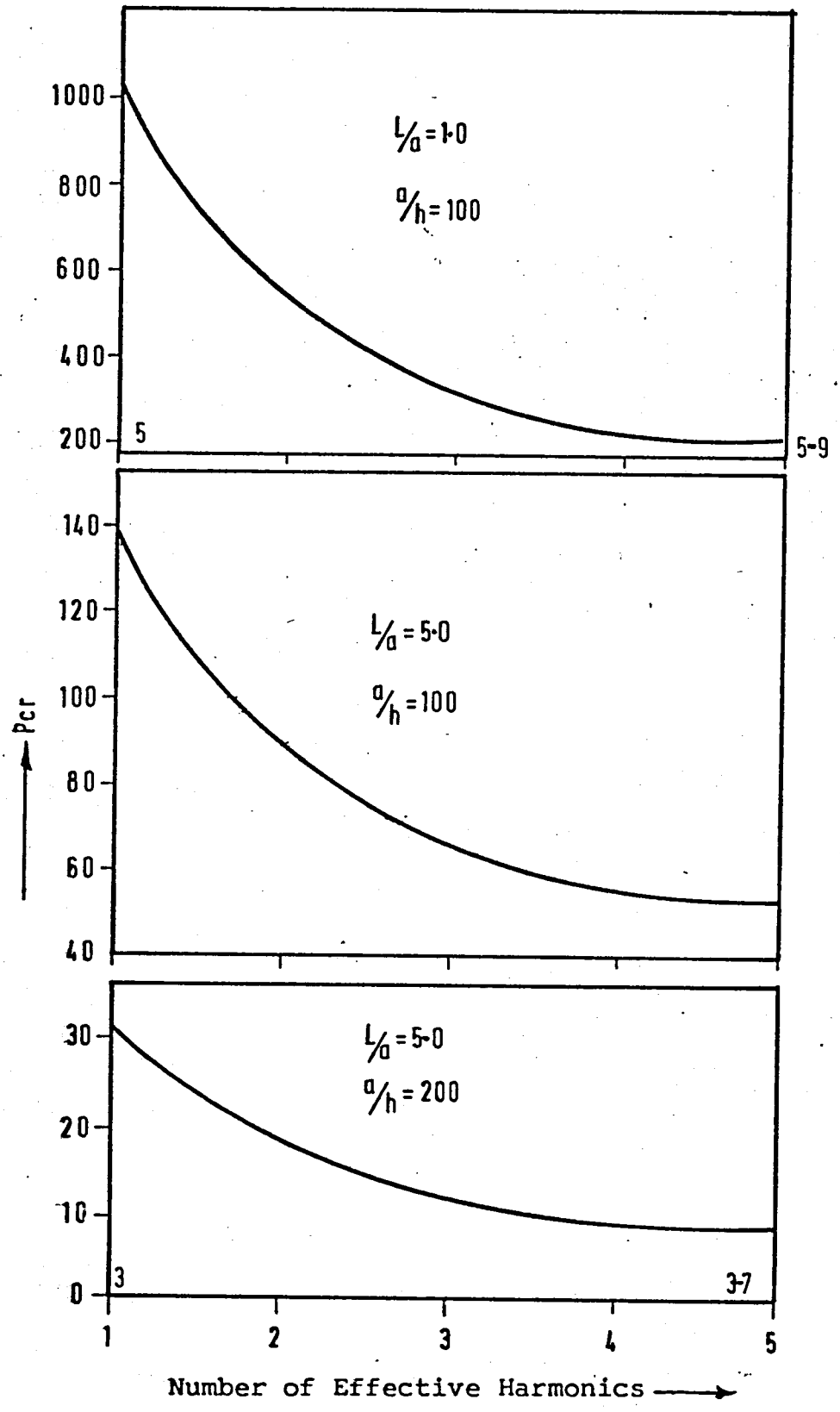

Figure 3.3 Convergence of the results with Fourier harmonics.

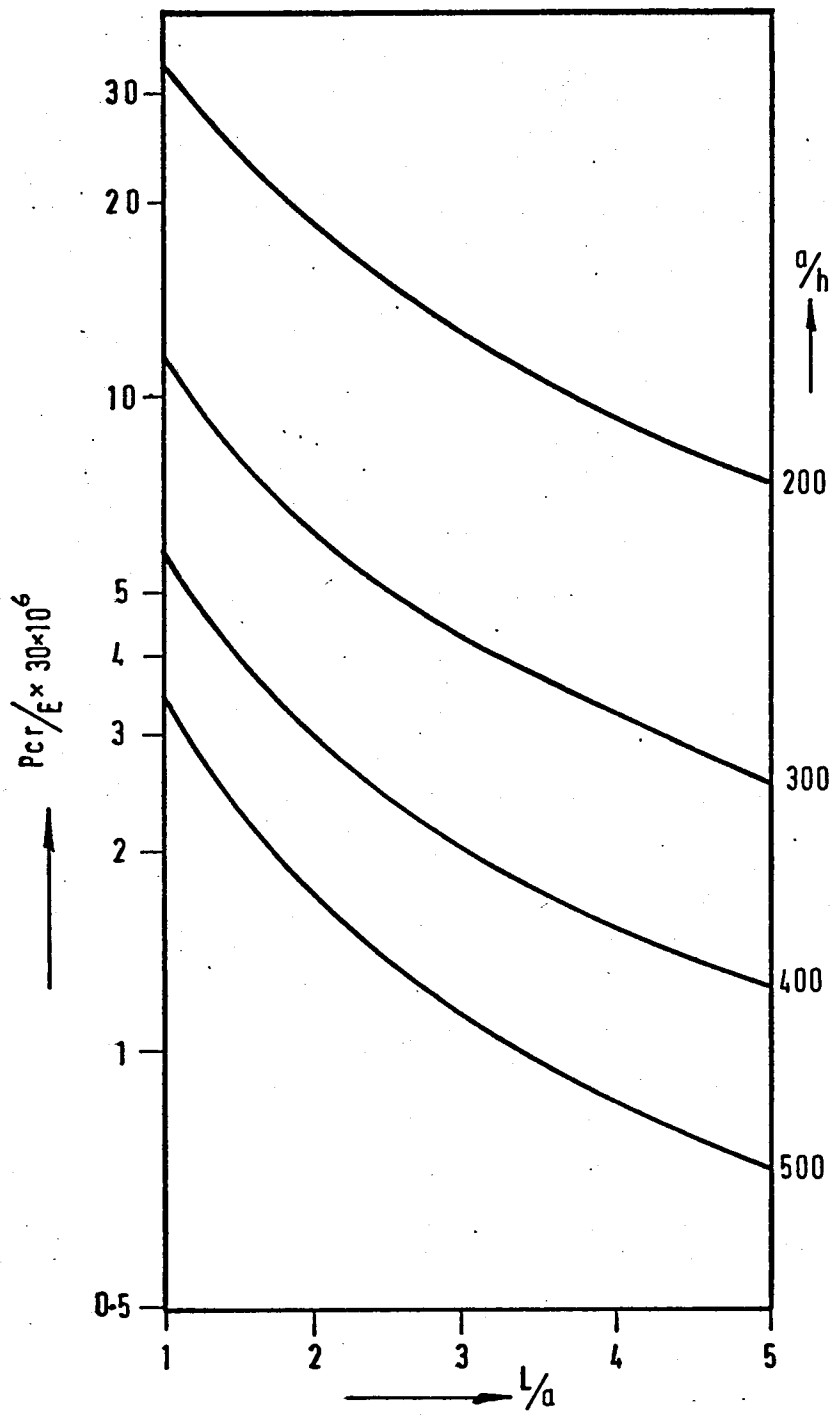

Fig. 3.4 Buckling pressures for different shell geometry.

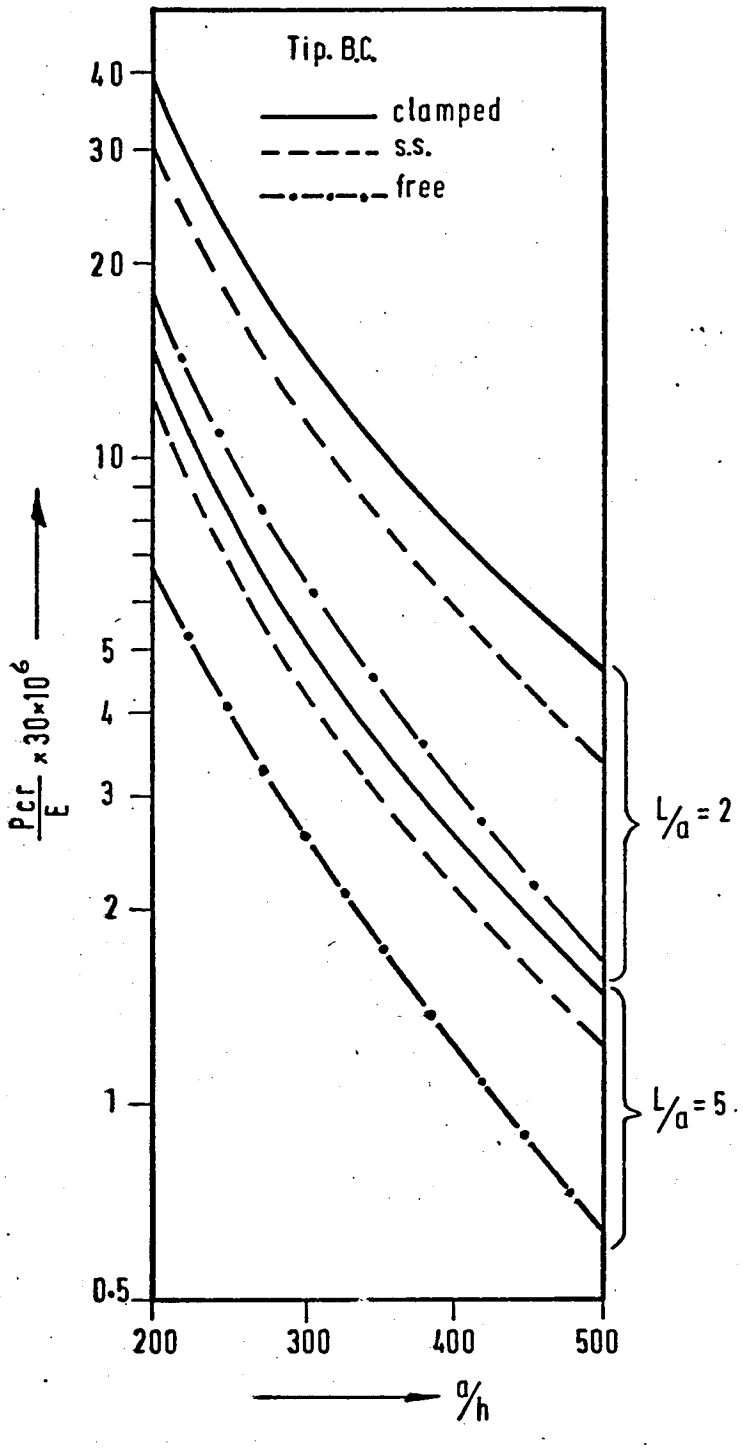

Fig. 3.5 Buckling pressures for different tip boundary conditions.

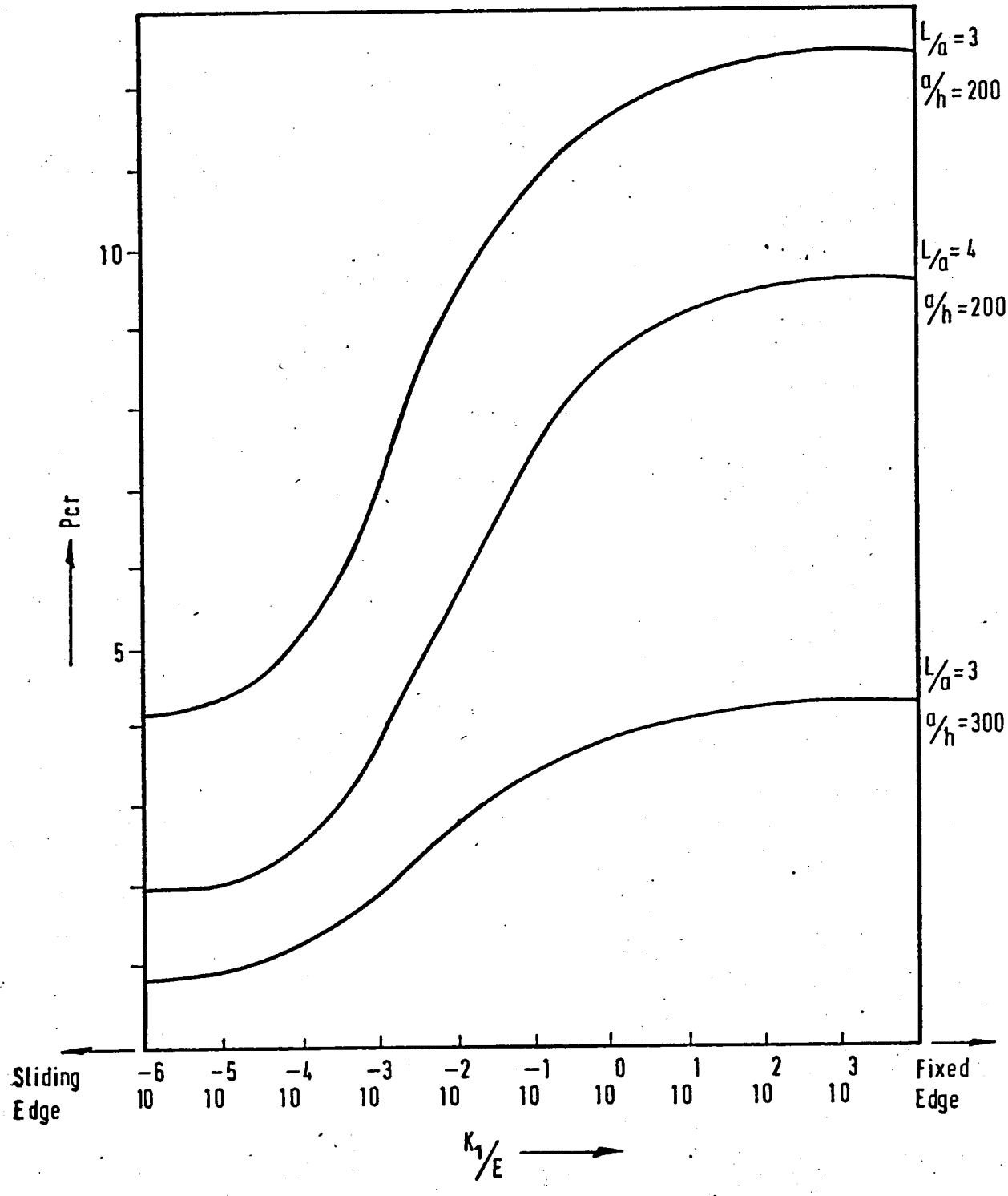

Fig. 3.6 Influence of axial displacement at the base on the buckling pressure.

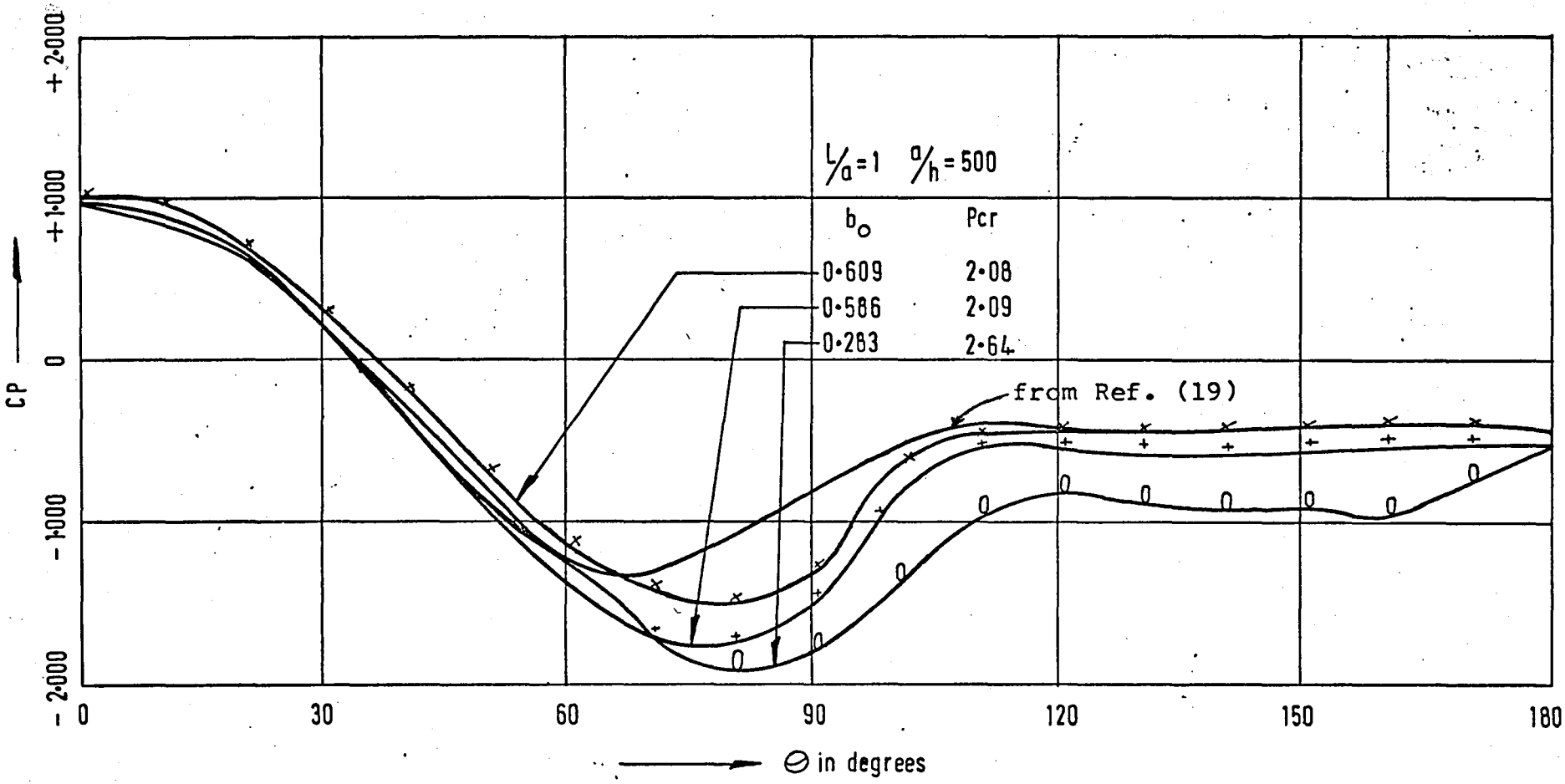

Fig. 3.7 Different pressure distributions considered (Gould Ref.(34))

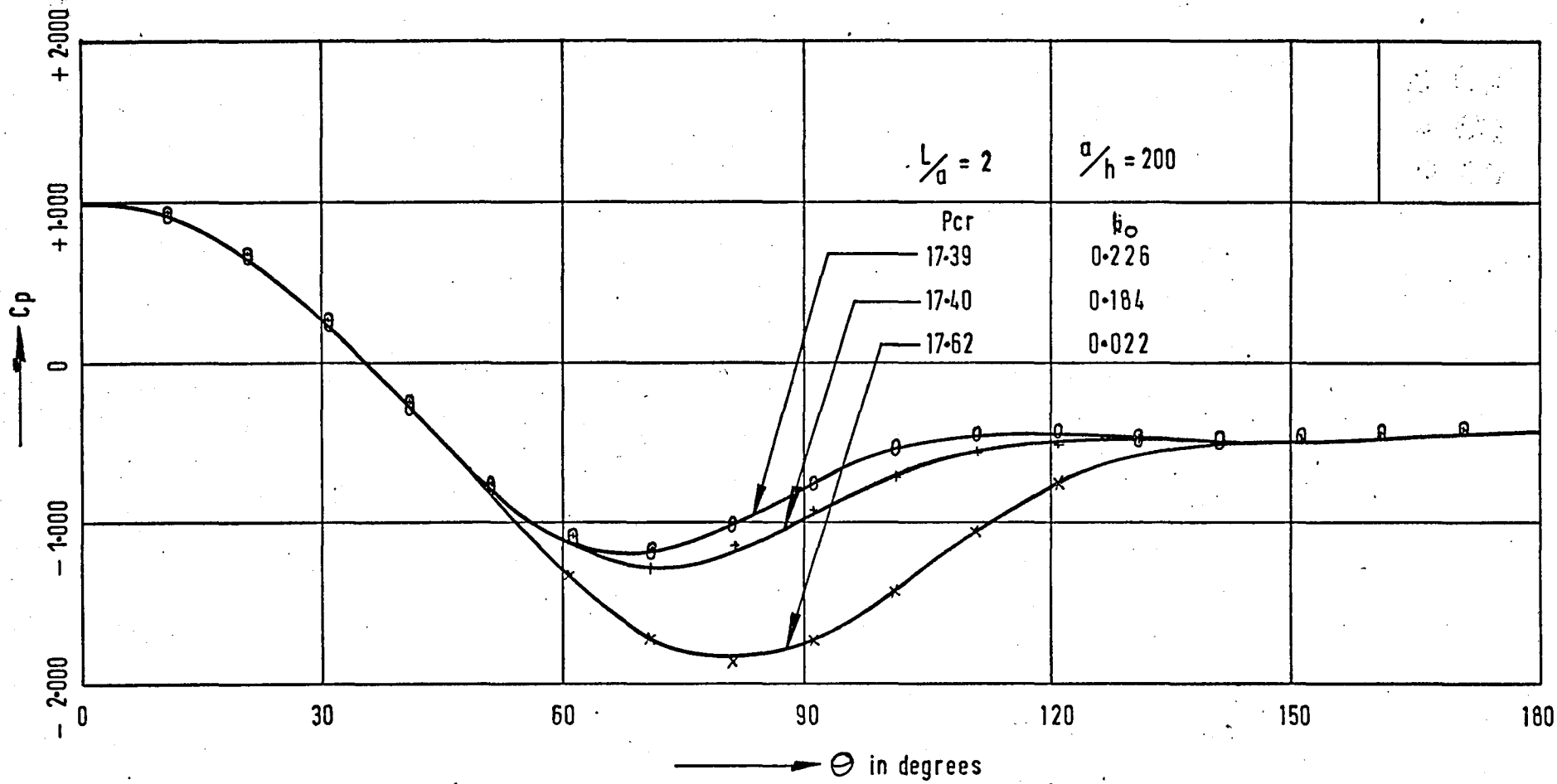

Fig. 3.8 Influence of suction peak on buckling pressures.

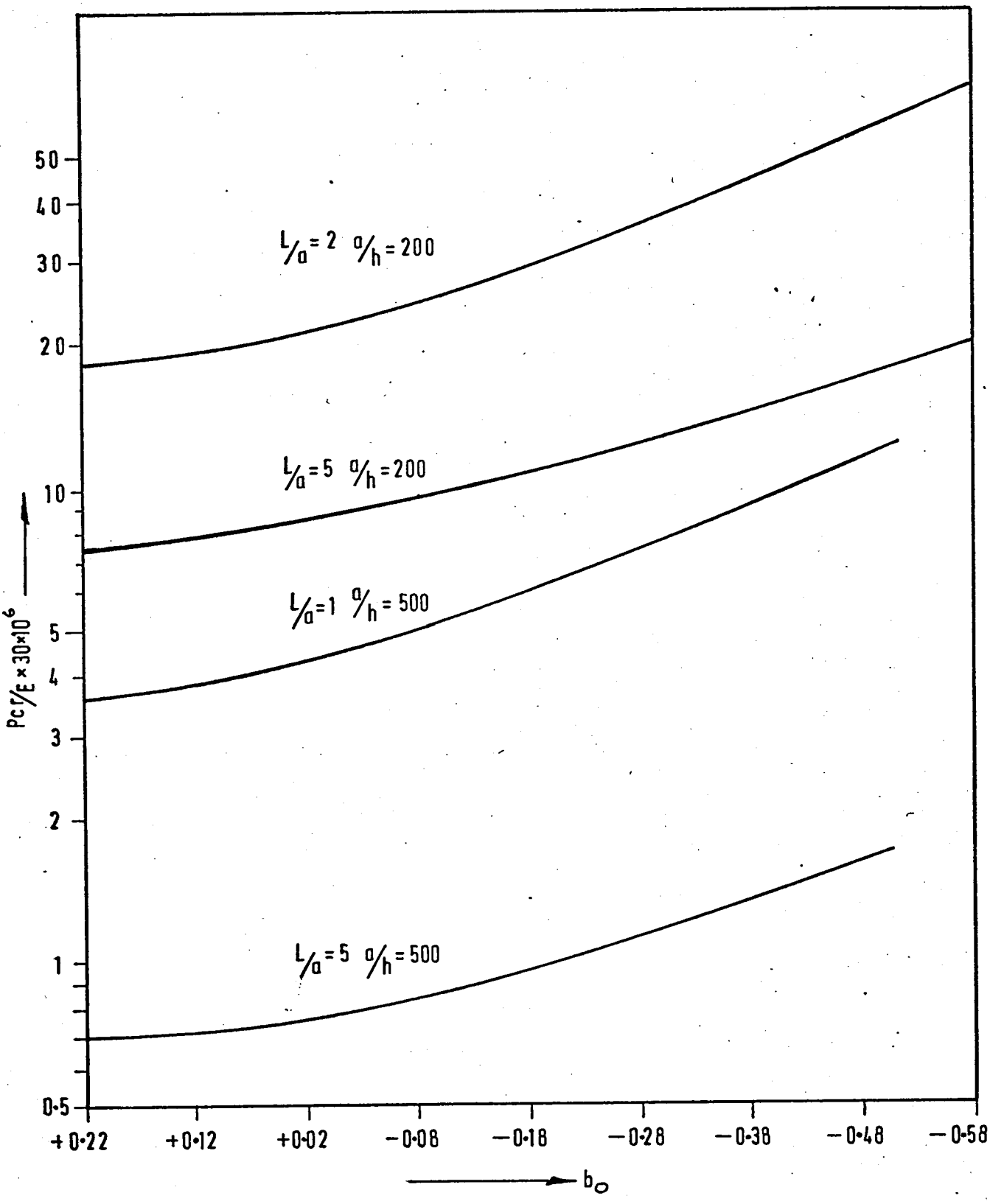

Fig. 3.9 Effect of b_o on critical buckling pressures.

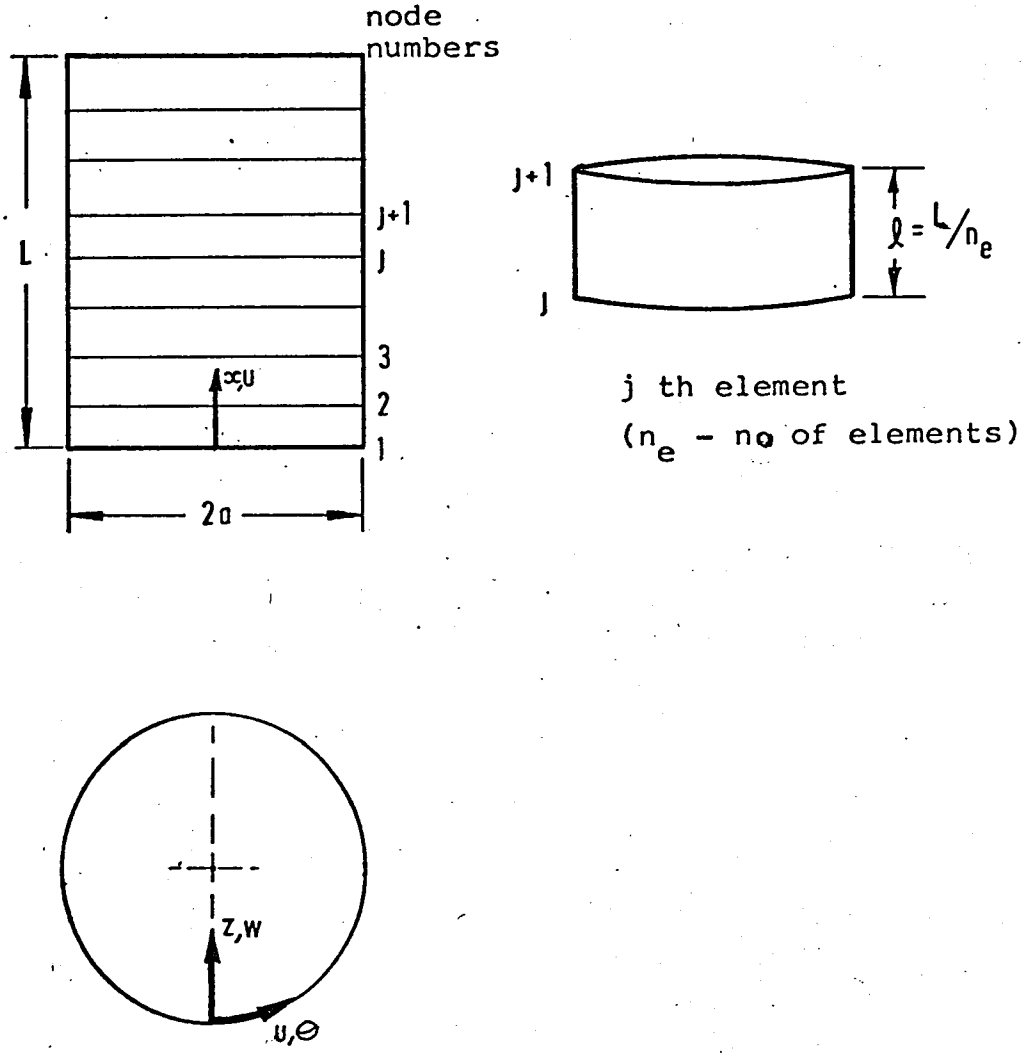

Fig. 4.1 Representation of shell as discrete elements.

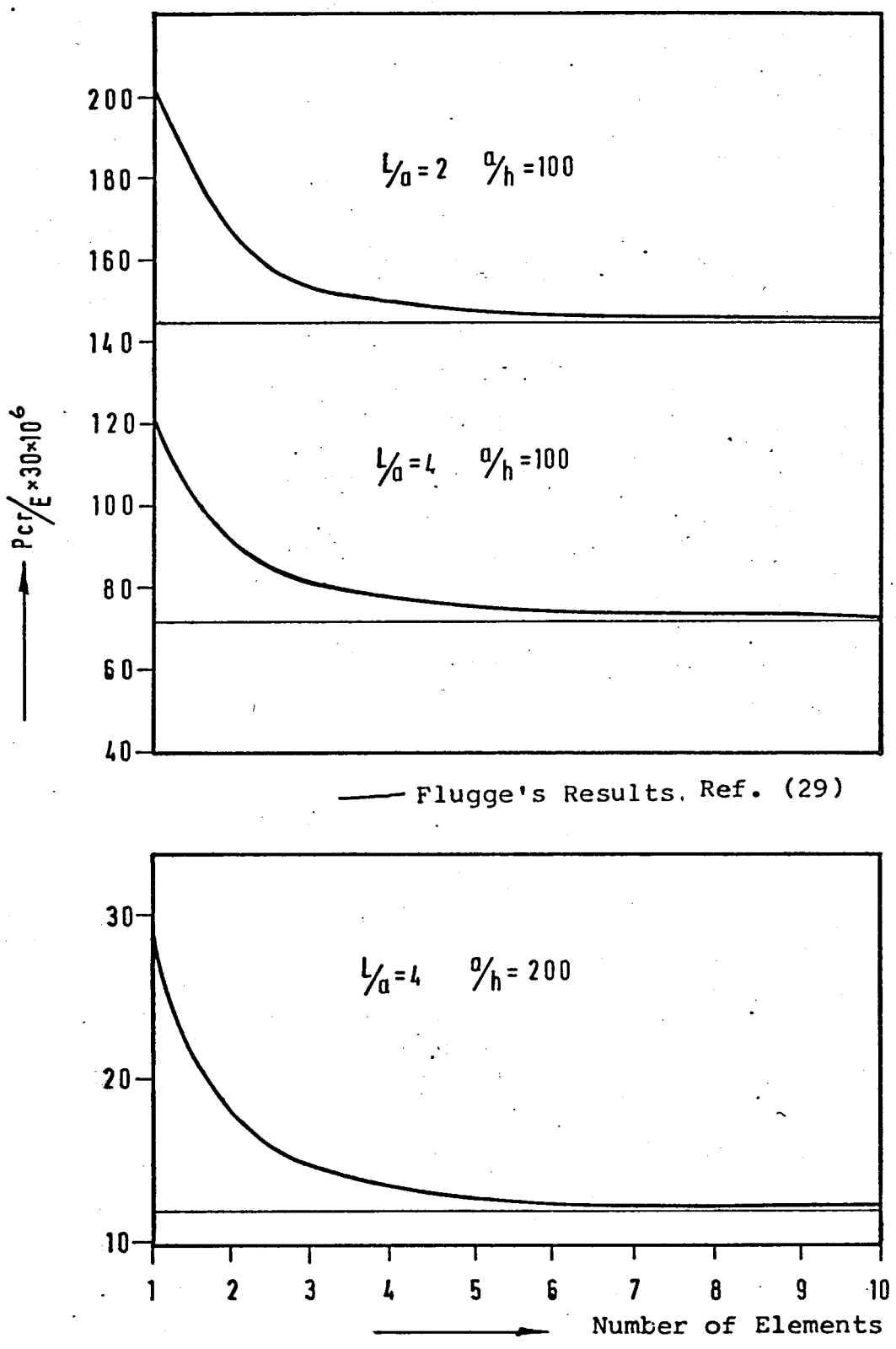

Fig. 4.2 Convergence of Results with no. of elements

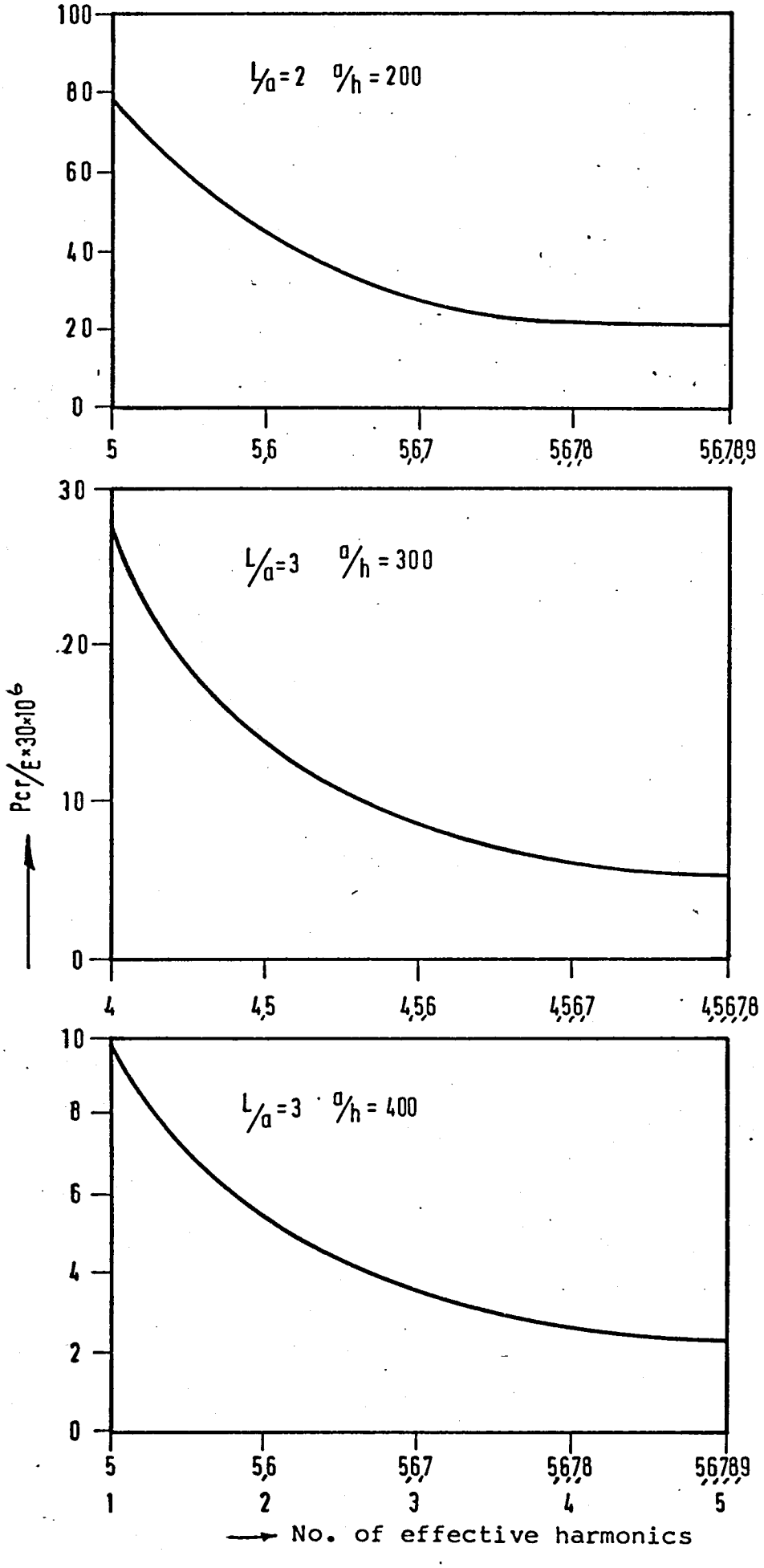

Fig. 4.3 Convergence of results with no. of harmonics.

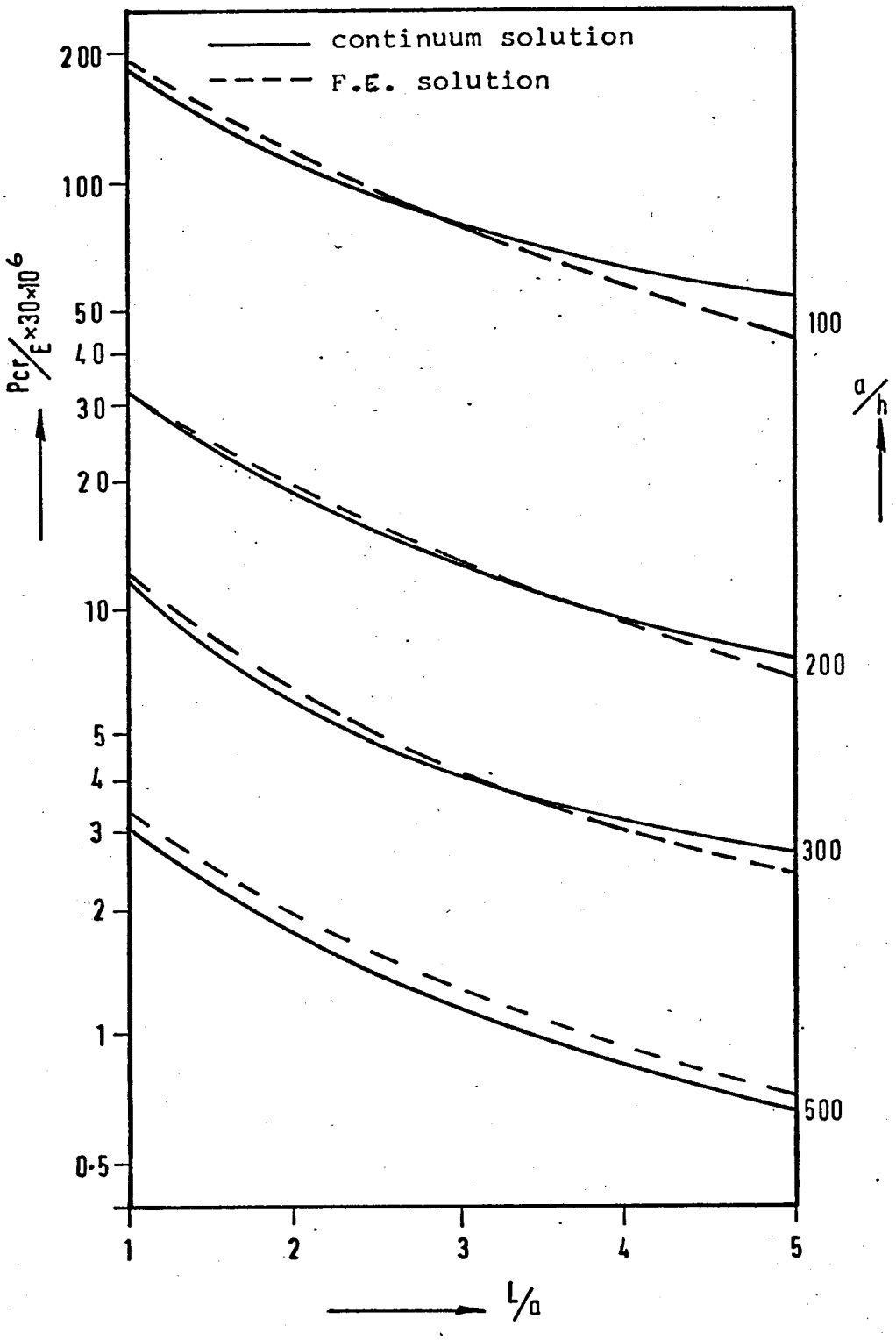

Fig. 4.4 Comparison of buckling pressures

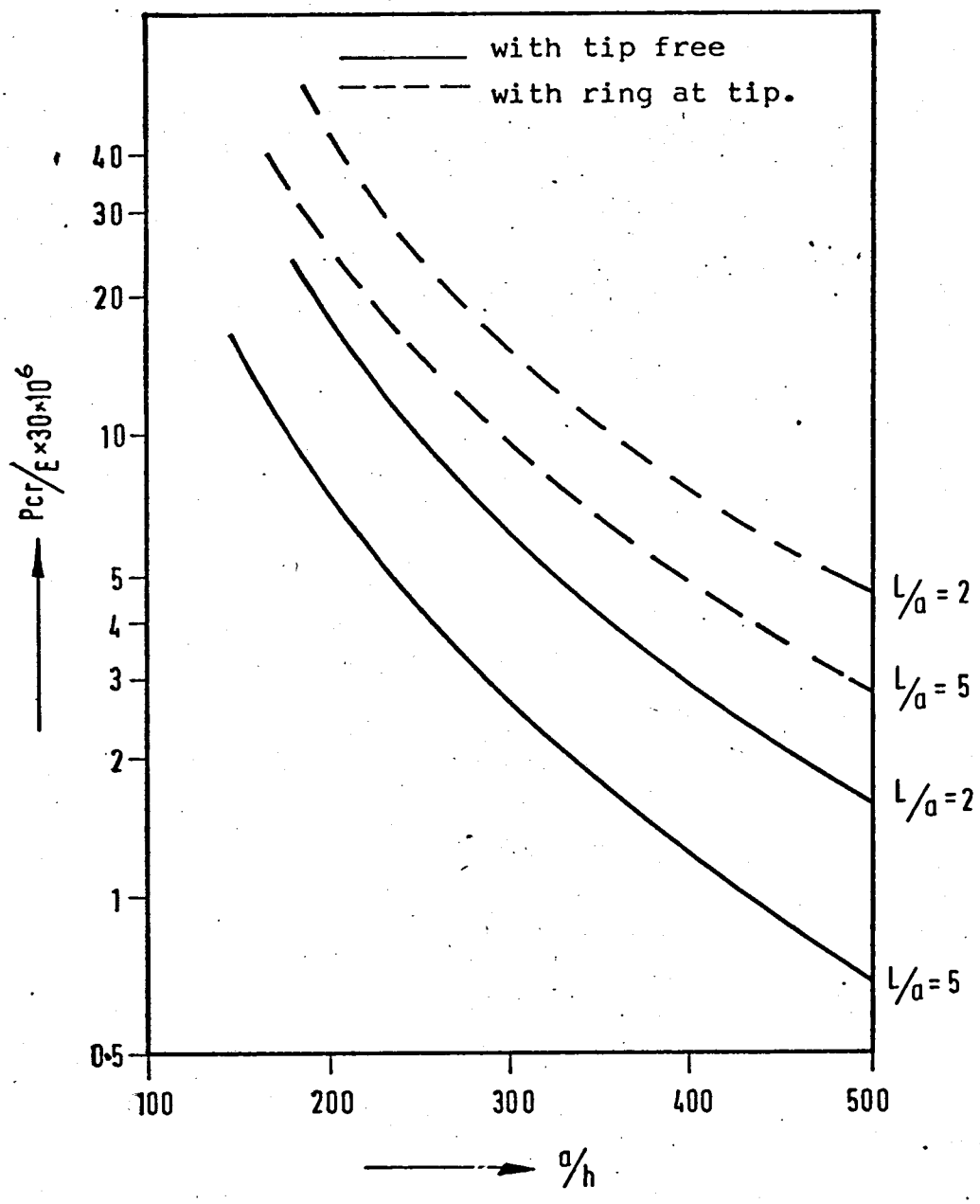

Fig. 4.5 Influence of ring stiffener on buckling pressure of a cantilever cylindrical shell. (Ring dimensions b = 20h, d = 100h)

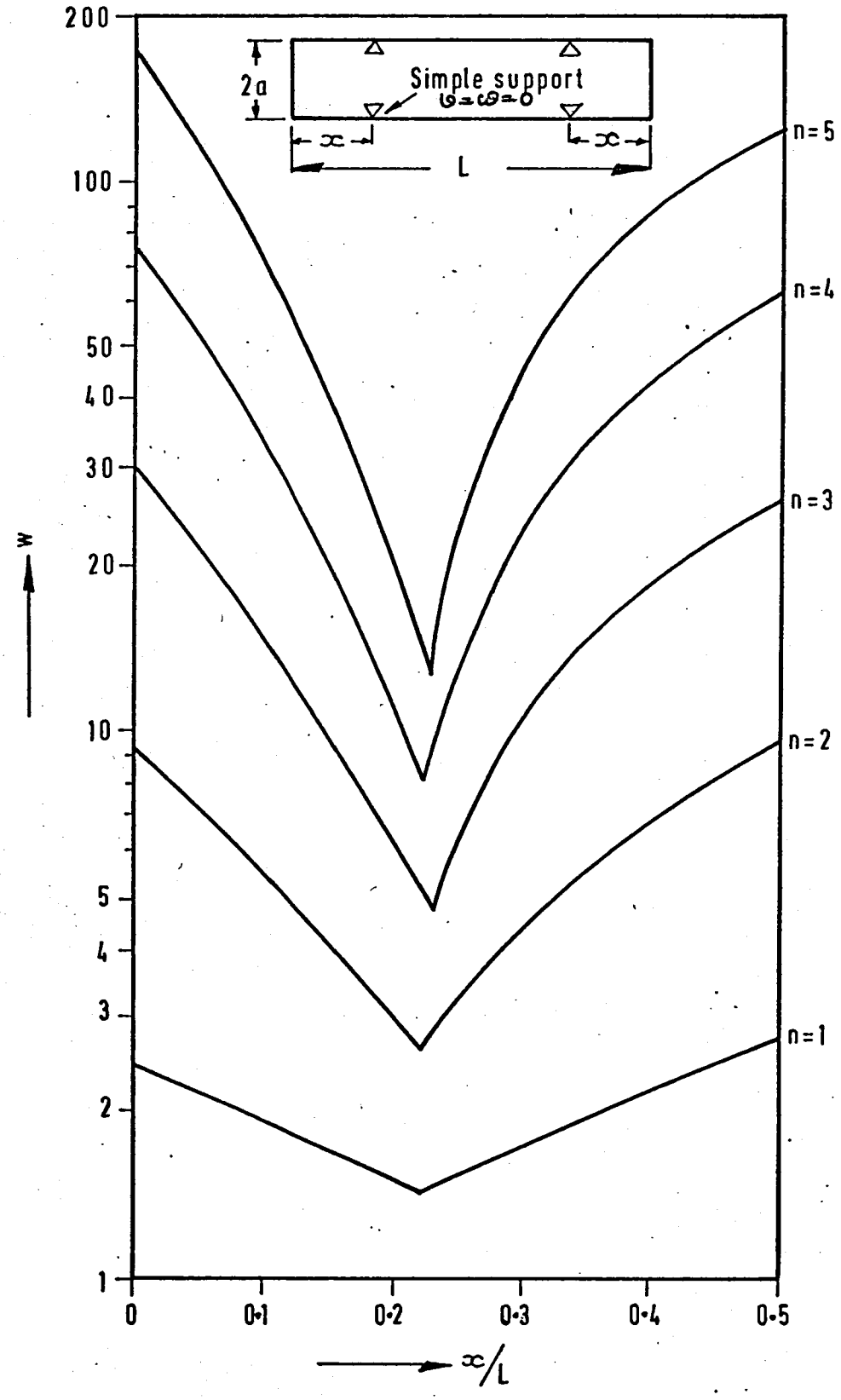

Fig. 4.6 Variation of radial displacement with support location for different harmonics.

(L/a = 2, a/h = 500)

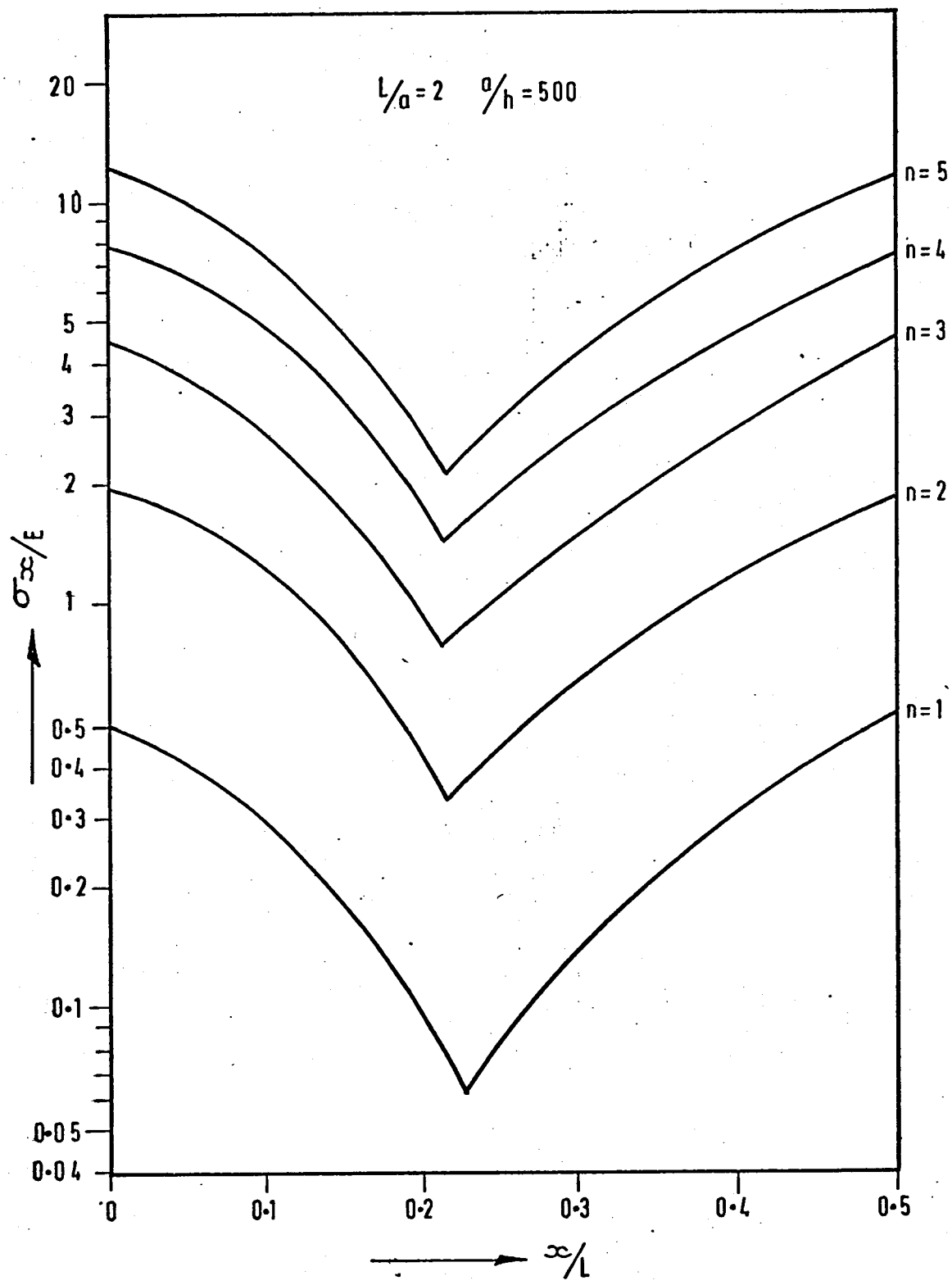

Fig. 4.7 Variation of axial stress with support location for different harmonics.

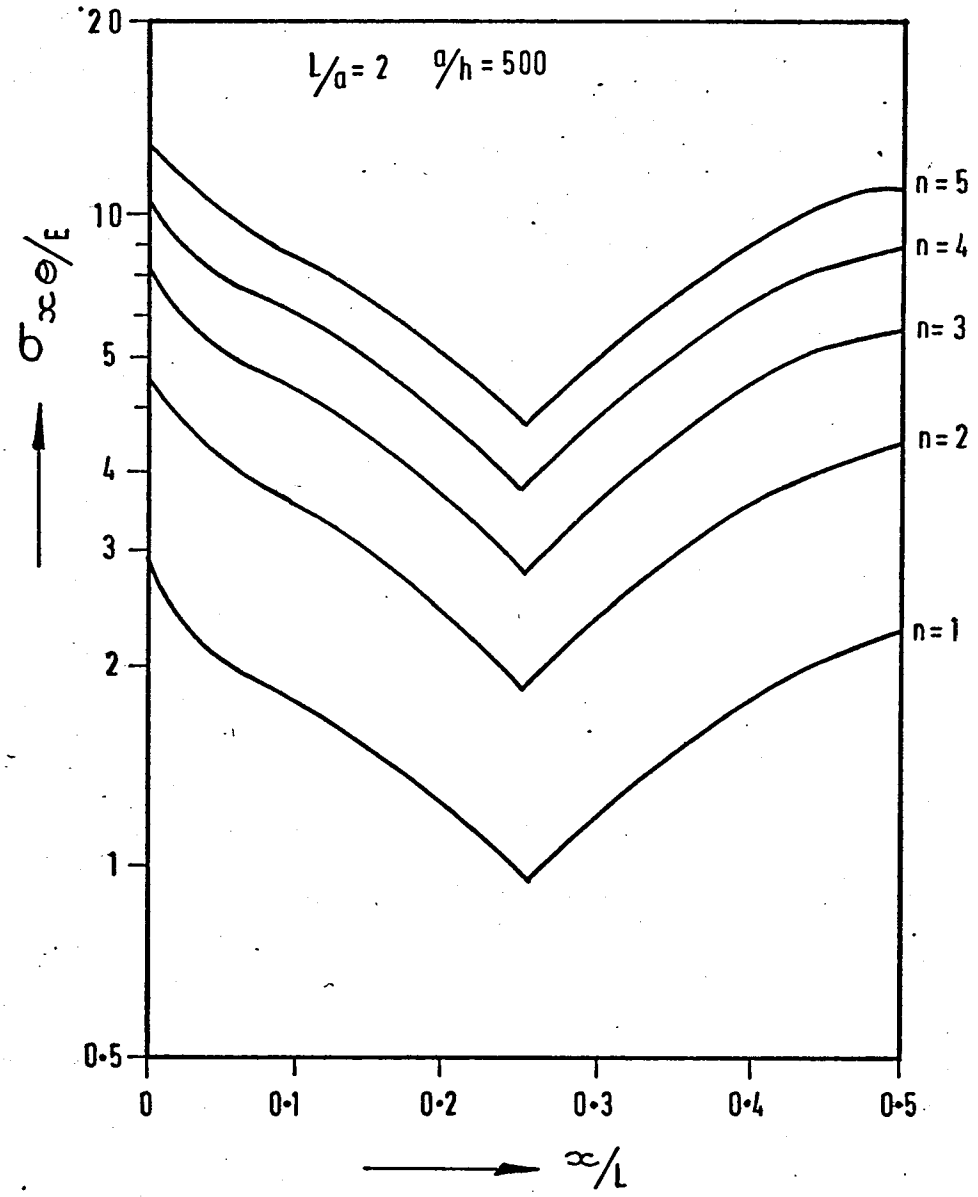

Fig. 4.8 Variation of shear stress with support location for different harmonics.

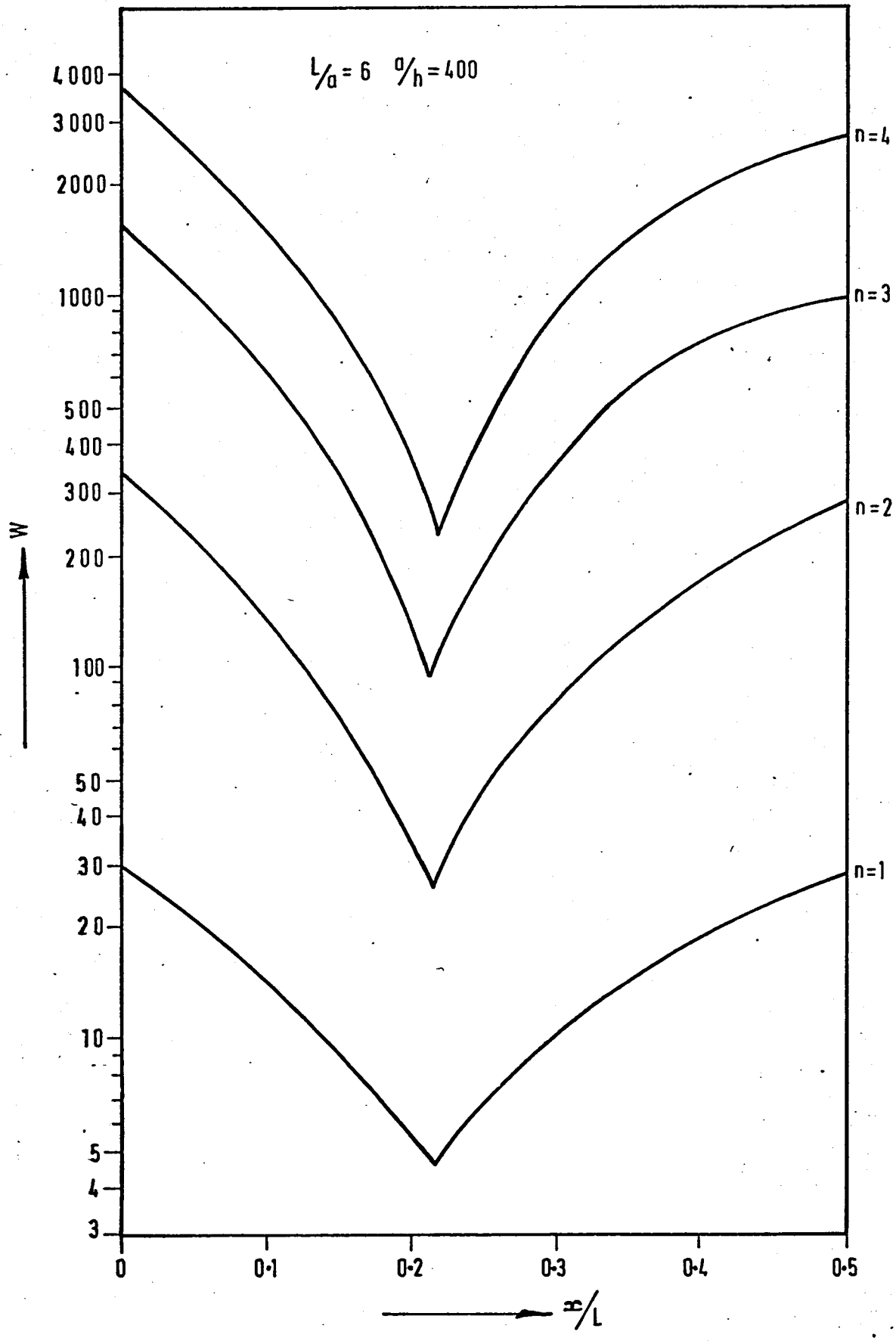

Fig. 4.9 Variation of radial displacement with support location for different harmonics.

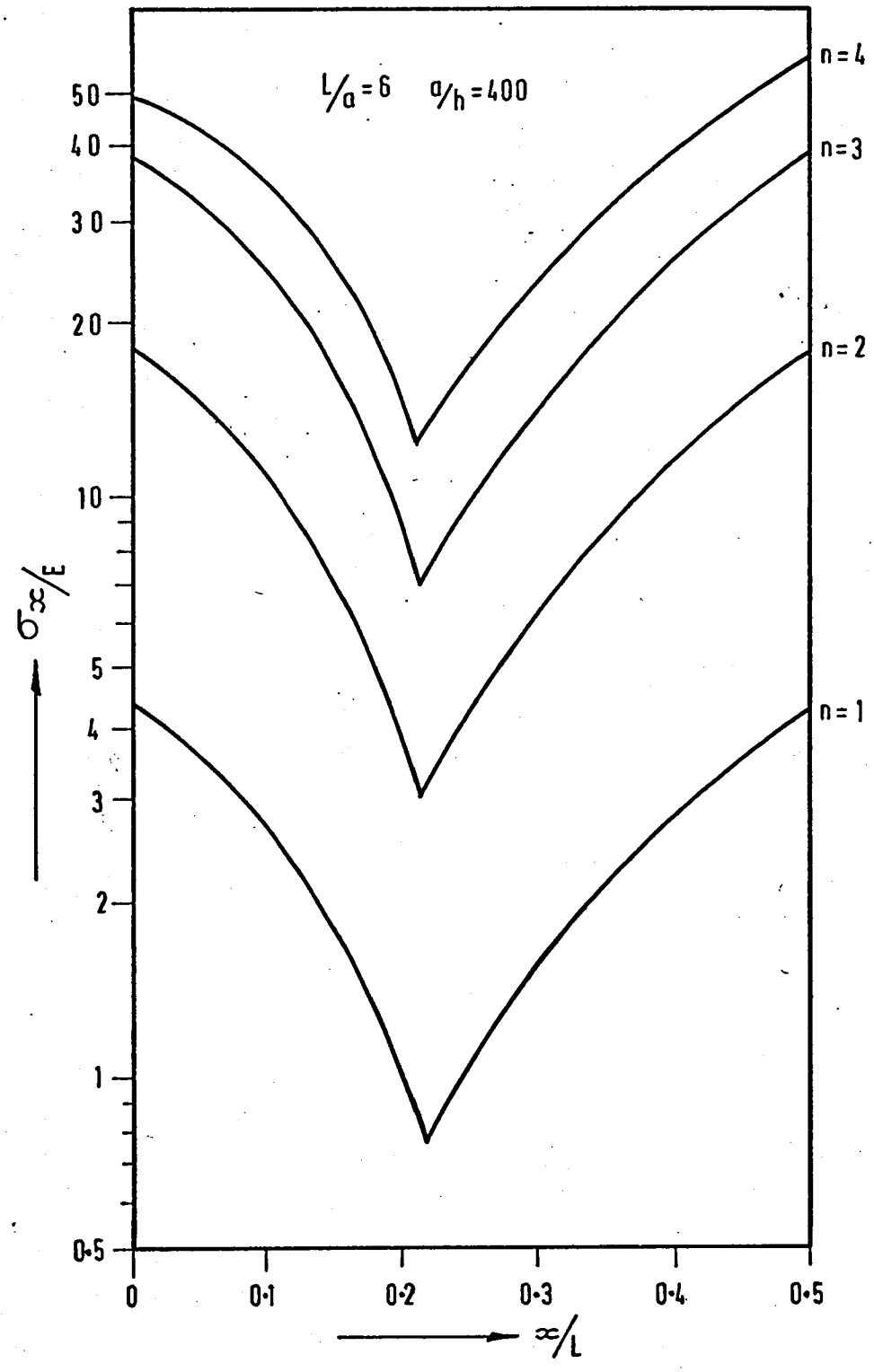

Fig. 4.10 Variation of axial stress for different harmonics with support location.

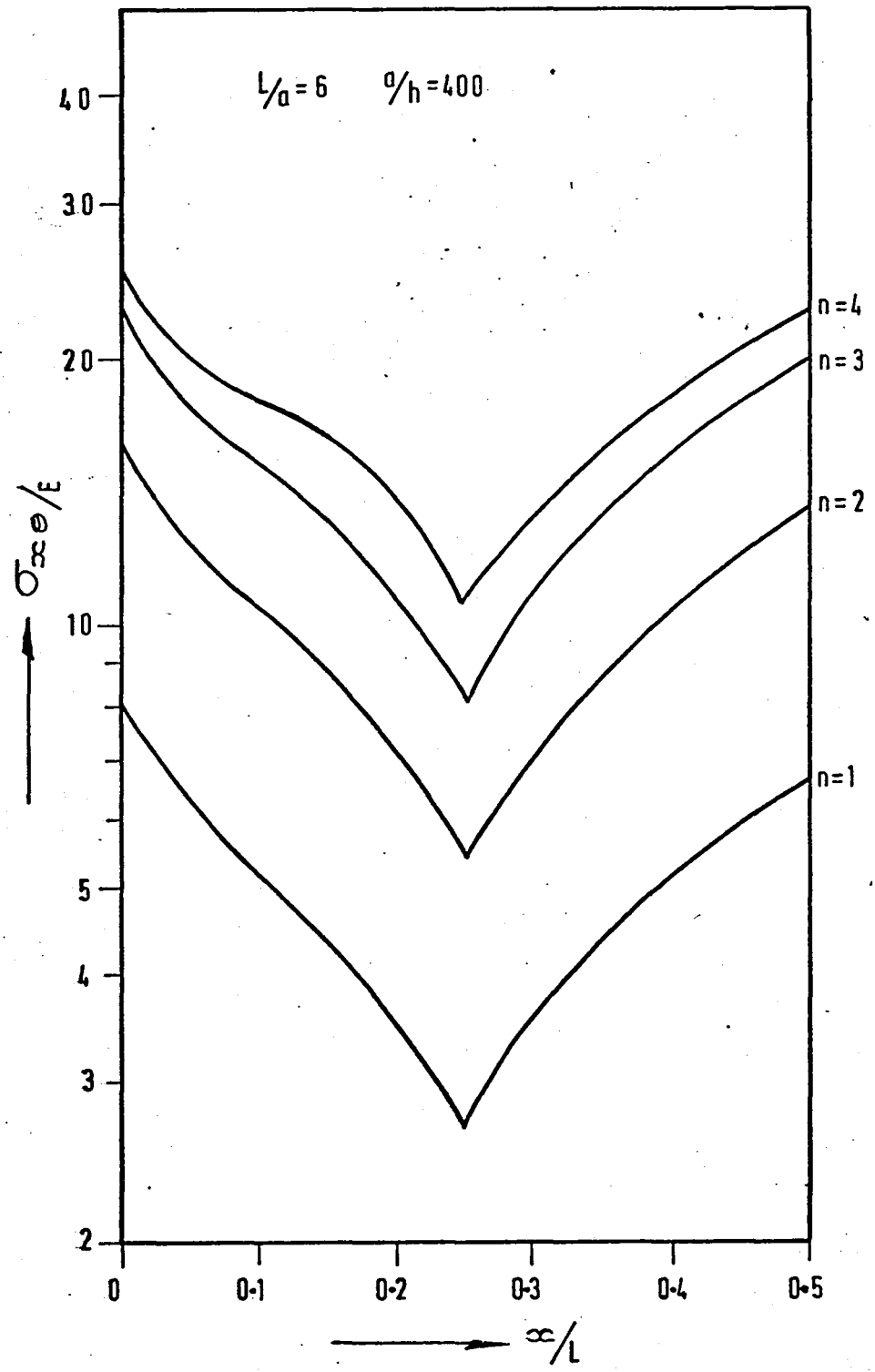

Fig. 4.11 Variation of shear stress with support location for different harmonics.

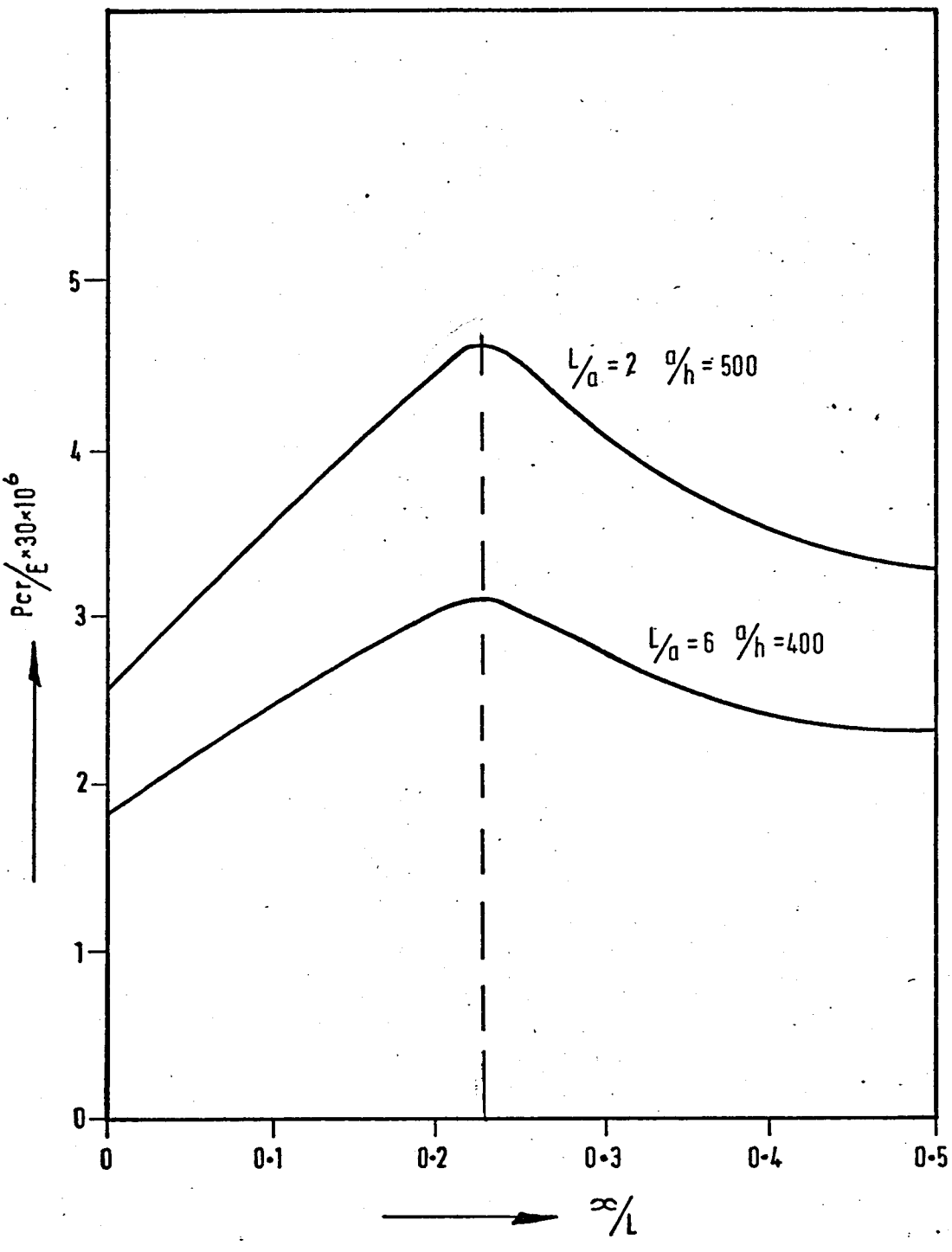

Fig. 4.12 Variation of buckling pressure with support location.

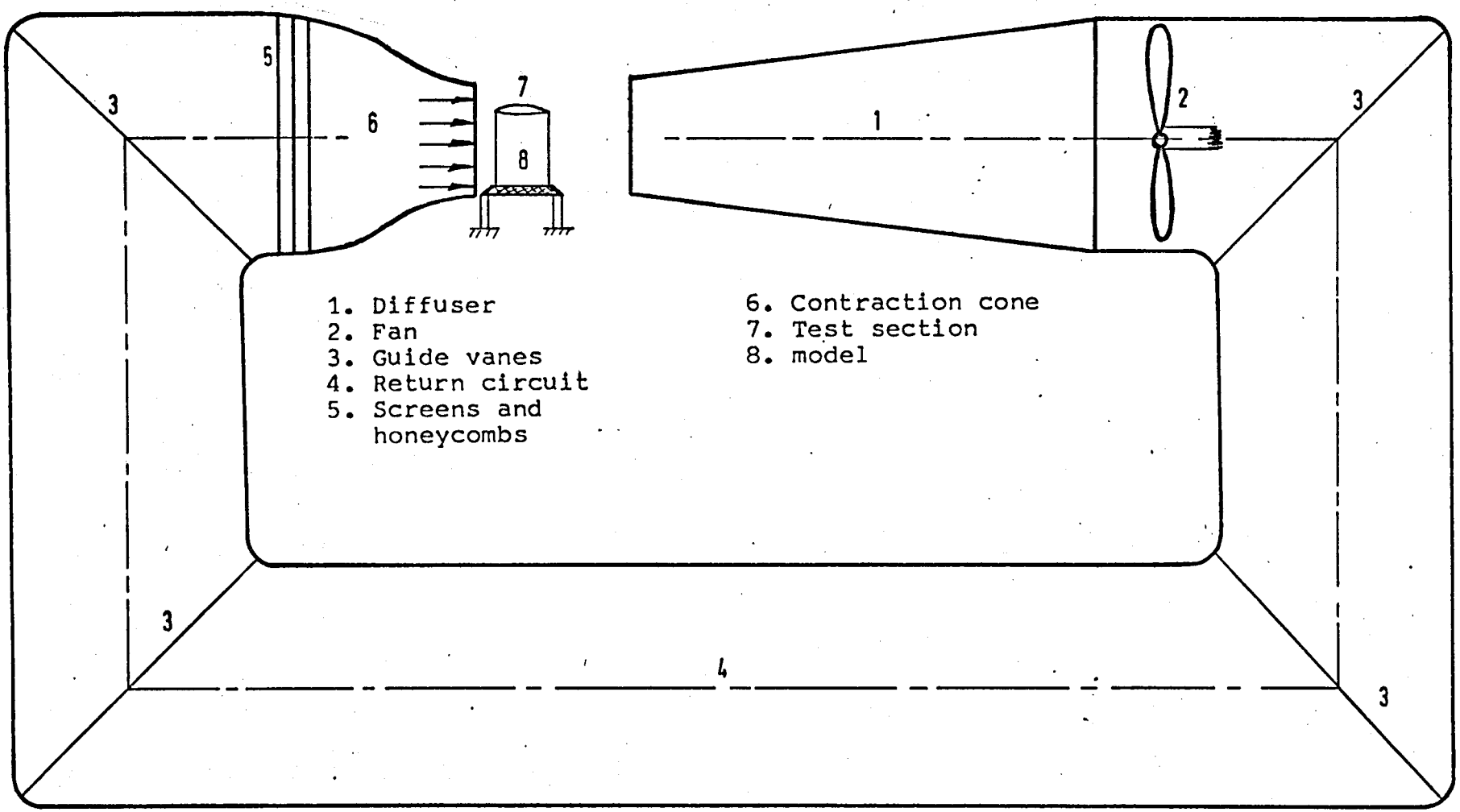

Fig. 5.1 The wind tunnel.

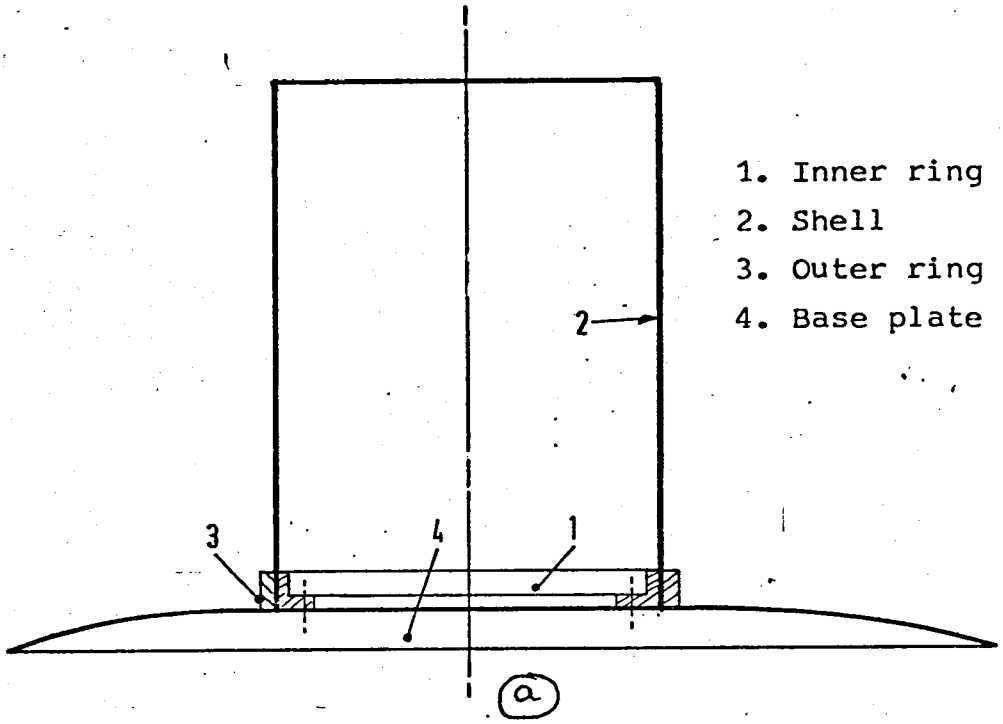

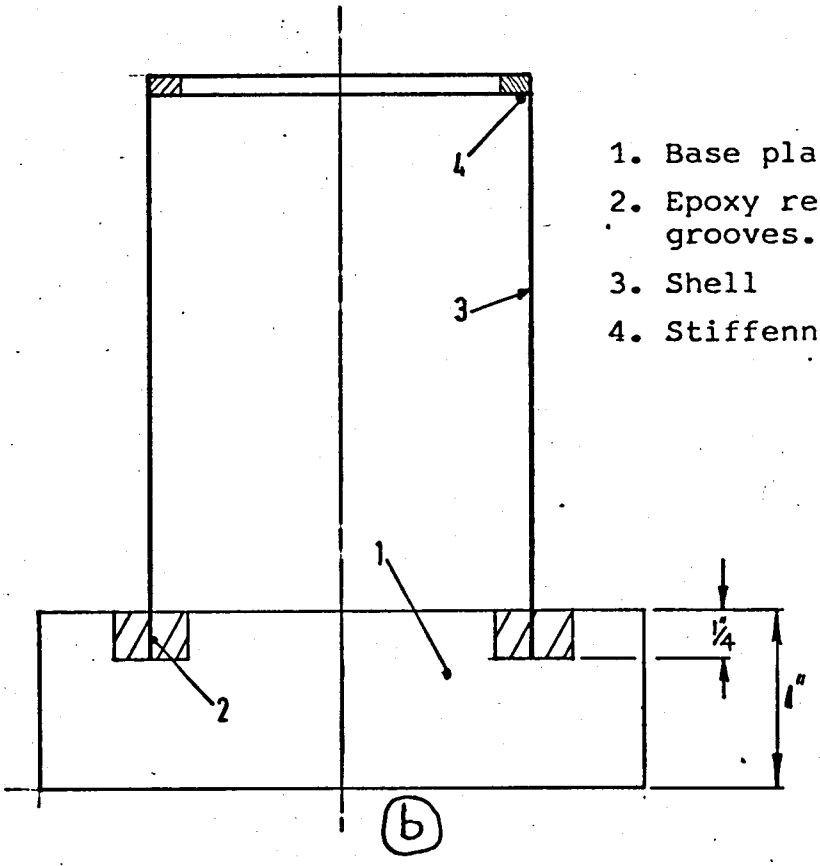

Fig. 5.2 Methods of clamping the shell.

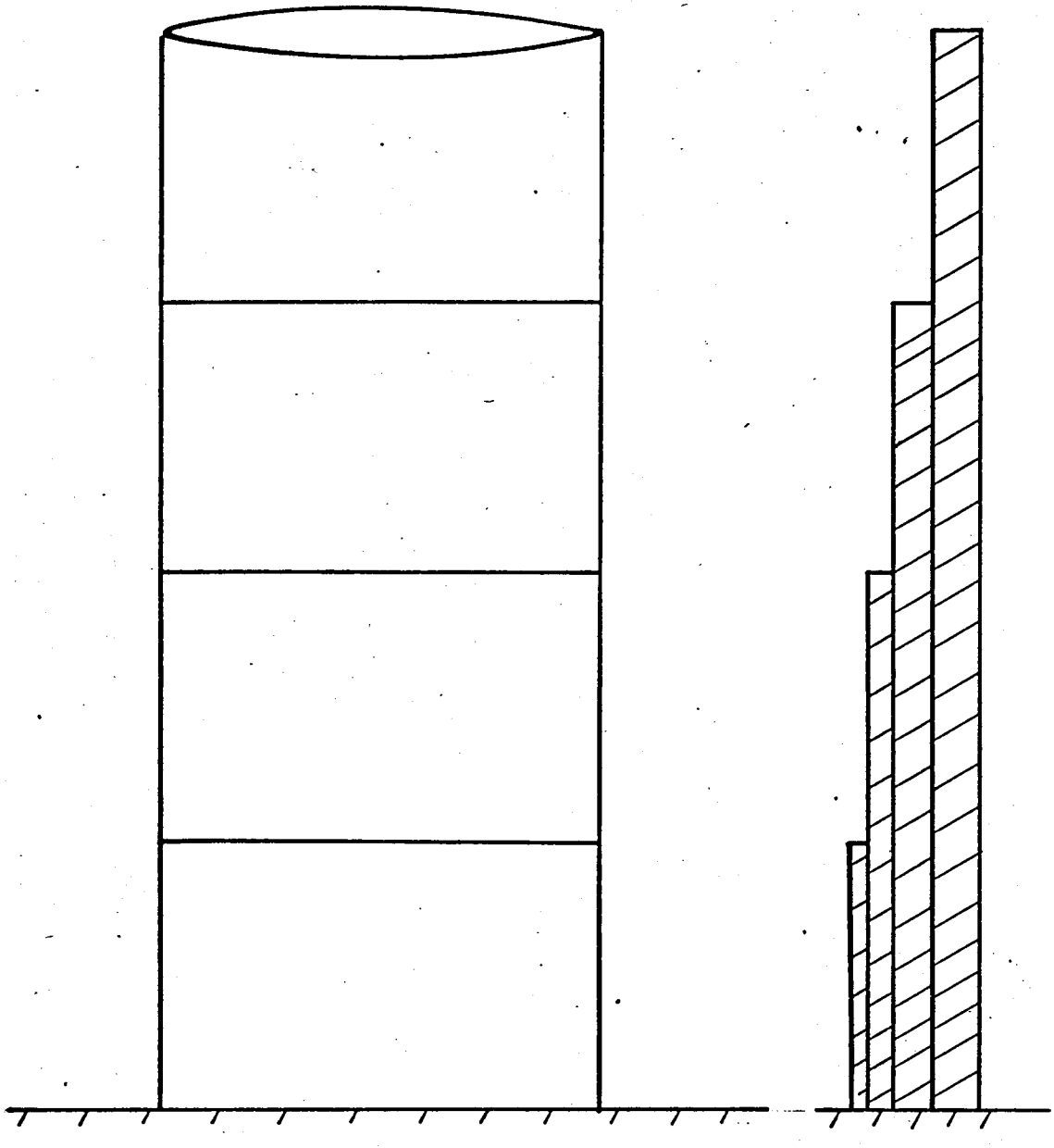

Fig. 5.3 Variable thickness shell.

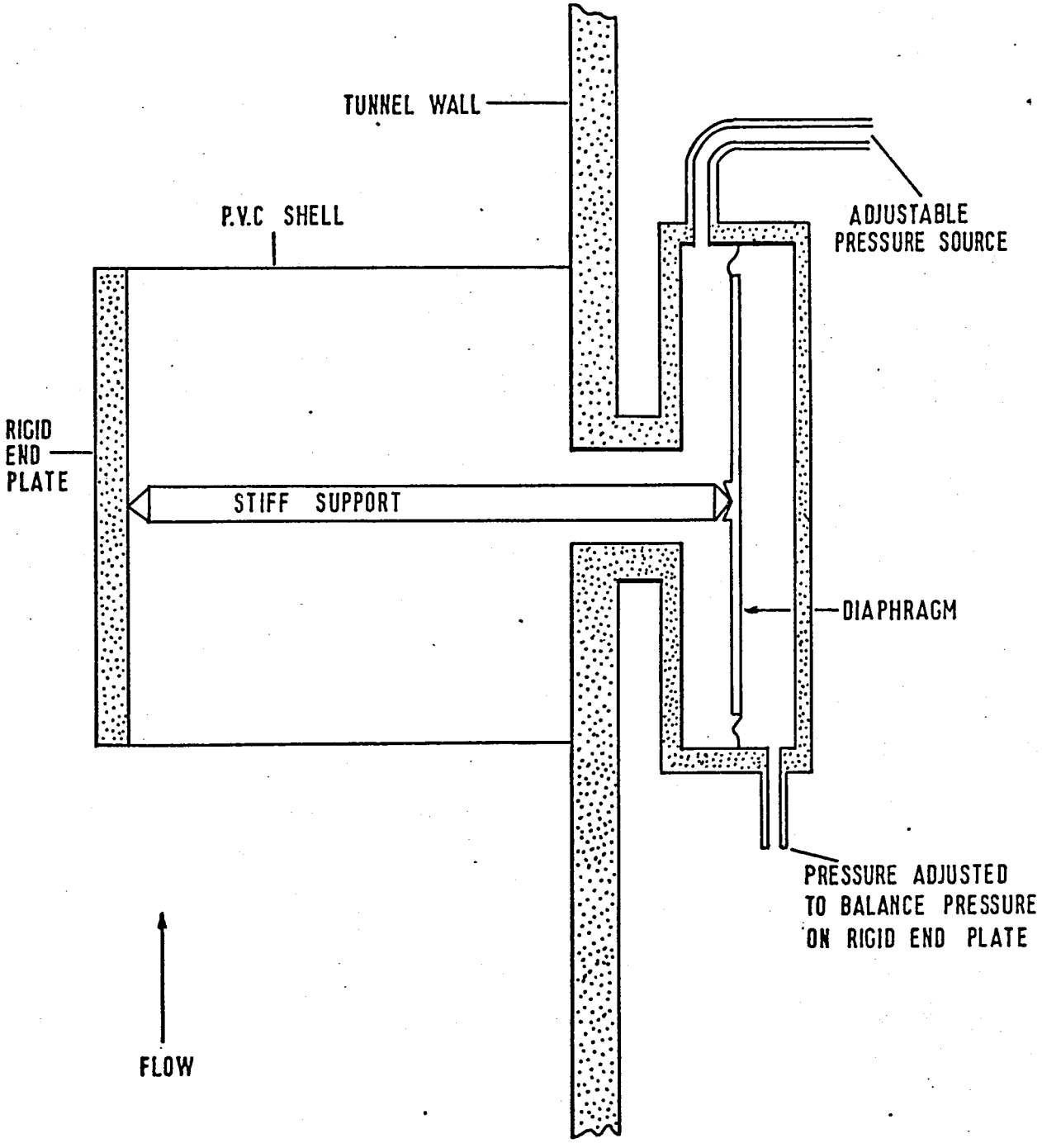

FIG. 5-4 TEST ARRANGEMENT IN WATER TUNNEL

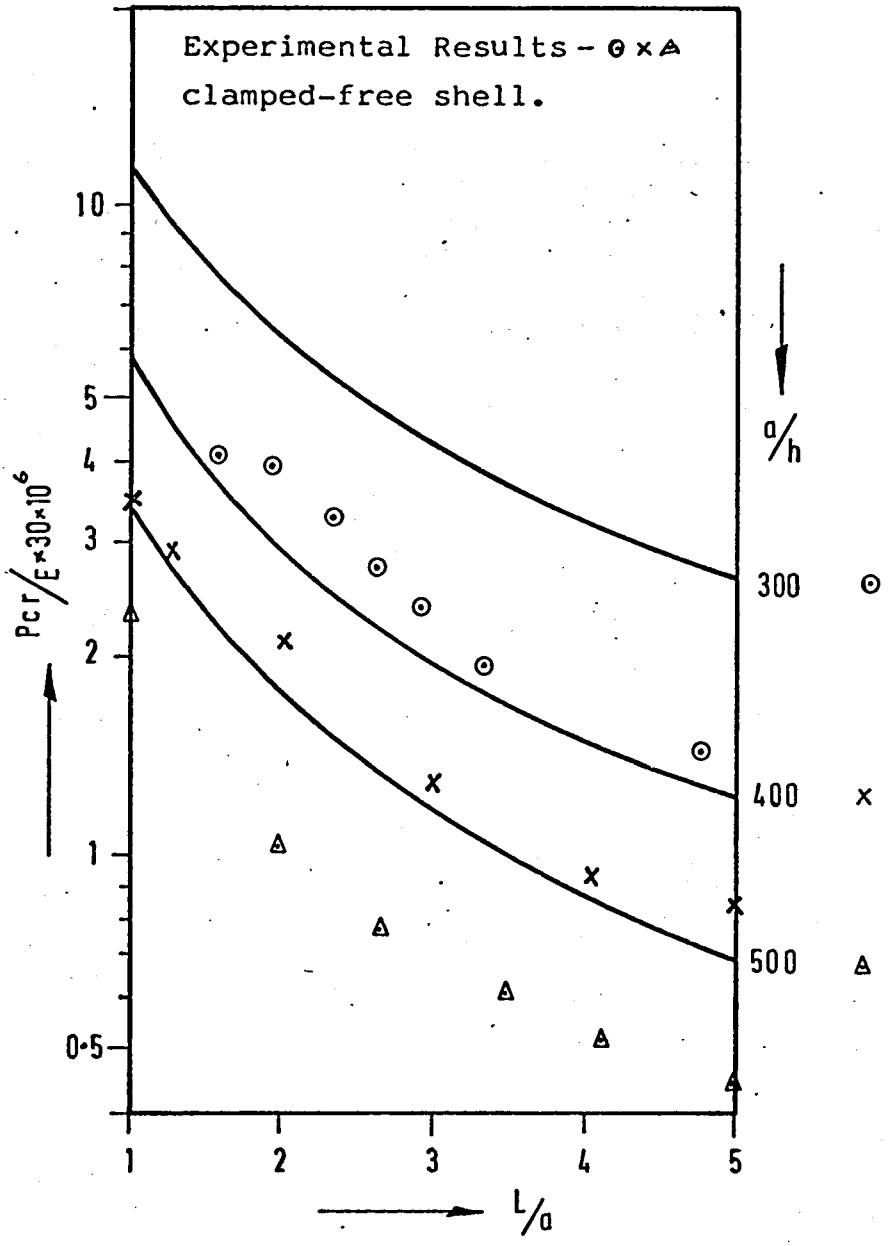

Fig. 5.5 Comparison with experiments.

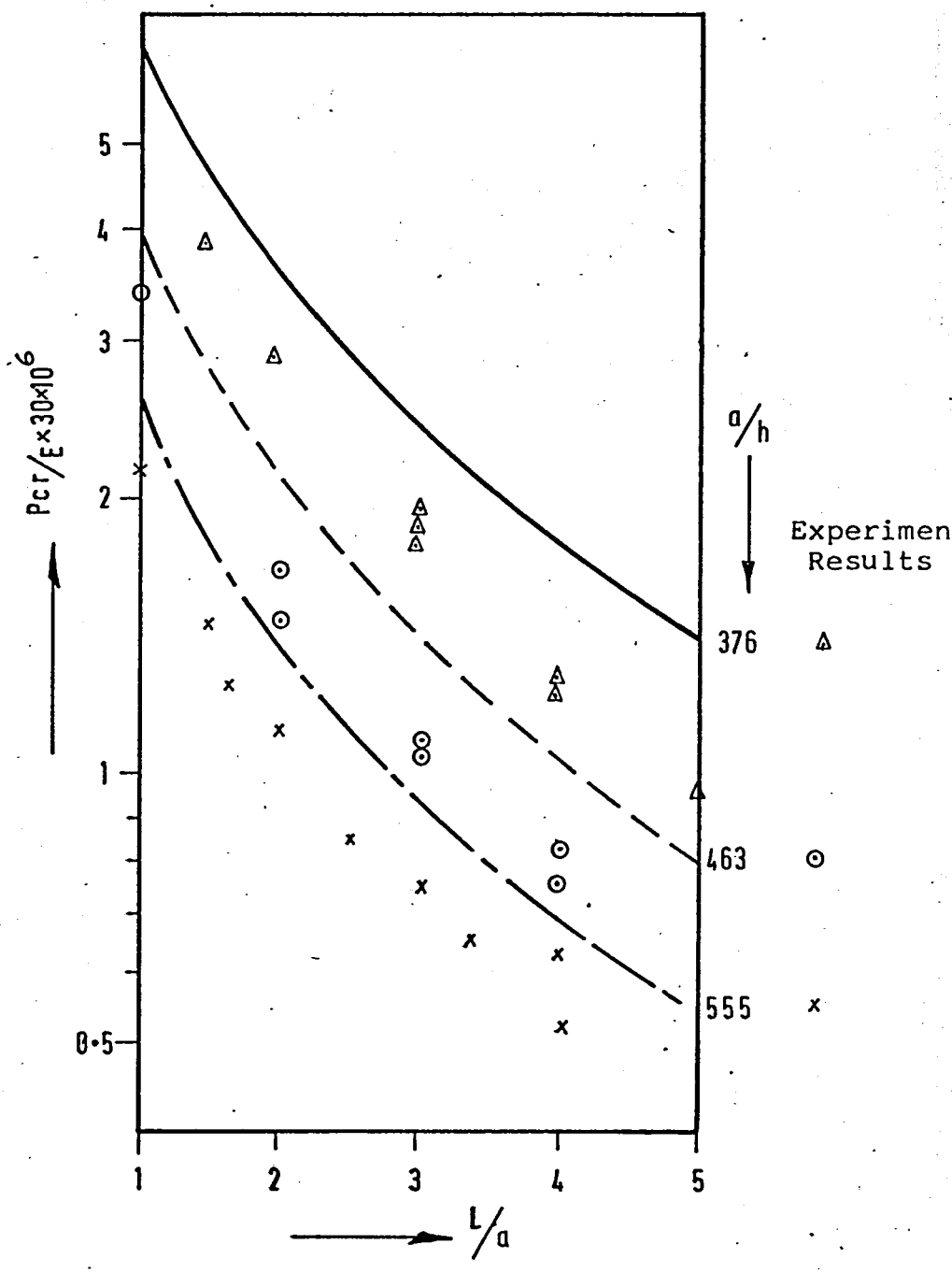

Fig. 5.6 Comparison of results with Experiments.

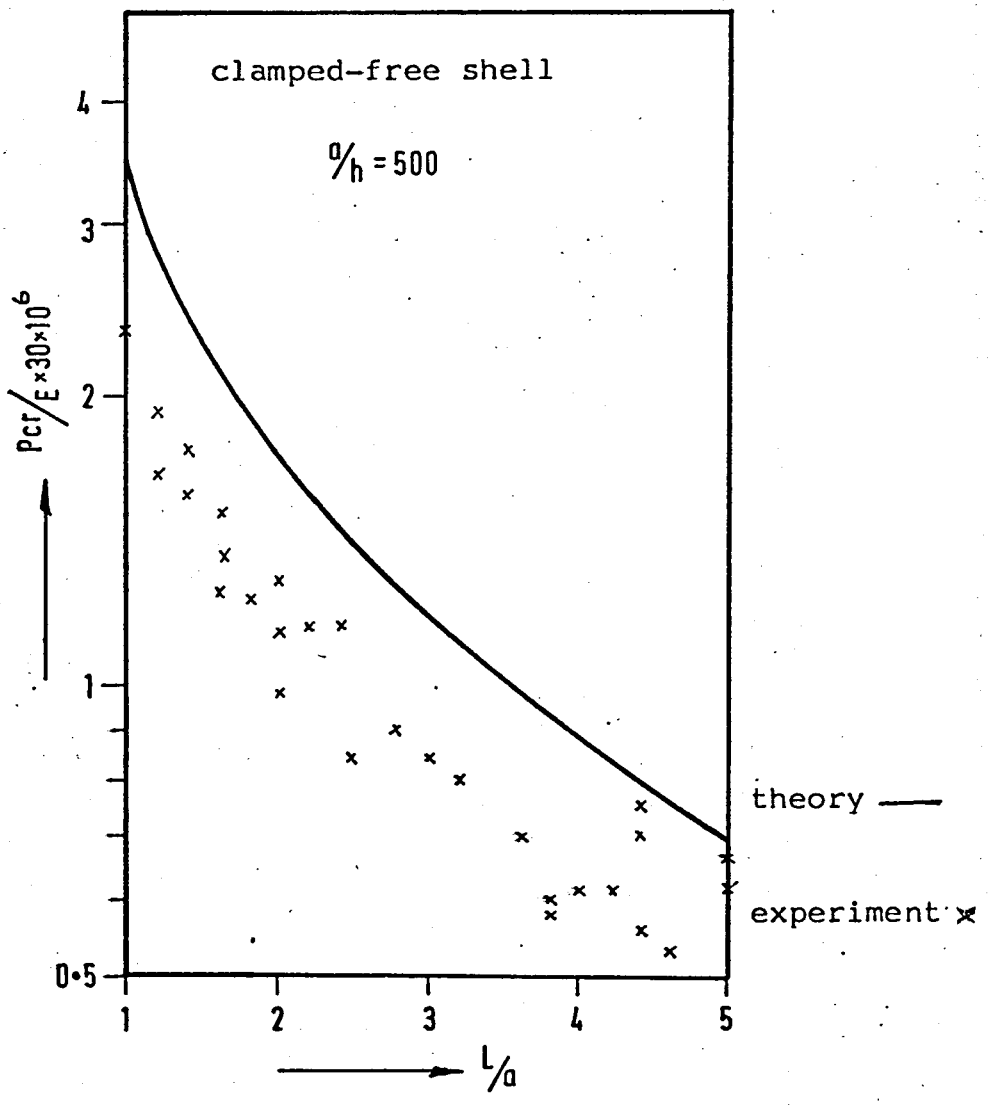

Fig. 5.7 Comparison of results

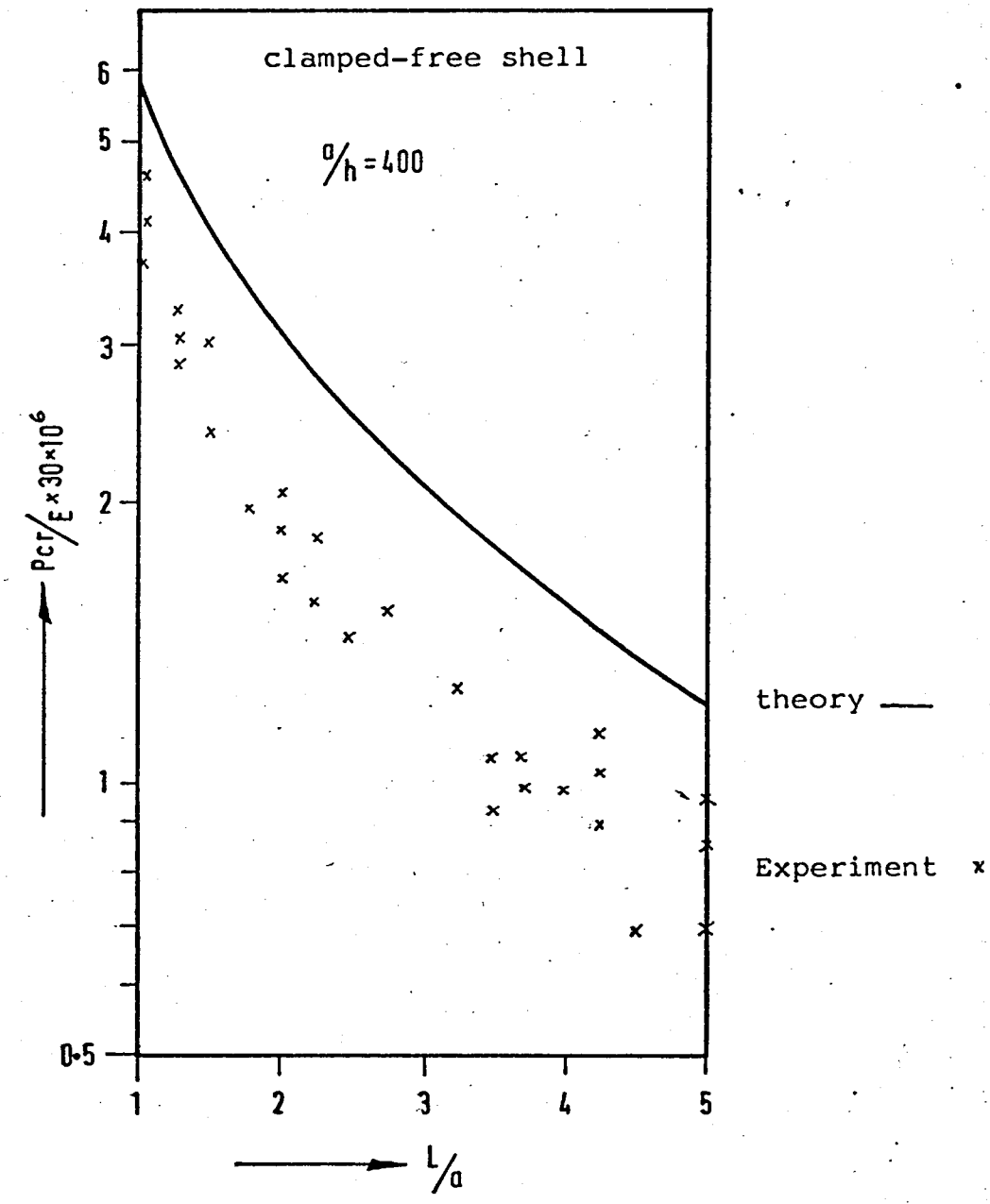

Fig. 5.8 Comparison of results.

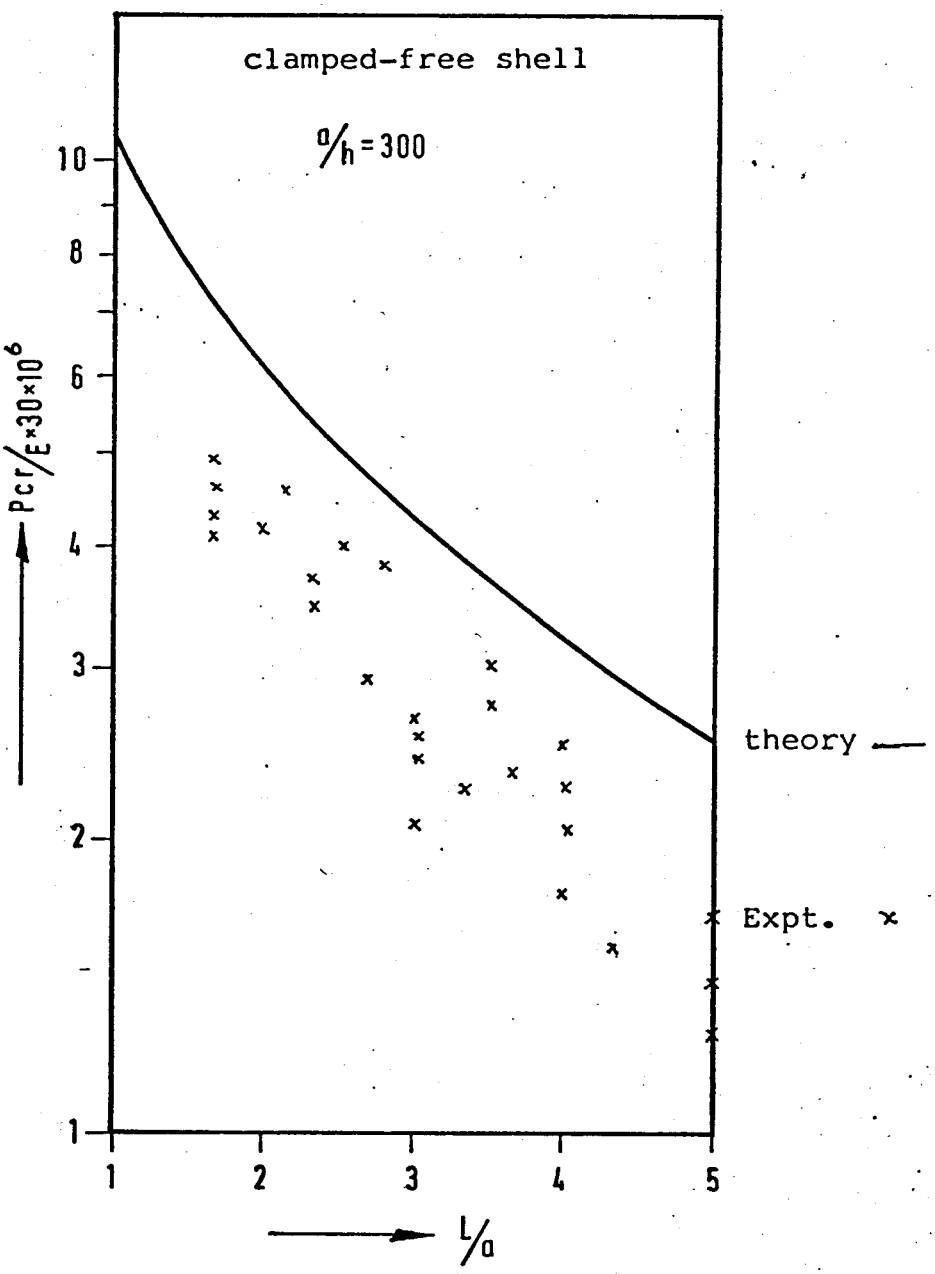

Fig. 5.9 Comparison of results.

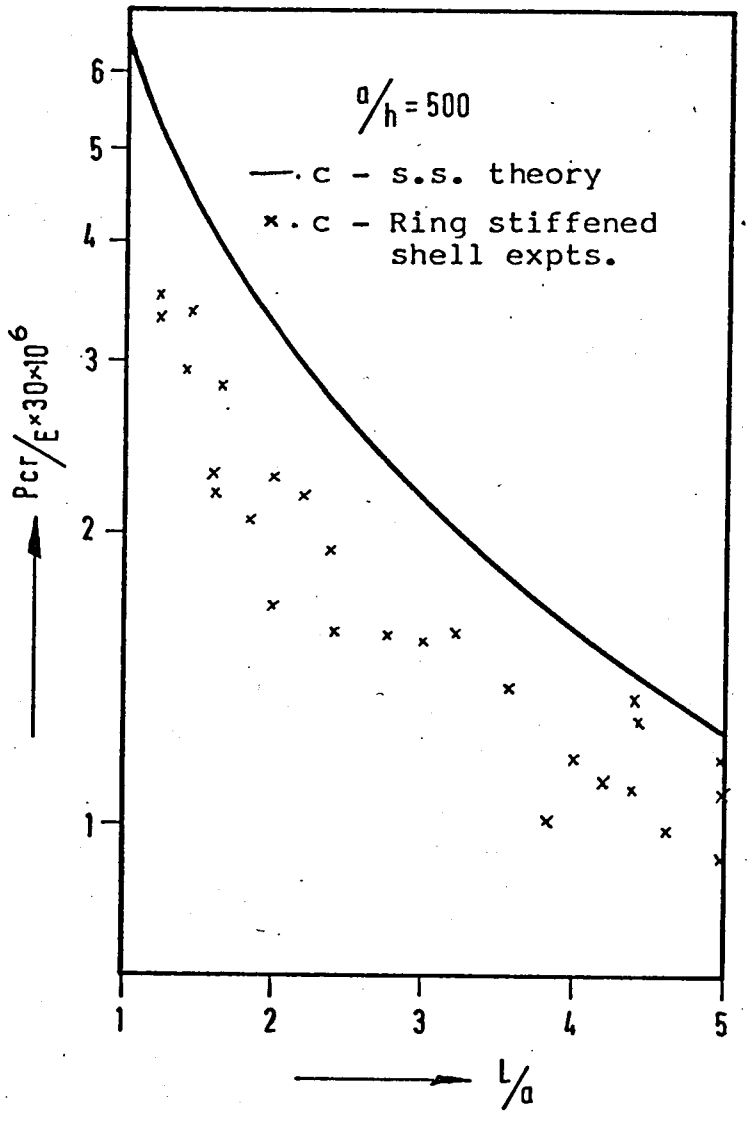

Fig. 5.10 Comparison of Results.

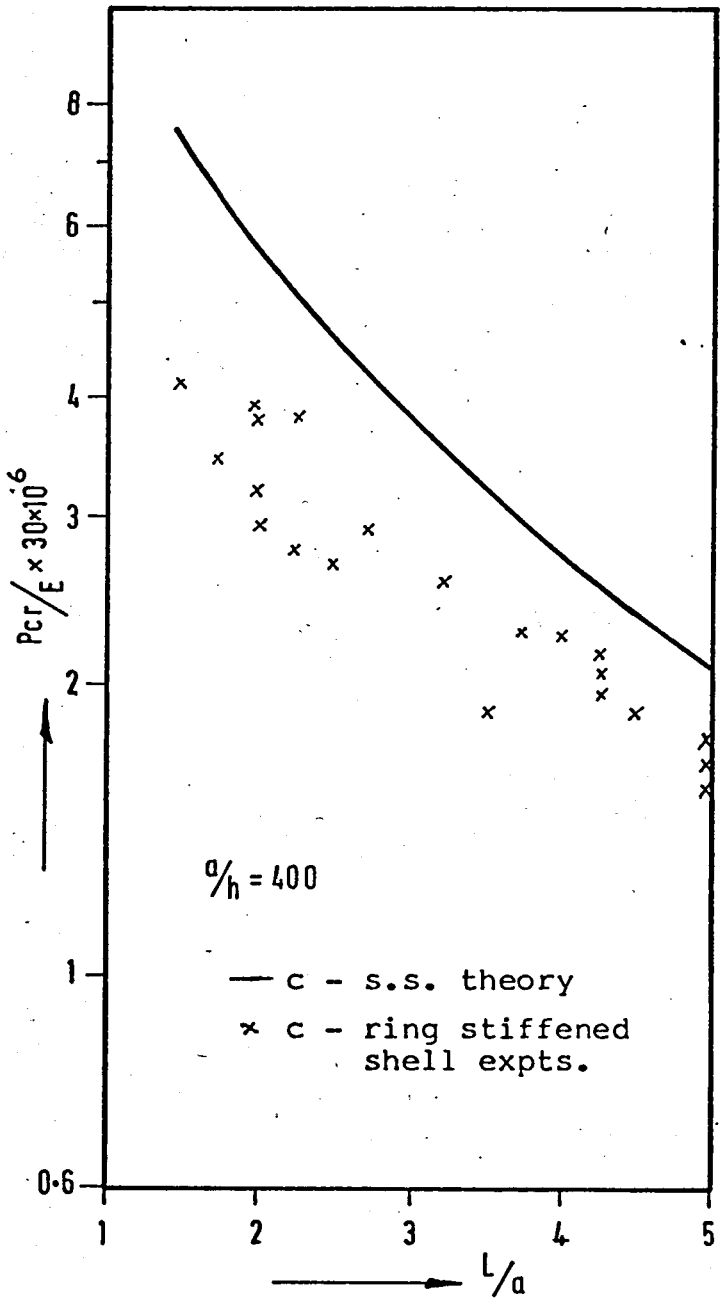

Fig. 5.11 Comparison of results.

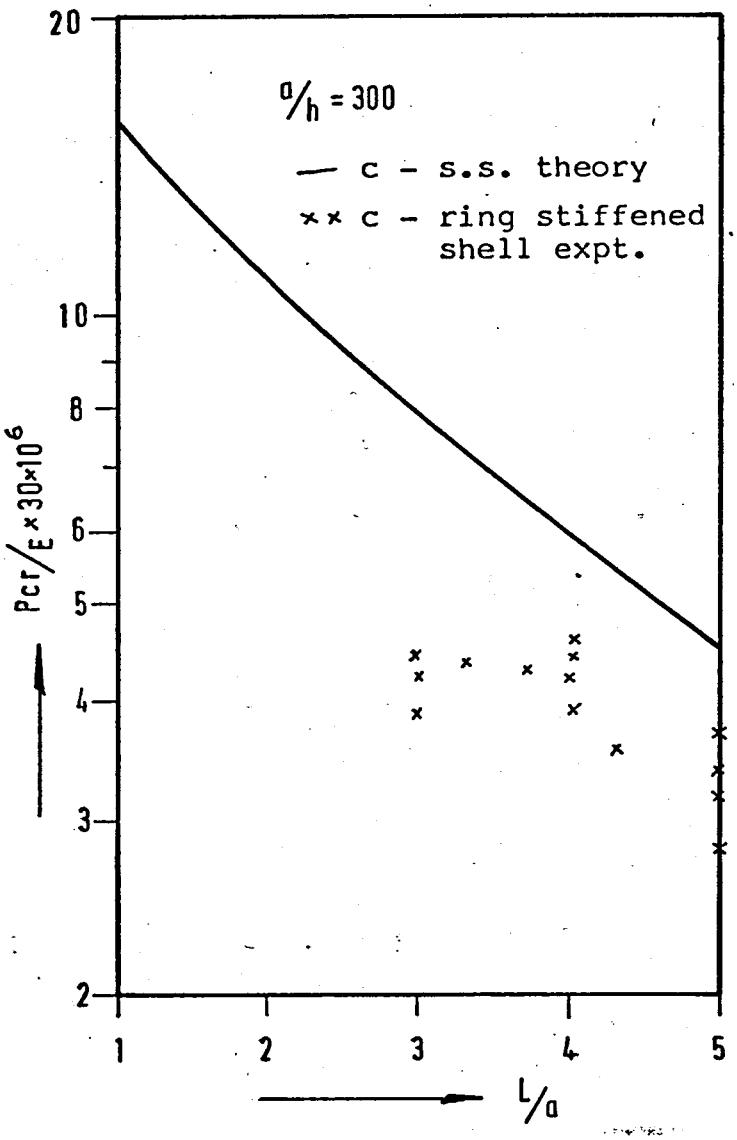

Fig. 5.12 Comparison of results.

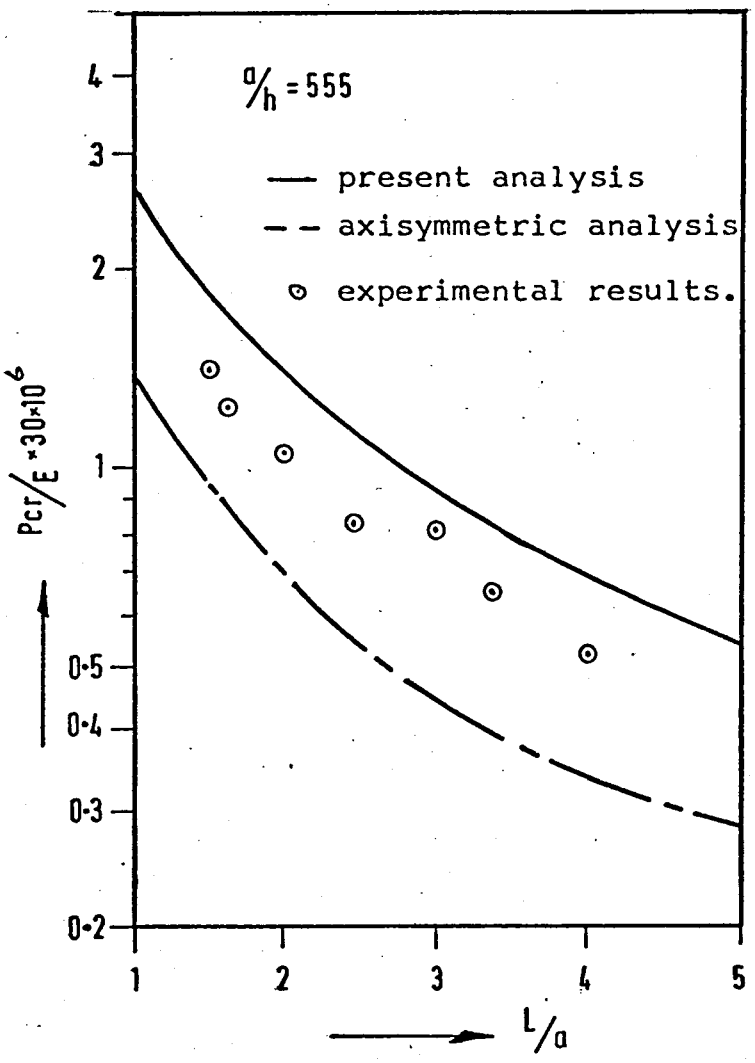

Fig. 6.1 Comparison of buckling pressures with current engineering practice

——— stagnation critical pressures (present analysis)

— — Gas buckling pressures (Axisymmetric analysis) Current engineering practice

⊙ ⊙ Experimental results.

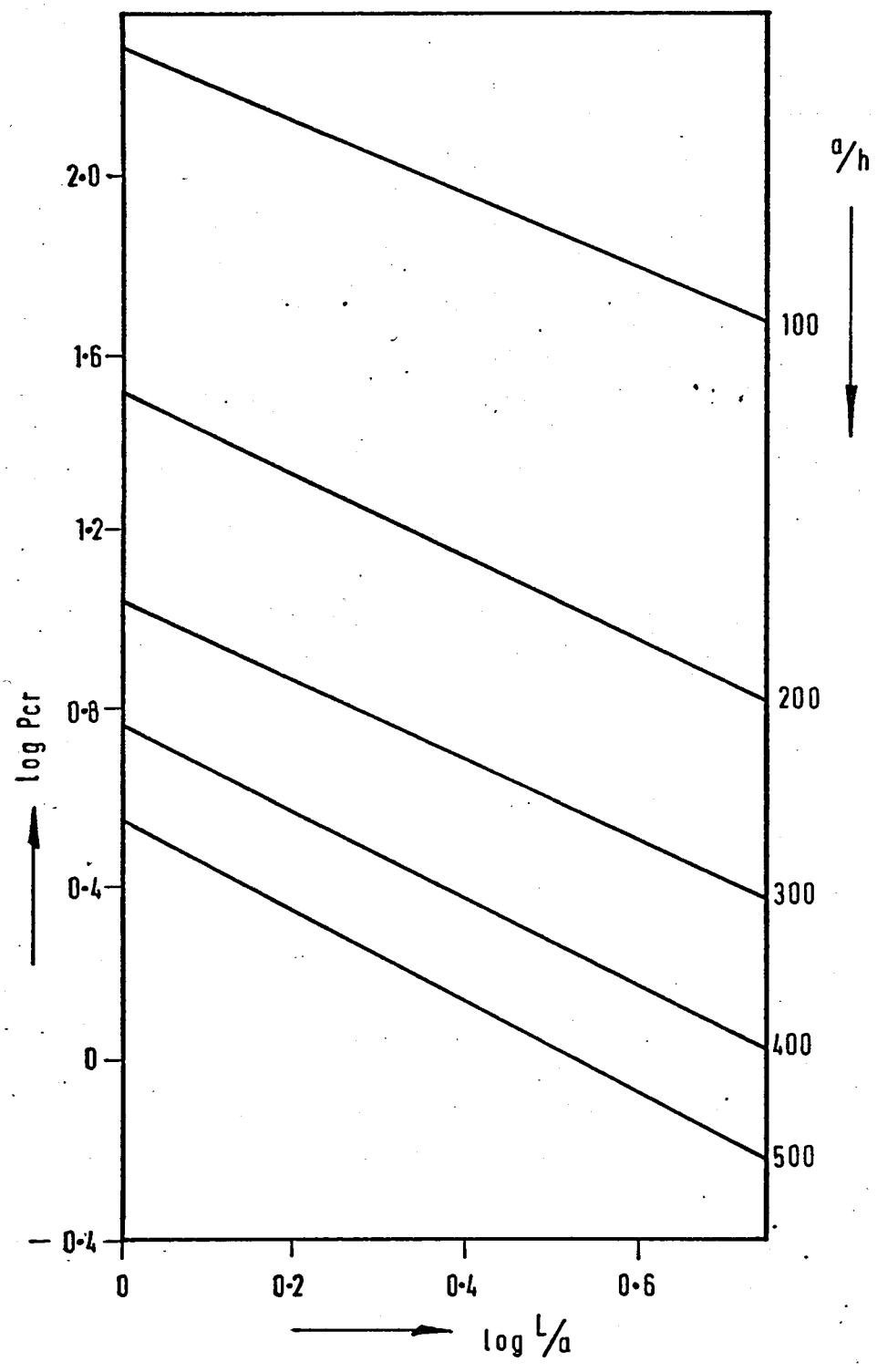

Fig. 6.2 log - log plots of buckling pressures

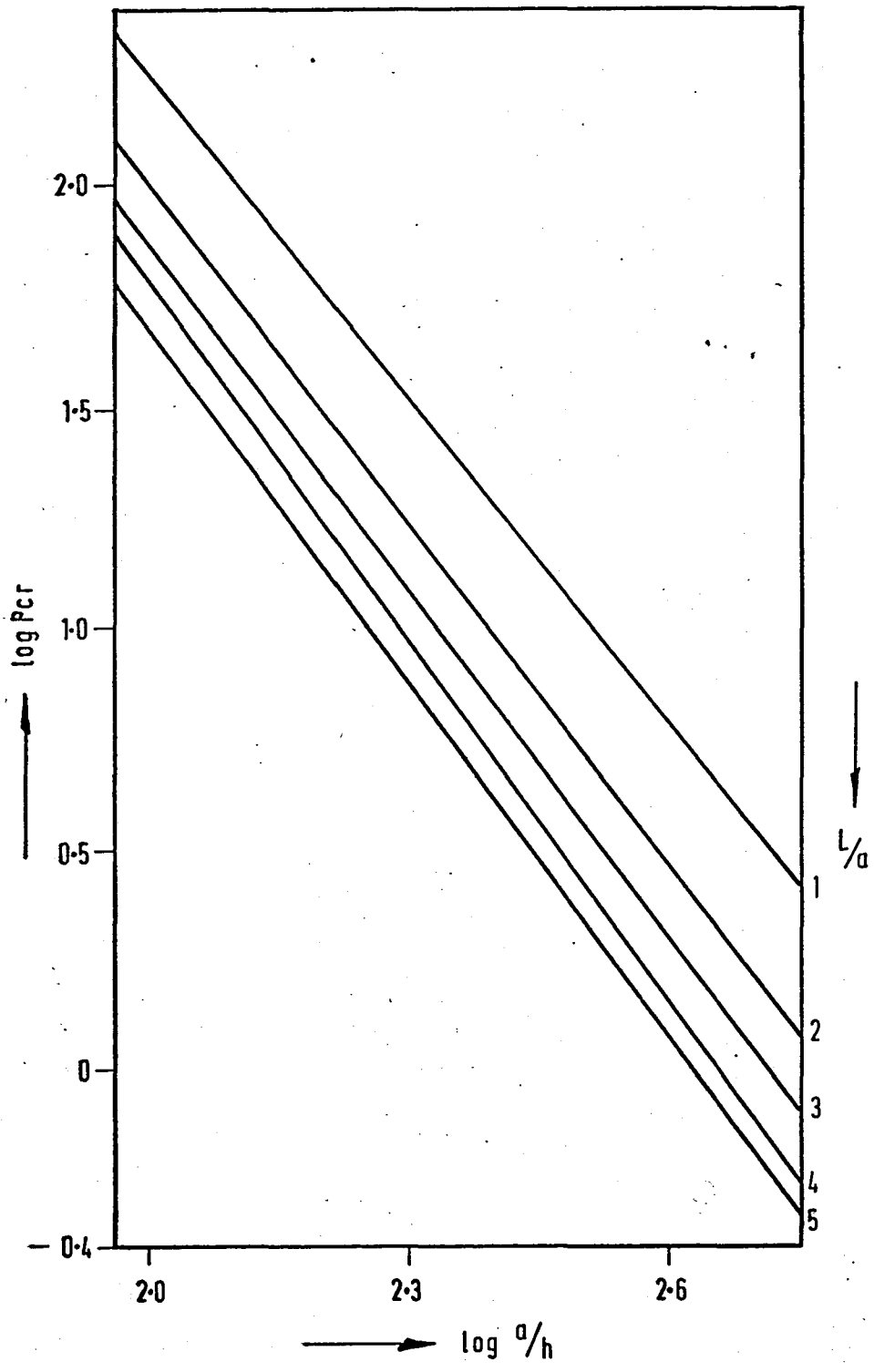

Fig. 6.3 log - log plots of buckling pressures

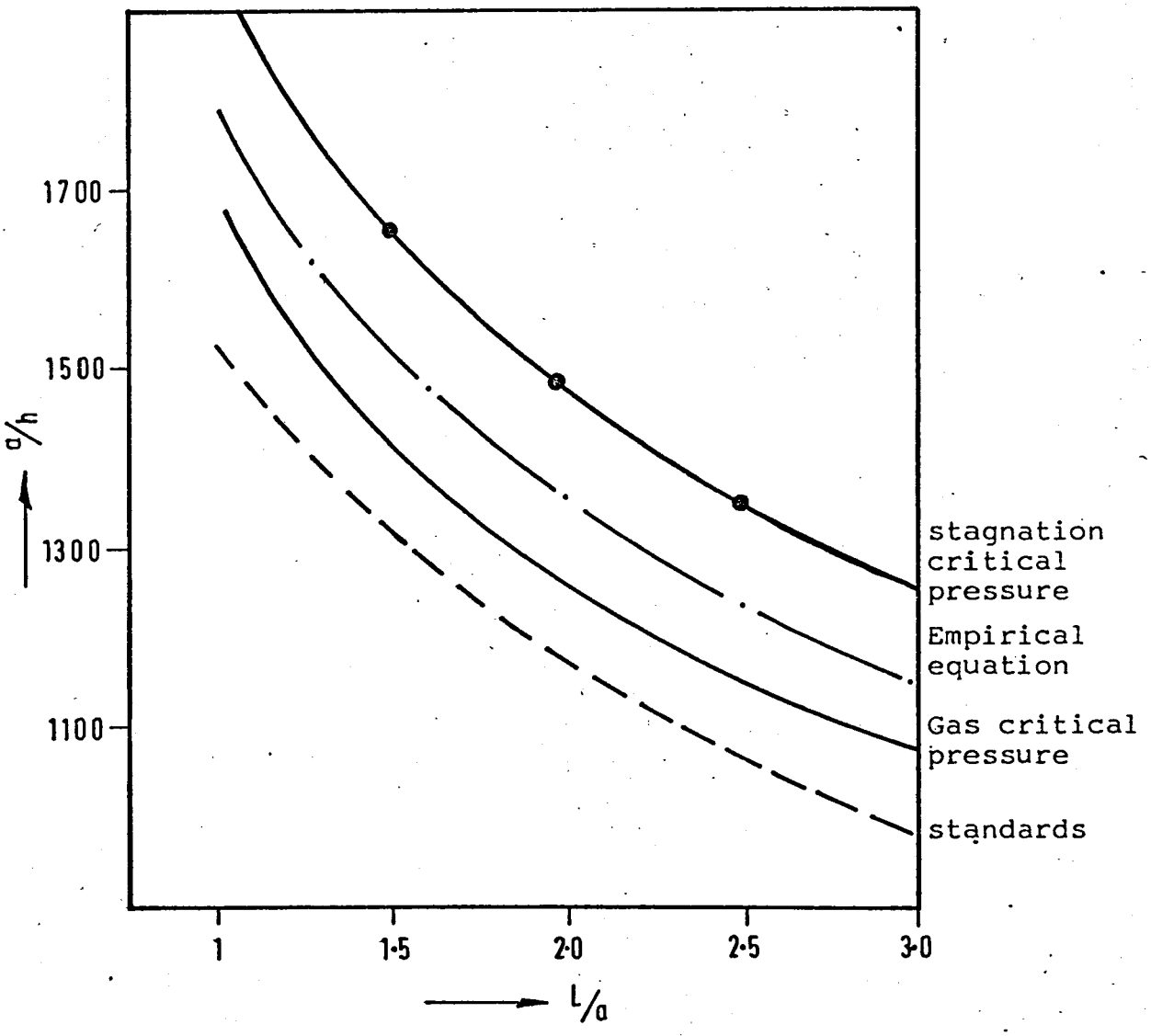

Fig. 6.4 Variation of thickness ratio with maximum permissible height (for s.s. ends and P_{cr} =0·25 psi)

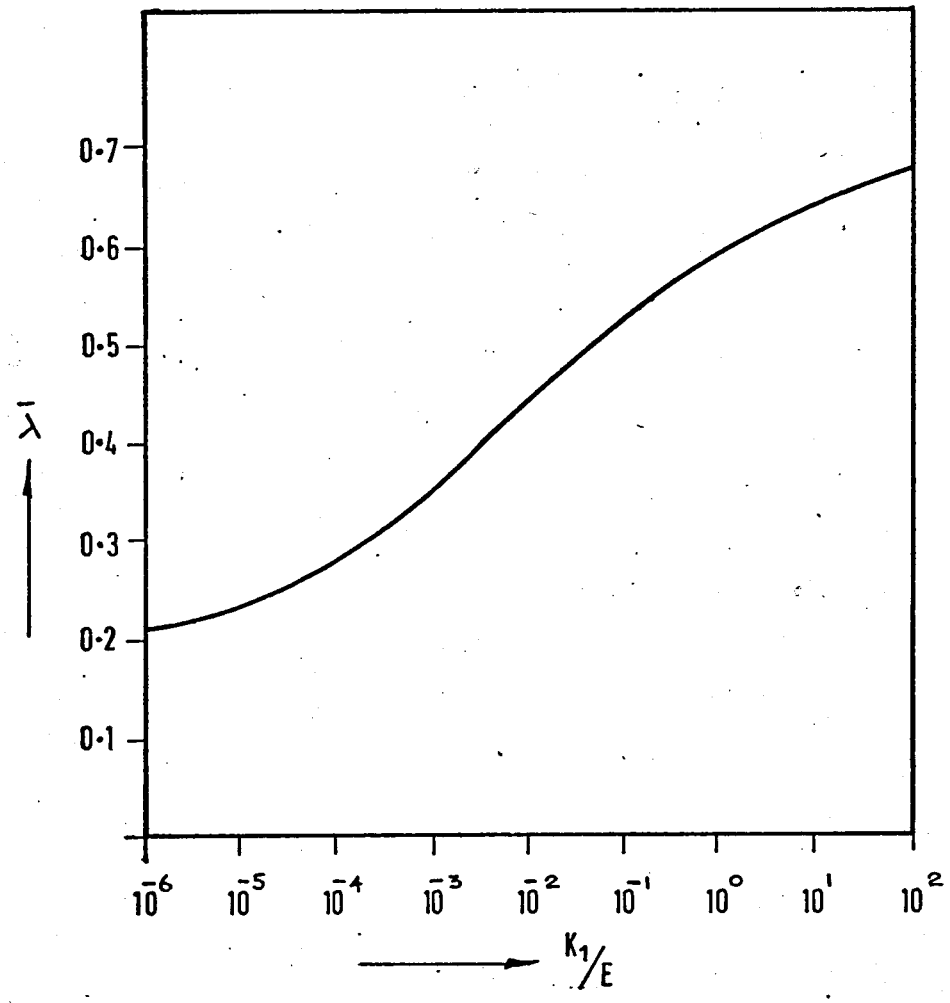

Fig. 6.5 Effect of stiffness of Elastic support on $\bar{\lambda}$

TABLES

COMPARISON OF DISPLACEMENTS BY DONNELL AND FLUGGE THEORIES

Shell Geometry		Boundary Conditions		Loading on the Shell	Max. u Displacement by		Max. v Displacement by		Max. w Displacement by	
		Root			Donnell	Flugge	Donnell	Flugge	Donnell	Flugge
1	500	C	F	$P = b_o = 1$	0.112×10^{-5}	0.115×10^{-5}	0	0	0.4×10^{-5}	0.399×10^{-5}
				$P = \cos\theta$	0.181×10^{-5}	0.181×10^{-5}	0.624×10^{-5}	0.624×10^{-5}	0.102×10^{-4}	0.102×10^{-4}
				$P = \cos 2\theta$	0.379×10^{-5}	0.379×10^{-5}	0.154×10^{-4}	0.154×10^{-4}	0.3490×10^{-4}	0.3489×10^{-4}
1	300	C	F	$P=1$	0.111×10^{-4}	0.109×10^{-4}	0	0	0.111×10^{-4}	0.110×10^{-4}
				$P = \cos\theta$	0.490×10^{-5}	0.505×10^{-5}	0.171×10^{-4}	0.173×10^{-4}	0.320×10^{-4}	0.288×10^{-4}
				$P = \cos 2\theta$	0.1046×10^{-4}	0.1056×10^{-4}	0.428×10^{-4}	0.429×10^{-4}	0.967×10^{-4}	0.973×10^{-4}
1	100	C	C	$P=1$	—	—	0	0	0.104×10^{-3}	0.104×10^{-3}
				$P = \cos\theta$	0.104×10^{-5}	0.105×10^{-5}	0.314×10^{-4}	0.314×10^{-4}	0.122×10^{-3}	0.122×10^{-3}
				$P = \cos 2\theta$	0.164×10^{-5}	0.164×10^{-5}	0.639×10^{-4}	0.640×10^{-4}	0.214×10^{-3}	0.214×10^{-3}
1	100	C	S.S.	$P=1$	-	-	0	0	0.106×10^{-3}	0.106×10^{-3}
				$P = \cos\theta$	0.167×10^{-4}	0.168×10^{-4}	0.298×10^{-4}	0.298×10^{-4}	0.125×10^{-3}	0.125×10^{-3}
				$P = \cos 2\theta$	0.449×10^{-4}	0.448×10^{-4}	0.664×10^{-4}	0.665×10^{-4}	0.217×10^{-3}	0.217×10^{-3}
5	500	C	F	$P=1$	0.6×10^{-4}	0.595×10^{-4}	0	0	0.4×10^{-4}	0.399×10^{-4}
				$P = \cos\theta$	0.891×10^{-4}	0.891×10^{-4}	0.456×10^{-3}	0.456×10^{-3}	0.46×10^{-3}	0.46×10^{-3}
				$P = \cos 2\theta$	0.336×10^{-3}	0.337×10^{-3}	0.269×10^{-2}	0.270×10^{-3}	0.554×10^{-2}	0.555×10^{-2}

COMPARISON OF DISPLACEMENTS BY DONNELL AND FLUGGE (Cont.) THEORIES

Shell Geometry		Boundary Conditions		Loading on the Shell	Max. u Displacement by		Max. v Displacement by		Max. w Displacement by	
		Root			Donnell	Flugge	Donnell	Flugge	Donnell	Flugge
1.0	10.0	C	F	P=1	0.997×10^{-2}	0.925×10^{-2}	0	0	0.102×10^{-1}	0.103×10^{-1}
				P= Cos θ	0.363×10^{-2}	0.365×10^{-2}	0.135×10^{-1}	0.136×10^{-1}	0.249×10^{-1}	0.248×10^{-1}
				P= Cos 2θ	0.679×10^{-2}	0.702×10^{-2}	0.268×10^{-1}	0.278×10^{-1}	0.665×10^{-1}	0.678×10^{-1}
1	100	C	F	P=1	0.10×10^{-3}	0.967×10^{-4}	0	0	0.999×10^{-4}	0.999×10^{-4}
				P= Cos θ	0.437×10^{-4}	0.437×10^{-4}	0.153×10^{-3}	0.153×10^{-3}	0.254×10^{-3}	0.254×10^{-3}
				P= Cos 2θ	0.920×10^{-4}	0.920×10^{-4}	0.378×10^{-3}	0.378×10^{-3}	0.859×10^{-3}	0.858×10^{-3}
1	100	C	F	$P=\sum_{n=0}^{6} b_n \cos n\theta$ (wind load)	0.179×10^{-3}	0.178×10^{-3}	0.666×10^{-3}	0.668×10^{-3}	0.158×10^{-2}	0.157×10^{-2}

COMPARISON OF STRESS RESULTANTS BY DONNELL AND FLUGGE THEORIES

Shell Geometry		Boundary Conditions		Loading on the Shell	Max. N_x		Max. N_θ		Max. $N_{x\theta}$	
		Root			Donnell	Flugge	Donnell	Flugge	Donnell	Flugge
1	500	C	F	$P = b_o = 1$	0	0	0.378×10^{-5}	0.378×10^{-5}	0	0
				$P = \cos\theta$	0.181×10^{-5}	0.181×10^{-5}	0.380×10^{-5}	0.380×10^{-5}	0.348×10^{-5}	0.348×10^{-5}
				$P = \cos 2\theta$	0.726×10^{-5}	0.726×10^{-5}	0.367×10^{-5}	0.367×10^{-5}	0.688×10^{-5}	0.688×10^{-5}
1	300	C	F	$P=1$	0	0	0.101×10^{-4}	0.1001×10^{-4}	0	0
				$P = \cos\theta$	0.503×10^{-5}	0.505×10^{-5}	0.119×10^{-4}	0.104×10^{-4}	0.947×10^{-5}	0.956×10^{-5}
				$P = \cos 2\theta$	0.201×10^{-4}	0.202×10^{-4}	0.102×10^{-4}	0.106×10^{-4}	0.184×10^{-4}	0.185×10^{-4}
1	100	C	C	$P=1$	0	0	0.949×10^{-4}	0.949×10^{-4}	0	0
				$P = \cos\theta$	0.268×10^{-4}	0.268×10^{-4}	0.946×10^{-4}	0.946×10^{-4}	0.384×10^{-4}	0.385×10^{-4}
				$P = \cos 2\theta$	0.373×10^{-4}	0.373×10^{-4}	0.946×10^{-4}	0.946×10^{-4}	0.746×10^{-4}	0.746×10^{-4}
1	100	C	S.S.	$P=1$	0	0	0.968×10^{-4}	0.968×10^{-4}	0	0
				$P = \cos\theta$	0.125×10^{-4}	0.125×10^{-4}	0.967×10^{-4}	0.967×10^{-4}	0.443×10^{-4}	0.443×10^{-4}
				$P = \cos 2\theta$	0.429×10^{-4}	0.429×10^{-4}	0.963×10^{-4}	0.963×10^{-4}	0.818×10^{-4}	0.819×10^{-4}
5	500	C	F	$P=1$	0	0	0.364×10^{-5}	0.364×10^{-5}	0	0
				$P = \cos\theta$	0.454×10^{-4}	0.454×10^{-4}	0.136×10^{-4}	0.136×10^{-4}	0.175×10^{-4}	0.175×10^{-4}
				$P = \cos 2\theta$	0.180×10^{-3}	0.181×10^{-3}	0.542×10^{-4}	0.543×10^{-4}	0.346×10^{-4}	0.346×10^{-4}

COMPARISON OF STRESS RESULTANTS BY DONNELL AND FLUGGE (cont.) THEORIES

Shell Geometry		Boundary Conditions		Loading on the Shell	Max. N_x		Max. N_θ		Max. $N_{x\theta}$	
		Root			Donnell	Flugge	Donnell	Flugge	Donnell	Flugge
1	10	C	F	P=1	0	0	-0.931×10^{-2}	-0.938×10^{-2}	0	0
				P= Cos θ	0.408×10^{-2}	0.412×10^{-2}	0.104×10^{-1}	0.102×10^{-1}	0.602×10^{-2}	0.605×10^{-2}
				P= Cos 2θ	0.128×10^{-1}	0.134×10^{-1}	0.117×10^{-1}	0.109×10^{-1}	0.92×10^{-2}	0.966×10^{-2}
1	100	C	F	P=1	0	0	-0.909×10^{-4}	-0.909×10^{-4}	0	0
				P= Cos θ	0.451×10^{-4}	0.451×10^{-4}	0.917×10^{-4}	0.915×10^{-4}	0.822×10^{-4}	0.822×10^{-4}
				P= Cos 2θ	0.179×10^{-3}	0.179×10^{-3}	0.967×10^{-4}	0.967×10^{-4}	0.159×10^{-3}	0.159×10^{-3}
1	100	C	F	$P=\sum_{n=0}^{6} b_n \cos n\theta$ (wind load)	0.351×10^{-3}	0.352×10^{-3}	0.105×10^{-3}	0.105×10^{-3}	0.251×10^{-3}	0.252×10^{-3}

COMPARISON OF MOMENT RESULTANTS BY DONNELL AND FLUGGE THEORIES

Shell Geometry		Boundary Conditions		Loading on the Shell	Max. M_x		Max. M_θ		Max. $M_{x\theta}$	
		Root			Donnell	Flugge	Donnell	Flugge	Donnell	Flugge
1	500	C	F	P= $b_o=1$	-0.660×10^{-2}	0.660×10^{-2}	-0.198×10^{-2}	0.198×10^{-2}	0	0
				P= $\cos\theta$	-0.811×10^{-2}	-0.811×10^{-2}	-0.243×10^{-2}	-0.243×10^{-2}	0.51×10^{-4}	0.457×10^{-4}
				P= $\cos 2\theta$	-0.126×10^{-2}	-0.126×10^{-2}	-0.378×10^{-2}	-0.378×10^{-2}	0.17×10^{-3}	0.161×10^{-3}
1	300	C	F	P= 1	-0.110×10^{-2}	-0.110×10^{-2}	-0.330×10^{-2}	-0.330×10^{-2}	0	0
				P= $\cos\theta$	-0.209×10^{-1}	-0.137×10^{-1}	0.627×10^{-2}	0.413×10^{-2}	-0.2×10^{-3}	0.122×10^{-3}
				P= $\cos 2\theta$	-0.222×10^{-1}	-0.219×10^{-1}	0.662×10^{-2}	0.659×10^{-2}	0.485×10^{-3}	0.46×10^{-3}
1	100	C	C	P= 1	-0.330×10^{-1}	-0.330×10^{-1}	-0.991×10^{-2}	-0.991×10^{-2}	0	0
				P= $\cos\theta$	0.388×10^{-1}	0.337×10^{-1}	0.101×10^{-1}	0.101×10^{-1}	0.596×10^{-3}	0.540×10^{-3}
				P= $\cos 2\theta$	0.435×10^{-1}	0.435×10^{-1}	0.130×10^{-1}	0.130×10^{-1}	0.164×10^{-2}	0.173×10^{-2}
1	100	C	S.S.	P= 1	-0.330×10^{-1}	-0.330×10^{-1}	-0.991×10^{-2}	-0.991×10^{-2}	0	0
				P= $\cos\theta$	0.350×10^{-1}	0.350×10^{-1}	0.105×10^{-1}	0.105×10^{-1}	0.960×10^{-3}	0.909×10^{-3}
				P= $\cos 2\theta$	0.435×10^{-1}	0.435×10^{-1}	0.130×10^{-1}	0.130×10^{-1}	0.225×10^{-2}	0.236×10^{-2}
5	500	C	F	P=1	-0.660×10^{-2}	0.660×10^{-2}	-0.198×10^{-2}	-0.198×10^{-2}	0	0
				P= $\cos\theta$	0.340×10^{-1}	0.340×10^{-1}	0.102×10^{-1}	0.102×10^{-1}	0.394×10^{-4}	0.263×10^{-4}
				P= $\cos 2\theta$	0.116	0.116	0.347×10^{-1}	0.348×10^{-1}	-	-

COMPARISON OF MOMENT RESULTANTS BY DONNELL AND FLUGGE (cont.)

THEORIES

Shell Geometry		Boundary Conditions		Loading on the Shell	Max. M_x		Max. M_θ		Max. $M_{x\theta}$	
		Root			Donnell	Flugge	Donnell	Flugge	Donnell	Flugge
1	10	C	F	P=1	-0.330	-0.330	-0.991×10^{-1}	-0.99×10^{-1}	0	0
				P= Cos θ	0.527	0.513	0.512	0.512	0.316×10^{-1}	0.22×10^{-1}
				P= Cos 2θ	0.950	0.934	0.268	0.276	0.128	0.115
1	100	C	F	P=1	-0.330×10^{-1}	-0.330×10^{-1}	-0.991×10^{-2}	-0.991×10^{-2}	0	0
				P= Cos θ	0.435×10^{-1}	0.434×10^{-1}	0.130×10^{-1}	0.130×10^{-1}	0.782×10^{-3}	0.657×10^{-3}
				P= Cos 2θ	0.754×10^{-1}	0.743×10^{-1}	0.222×10^{-1}	0.222×10^{-1}	0.293×10^{-2}	0.267×10^{-2}
1	100	C	F	$P=\sum_{n=0}^{6} b_n \cos n\theta$ (wind load)	0.127	0.124	0.374×10^{-1}	0.373×10^{-1}	0.696×10^{-2}	0.670×10^{-2}

TABLE 3.1

L/a	critical buckling pressure $(P_{cr}/E) \times 30.10^6$		
	present analysis	Wang and Billington	Cole
1	169	174	
2	83.7	84.2	86.1
3	54.4	54.9	
4	44.3	45.5	
5	31.5	32.1	35.2
6	26.9	27.2	
7	24.8	24.9	
8	23.7	23.8	
9	20.2	20.9	
10	16.1	16.6	21.2

Comparison of critical buckling pressures for clamped-free cylindrical shell (under uniform radial load, $a/h = 100$).

TABLE 3.2

Variation of Buckling pressure P_{cn} with the single harmonic selected for the virtual displacement

L/a	a/h	The harmonic selected n								
		3	4	5	6	7	8	9	10	11
1	200	3599.0	1125.	385.9	187.0	132.2	125.4	138.1	157.0	1036.
	300	2278.0	736.5	241.0	103.0	59.59	46.84	45.90	49.04	362.9
	400	1672.0	549.1	176.5	71.60	37.2	25.47	22.3	22.23	164.4
	500	1321.0	437.9	139.6	55.18	26.98	16.80	13.35	12.40	91.86
2	200	525.2	130.4	66.23	63.32	76.82	97.31	122.2	150.5	664.6
	300	321.7	76.65	30.02	22.19	23.92	29.16	36.16	43.91	226.2
	400	227.5	54.78	18.87	11.48	10.93	12.64	15.38	18.43	106.4
	500	174.5	42.82	13.76	7.29	6.16	6.72	7.89	9.45	60.03
3	200	142.7	48.72	44.22	56.81	75.57	98.31	124.4	154.9	564.4
	300	83.18	22.57	14.95	17.09	22.1	28.59	36.2	45.0	180.7
	400	57.55	14.34	7.52	7.54	9.35	11.97	15.11	18.67	83.17
	500	43.55	10.51	4.68	4.11	4.86	6.13	7.07	9.45	45.74
4	100	202.9	219.3	320.5	456.1	618.6	789.7	1024.2	1259.6	7045.
	200	58.96	33.32	41.13	56.92	76.80	99.99	126.3	158.2	1436.
	300	32.22	12.52	12.59	16.69	22.38	29.19	36.98	46.07	166.0
	400	21.59	6.84	5.61	7.03	9.32	12.12	15.38	19.18	71.41
	500	16.01	4.53	3.11	3.63	4.73	6.14	7.77	9.69	38.50
5	100	141.8	204.6	313.3	451.5	608.1	857.7	971.5	1260.2	6504.
	200	32.59	28.68	40.29	50.07	77.30	100.72	127.4	150.8	1179.
	300	16.31	9.65	12.09	16.81	22.72	29.61	37.40	46.12	185.0
	400	10.49	4.72	5.18	7.03	9.47	12.35	15.65	19.50	71.09
	500	7.57	2.84	2.72	3.58	4.78	6.24	7.92	9.88	35.48

TABLE 3.3

Variation of buckling pressures with n_1 $(n_2 = n_1 + 4)$

L/a	a/h	$(P_{cr}/E) \times 30 \times 10^6$ for n_1 =						
		2	3	4	5	6	7	8
1.0	100	414.2	268.4	211.1	190.4	185.4	224.5	292.7
	200	130.9	68.9	46.1	36.2	32.4	32.9	40.0
	300	76.0	35.4	21.14	15.1	12.4	11.68	13.41
	400	53.9	23.4	12.89	8.54	6.56	5.86	8.61
	500	42.0	17.5	9.09	5.67	4.13	3.54	4.93
2.0	100	139.2	112.5	108.0	124.8	159.0	204.3	277.4
	200	29.0	20.8	17.8	17.6	20.3	25.3	34.17
	300	12.66	8.30	6.63	6.09	6.45	7.67	10.21
	400	7.39	4.5	3.39	2.96	2.95	3.36	4.38
	500	5.03	2.86	2.05	1.72	1.64	1.78	2.29
3.0	100	89.95	80.61	89.86	119.4	158.2		
	200	16.0	12.9	12.4	14.55	18.67	23.9	32.5
	300	6.26	4.72	4.24	4.52	5.54	7.05	9.57
	400	3.31	2.38	2.04	2.02	2.39	3.0	4.07
	500	2.06	1.42	1.18	1.14	1.26	1.56	2.04
4.0	100	67.47	64.34	81.13	108.5	134.7	159.9	
	200	11.21	9.49	10.01	12.77	1. .14	19.6	25.9
	300	4.18	3.34	3.23	3.89	4.98	6.08	8.13
	400	2.1	1.64	1.51	1.70	2.04	2.67	3.60
	500	1.28	0.962	0.866	0.957	1.04	1.39	1.97
5.0	100	52.4	51.9	67.79	83.39	96.9	111.0	144.0
	200	8.31	7.28	8.27	10.29	12.06	13.82	17.48
	300	3.08	2.53	2.62	3.24	3.89	4.5	5.85
	400	1.55	1.23	1.22	1.48	1.94	2.02	2.7
	500	0.923	0.713	0.676	0.908	0.98	1.04	1.81

TABLE 3.3(b)

Variation of P_{cn} with n_1

L/a	a/h	$(P_{cn}/E) \cdot 30 \times 10^6$ for n_1 =			
		1	2	3	4
1	200	368.1	130.9	68.9	46.1
2	300	29.5	12.66	8.30	6.63
3	100	127.7	89.9	80.6	89.86
5	300	4.6	3.08	2.53	2.62
6	50	330.0	308	315	
7	200		4.97	4.60	5.36
10	100	21.32	18.21	19.21	22.74
10	50	169.6	160.1	170.0	
10	20	2998	3239	4443	

TABLE 3.4

Influence of various combination of harmonics on buckling pressure $\left(\frac{P_{cr}}{E}.30\times10^{6}\right)$

L/a	a/h	The buckling pressure when the harmonics selected are -			
		Five consecutive ones $(n_1 \text{ to } n_2)$	1,3,5,7 and 9	2,4,6,8 and 10	2,3,7,8 and 9
1.0	300.0	11.68 (7-11)	22.93	19.79	17.66
	400.0	5.86 (7-11)	12.48	10.24	9.54
	500.0	3.54 (7-11)	8.03	6.29	6.17
2.0	300.0	6.09 (5-9)	9.98	9.60	10.0
	400.0	2.95 (6-10)	4.88	4.57	4.43
	500.0	1.64 (6-10)	2.81	2.60	2.40
3.0	300.0	4.24 (4-8)	6.78	6.94	9.30
	400.0	2.02 (5-9)	3.18	3.23	3.95
	500.0	1.14 (5-9)	1.803	1.90	2.02

TABLE 3.5

shell geometry →	$L/a=1$ $a/h=100$	$L/a=2$ $a/h=200$	$L/a=5$ $a/h=100$
No. of terms	Buckling pressures $(P_{cn}/E)\times 30\times10^{6}$		
2	212.6	18.99	56.71
3	193.9	17.77	53.40
4	192.3	17.73	52.22
5	190.4	17.69	51.93

Convergence of buckling pressures with no. of terms in axial direction

TABLE 3.6

shell geometry →	$L/a=1$ $a/h=100$	$L/a=1$ $a/h=500$	$L/a=5$ $a/h=100$	$L/a=5$ $a/h=200$	$L/a=5$ $a/h=500$
No. of terms	Buckling pressures $(P_{cn}/E).30\times10^{6}$				
1	1037.5	26.98	141.8	32.5	2.84
2	514.1	12.70	91.5	16.3	1.54
3	305.0	6.63	65.4	10.9	1.03
4	224.1	4.37	55.6	8.3	0.781
5	190.4	3.54	51.9	7.3	0.676

Convergence of buckling pressures with number of terms in circumferential direction

TABLE 3.7 (a)

VARIATION OF Pcr WITH N_1 and tip B.C.

	a/h	200					300				
	B.C.	F	S.S	P	C.S	C	F	S.S	P	C.S.	C
		L/a = 2									
5		17.6	33.06	41.5	36.07		6.09	14.07	18.87	15.80	
6		20.3	29.64	35.36	31.95	35.94	6.45	11.53	14.61	12.75	14.77
7		25.3	30.21	34.3	32.08	34.78	7.67	10.85	13.10	11.81	13.20
8						40.26		12.34		13.24	14.42
		L/a = 5									
3		7.28	13.98	17.23	15.9	17.27	2.541	5.41			6.99
4		8.27	12.72	14.81	14.09	14.81	2.63	4.58	5.54	5.24	5.57
5		10.29	13.97	15.11	14.84	15.12	3.24	4.58	5.08	5.04	5.22
6		12.06	17.74				3.87	5.08	5.63	5.46	5.46

TABLE 3.7 (b)

VARIATION OF Pcr WITH N_1 and tip B.C.

N_1	a/h	L/a = 2									
		400					500				
	B.C.	F	S.S	P	C.S.	C	F	S.S	P	C.S.	C
5		2.96					1.72				
6		2.95	6.19	8.25	7.04	8.34	1.64	3.94	5.49	4.60	5.57
7		3.36	5.51	6.99	6.17	7.05	1.78	3.36	4.44	3.86	4.50
8		4.38	6.02	7.40	6.68	7.46	2.29	3.57	4.60	4.06	4.65
		L/a = 5									
3		1.23	2.84			3.80	0.71	1.6			2.54
4		1.22	2.28	2.58	2.68	2.85	0.67	1.36	1.73	1.638	1.75
5		1.48	2.07	2.53	2.43	2.54	0.908	1.23	1.48	1.42	1.48
6		1.94	2.35	2.56	2.53	2.57	0.98	1.908	1.64	1.61	1.49

TABLE 3.8

Buckling pressures for different tip B.C. with base clamped

$\left(\frac{P_{cr}}{E} \cdot 30\times10^{6}\right)$

L/a	a/h	Tip Boundary condition				
		Free	Simply supported	Pinned	Clamped-sliding	Clamped
2.0	200.0	17.6	29.64	34.3	31.95	34.78
	300.0	6.09	10.85	13.10	11.81	13.20
	400.0	2.95	5.51	6.99	6.17	7.05
	500.0	1.64	3.36	4.44	3.86	4.50
5.0	200.0	7.28	12.72	14.81	14.09	14.81
	300.0	2.53	4.58	5.22	5.04	5.22
	400.0	1.22	2.07	2.51	2.43	2.53
	500.0	0.676	1.23	1.44	1.42	1.44

TABLE 3.9

Influence of base notation on buckling pressure $\left(\frac{P_{cr}}{E}.30\times10^{6}\right)$

Shell geometry		Buckling pressure when	
L/a	a/h	Base notation is relaxed (pinned condition)	Base is clamped $(w_{,x}(0)=0)$
1	100	188.68	190.4
1	500	3.50	3.54
3	300	4.22	4.24
4	300	3.24	3.22

TABLE 3.10

	Fourier coefficients for the pressure data		
b_0	0.233	0.586	0.609
b_1	0.491	0.329	0.340
b_2	0.913	0.846	0.766
b_3	0.425	0.538	0.476
b_4	-0.049	-0.043	-0.053
b_5	-0.161	-0.092	-0.086
b_6	0.0891	0.0158	0.0283

Fourier pressure coeffients (for the pressure distribution in Figure 3.7).

TABLE 4.1

Quantity compared	Theory used	The loading harmonic selected for comparison: 1	2	3	4	5	6
$\frac{w_{max}}{a}$	Donnell	2.54	8.59	23.0	48.86	73.5	71.7
	F.E.	2.54	8.59	23.0	49.10	74.8	73.2
$\frac{\sigma_{x\,max}}{E}$	Donnell	0.451	1.79	3.93	6.33	7.34	58.9
	F.E.	0.437	1.74	3.88	6.31	7.41	59.8
$\frac{\sigma_{\theta\,max}}{E}$	Donnell	0.917	0.953	-1.06 +1.17	1.90	2.20	1.77
	F.E.	0.915	0.947	+1.17 -1.04	1.91	2.22	1.785
$\frac{\sigma_{x\theta\,max}}{E}$	Donnell	0.825	1.59	2.32	2.83	2.80	-
	F.E.	0.872	1.69	2.54	3.12	3.12	-

Comparison of Results by FINITE ELEMENT ANALYSIS with CONTINUUM ANALYSIS

For a cantilever shell of L/a = 1 and a/h = 100

The loading is $\frac{P_a a}{E h} = 1$

TABLE 4.2

Quantity compared		The loading harmonic selected for comparison					
	Theory used	1	2	3	4	5	6
$\frac{w_{max}}{a}$	Donnell	2.56	8.74	23.9	55.3	111.4	198
	F.E.	2.56	8.72	23.8	55.3	111.7	197
$\frac{\sigma_{x\,max}}{E}$	Donnell	0.453	1.82	4.07	7.20	11.05	15.2
	F.E.	0.409	1.73	3.98	7.05	10.78	14.9
$\frac{\sigma_{\theta\,max}}{E}$	Donnell	0.95	0.962	0.95	1.05	1.29	1.81
	F.E.	0.948	0.948	0.945	1.035	1.27	1.75
$\frac{\sigma_{z\theta\,max}}{E}$	Donnell	0.87	1.72	2.47	3.41	4.19	-
	F.E.	0.961	1.86	2.72	3.59	4.46	-

Comparison of Results by FINITE ELEMENT ANALYSIS with CONTINUUM ANALYSIS

For a cantilever shell of L/a = 1 and a/h = 500

The loading is $\frac{P_0}{E}\left(\frac{a}{h}\right) = 1$.

TABLE 4.3

Quantity compared	Theory used	The loading harmonic selected for comparison: 1	2	3	4	5	6
$\frac{w_{max}}{a}$	Donnell	115.0	1383.0	5890	8940	5440	2470
	F.E.	114.8	1385.0	5970	9540	5850	2620
$\frac{\sigma_{x\,max}}{E}$	Donnell	11.35	45.2	91.7	90.0	55.6	38.4
	F.E.	11.4	45.4	93.6	95.4	58.4	39.4
$\frac{\sigma_{\theta\,max}}{E}$	Donnell	0.938	+13.4	27.7	27.10	16.73	11.52
	F.E.	0.940	+13.65	28.1	28.6	17.50	11.84
$\frac{\sigma_{x\theta\,max}}{E}$	Donnell	0.438	8.0	11.35	7.71	6.25	-
	F.E.	0.440	8.80	10.98	9.08	7.20	-

Comparison of Results by FINITE ELEMENT ANALYSIS WITH CONTINUUM ANALYSIS

For a cantilever shell of L/a = 5 and a/h = 500

The loading is $\frac{P_0}{E}\frac{a}{h} = 1$

TABLE 4.4

Shell geometry		buckling pressure by P_{cr} psi	
L/a	a/h	F.E.Method	Flugge
2	100	148.4	142.0
	200	26.09	24.8
4	100	75.73	72.50
	200	12.95	11.6

COMPARISON OF BUCKLING PRESSURES WITH FLUGGE'S RESULTS (for the case of axisymmetric radial compression)

TABLE 4.5

Shell geometry		buckling pressures by P_{cr} psi	
L/a	a/h	F.E.Method	Almroth
$\pi/2$	100	221.5	216.0
π	200	19.39	18.0
2π	200	10.53	10.45
2π	400	1.84	1.69

COMPARISON OF BUCKLING PRESSURES WITH ALMROTH'S RESULTS (for the case of non-uniform pressure of the type $P = P_0 (b_0 + b_1 \cos \theta)$.

TABLE 4.6

Shell geometry			Buckling pressure
No. of courses	for successive courses from base		
	L/a	a/h	$\frac{P_{cr}}{E}.30\times10^6$
5	0.2 for each	100, 200, 300, 400 and 500	6.19
4	0.2, 0.2, 0.2 and 0.4	100, 200, 300 and 500	5.37
5	0.1 for each	1055, 1405, 1898, 2918 and 3075	0.111
5	0.066 for each	1115, 1312, 1990, 3058, 3740	0.125
3	0.2, 0.2 and 0.6	100, 200 and 500	4.72
2	0.2 and 0.8	100 and 500	4.20
2	1.66 and 2.5	150 and 300	4.0
3	0.84, 1.66 and 1.66	150, 200 and 300	4.1
2	1.33 and 2.0	150 and 300	5.17
2	1.66 and 1.66	200 and 300	5.28

BUCKLING PRESSURE FOR VARIABLE THICKNESS SHELLS UNDER WIND LOADS

TABLE 5.1

Shell Geometry				Buckling Pressure by $(P_{cr}/E).30\times10^6$	
$L/_a$	No. of Courses	For Each Course		Experiments	F.E. Method
		$1/_a$	$a/_h$		
4.16	2	1.66 2.5	150 300	3.10	4.0
4.16	3	0.84 1.66 1.66	150 200 300	3.33	4.10
3.33	2	1.33 2.0	150 300	3.94	5.17
3.33	2	1.66 1.66	200 300	3.98	5.28

COMPARISON OF BUCKLING PRESSURES

FOR VARIABLE THICKNESS SHELLS

Shell Geometry		Type of Flow	Buckling Pressure By (P_{cr} psi)		
			Experiment	Theory	
$L/_a$	$a/_h$			(a)	(b)
1.833	214.0	Smooth Flow	0.286	0.433	0.278
		Turbulent Flow	0.288		
		Turbulent Shear Flow	0.281		
4.728	149.0	Smooth Flow	0.238	0.422	0.37
		Turbulent Flow	0.250		
		Turbulent Shear Flow	0.240		

COMPARISON OF BUCKLING PRESSURES FOR AXISYMMETRIC COMPRESSION

(VELOCITY $V = 0$)

Type of Flow	Velocity of Flow In/Sec	Buckling Pressure By (P_{cr} p.s.i)						
		Experiments: when the Number of Lobes is					Theory	
		1	3	5	7	8	(a)	(b)
Smooth Flow	73.0	0.189	0.306	0.526	0.460	0.460	0.443	0.264
	52.2	0.245	0.294	0.396	0.387	0.387	0.434	0.286
Turbulent Flow	73.0	0.187	0.335	0.491	0.491	0.476	0.435	0.325
	52.2	0.262	0.305	0.395	0.408	0.408	0.472	0.325
Turbulent Shear Flow	73.0	0.226	0.330	0.458	0.442	0.442	0.443	0.326
	52.2	0.267	0.296	0.374	0.374	0.374	0.47	0.352

COMPARISON OF BUCKLING PRESSURES

(For the Shell with $L/_a$ = 1.833 and $a/_h$ = 214)

Type Of Flow	Velocity Of Flow In/Sec	Buckling Pressures By (P_{cr} P.S.I)			
		Experiments		Theory	
		When the No. of Lobes is			
		1	2,3,4 and 5	(a)	(b)
Smooth Flow	73.0 52.2	0.112 0.183	0.365 0.30	0.516 0.465	0.37 0.442
Turbulent Flow	73.0 52.2	0.117 0.195	0.405 0.331	0.49 0.49	0.38 0.427
Turbulent Shear Flow	77.8 54.3	0.147 0.20	0.360 0.307	0.478 0.466	0.402 0.43

COMPARISON OF BUCKLING PRESSURES

(For the Shell with $L/_a = 4.728$ and $a/_h = 149.0$)

TABLE 6.1

VALUES OF $\bar{\lambda}$ FOR DIFFERENT END BOUNDARY CONDITIONS

TOP	FREE	SIMPLE SUPPORT	FREE	CLAMPED	FREE
BASE	CLAMPED	SIMPLE SUPPORT	CLAMPED-SLIDING	CLAMPED	ELASTIC SUPPORT
$\bar{\lambda}$	0.66	1.1	0.22	1.3	Ref.Fig. (6.5)

TABLE 6.2

TYPICAL TANK WIDTH 96 IN BUTT WELD COURSES (APPENDIX A TYPE TANKS)

1 TANK RADIUS	2 SHELL THICKNESS	3 TANK HEIGHT	4 (MAX PERMISSIBLE HEIGHT) STANDARDS	5 PRESENT ANALYSIS	6 MAX FREE HEIGHT CLAMPED-FREE
50.0	0.34	24.0	40.44	50.45	30.27
50.0	0.46	32.0	86.11	107.41	64.45
50.0	0.57	40.0	147.18	183.59	110.15
50.0	0.69	48.0	237.29	296.00	177.60
60.0	0.41	24.0	49.13	61.28	36.77
60.0	0.55	32.0	102.40	127.73	76.64
60.0	0.60	40.0	127.28	158.77	95.26
60.0	0.83	48.0	286.47	357.35	214.41
70.0	0.47	24.0	54.85	68.43	41.06
70.0	0.64	32.0	118.69	148.06	88.83
70.0	0.80	40.0	207.34	258.64	155.19
70.0	0.96	48.0	327.07	407.99	244.80
80.0	0.54	24.0	63.53	79.24	47.55
80.0	0.73	32.0	134.98	168.38	101.03
80.0	0.91	40.0	234.19	292.14	175.28
80.0	1.00	48.0	296.46	369.82	221.89
90.0	0.61	24.0	72.20	90.07	54.04
90.0	0.82	32.0	151.28	188.71	113.23
90.0	1.03	40.0	267.51	333.70	200.22
90.0	1.24	48.0	425.40	530.65	318.39
100.0	0.67	24.0	77.95	97.23	58.34
100.0	0.91	32.0	167.58	209.04	125.42
100.0	1.14	40.0	294.35	367.18	220.31
100.0	1.37	48.0	466.02	581.33	348.80

shell thickness in inches, other dimensions in feet.

TABLE 6.3

TYPICAL API TANKS BASED ON APPENDIX K METHOD

TANK DIAM	TANK HEIGHT	NUMBER OF COURSES	REDUCED HEIGHT	MAX PERMISSIBLE HEIGHT STANDARD	MAX PERMISSIBLE HEIGHT PRESENT ANALYSIS	INTERMEDIATE GIRDER API	PRESENT ANALYSIS
1	2	3	4	5	6	7	8
160	40		77.38	66.03	82.36	YES	NO
180	40		85.15	70.15	87.51	YES	NO
200	40		94.24	74.28	92.65	YES	YES
220	40	5	87.92	84.29	105.15	YES	NO
240	40		97.39	90.54	112.94	YES	NO
260	40		107.70	96.40	120.25	YES	NO
280	40		118.76	101.83	127.03	YES	NO
140	48		97.74	87.68	109.38	YES	NO
160	48		113.08	94.45	117.82	YES	NO
180	48		125.77	101.67	126.83	YES	NO
200	48	6	143.38	111.50	139.09	YES	YES
220	48		132.59	124.83	155.72	YES	NO
227	48		137.46	128.05	159.73	YES	NO
120	56		111.02	109.73	136.88	YES	NO
140	56		135.30	118.75	148.14	YES	NO
160	56	7	157.70	129.89	162.03	YES	NO
180	56		180.84	145.29	181.24	YES	NO
189	56		190.38	149.91	187.00	YES	YES
120	64		147.01	143.15	178.57	YES	NO
140	64		180.67	157.54	196.51	YES	NO
160	64	8	213.19	173.98	217.03	YES	NO
165	64		217.68	176.96	220.74	YES	NO

all dimensions in feet

TABLE 6.4

TYPICAL APPENDIX D TANKS BASED ON APPENDIX K METHOD

TANK DIAM	TANK HEIGHT	NUMBER OF COURSES	REDUCED HEIGHT	MAX PERMISSIBLE HEIGHT STANDARD	MAX PERMISSIBLE HEIGHT PRESENT ANALYSIS	INTERMEDIATE GIRDER API	PRESENT ANALYSIS
1	2	3	4	5	6	7	8
200	40		75.39	43.26	53.96	YES	YES
220	40		67.41	49.25	61.43	YES	YES
240	40		75.66	51.08	63.72	YES	YES
260	40	5	82.00	54.29	67.72	YES	YES
280	40		88.28	57.51	71.74	YES	YES
300	40		94.98	60.51	75.48	YES	YES
320	40		102.25	63.32	78.98	YES	YES
340	40		110.42	66.25	82.65	YES	YES
360	40		118.12	68.44	85.38	YES	YES
380	40		126.55	70.73	88.23	YES	YES
180	48		96.93	59.18	73.82	YES	YES
200	48		110.35	61.99	77.32	YES	YES
220	48		99.17	70.84	88.37	YES	YES
240	48	6	113.01	74.82	93.34	YES	YES
260	48		123.01	79.60	99.29	YES	YES
280	48		132.48	84.30	105.16	YES	YES
298	48		141.61	88.30	110.15	YES	YES
160	56		115.24	75.53	94.22	YES	YES
180	56		134.07	80.46	100.37	YES	YES
200	56		155.90	86.43	107.82	YES	YES
220	56	7	139.47	98.03	122.29	YES	YES
240	56		159.57	104.09	129.85	YES	YES
247	56		165.69	106.28	132.57	YES	YES
160	64		152.88	98.77	123.20	YES	YES
180	64		180.66	106.28	132.57	YES	YES
200	64	8	211.99	116.42	145.22	YES	YES
212	64		178.14	127.35	158.85	YES	YES

all dimensions in feet

TABLE 6.5

TYPICAL APPENDIX G TANKS BASED ON APPENDIX K METHOD

TANK DIAM	TANK HEIGHT	NUMBER OF COURSES	REDUCED HEIGHT	MAX PERMISSIBLE HEIGHT STANDARD	MAX PERMISSIBLE HEIGHT PRESENT ANALYSIS	INTERMEDIATE GIRDER API	PRESENT ANALYSIS
1	2	3	4	5	6	7	8
240	40		56.06	31.41	39.18	YES	YES
260	40		60.13	31.82	39.69	YES	YES
280	40		65.93	32.95	41.10	YES	YES
300	40	5	74.93	35.57	44.38	YES	YES
320	40		79.25	35.10	43.79	YES	YES
340	40		83.59	36.60	45.66	YES	YES
360	40		88.08	38.08	47.50	YES	YES
220	48		73.52	41.85	52.20	YES	YES
240	48		79.74	43.27	53.98	YES	YES
260	48		87.86	45.30	56.50	YES	YES
280	48		96.83	47.26	58.95	YES	YES
300	48	6	106.77	49.16	61.33	YES	YES
320	48		117.50	51.00	63.62	YES	YES
340	48		124.62	53.14	66.29	YES	YES
360	48		131.15	55.32	69.01	YES	YES
200	56		109.29	48.96	61.08	YES	YES
220	56		100.03	55.56	69.30	YES	YES
240	56		110.58	58.73	73.26	YES	YES
260	56		122.28	61.80	77.10	YES	YES
280	56	7	135.50	64.88	80.93	YES	YES
300	56		149.69	67.73	84.49	YES	YES
320	56		165.18	70.55	88.01	YES	YES
328	56		169.42	71.75	89.50	YES	YES
200	64		144.86	63.92	79.73	YES	YES
220	64		133.17	72.78	90.79	YES	YES
240	64		147.76	77.37	96.52	YES	YES
260	64	8	164.03	81.73	101.96	YES	YES
280	64		182.05	86.12	107.43	YES	YES

all dimensions in feet

COMPUTER PROGRAMS

```
JOB B501,B,KSP1650
JOBCORE 45K
LUFORTRAN
RUN ,,6000
****
DOCUMENT SOURCE
      LIBRARY (ED,SUBGROUPNAGF)
      PROGRAM (B501)
      EXTENDED DATA
      INPUT 1 = CR0
      OUTPUT 2 = LP0
      TRACE 1
      END
      MASTER PRABHU
C     ' COMPUTATION OF CRITICAL BUCKLING PRESSURES OF CYLINDRICAL SHELLS
C       UNDER WIND LOADS BY CONTINUUM ANALYSIS  '
      REAL MU
      DOUBLE PRECISION UK1,UK,WM,ALF1,BET1,ALF2,BET2,AM1,AM2,BM1,BM2,
     1HM1,HM1P,HM2,HM2P,HN1,HN1P,HN2,HN2P,S1,S2,S1P,S2P,TEH1,TEH1P,TEH2,
     2TEH2P,CB1,CB2,SB1,SB2,HYP1,HYP2,H1,H2,V1,V2,C1,C2,QS1,QD1,QS2,QD2,
     3HA,HB,ATUK,BTUK,CTUK,DTUK,ETUK
      DIMENSION B(7),Z(64),E(8),Y(8),G1(6,15),G2(6,15),G3(6,15),F1(21)
     1,F2(21),F3(21),F4(21),G4(15),EC(6,6,6),ES(6,6,6),RC(6,6),RS(6,6),
     2DE(20,20),SC(15,6,6),SS(15,6,6),TS(15,6,6),US(15,6,6),WS(15,6,6),
     3AA(8,8),BB(8),BC(95,95),CMD1(8),CMD2(8),ZZ(95),XXX(20),DD(20)
     4,CN(15)
      PI=3.141592653
      MU=0.3
C     ' GEOMETRIC PARAMETERS OF THE SHELL  '
C     ' AL = LENGTH / RADIUS  AND   AH = RADIUS / THICKNESS  '
      AL=4.0
      AH=300.0
      RO=1./AL
C     ' ASSUMED WIND LOAD COEFFICIENTS  '
      B(1)=0.22
      B(2)=0.338
      B(3)=0.233
      B(4)=0.471
      B(5)=0.166
      B(6)=-0.066
      B(7)=-0.055
      MA=5
      MAA=MA+1
      M1=2*MA+3+2
      MM=3*MA*MA
C     ' PREBUCKLING ANALYSIS BY DONNELL'S THEORY  '
      U1=SQRT(2.75)
C     ' ANALYSIS FOR THE CASE OF AXISSYMETRIC LOADING  '
      U=SQRT(U1*AH)
C     'THE EDGE X=L IS S.S,  '
```

```
      V=AL*U
       X1=COS(V)/EXP(V)
       X2=SIN(V)/EXP(V)
      X3=COS(V)*EXP(V)
      X4=SIN(V)*EXP(V)
C   'THE EDGE X=0 IS CLAMPED AND THE EDGE X=L IS SIMPLY SUPPORTED  '
      Z(1)=1.
      Z(2)=-1.
      Z(3)=X1
      Z(4)=-X1-X2
      Z(5)=0
      Z(6)=1.
      Z(7)=X2
      Z(8)=-X2+X1
      Z(9)=1.
       Z(10)=1.
       Z(11)=X3
       Z(12)=X3-X4
      Z(13)=0
      Z(14)=1.
      Z(15)=X4
      Z(16)=X3+X4
      Z(4)=X2
      Z(8)=-X1
      Z(12)=-X4
      Z(16)=X3
      E(1)=-1.
      E(2)=0.
      E(3)=-1.
      E(4)=0.
      DO 137 I=1,4
      DO 137 J=1,4
  137 DE(I,J)=Z(I+4*(J-1))
        DO 138 I=1,4
      DE(I,3)=DE(I,3)/EXP(V)
  138 DE(I,4)=DE(I,4)/EXP(V)
      CALL F04AEF (DE,20,E,8,4,1,Y,8,BB,AA,8,DD,20,IFAIL)
       Y(3)=Y(3)/EXP(V)
      Y(4)=Y(4)/EXP(V)
      DO 41 MJ=1,21
      X=(MJ-1)*AL/20.
      V=U*X
      F4(MJ)=1+(Y(1)*COS(V)+Y(2)*SIN(V))/EXP(V)+(Y(3)*COS(V)+
     1Y(4)*SIN(V))*EXP(V)
      F4(MJ)=F4(MJ)*B(1)/(AH*AH)
   41 CONTINUE
      DO 442 M=1,M1
      G4(M)=F4(21)*AL**M/AL
      Q=4.
      DO 43 MJ=2,20
```

```
      X=((MJ-1)*AL/20.)**(M-1)
      G4(M)=G4(M)+F4(MJ)*X*Q
   43 Q=6.-Q
      G4(M)=G4(M)*AL/60.
  442 CONTINUE
      UK1=DSQRT(2.73)
      UK=DSQRT(UK1*AH)
C     ' ANALYSIS FOR THE CASE OF OTHER HARMONIC LOADING  '
      DO 1 N=1,6
      ANUK=1.*N
      ATUK=ANUK**4.
      BTUK=(UK**4.)/4.
      CTUK=ATUK+BTUK
      DTUK=DSQRT(CTUK)
      ETUK=DTUK-UK*UK/2.
      WM=DSQRT(ETUK)
      ALF1=(WM+UK+N*N/WM)/2.
      BET1=(WM-UK-N*N/WM)/2.
      ALF2=(WM-UK+N*N/WM)/2.
      BET2=(WM+UK-N*N/WM)/2.
      AM1=(ALF1**2-BET1*BET1)
      AM2=(ALF2**2-BET2**2)
      BM1=(ALF1**2+BET1**2)
      BM2=(ALF2**2+BET2**2)
      HM1=N*N*AM1/BM1**2-(2+MU)
      HM1P=N*N*2*ALF1*BET1/BM1**2
      HM2=N*N*AM2/BM2**2-(2+MU)
      HM2P=N*N*2*ALF2*BET2/BM2**2
      HN1=(N*N/BM1+MU)*ALF1
      HN1P=(N*N/BM1-MU)*BET1
      HN2=(N*N/BM2+MU)*ALF2
      HN2P=(N*N/BM2-MU)*BET2
      S1=-AM1+MU*N*N
      S2=-AM2+MU*N*N
      S1P=2.*ALF1*BET1
      S2P=2.*ALF2*BET2
      TEH1=ALF1**3-3.*ALF1*BET1**2-ALF1*N*N*(2-MU)
      TEH2=ALF2**3.-3.*ALF2 *BET2**2.-ALF2*N*N*(2-MU)
      TEH1P=BET1**3-3.*BET1*ALF1**2+BET1*N*N*(2-MU)
      TEH2P=BET2**3.-3.*BET2*ALF2**2.+BET2*N*N*(2-MU)
      CB1=DCOS(BET1*AL)
      CB2=DCOS(BET2*AL)
      SB1=DSIN(BET1*AL)
      SB2=DSIN(BET2*AL)
      HYP1=DEXP(ALF1*AL)
      HYP2=DEXP(ALF2*AL)
C     ' THE COEFFICIENT MATRIX FOR THE CLAMPED FREE SHELL  '
      Z(1)=-HN1P
      Z(2)=HM1P
      Z(3)=1.
```

```
Z(4)=-ALF1
Z(5)=(S1*CB1-S1P*SB1)/HYP1
Z(6)=(-TEH1*CB1+TEH1P*SB1)/HYP1
Z(7)=(SB1)/HYP1
Z(8)=-(BET1*CB1-ALF1*SB1)/HYP1
Z(9)=HN1
Z(10)=-HM1
Z(11)=0.
Z(12)=BET1
Z(13)=(S1P*CB1+S1*SB1)/HYP1
Z(14)=(-TEH1P*CB1-TEH1*SB1)/HYP1
Z(15)=-CB1/HYP1
Z(16)=-(ALF1*CB1+BET1*SB1)/HYP1
Z(17)=-HN2P
Z(18)=HM2P
Z(19)=1.
Z(20)=-ALF2
Z(21)=(S2*CB2-S2P*SB2)/HYP2
Z(22)=(-TEH2*CB2+TEH2P*SB2)/HYP2
Z(23)=SB2/HYP2
Z(24)=-(BET2*CB2-ALF2*SB2)/HYP2
Z(25)=HN2
Z(26)=-HM2
Z(27)=0.
Z(28)=BET2
Z(29)=(S2P*CB2+S2*SB2)/HYP2
Z(30)=(-TEH2P*CB2-TEH2*SB2)/HYP2
Z(31)=-CB2/HYP2
Z(32)=-(ALF2*CB2+BET2*SB2)/HYP2
Z(33)=HN1P/HYP1
Z(34)=HM1P/HYP1
Z(35)=1./HYP1
Z(36)=ALF1/HYP1
Z(37)=(S1*CB1+S1P*SB1)
Z(38)=(TEH1*CB1+TEH1P*SB1)
Z(39)=-SB1
Z(40)=(BET1*CB1+ALF1*SB1)
Z(41)=-HN1/HYP1
Z(42)=-HM1/HYP1
Z(43)=0.
Z(44)=-BET1/HYP1
Z(45)=(S1P*CB1-S1*SB1)
Z(46)=(TEH1P*CB1-TEH1*SB1)
Z(47)=-CB1
Z(48)=(ALF1*CB1-BET1*SB1)
Z(49)=HN2P/HYP2
Z(50)=HM2P/HYP2
Z(51)=1./HYP2
Z(52)=ALF2/HYP2
Z(53)=(S2*CB2+S2P*SB2)
```

```
      Z(54)=(TEH2*CB2+TEH2P*SB2)
      Z(55)=-SB2
      Z(56)=(BET2*CB2+ALF2*SB2)
      Z(57)=-HN2/HYP2
      Z(58)=-HM2/HYP2
      Z(59)=0.
      Z(60)=-BET2/HYP2
      Z(61)=(S2P*CB2-S2*SB2)
      Z(62)=(TEH2P*CB2-TEH2*SB2)
      Z(63)=-CB2
      Z(64)=(ALF2*CB2-BET2*SB2)
      E(1)=0.
      E(2)=-12.*(1-MU*MU)*B(N+1)*2*UK*UK/N**6
      E(3)=-12.*(1-MU*MU)*B(N+1)/N**4
      E(4)=0.
      E(5)=-MU*12*(1-MU*MU)*B(N+1)/N**2
      E(6)=0.0
      E(7)=0.
      E(8)=0.
      DO 544 JI=1,8
       CMD1(JI)=1.
        CMD2(JI)=0.0
  544 Y(JI)=0.
C   ' THE CONSTRAINTS AT THE FREE TIP ARE CONSIDERED BELOW  '
      DO 35 II=1,64
   35 ZZ(II)=0.0
C   '  THE CONDITION  W'(L)=0
      ZZ(5)=-(ALF1*CB1+BET1*SB1)/HYP1
      ZZ(13)=(-ALF1*SB1+BET1*CB1)/HYP1
      ZZ(21)=(-ALF2*CB2-BET2*SB2)/HYP2
      ZZ(29)=(-ALF2*SB2+BET2*CB2)/HYP2
      ZZ(37)=ALF1*CB1-BET1*SB1
      ZZ(45)=ALF1*SB1+BET1*CB1
      ZZ(53)=ALF2*CB2-BET2*SB2
      ZZ(61)=ALF2*SB2+BET2*CB2
C   '  THE CONDITION W(L)=0  '
      ZZ(6)=CB1/HYP1
      ZZ(14)=SB1/HYP1
      ZZ(22)=CB2/HYP2
      ZZ(30)=SB2/HYP2
      ZZ(38)=CB1
      ZZ(46)=-SB1
      ZZ(54)=CB2
       ZZ(62)=-SB2
C   '  THE CONDITION  U(L)=0  '
      ZZ(7)=-(HNP1*CB1+HN1*SB1)/HYP1
      ZZ(15)=(HN1*CB1-HN1P*SB1)/HYP1
      ZZ(23)=-(HN2P*CB2+HN2*SB2)/HYP2
      ZZ(31)=(HN2*CB2-HN2P*SB2)/HYP2
      ZZ(39)=HN1P*CB1-HN1*SB1
```

```
      ZZ(47)=-(HN1*CB1+HN1P*SB1)
      ZZ(55)=HN2P*CB2-HN2*SB2
      ZZ(63)=-(HN2*CB2+HN2P*SB2)
C     '   THE CONDITION    V(L)=0   '
      ZZ(8)=+(HM1P*CB1+HM1*SB1)/HYP1
      ZZ(16)=(-HM1*CB1+HM1P*SB1)/HYP1
      ZZ(24)=(HM2P*CB2+HM2*SB2)/HYP2
      ZZ(32)=(-HM2*CB2+HM2P*SB2)/HYP2
      ZZ(40)=HM1P*CB1-HM1*SB1
      ZZ(48)=-(HM1*CB1+HM1P*SB1)
      ZZ(56)=HM2P*CB2-HM2*SB2
      ZZ(64)=-(HM2*CB2+HM2P*SB2)
      Y(4)=E(5)
       Y(6)=E(3)
      Y(8)=E(2)
C     ' AS THE EDGE X=L IS S.S. THE CORRESPONDING B.C. AT X=L ARE ALTERED '
      CMD1(6),CMD1(8)=0.0
      CMD2(6),CMD2(8)=1.0
      DO 36 KJ=1,8
      DO 36 KI=1,8
      II=  KI+(KJ-1)*8
      E(KI)=CMD1(KI)*E(KI)+CMD2(KI)*Y(KI)
   36 Z(II)=CMD1(KI)*Z(II)+CMD2(KI)*ZZ(II)
      DO 543 IJK=1,8
  543 Y(IJK)=0.0
      NN=8
      NA=64
      NB=8
  279 FORMAT  (/,8E14.6)
      WRITE (2,279) (Z(I),I=1,64)
       WRITE(2,279) (E(I),I=1,8)
      DO 37 I=1,NN
      DO 37 J=1,NN
   37 DE(I,J)=Z(I+NN*(J-1))
      CALL F04AEF (DE,20,E,NB,NN,1,Y,NB,BB,AA,NN,DD,20,IFAIL)
  620 FORMAT (4E20.10)
      WRITE (2,620) (Y(I),I=1,8)
      DO 2 MJ=1,21
      X=(MJ-1)*AL/20.
      C1=DCOS(BET1*X)
      C2=DCOS(BET2*X)
      V1=DSIN(BET1*X)
      V2=DSIN.BET2*X)
      H1=DEXP(ALF1*X)
      H2=DEXP(ALF2*X)
      HA=DEXP(ALF1*(X-AL))
      HB=DEXP(ALF2*(X-AL))
      QS1=HN1*ALF1+HN1P*BET1
      QD1=HN1P*ALF1-HN1*BET1
      QS2=HN2*ALF2+HN2P*BET2
```

```
      QD2=HN2P*ALF2-HN2*BET2
      F=(C1*QD1+V1*QS1)*Y(1)/H1+(-C1*QS1+V1*QD1)*Y(2)/H1+
     C(C2*QD2+V2*QS2)*Y(3)/H2+(-C2*QS2+V2*QD2)*Y(4)/H2 +
     C(C1*QD1+V1*(-QS1))*Y(5)*HA+(-C1*QS1-V1*QD1)*Y(6)*HA    +
     C(C2*QD2-V2*QS2)*Y(7)*HB+(-C2*QS2-V2*QD2)*Y(8)*HB
      F1(MJ)=F/(2.*UK*UK)
      F2(MJ)=(C1*HM1P+V1*HM1)*Y(1)/H1-(C1*HM1-V1*HM1P)*Y(2)/H1+
     C(C2*HM2P+V2*HM2)*Y(3)/H2-(C2*HM2-V2*HM2P)*Y(4)/H2   +
     C(C1*HM1P-V1*HM1)*Y(5)*HA-(C1*HM1+V1*HM1P)*Y(6)*HA   +
     C(C2*HM2P-V2*HM2)*Y(7)*HB-(C2*HM2+V2*HM2P)*Y(8)*HB
      F2(MJ)=F2(MJ)*N*N/(2.*UK*UK)
      F2(MJ)=F2(MJ)-(Y(1)*C1+Y(2)*V1)/H1-(Y(3)*C2+Y(4)*V2)/H2
     C-(Y(5)*C1-Y(6)*V1)*HA-(Y(7)*C2-Y(8)*V2)*HB
      F3(MJ)=-Y(1)*(BET1*CB1-ALF1*SB1)/H1-Y(2)*(ALF1*CB1+BET1*SB1)/H1
     C-Y(3)*(BET2*CB2-ALF2*SB2)/H2-Y(4)*(ALF2*CB2+BET2*SB2)/H2
     C+Y(5)*(BET1*CB1+ALF1*SB1)*HA+Y(6)*(ALF1*CB1-BET1*SB1)*HA
     C+Y(7)*(BET2*CB2+ALF2*SB2)*HB+Y(8)*(ALF2*CB2-BET2*SB2)*HB
      F3(MJ)=2.*(1-MU)*N*F3(MJ)/(2.*UK*UK)
      F3(MJ)=F3(MJ)*1.5/0.7
    2 CONTINUE
      DO 3 M=1,M1
      IF(M-1) 97,97,98
   97 G1(N,M)=F1(1)+F1(21)
      G2(N,M)=F2(1)+F2(21)
      G3(N,M)=F3(1)+F3(21)
      GO TO 96
   98 G1(N,M)=F1(21)*AL**(M-1)
      G2(N,M)=F2(21)*AL**(M-1)
      G3(N,M)=F3(21)*AL**(M-1)
   96 Q=4.
      DO4 MJ=2,20
      X=((MJ-1.)*AL/20.)**(M-1)
      G1(N,M)=G1(N,M)+F1(MJ)*X*Q
      G2(N,M)=G2(N,M)+F2(MJ)*X*Q
      G3(N,M)=G3(N,M)+F3(MJ)*X*Q
      Q=6-Q
    4 CONTINUE
      G1(N,M)=G1(N,M)*AL/60.
      G2(N,M)=G2(N,M)*AL/60.
      G3(N,M)=G3(N,M)*AL/60.
    3 CONTINUE
    1 CONTINUE
C   ' THE BUCKLING ANALYSIS STARTS FROM HERE  '
      DO 5 N=1,20
      DO 5 J=1,20
      IF (N-J) 7,6,7
 6    DE(N,J)=1.
      GO TO 8
 7    DE(N,J)=0.
 8    CONTINUE
```

```
 5     CONTINUE
C    ' THE RANGE OF HARMONICS SELECTED ARE  NL TO  NU  '
C    ' THE BUCKLING PRESSURES ARE CALCULATED FOR DIFFERENT VALUES OF  NL  '
      DO 777 NL=4,6
      NU=NL+4
      MA1=NU-NL+1
       NLL=NL-1
C    ' THE CIRCUMFERENTIAL INTEGRATION FUNCTIONS  '
      DO 9 JR=1,6
       DO 9 N=NLL,NU
      DO 9 J=NLL,NU
      NN=N-NL+2
       JJ=J-NL+2
      IF(N-J) 10,11,10
 11   NT=N+J
      EC(JR,NN,JJ)=DE(NT,JR)*PI/2.
      ES(JR,NN,JJ)=-DE(NT,JR)*PI/2.
      GO TO 12
 10   NJ=IABS(N-J)
      NT=N+J
      ES(JR,NN,JJ)=(-DE(NT,JR)+DE(NJ,JR))*PI/2.
      EC(JR,NN,JJ)=(DE(NT,JR)+DE(NJ,JR))*PI/2.
 12   CONTINUE
 9    CONTINUE
      DO 13 M=1,M1
      DO 13 N=2,MAA
      DO 13 J=2,MAA
      RC(N,J)=B(1)*DE(N,J)
      RC(N,J)=RC(N,J)*PI
      RS(N,J)=B(1)*DE(N,J)
      RS(N,J)=RS(N,J)*PI
      SS(M,N,J)=0.
      SC(M,N,J)=0.
      TS(M,N,J)=0.
      US(M,N,J)=0.
      WS(M,N,J)=0.
      DO 14 JR=1,6
      RS(N,J)=RS(N,J)+B(JR+1)*ES(JR,N,J)
      RC(N,J)=RC(N,J)+B(JR+1)*EC(JR,N,J)
      SC(M,N,J)=SC(M,N,J)+G1(JR,M)*EC(JR,N,J)
      SS(M,N,J)=SS(M,N,J)+G1(JR,M)*ES(JR,N,J)
      TS(M,N,J)=TS(M,N,J)+G2(JR,M)*ES(JR,N,J)
      WS(M,N,J)=WS(M,N,J)+G2(JR,M)*EC(JR,N,J)
      US(M,N,J)=US(M,N,J)+G3(JR,M)*ES(N,JR,J)
 14   CONTINUE
 13   CONTINUE
      LMN=0
      DO 21 KX=1,20
      DO 143 I=1,95
      DO 143 J=1,95
```

```
  143 BC(I,J)=0.0
      IF ( LMN ) 202,202,40
      IF(KX-2) 38,39,40
   38 XXX(1)=0.0
      GO TO 42
   39 XXX(2)=5.0
  202 XXX(KX)=(KX-1)*1.0
      XXX(KX)=(KX-1)*(200./AL)*(100./AH)**2.5
      GO TO 42
   40 XXX(KX)=(XXX(KX-2)*DD(KX-1)                                    -XXX(KX-1)*
     CDD(KX-2))/(DD(KX-1)                                  -DD(KX-2))
   42 XX=XXX(KX)
       PR=XX
      X=PR*AH**3/(30.*10.**6)
C     GENERATION OF THE ELEMENTS OF THE BUCKLING DETERMINANT
      DO 20 III=1,MA
       DO 20 J=NL,NU
      DO 20 MMM=1,MA
      DO 20 N=NL,NU
      I=III
      M=MMM
      K=N-NL+1+(M-1)*MA 1
      L=J-NL+1+(I-1)*MA 1
      LL=L+MA*MA1
      KK=K+MA*MA 1
      LLL=L+2*MA*MA 1
      KKK=K+2*MA*MA 1
      AM=M+I-1
      BM=M+I
      NN=N-NL+2
      JJ=J-NL+2
      DDLK=(2*M*I*AL**(M+I-1)*DE(N,J)*PI)/(AM)+N*J*(1-MU)*AL**(M+I
     C+1)*DE(N,J)*PI/(M+I+1)
      DDLKK=(2.*MU*I*N*AL**(M+I)*DE(N,J)/(BM)-(1-MU)*J*M*AL**(M+I)*
     CDE(N,J)/(BM))*PI
      DDLLK=(2.*MU*M*J+(MU-1)*N*I)*AL**(M+I)*DE(N,J)*PI/(BM)
      DDLLKK    =2.*N*J*AL**(M+I+1)*PI*DE(N,J)/(M+I+1)+2.*(1-MU)*M*I*PI*
     CAL**(M+I-1)*DE(N,J)/(2.*AM)
      ELK=0.
      ELKK=0.
      ELLK=0.
      ME=M+I+1
      ELLKK=2.*MU*SS(ME,NN,JJ)+2.*(1-MU*MU)*AH*AL**(M+I+1)*RS(NN,JJ)/((M+
     C+I+1)*AH**3)+2.*TS(ME,NN,JJ)
     C-(1-MU*NU)*2*PI*DE(N,J)*G4(ME)
      DDLKKK    =-2.*MU*I*AL**(M+I+1)*DE(N,J)*PI/(M+I+1)
      DDLLKKK=-2.*J*AL**(M+I+2)*PI*DE(N,J)/(M+I+2)
      ELKKK= (1-MU*MU)*AH*AL**(M+I+1)*(M-I+1)*RC(NN,JJ)/((M+I+1)*AH
     C**3)
      ME=M+I+1
```

```
      MEE=M+I+2
      ELLKKK    =-2.*MU*N*SS(MEE,NN,JJ)-2.*(1-MU*MU)*AH*N*AL**(M+I+2)*RS(N
     CNN,JJ)/((M+I+2)*AH**3)
     C-2*N*TS(MEE,NN,JJ)+(1-MU)*(M+1)*US(ME,NN,JJ)
     C+2.*(1-MU*MU)*PI*DE(N,J)*G4(MEE)*N
      DDLLLK    =-2*MU*M*DE(N,J)*PI*AL**(M+I+1)/(M+I+1)
      DDLLLKK    =-2*N*PI*DE(N,J)*AL**(M+I+2)/(M+I+2)
      ELLLK    =((1-MU*MU))   *AH*AL**(M+I+1)*RC(NN,JJ)*(-M+I+1)/((M+I+1)*A
     CAH**3)
      ME=M+I+1
      MEE=M+I+2
      ELLLKK=-2.*MU*J*SS(MEE,NN,JJ)-2.*(1-MU*MU)*AH*J*RS(NN
     C,JJ)*AL**(M+I+2)/((M+I+2)*AH**3)
     C-2*J*TS(MEE,NN,JJ)+(1-MU)*(I+I)*US(ME,JJ,NN)
     C+(1-MU*MU)*PI*2*DE(N,J)*G4(MEE)*J
      DDLLLKKK    =2.*PI*DE(N,J)*AL**(M+I+3)/(M+I+3)+(M*I*(M+1)*(I+1)*
     CAL**(M+I-1)/(AM)+(1-N*N)*(1-J*J)*AL**(M+I+3)/(M+I+3)+MU*M*(M+1)
     C*(1-J*J)*AL**(M+I+1)/(M+I+1)+MU*I*(I+1)*(1-N*N)*AL**(M+I+1)/(M+I+1
     C)+2.*(1-MU)*(1+M)*(1+I)*N*J*AL**(M+I+1)/(M+I+1))*PI*DE(N,J)/(6.
     C*AH*AH)
      ME=M+I+1
      MEE=M+I+2
      MEA=M+I+3
      ELLLKKK    =2.*MU*J*N*SS(MEA,NN,JJ)+2.*(1-MU*MU)*AH*RC(NN,JJ)*AL**(M
     CM+I+3)/((M+I+3)*AH**3)+2.*(M+1)*(I+1)*SC(ME,NN,JJ)
     C+2.*N*J*TS(MEA,NN,JJ)+2.*MU*(M+1)*(I+1)*WS(ME,NN,JJ)
     C-(1-MU)*(M+1)*J*US(MEE,NN,JJ)-(1-MU)*(1+I)*N*US(MEE,JJ,NN)
     C-2*(1-MU*MU)*PI*DE(N,J)*G4(MEA)*N*J
C     MODIFICATION TO THE VIRTUAL DISPLACEMENTS
      DDLKK=DDLKK-RO*PI*DE(N,J)*AL**(M+I+1)*(0.6*I*N-0.7*J*(M+1))/(M+I+1)
     1)
      DDLLK=DDLLK-RO*PI*DE(N,J)*AL**(M+I+1)*(.6*J*M-.7*N*(I+1))/(M+I+1)
      DDLKKK=DDLKKK+RO*0.6*PI*DE(N,J)*I*AL**(M+I+2)/(M+I+2)
      DDLLLK=DDLLLK+RO*0.6*PI*DE(N,J)*M*AL**(M+I+2)/(M+I+2)
      DDLLKK=DDLLKK+2.*PI*DE(N,J)*(RO*(-2.*N*J*AL**(M+I+2)/(M+I+2)-0.35*
     1(2*M*I+M+I)*AL**(M+I)/(M+I))+RO*RO*(N*J*AL**(M+I+3)/(M+I+3)+0.35*(
     2M+1)*(I+1)*AL**(M+I+1)/(M+I+1)))
      DDLLKKK=DDLLKKK+2.*RO*2*PI*DE(N,J)*J*AL**(M+I+3)/(M+I+3)-RO*RO*2.
     1*PI*DE(N,J)*J*AL**(M+I+4)/(M+I+4)
      DDLLLKK=DDLLLKK+2.*RO*PI*DE(N,J)*N*AL**(M+I+3)*(2.-RO*AL*(M+I+3)/(
     1M+I+4))/(M+I+3)
      DDLLLKKK=DDLLLKKK-4.*RO*PI*DE(N,J)*(AL**(M+I+4)/(M+I+4)+(1./(12.*A
     1H*AH))*((M+1)*(I+1)*(M*I+M+I)*AL**(M+I)/(M+I)+(1-N*N)*(1-J*J)*AL
     2**(M+I+4)/(M+I+4)+0.3*(1+M)**2*(1-J*J)*AL**(M+I+2)/(M+I+2)+0.7*N*J
     3*(2*M*I+3*(M+I)+4)*AL**(M+I+2)/(M+I+2)))+RO*RO*2.*PI*DE(N,J)*(AL
     4**(M+I+5)/(M+I+5)+((M+1)*(M+2)*(I+1)*(I+2)*AL**(M+I+1)/(M+I+1)+
     5(1-N*N)*(1-J*J)*AL**(M+I+5)/(M+I+5)+0.3*(M+1)*(M+2)*(1-J*J)*AL**(M
     6+I+3)/(M+I+5)+1.4*N*J*(M+2)*(I+2)*AL**(M+I+3)/(M+I+3))/(12*AH*AH))
      DDLLLKKK=DDLLLKKK+(2.*RO*PI*DE(N,J)*0.3*(1-N*N)*(-2.*(1+I)**2/(
     1M+I+2)+RO*(I+1)*(I+2)*AL/(M+I+3))*AL**(M+I+2) )/(12.*AH*AH)
```

```
      ELKKK=ELKKK-RO*0.91*RC(NN,JJ)*(M+2-I)*AL**(M+I+2)/((M+I+2)*AH*AH)
      ELLLK=ELLLK-RO*0.91*RC(NN,JJ)*(I+2-M)*AL**(M+I+2)/((M+I+2)*AH*AH)
      ELLKK=ELLKK-2.*RO*(0.6*SS(M+I+2,NN,JJ)+2.*TS(M+I+2,NN,JJ)+1.82*RS
     1(NN,JJ)*AL**(M+I+2)/((M+I+2)*AH*AH)-0.91*2*PI*DE(N,J)*G4(M+I+2))+
     2RO*RO*(0.6*SS(M+I+3,NN,JJ)+2.*TS(M+I+3,NN,JJ)+1.82*RS(NN,JJ)*AL**(
     3M+I+3)/((M+I+3)*AH*AH)-1.82*PI*DE(N,J)*G4(M+I+3))
      ELLKKK=ELLKKK-2.*RO*(-0.6*N*SS(M+I+3,NN,JJ)-2.*N*TS(M+I+3,NN,JJ)+
     11.82*N*PI*DE(N,J)*G4(M+I+3)-1.82*N*RS(NN,JJ)*AL**(M+I+3)/((M+I+3)
     2*AH*AH)+0.35*(2*M+3)*US(M+I+2,NN,JJ))+RO*RO*(-0.6*N*SS(M+I+4,NN,J
     3J)-2.*N*TS(M+I+4,NN,JJ)+1.82*PI*DE(N,J)*G4(M+I+4)*N-1.82*N*RS(NN,
     4JJ)*AL**(M+I+4)/((M+I+4)*AH*AH)+0.7*(2+M)*US(M+I+3,NN,JJ)     )
      ELLLKK=ELLLKK-2.*RO*(-0.6*J*SS(M+I+3,NN,JJ)-2.*J*TS(M+I+3,NN,JJ)+
     11.82*J*PI*DE(N,J)*G4(M+I+3)-1.82*J*RS(NN,JJ)*AL**(M+I+3)/((M+I+3
     2)*AH*AH)+0.35*(2.*I+3)*US(M+I+2,JJ,NN))+RO*RO*(-0.6*J*SS(M+I+4,NN
     3,JJ)-2*J*TS(M+I+4,NN,JJ)+1.82*PI*J*DE(N,J)*G4(M+I+4)-1.82*J*RS(
     4NN,JJ)*AL**(M+I+4)/((M+I+4)*AH*AH)+0.7*(2+I)*US(M+I+3,JJ,NN) )
      ELLLKKK=ELLLKKK-2.*RO*(0.6*N*J*SS(M+I+4,NN,JJ)+1.82*RC(NN,JJ)*AL**
     1(M+I+4)/((M+I+4)*AH*AH)+(2*M*I+3*M+3*I+4)*(SC(M+I+2,NN,JJ)+0.3*WS
     2(M+I+2,NN,JJ))+2*N*J*TS(M+I+4,NN,JJ)-.35*J*(2*M+3)*US(M+I+3,NN,JJ)
     3-1.82*N*J*PI*DE(N,J)*G4(M+I+4))+RO*RO*(2.*N*J*(SS(M+I+5,NN,JJ)*0.3+
     4+TS(M+I+5,NN,JJ))+1.82*RC(NN,JJ)*AL**(M+I+5)/((M+I+5)*AH*AH)+2.*(
     4M+2)*(I-2)*(SC(M+I+3,NN,JJ)+0.3*WS(M+I+3,NN,JJ))-0.7*J*(M+2)*US(
     5M+I+4,NN,JJ)-1.82*N*J*PI*DE(N,J)*G4(M+I+5))
      ELLLKKK=ELLLKKK+0.7*RO*N*((2.*I+3)*US(M+I+3,JJ,NN)-RO*(I+2)*US(M+I+
     1+4,JJ,NN))
      BC(L,K)=DDLK+X*ELK
      BC(L,KK)=DDLKK+X*ELKK
      BC(L,KKK)=DDLKKK+X*ELKKK
      BC(LL,K)=DDLLK+X*ELLK
      BC(LL,KK)=DDLLKK+X*ELLKK
       BC(LL,KKK)=DDLLKKK+X*ELLKKK
      BC(LLL,K)=DDLLLK+X*ELLLK
      BC(LLL,KK)=DDLLLKK+X*ELLLKK
      BC(LLL,KKK)=DDLLLKKK+X*ELLLKKK
20    CONTINUE
      MAS=3*MA*MA1
      DO 27 I=1,MAS
        DO 27 J=1,MAS
27    BC(I,J)=BC(I,J)/(2.**((AL-2)*3.))
      IFAIL=1
      CALL F03AAF (BC,95,MAS,D,ZZ,IFAIL)
      WRITE (2,100) IFAIL
100   FORMAT (10X,I3)
      WRITE (2,22) AL,AH,PR,D
22    FORMAT (4E20.10)
      DD(KX)=0
      IF (LMN.GT.0) GO TO 45
      IF (D) 201,776,21
201   LMN=1
      IF (KX-2) 21,21,45
```

```
   45 QRS=ABS((XXX(KX)-XXX(KX-1))/XXX(KX))
      IF (  QRS .LE.0.01  ) GO TO  776
 21   CONTINUE
  776 WRITE (2,25) (NL,AL,AH,PR)
   25 FORMAT ( //,3X,30HTHE LOWEST HORMONIC SELECTED =,I2,/,3X,23HLENGTH
     C TORADIUS RATIO =,F4.1,/,3X,24H RADIUS TO THICK RATIO =,F5.1,/,3X,
     C  19H BUCKLING PRESSURE=,F10.5 )
  777 CONTINUE
  555 CONTINUE
      STOP
      END
      FINISH
****
****
```

Computer program based on F.E. Analysis.

```
      MASTER RINGELH
C   'LENIAR SHELL ANALYSIS BY A HIGHER ORDER RING ELEMENT'
      DIMENSION WLC(7),C(14),SQ(14),B(14,14),BT(14,14),D(14,14),SK(14,14
     1),Z(14,14),Q( 77),BK(100,100),DI(77),G(5,7),WKSP(100)
     2,AS(11),CS(11),SS(11),F1(5,6,7),F2(5,6,7),F3(5,6,7),AH1(10),AH2(5)
     3,SG(8,8),CSS(6,5 ,5 ),CCC(6,5 ,5 ),XXX(20),DD(20) ,CS1(5,6,5)
     4,G1(10,7),SG1(8,8) ,RK1(7,7),RK2(4,4) ,ETR(7) ,GRK(4,4)
      COMMON/BLOCK/RB,RD,RE,RA,RIX,RIZ,RJ
C   'GEOMETRY OF THESHELL'
      PI=3.141592653
      AL=3.0
      AL=2.0
      AL=1.0
      DO 3 I=1,5
      II=I+5
    3 AH1(I),AH1(II),AH2(I)=500.0
      AL=0.333
      AH1(1),AH1(2),AH2(1)=1115
      AH1(3),AH1(4),AH2(2)=1312
      AH1(5),AH1(6),AH2(3)=1990
      AH1(7),AH1(8),AH2(4)=3058
      AH1(9),AH1(10),AH2(5)=3740
      AL=5.0
      AH1(1),AH1(2),AH2(1)=100.0
      AH1(3),AH1(4),AH2(2)=200.0
      AH1(5),AH1(6),AH2(3)=300.0
      AH1(7),AH1(8),AH2(4)=400.0
      AH1(9),AH1(10),AH2(5)=500.0
C  ' GEOMETRIC PARAMETERS OF THE RING '
      AH=AH1(1)
      RB=20./AH
      RD=100./AH
      RB=5.0/AH
      RD=15.0/AH
      RE=RD/2.
      RA=RB*RD
      RIX=RB*RD**3/12.
      RIZ=RD*RB**3/12.
      RJ=4.*RIZ
  100 FORMAT (/,6E20.10)
  101 FORMAT (/,7E17.8)
  102 FORMAT (/,10E12.4)
  103 FORMAT (1X,4E20.10)
  104 FORMAT (10E12.4)
C   ' THE ASSUMED WIND LOAD COEFFICIENTS  '
      WLC(1)=0.22
      WLC(2)=0.336
      WLC(3)=0.533
      WLC(4)=0.471
      WLC(5)=0.166
```

```
      WLC(6)=-0.066
      WLC(7)=-0.055
      DO 1 I=1,14
      C(I)=0.0
      SQ(I)=0.0
      DO 1 J=1,14
      B(I,J)=0.0
      BT(I,J)=0.0
      D(I,J)=0.0
      SK(I,J)=0.0
    1 Z(I,J)=0.0
      NE=10
      NEB=5
      ELL=AL/NE
      ELLR=1.0/ELL
C 'ANALYSIS FOR AXISYMMETRIC  CASE'  N=0
C  'GENERATE THE DISPLACEMENT TRASFORMATION MATRIX'
      CALL DISTRAN (B,BT,ELLR)
      DO 231 I=1,14
      DO 231 J=1,3
  231 B(I,J+9)=B(I,J+11)
      DO 232 I=1,14
      DO 232 J=1,8
  232 B(I,J+2)=B(I,J+4)
      DO 233 I=1,6
      DO 233 J=1,10
  233 B(I+4,J)=B(I+8,J)
      DO 234 I=1,10
      DO 234 J=1,10
  234 BT(I,J)=B(J,I)
C  ' THE ELEMENT LOAD VECTOR   '
      DO 22  I=1,6
   22 C(8+I)=ELL**I/I
      DO 1032 I=1,10
 1032 C(I)=C(I+4)
      CALL MATMULT (14,14,1,14,1,14,10,10,1,BT,C,SQ)
      DO 33 MI=1,NE
      ALP=1./(12.*AH1(MI)**2)
      CALL ELSTIF (N,ALP,ELL,D)
      CALL MATMULT (14,14,14,14,14,14,10,10,10,BT,D,Z)
      CALL MATMULT (14,14,14,14,14,14,10,10,10,Z,B,SK)
C 'ASSENBLE THE ELEMENT STIFFNESS AND LOAD MATRICES
      DO 33 I=1,10
      II=(MI-1)*5+I
      Q(II)=Q(II)+SQ(I)
      DO 33 J=1,10
      JJ=(MI-1)*5+J
C    ' DUE TO VARIATION OF THICKNRSS   '
      SK(I,J)=SK(I,J)*AH1(1)/AH1(MI)
   33 BK(II,JJ)=BK(II,JJ)+SK(I,J)
```

```
      NI=5*NE+5
C   ' THE SHELL IS CLAMPDE ATTHE BASE AND RING STIIFFENED AT THE TOP   '
      DO 34 I=1,NI
      BK(1,I),BK(I,1),BK(3,I),BK(I,3),BK(4,I),BK(I,4)=0.0
   34 CONTINUE
      Q(1),Q(3),Q(4)=0.0
      BK(1,1),BK(3,3),BK(4,4)=1.0
C 'WITH A RING AT THE TOP OF THE SHELL '
      CALL RISTIF (RK1,RK2,N,AH)
      BK(53,53)=BK(53,53)+RK2(3,3)
      BK(54,54)=BK(54,54)+RK2(4,4)
      CALL F04AAF (BK,100,Q, 77,NI,1,DI, 77,WKSP,IFAIL).
      WRITE (2,100) (DI(I),I=1,NI)
      DO 36 I=1,NI
   36 DI(I)=WLC(1)*DI(I)
      ETR(1)=-DI(53)
      DO 128 K=1,NEB
      DO 128 M=1,7
      IF (M-1) 129,129,130
  129 G(K,M)=(ELL/3.)*(DI(K*10-7)+4.*DI(K*10-2)+DI(K*10+3))
      GO TO 128
  130 G(K,M)=(ELL/3.)*(4.*DI(K*10-2)*ELL**(M-1)+DI(K*10+3)*(2.*ELL)
     1**(M-1))
  128 CONTINUE
      WRITE (2,101) ((G(K,M),K=1,5),M=1,7)
C 'THE ABOVE FUNCTION IS FOR N=0 '
C 'ANALYSIS  FOR ANY  HORMONIC LOADING'
       CALL DISTRAN (B,BT,ELLR)
C   ' THE ELEMENT LOAD VECTOR    '
      DO 14 I=1,14
   14 C(I)=0.0
      DO 15 I=1,6
   15 C(I+8)=ELL**I/I
      CALL MATMULT (14,14,14,1,14,1,14,14,1,BT,C,SQ)
      DO 13 N=1,6
      DO 2 I=1,77
      Q(I)=0.0
      DO 2 J=1,77
    2 BK(I,J)=0.0
C 'GENERATION OF ELEMENT STIFFNESS MATRIX'  (IN ELEMENT COORDINATES )
      DO 23 MI=1,NE
      ALP=1./(12.*AH1(MI)**2)
      CALL ELSTIF (N,ALP,ELL,D)
      CALL MATMULT (14,14,14,14,14,14,14,14,14,BT,D,Z)
      CALL MATMULT (14,14,14,14,14,14,14,14,14,Z,B,SK)
      DO 23  I=1,14
      II=(MI-1)*7+I
      Q(II)=Q(II)+SQ(I)
      DO 23  J=1,14
      JJ=(MI-1)*7+J
```

```
C    ' DUE TO VARIATION OF THICKNRSS    '
      SK(I,J)=SK(I,J)*AH1(1)/AH1(MI)
   23 BK(II,JJ)=BK(II,JJ)+SK(I,J)
      NI=7*(NE+1)
      DO 24 I=1,NI
      BK(1,I),BK(I,1),BK(3,I),BK(I,3),BK(5,I),BK(I,5),BK(6,I),BK(I,6)=0.
   24 CONTINUE
      Q(1),Q(3),Q(5),Q(6)=0.0
      BK(1,1),BK(3,3),BK(5,5),BK(6,6)=1.0
C 'THE RING IS LOCATED AT TOP OF THE SHELL '
      CALL RISTIF (RK1,RK2,N,AH)
      DO 4 I=1,7
      DO 4 J=1,7
    4 BK(70+I,70+J)=BK(70+I,70+J)+RK1(I,J)
      CALL F04AAF (BK,100,Q, 77,NI,1,DI, 77,WKSP,IFAIL)
      WRITE (2,140) N
  140 FORMAT (/,3X,'THE DISPLACEMENT VECTOR FOR THE HARMONIC =',I2,/)
      WRITE (2,100) (DI(I),I=1,NI)
      DO 37 I=1,NI
   37 DI(I)=WLC(N+1)*DI(I)
C ' COMPUTE PRE-BUCKLE STRAINS OF THE RING '
      ETR(N+1)=N*DI(73)-DI(75)
C 'TO COMPUTE THE PREBUCKLE STRAINS' AND DISPLACEMENTS
      NEE=NE+1
      DO 26 I=1,NEE
      II=7*(I-1)
      AS(I)=DI(2+II)+0.3*(DI(3+II)*N-DI(5+II))
      CS(I)=N*DI(3+II)-DI(5+II)+0.3*DI(2+II)
   26 SS(I)=-N*DI(1+II)+DI(4+II)
      WRITE (2,141)
  141 FORMAT (/,3X,'THE AXIAL STRESS DISTRIBUTION ',/)
      WRITE (2,100) (AS(I),I=1,11)
      WRITE (2,142)
  142 FORMAT (/,3X,'THE CIRCUMFERENTIAL STRESS DISTRIBUTION ',/)
      WRITE (2,100) (CS(I),I=1,11)
      WRITE (2,143)
  143 FORMAT (/,3X,'THE SHEAR STRESS DISTRIBUTION ',/)
      WRITE (2,100) (SS(I),I=1,11)
C 'CALCULATION OF FUNCTIONS INVOLVING THE PREBUCKE STRAINS'
      DO 137 K=1,NEB
      DO 137 M=1,7
      IF (M-1) 138,138,139
  138 F1(K,N,M)=(ELL/3.)*(AS(2*K-1)+4.*AS(2*K)+AS(2*K+1))
      F2(K,N,M)=(ELL/3.)*(CS(2*K-1)+4.*CS(2*K)+CS(2*K+1))
      F3(K,N,M)=(ELL/3.)*(SS(2*K-1)+4.*SS(2*K)+SS(2*K+1))
      GO TO 137
  139 F1(K,N,M)=(ELL/3.)*(4.*AS(2*K)*ELL**(M-1)+AS(2*K+1)*
     1(ELL*2.)**(M-1))
      F2(K,N,M)=(ELL/3)*(4*CS(2*K)*(ELL  )**(M-1)+CS(2*K+1)*
     1(ELL*2.)**(M-1))
```

```
      F3(K,N,M)=(ELL/3.)*(4.*SS(2*K)*ELL**(M-1)+SS(2*K+1)*
     1(ELL*2.)**(M-1))
  137 CONTINUE
C 'THE ABOVE FUNCTIONS ARE FOR DIFFERENT HORMONICS AND ELEMENTS'
   13 CONTINUE
C  'END OF PRE-BUCKLING ANALYSIS  '
C  ' STABILITY ANALYSIS STARTS FROM HERE  '
      NEB=5
      ELL=AL/NEB
      BEL=AL/NEB
      BELR=1./BEL
      CALL BUDITR (B,BT,BELR)
      DO 47 K=1,NEB
      DO 47 M=1,7
      G(K,M)=G(K,M)*0.91*AH1(1)/AH2(K)
      DO 47 N=1,6
      F1(K,N,M)=F1(K,N,M)    *0.91*AH1(1)/AH2(K)
      F2(K,N,M)=F2(K,N,M)    *0.91*AH1(1)/AH2(K)
   47 F3(K,N,M)=F3(K,N,M)    *0.91*AH1(1)/AH2(K)
        DO 777 NL=11,12
      NU=NL+4
C 'CIRCUMFERENTIAL INTEGRATION'
      DO 48 N=1,6
      DO 48 I=NL,NU
      I1=I-NL+1
      DO 48 J=NL,NU
      J1=J-NL+1
      CSS(N,I1,J1),CCC(N,I1,J1)=0.0
      IPJ=I+J
      IF (N-IPJ) 49,50,49
   50 CSS(N,I1,J1)=-PI/2
      CCC(N,I1,J1)=PI/2
   49 IF (I-J) 51,48,51
   51 IMJ=IABS(I-J)
      IF (N-IMJ) 48,52,48
   52 CSS(N,I1,J1),CCC(N,I1,J1)=PI/2
   48 CONTINUE
      DO 53 I=NL,NU
      I1=I-NL+1
      DO 53 N=1,6
      DO 53 J=NL,NU
      J1=J-NL+1
      CS1(I1,N,J1)=0.0
      NPJ=N+J
      IF (I-NPJ) 54,55,54
   55 CS1(I1,N,J1)=-PI/2
   54 IF (N-J) 56,53,56
   56 NMJ=IABS(N-J)
      IF (I-NMJ) 53,57,53
   57 CS1(I1,N,J1)=PI/2
```

```
   53 CONTINUE
      IBK=4*(  NEB)*(NU-NL+1)
C 'CALCULATION OF CRITICAL LOAD  BY DETERMINENT SEARCH METHOD '
       LMN=0
      DO 75 KX=1,20
      DO 74 I=1,100
      DO 74 J=1,100
   74 BK(I,J)=0.0
      IF (LMN) 204,204,70
  204 XXX(KX)=(KX-1)*((200./AL)*(100/AH)**2.5)
      XXX(KX)=(KX-1)*(200./AL)*(100./AH1(10))**2.5
       XXX(KX)=XXX(KX)*4.0
      GO TO 73
   70 IF (KX-2) 71,71,72
   71 XXX(2)=5.0
      GO TO 73
   72 XXX(KX)=(XXX(KX-2)*DD(KX-1)-XXX(KX-1)*DD(KX-2))/(DD(KX-1)-DD(KX
     1-2))
   73 PR=XXX(KX)
      X=PR*AH1(1)/(30.*10.**6)
C 'CALCULATION OF THE ELEMENTS OF GEOMETRIC STIFFNESS '
C 'THE FOLLOWING ARE THE ELEMENTS OF`SG'MATRIX
      DO 60 I=NL,NU
      I1=I-NL+1
      DO 60 J=NL,NU
      J1=J-NL+1
      DO 60 K=1,NEB
      CALL GEOSTIF (I ,J ,K,SG,WLC,ELL,G,F1,F2,F3,CCC,CSS,CS1,I1,J1)
      CALL MATMULT (14,14,8,8,14,14,8,8,8,BT,SG,Z)
      CALL MATMULT (14,14,14,14,8,8,8,8,8,Z,B,SG)
      IF (K-1) 66,66,67
   66 DO 68 II=1,4
      DO 68 JJ=1,4
      III=II+20*(I-NL)
      JJJ=JJ+20*(J-NL)
   68 BK(III,JJJ)=BK(III,JJJ)+X*SG(II+4,JJ+4)
      GO TO 601
   67 DO 65 II=1,8
      DO 65 JJ=1,8
      III=II+20*(I-NL)+(K-2)*4
      JJJ=JJ+20*(J-NL)+(K-2)*4
   65 BK(III.JJJ)=BK(III,JJJ)+X*SG(II,JJ)
C 'ADD THE GEOMETRIC STIFFNESS CONTRIBUTION DUE TO RING '
  601 CONTINUE
      IF (NEB -K ) 60,61,60
   61 CALL RIGEM (  I,J,ETR,CSS,AH,GRK,I1,J1)
      DO 62 II=1,4
      DO 62 JJ=1,4
      III=(I-NL)*20+16+II
      JJJ=(J-NL)*20+16+JJ
```

```
   62 BK(III,JJJ)=BK(III,JJJ)+X*GRK(II,JJ)
   60 CONTINUE
C 'GENERATION OF ELASTIC STIFFNESS MATRIC FOR BUCKLING '
C 'THE ELEMENT STIFFNESS MATRIC IS OF  8X8 '
C 'THIS IS TO BE ASSEMBLED FOR  ALL ELEMENTS AND  HARMANICS'
      DO 150 N=NL,NU
      DO 150 K=1,NEB
      ALP=1./(12.*AH2(K)**2)
      CALL BUCELSTIF (N,SK,B,D,BT,Z,ALP,BEL)
      IF (K-1) 151,151,152
  151 DO 153 I=1,4
      DO 153 J=1,4
      II=I+(N-NL)*20
      JJ=J+(N-NL)*20
  153 BK(II,JJ)=BK(II,JJ)+PI*SK(I+4,J+4)*AH1(1)/AH2(K)
      GO TO 1501
  152 DO 154 I=1,8
      DO 154 J=1,8
      II=I+20*(N-NL)+(K-2)*4
      JJ=J+20*(N-NL)+(K-2)*4
  154 BK(II,JJ)=BK(II,JJ)+PI*SK(I,J)*AH1(1)/AH2(K)
C 'ADD ELASTIC STIFFNESS OF RING  TO THE BUCKLING DETERMINANT '
 1501 CONTINUE
      IF (NEB-K) 150,1154,150
 1154 CALL RISTIF (RK1,RK2,N,AH)
      DO 155 I=1,4
      DO 155 J=1,4
      II = I+(N-NL)*20+16
      JJ = J+(N-NL)*20+16
  155 BK(II,JJ)=BK(II,JJ)+PI*RK2(I,J)
  150 CONTINUE
      CALL F03AAF (BK,100,IBK,DET,WKSP,IFAIL)
      WRITE (2,202) (AL,AH,PR,DET)
  202 FORMAT (4E20.10)
      DD(KX)=D ET
      IF (LMN.GT.0) GO TO 76
      IF ( DET ) 1205,77,75
 1205 LMN=1
      IF (KX-2) 75,75,76
   76 QRS=ABS ((XXX(KX)-XXX(KX-1))/XXX(KX))
       IF  ( QRS .LE. 0.01) GO TO 77
   75 CONTINUE
   77 WRITE (2,203) (NL,AL,AH,PR)
  203 FORMAT (//,3X,'THELOWEST  HARMONIC SELE CTED =',I2,/,3X,'LENGTH TO
     1 RADIOS RATIO = ',F4.1,/,3X,'RADIOS TO THICKNESS RATIO =',F6.2,/,
     23X, 'BUCKLING PRESSURE = ',F10.5,/)
  777 CONTINUE
  555 CONTINUE
      STOP
      END
```

```
      SUBROUTINE GEMSTIF (I,J,K,SG,WLC,ELL,G,F1,F2,F3,CCC,CSS,CS1,I1,J1)
      DIMENSION SG(8,8),WLC(7),G(5,7),F1(5,6,7),F2(5,6,7),F3(5,6,7)
     1,CCC(6, 5, 5),CSS(6, 5, 5) ,CS1(5,6,5)
      PI=3.141592653
      DO 63 II=1,8
      DO 63 JJ=1,8
   63 SG(II,JJ)=0.0
      IF (I-J) 21,20,21
   20 SG(1,6)=0.91*WLC(1)*ELL
      SG(2,5)=-SG(1,6)
      SG(1,7)=SG(1,6)*ELL
      SG(1,8)=SG(1,7)*ELL
      SG(2,7)=SG(1,8)/3.
      SG(2,8)=SG(1,8)*ELL/2.
      SG(3,3)=SG(1,6)-0.91*G(K,1)
      SG(3,4),SG(4,3)=SG(1,7)/2.-0.91*G(K,2)
      SG(3,5),SG(5,3)=-I* SG(3,3)
      SG(3,6),SG(6,3),SG(4,5),SG(5,4)=-I*SG(3,4)
      SG(4,4)=-0.91*G(K,3)+SG(2,7)
      SG(3,7),SG(7,3),SG(4,6),SG(6,4)=-I*SG(4,4)
      SG(3,8),SG(4,7),SG(7,4)=-I*(2.*SG(2,8)-0.91*G(K,4))
      SG(8,3)=SG(3,8)
      SG(4,8)=-I*0.91*(WLC(1)*ELL**5/5.-G(K,5))
      SG(8,4)=SG(4,8)
      SG(5,5)=0.91*(-I*J*G(K,1)+WLC(1)*ELL)
      SG(5,6),SG(6,5)=0.91*(-I*J*G(K,2)+WLC(1)*ELL**2/2.)
      SG(5,7),SG(7,5),SG(6,6)=0.91*(-I*J*G(K,3)+WLC(1)*ELL**3/3.)
      SG(5,8),SG(8,5),SG(6,7),SG(7,6)=0.91*(-I*J*G(K,4)+WLC(1)*ELL**4/4.
     1)
      SG(6,8),SG(8,6),SG(7,7)=0.91*(-I*J*G(K,5)+WLC(1)*ELL**5/5.)
      SG(7,8),SG(8,7)=0.91*(-I*J*G(K,6)+WLC(1)*ELL**6/6.)
      SG(8,8)=0.91*(-I*J*G(K,7)+WLC(1)*ELL**7/7.)
      DO 323 II=1,8
      DO 323 JJ=1,8
  323 SG(II,JJ)=SG(II,JJ)*PI
   21 DO 324 N=1,6
      SG(1,6)=SG(1,6)+0.91*CCC(N,I1,J1)*WLC(N+1)*ELL
      SG(1,7)=SG(1,7)+0.91*CCC(N,I1,J1)*WLC(N+1)*ELL**2
      SG(1,8)=SG(1,8)+0.91*CCC(N,I1,J1)*WLC(N+1)*ELL**3
      SG(2,5)=SG(1,6)
      SG(2,5)=SG(2,5)*(-1)
      SG(2,6)=0.
      SG(2,7)=SG(1,8)/3.
      SG(2,8)=SG(2,8)+0.91*CCC(N,I1,J1)*WLC(N+1)*ELL**4/2.
      SG(3,3)=SG(3,3)+CSS(N,I1,J1)*(0.91*WLC(N+1)*ELL+F2(K,N,1))
      SG(3,4),SG(4,3)=SG(3,4)+CSS(N,I1,J1)*(0.91*WLC(N+1)*ELL**2/2
     1+F2(K,N,2))
      SG(3,5)=-J*SG(3,3)
      SG(5,3)=-I*SG(3,3)
      SG(3,6),SG(4,5)=-J*SG(3,4)
```

```
      SG(6,3)=-I*SG(3,4)+0.7*CS1(I1,N,J1)*F3(K,N,1)
      SG(4,4)=SG(4,4)+CSS(N,I1,J1)*(0.91*WLC(N+1)*ELL**3/3+F2(K,N,3))
      SG(3,7),SG(4,6)=-J*SG(4,4)
      SG(7,3)=-I*SG(4,4)+1.4*CS1(I1,N,J1)*F3(K,N,2)
      SG(6,4)=-I*SG(4,4)+0.7*CS1(I1,N,J1)*F3(K,N,2)
      SG(5,4)=-I*SG(3,4)
      SG(3,8),SG(4,7)=SG(3,8)-J*CSS(N,I1,J1)*(0.91*WLC(N+1)*ELL**4/4.
     1+F2(K,N,4))
      SG(8,3)=SG(8,3)+(0.91*WLC(N+1)*ELL**4/4.+F2(K,N,4))*(-I)*CSS(N,I1,
     1J1)+2.1*CS1(I1,N,J1)*F3(K,N,3)
      SG(7,4)=SG(7,4)-I*CSS(N,I1,J1)*(0.91*WLC(N+1)*ELL**4/4.+F2(K,N,4))
     2+1.4*CS1(I1,N,J1)*F3(K,N,3)
      SG(4,8)=SG(4,8)-J*(0.91*WLC(N+1)*ELL**5/5.+F2(K,N,5))*CSS(N,I1,J1)
      SG(8,4)=SG(8,4)-I*CSS(N,I1,J1)*(0.91*WLC(N+1)*ELL**5/5.+F2(K,N,5))
     1+2.1*CS1(I1,N,J1)*F3(K,N,4)
      SG(5,5)=SG(5,5)+0.91*CCC(N,I1,J1)*WLC(N+1)*ELL+I*J*CSS(N,I1,J1)*
     1F2(K,N,1)
      SG(5,6)=SG(5,6)+0.91*CCC(N,I1,J1)*WLC(N+1)*ELL**2/2.+I*J
     1*CSS(N,I1,J1)*F2(K,N,2)
      SG(5,7)=SG(5,7)+0.91*CCC(N,I1,J1)*WLC(N+1)*ELL**3/3.+I*J
     1*CSS(N,I1,J1)*F2(K,N,3)
      SG(5,8)=SG(5,8)+0.91*CCC(N,I1,J1)*WLC(N+1)*ELL**4/4.+I*J
     1*CSS(N,I1,J1)*F2(K,N,4)
      SG(6,5)=SG(5,6)+0.7*(-J)*CS1(I1,N,J1)*F3(K,N,1)
      SG(7,5)=SG(5,7)-1.4*J*CS1(I1,N,J1)*F3(K,N,2)
      SG(8,5)=SG(5,8)-2.1*J*CS1(I1,N,J1)*F3(K,N,3)
      SG(6,6)=SG(5,7)+CCC(N,I1,J1)*F1(K,N,1)-0.7*J*CS1(I1,N,J1)*F3(K,N,2
     1)
      SG(6,7)=SG(5,8)+CCC(N,I1,J1)*F1(K,N,2)*2.-0.7*J*CS1(I1,N,J1)*F3(K,
     1N,3)
      SG(7,6)=SG(5,8)+2.*CCC(N,I1,J1)*F1(K,N,2)-1.4*J*CS1(I1,N,J1)*F3(K,
     1N,3)
      SG(6,8)=SG(6,8)+(0.91*WLC(N+1)*ELL**5/5.+3.*F1(K,N,3))*CCC(N,I1,J1
     1)+I*J*CSS(N,I1,J1)*F2(K,N,5)-0.7*J*CS1(I1,N,J1)*F3(K,N,4)
      SG(8,6)=SG(8,6)+(0.91*WLC(N+1)*ELL**5/5.+3.*F1(K,N,3))*CCC(N,I1,J1
     1)+I*J*CSS(N,I1,J1)*F2(K,N,5)-2.1*J*CS1(I1,N,J1)*F3(K,N,4)
      SG(7,7)=SG(7,7)+(0.91*WLC(N+1)*ELL**5/5.+4.*F1(K,N,3))*CCC(N,I1,J1
     1)+I*J*CSS(N,I1,J1)*F2(K,N,5)-1.4*J*CS1(I1,N,J1)*F3(K,N,4)
      SG(7,8)=SG(7,8)+(0.91*WLC(N+1)*ELL**6/6.+6.*F1(K,N,4))*CCC(N,I1,J1
     1)+I*J*CSS(N,I1,J1)*F2(K,N,6)-1.4*J*CS1(I1,N,J1)*F3(K,N,5)
      SG(8,7)=SG(8,7)+(0.91*WLC(N+1)*ELL**6/6.+6.*F1(K,N,4))*CCC(N,I1,J1
     1)+I*J*CSS(N,I1,J1)*F2(K,N,6)-2.1*J*CS1(I1,N,J1)*F3(K,N,5)
  324 SG(8,8)=SG(8,8)+(0.91*WLC(N+1)*ELL**7/7.+9.*F1(K,N,5))*CCC(N,I1,J1
     1)+I*J*CSS(N,I1,J1)*F2(K,N,7)-2.1*J*CS1(I1,N,J1)*F3(K,N,6)
      RETURN
      END
```

```
      SUBROUTINE DISTRAN (B,BT,ELLR)
      DIMENSION B(14,14),BT(14,14)
      DO 1 I=1,14
      DO 1J=1,14
      BT(I,J)=0.
    1  B(I,J)=0.0
      B(1,1),B(2,2),B(5,3),B(6,4),B(9,5),B(10,6)=1.0
      B(3,9),B(7,11)=-ELLR
      B(11,7)=0.5
      B(12,14)=0.5*ELLR
      B(12,7)=-1.5*ELLR
      B(3,2),B(7,4)=-2.*ELLR
      B(4,2),B(4,9),B(13,14)=ELLR**2
      B(13,14)=-B(13,14)
      B(12,6)=-6.*ELLR**2
      B(12,13)=-4.*ELLR**2
      B(13,7)=1.5*ELLR**2
      B(8,4),B(8,11)=ELLR**2
      B(3,1),B(7,3)=-3.*ELLR**2
      B(3,8),B(7,10)=3.*ELLR**2
      B(4,1),B(8,3)=2.*ELLR**3
      B(4,8),B(8,10)=-2.*ELLR**3
      B(12,5)=-10.*ELLR**3
      B(12,12)=10.*ELLR**3
      B(13,6)=8.*ELLR**3
      B(13,13)=7.*ELLR**3
      B(14,7)=-0.5*ELLR**3
      B(14,5)=-6.*ELLR**5
      B(14,14)=0.5*ELLR**3
      B(13,5)=15.*ELLR**4
      B(13,12)=-15.*ELLR**4
      B(14,6),B(14,13)=-3.*ELLR**4
      B(14,12)=6.*ELLR**5
      DO 2 I=1,14
      DO 2 J=1,14
    2 BT(I,J)=B(J,I)
      RETURN
      END
```

```
      SUBROUTINE ELSTIF (N,ALP,ELL,D)
      DIMENSION D(14,14)
      DO 1 I=1,14
      DO 1 J=1,14
    1 D(I,J)=0.0
      DO 4 J=2,4
      DO 4 I=2,J
    4 D(I,J)=(I-1)*(J-1)*ELL**(I+J-3)/(I+J-3)+D(I,J)
      DO 5 J=1,4
      DO 5 I=1,4
    5 D(J+4,I+4)=N**2*ELL**(I+J-1)/(I+J-1)+D(J+4,I+4)
      DO 6 J=1,6
      DO 6 I=1,4
    6 D(I+4,J+8)=D(I+4,J+8)-N*ELL**(I+J-1)/(I+J-1)
      DO 7 J=1,6
      DO 7 I=1,J
    7 D(I+8,J+8)=D(I+8,J+8)+ELL**(I+J-1)/(I+J-1)
      DO 8 I=2,4
      DO 8 J=1,4
    8 D(I,J+4)=D(I,J+4)+N*(I-1)*ELL**(I+J-2)/(I+J-2)*(0.3)
      DO 9 I=2,4
      DO 9 J=1,6
    9 D(I,J+8)=D(I,J+8)-(I-1)* ELL**(I+J-2)/(I+J-2)* (0.3)
      DO 10 J=1,4
      DO 10 I=1,J
   10 D(I,J)=D(I,J)+0.35*N*N*ELL**(I+J-1)/(I+J-1)
      DO 11 I=1,4
      DO 11 J=2,4
   11 D(I,J+4)=D(I,J+4)-0.35*N*(J-1)*ELL**(I+J-2)/(I+J-2)
      DO 12 J=2,4
      DO 12 I=2,J
   12 D(I+4,J+4)=D(I+4,J+4)+(0.35*ELL**(I+J-3)/(I+J-3))*((I-1)*(J-1))
      DO 13 J=1,4
      DO 13 I=1,J
   13 D(I+10,J+10)=D(I+10,J+10)+ALP*(I+1)*I*(J+1)*J*ELL**(I+J-1)/(I+J-1
      DO 14 J=1,6
      DO 14 I=1,J
   14 D(I+8,J+8)=D(I+8,J+8)+ALP*(1-N*N)**2*ELL**(I+J-1)/(I+J-1)
      DO 15 J=2,6
      DO 15 I=2,J
   15 D(I+8,J+8)=D(I+8,J+8)+(2.*N*N*0.7*ALP*ELL**(I+J-3)/(I+J-3))*
     1((I-1)*(J-1))
      DO 16 J=1,4
      IK=0
      DO 18 K=1,J
   18 IK=IK+K
      DO 17 I=1,2
   17 D(I+8,J+10)=D(I+8,J+10)+0.3*ALP*(1-N*N)*2.*IK*ELL**(I+J-1)/(I+J-1
      DO 19 I=1,4
      KI=0.0
```

```
      DO 20 K=1,I
   20 KI=KI+K
   19 D(I+10,J+10)=D(I+10,J+10)+0.6*ALP*(1-N*N)*(IK+KI)*ELL**(I+J+1)/
     1(I+J+1)
   16 CONTINUE
      DO 21 I=1,14
      DO 21 J=1,I
   21 D(I,J)=D(J,I)
       IF ( N ) 22,23,22
   23 CONTINUE
      DO 1030 I=1,14
      DO 1030 J=1,6
 1030 D(I,J+4)=D(I,J+3)
      DO 1031 I=1,6
      DO 1031 J=1,10
 1031 D(I+4,J)=D(I+8,J)
   22 CONTINUE
      RETURN
      END
```

```
      SUB ROUTINE BUCELSTIF (N,SK,B,D,BT,Z,ALP,ELL)
      DIMENSION B(14,14),BT(14,14),D(14,14),Z(14,14),SK(14,14)
      DO 1 I=1,8
      DO 1 J=1,8
      SK(I,J)=0.0
    1 D(I,J)=0.0
      D(1,1)=0.35*N*N*ELL
      D(1,2)=0.35*N*N*ELL**2/2.
      D(1,4)=-0.35*N*ELL
      D(2,2)=ELL  +0.35*N*N*ELL**3/3.
      D(2,3)=0.3*N *ELL
      D(2,4)=N*(-0.05)*ELL**2/2.
      DO 3  I=1,4
      D(2,4+ I)=-0.3*ELL** I/ I
      D(3,4+ I)=-N*ELL** I/ I
    3 D(4,4+ I)=-N*ELL**( I+1)/( I+1)
      D(4,4)=0.35*ELL+N*N*ELL**3/3.
      D(3,3)=N*N*ELL
      D(3,4)=N*N*ELL**2/2.
      BE=(1-N*N)**2+1./ALP
      D(5,5)=BE*ELL
      D(5,6)=BE*ELL**2/2.
      D(5,7)=BE*ELL**3/3.+0.6*(1-N*N)*ELL
      D(5,8)=BE*ELL**4/4.+1.8*(1-N*N)*ELL**2/2.
      D(6,6)=BE*ELL**3/3.+1.4*N*N*ELL
      D(6,7)=BE*ELL**4/4.+0.6*(1-N*N)*ELL**2/2.+2.8*N*N*ELL**2/2.
      D(6,8)=BE*ELL**5/5.+1.8*(1-N*N)*ELL**3/3. +4.2*N*N*ELL**3/3.
      D(7,7)=BE*ELL**5/5.+4.*ELL+(1.2*(1-N*N)+5.6*N*N)*ELL**3/3.
      D(7,8)=BE*ELL**6/6.+6.*ELL**2+(2.4*(1-N*N)+8.4*N*N)*ELL**4/4.
      D(8,8)=BE*ELL**7/7.+36.*ELL**3/3+(3.6*(1-N*N)+12.6*N*N)*ELL**5/5.
      DO 4 I=1,8
      DO 4 J=1,I
    4 D(I,J)=D(J,I)
      DO 12 I=5,8
       DO 12 J=5,8
   12 D(I,J)=ALP*D(I,J)
      CALL MATMULT (14,14,14,14,14,14,8,8,8,BT,D,Z)
      CALL MATMULT (14,14,14,14,14,14,8,8,8,Z,B,SK)
      RETURN
      END
```

```
      SUBROUTINE BUDITR (B,BT,ELLR)
      DIMENSION B(14,14),BT(14,14)
      DO 1 I=1,8
      DO 1 J=1,8
      B(I,J)=0.0
    1 BT(I,J)=0.0
      B(1,1),B(3,2)=1.0
      B(2,5),B(4,6)=ELLR
      B(2,1),B(4,2),B(7,8)=-ELLR
      B(5,3),B(6,4)=1.
      B(7,4)=-2.*ELLR
      B(8,4),B(8,8)=ELLR**2
      B(7,3)=-3.*ELLR**2
      B(7,7)= 3.*ELLR**2
      B(8,3)=2.*ELLR**3
      B(8,7)=-B(8,3)
      DO 2 I=1,8
      DO 2 J=1,8
    2 BT(I,J)=B(J,I)
      RETURN
      END
```

```
      SUBROUTINE MATMULT (II,JJ,KK,LL,MM,NN,K,L,M,AA,BB,CC )
      DIMENSION  AA(II,JJ),BB(KK,LL),CC(MM,NN)
      DO 1 I=1,MM
      DO 1 J=1,NN
    1 CC(I,J)=0.0
      DO 2 I=1,K
      DO 2 N=1,M
      DO 2 J=1,L
    2 CC(I,N)=CC(I,N)+AA(I,J)*BB(J,N)
      RETURN
      END
```

```
      SUBROUTINE RISTIF (RK1,RK2,N,AH)
      DIMENSION RK1(7,7),RK2(4,4)
      COMMON/BLOCK/RB,RD,RE,RA,RIX,RIZ,RJ
      DO 1 I =1,7
      DO 1 J =1,7
    1 RK1(I,J)=0.0
      DO 2 I= 1,4
      DO 2 J= 1,4
    2 RK2(I,J)=0.0
      RK1(1,1),RK2(1,1)=(N/(1+RE))**2*(N*N*RIZ +RJ/2.6)
       RK1(1,6)=(N*N/(1+RE))*(RIZ*(RE*N*N/(1+RE)-1)-RJ/(2.6*(1+RE)))
      RK1(6,1),RK2(1,4),RK2(4,1)=RK1(1,6)
      RK1(3,3),RK2(2,2)=RA*(N*(1+RE))**2
      RK1(3,5),RK1(5,3),RK2(2,3),RK2(3,2)=-RA*N*(1+RE)*(1+N*N*RE)
      RK1(5,5),RK2(3,3)=RIX*(1-N*N)**2/(1+RE)**2+RA*(1+N*N*RE)**2
      RK1(6,6),RK2(4,4)=RIZ*(1-RE*N*N/(1+RE))**2+RJ*(N/(1+RE))**2/2.6
      DO 3 I=1,7
      DO 3 J=1,7
    3 RK1(I,J)=RK1(I,J)*0.91*AH/(1+RE)
      DO 4 I=1,4
      DO 4 J=1,4
    4 RK2(I,J)=RK2(I,J)*0.91*AH/(1+RE)
      RETURN
      END
```

```
      SUBROUTINE RIGEM (I,J,ETR,CSS,AH,GRK,I1,J1)
      DIMENSION ETR(7),CSS(6,5,5),GRK(4,4)
      COMMON/BLOCK/RB,RD,RE,RA,RIX,RIZ,RJ
      PI=3.141592653
      DO 1 II=1,4
      DO 1 JJ=1,4
    1 GRK(II,JJ)=0.0
      IF (I-J) 2,3,2
    3 GRK(2,2)=PI*ETR(1)
      GRK(2,3),GRK(3,2)=-PI*ETR(1)*I/2.
      GRK(3,3)=PI*ETR(1)*I*J
    2 DO 4 N=1,6
      GRK(2,2)=GRK(2,2)+ETR(N+1)*CSS(N,I1,J1)
      GRK(2,3)=GRK(2,3)+ETR(N+1)*CSS(N,I1,J1)*(-J/2.)
      GRK(3,2)=GRK(3,2)+ETR(N+1)*CSS(N,I1,J1)*(-I/2.)
      GRK(3,3)=GRK(3,3)+ETR(N+1)*CSS(N,I1,J1)*I*J
    4 CONTINUE
      DO 5 II=1,4
      DO 5 JJ=1,4
    5 GRK(II,JJ)=GRK(II,JJ)*0.91*AH*RA
      RETURN
      END
```